Investigations on synaptic plasticity: new tools and perspectives

A thesis submitted for the degree of
Doctor of Philosophy

Carla Christianne Schmidt
New College

Michaelmas 2021

Acknowledgements

I would first like to thank my supervisor Nigel Emptage, whose expertise, continuous support and invaluable advice made my time in Oxford a thoroughly enjoyable experience. I would also like to thank Rudi Tong and Raphaël Turcotte for their mentoring and for providing insightful feedback which pushed me to sharpen my thinking and brought my work to a higher level. Thank you both for numerous scientific discussions and excellent teamwork, even across continents. In addition, I would like to acknowledge other former and current members from the Emptage lab: Alex, Peter and Henry for advice on everything scientific and technical, and for being so welcoming. Sebastian, Caroline and Jiahe for their help and for being so friendly. Thank you all for making my time in the Emptage lab fun and memorable. Furthermore, I would like to thank the MRC for supporting me throughout my studies. I would also like to thank all my friends from Oxford (OURFC and beyond). Thanks to you, I had a wonderful and unforgettable time in the UK. To my friends in Germany: I could not have completed this PhD without you and thank you for listening to my worries despite the distance. Finally, I would like to thank my family, especially my parents Heidi and Bruno whom without this PhD would have not been possible. Thank you both for always being there and for your unlimited support.

Abstract

For decades, neuroscientists have sought to understand the neural basis of learning and memory. As yet no unified model has emerged, although it is widely agreed that synaptic plasticity plays a pivotal role. In consequence, a great deal of research has focused upon the characterisation of synaptic plasticity both *in vitro* and *in vivo*. While the advances have been impressive, substantial gaps remain that may be slowing the identification of the precise relationship between synaptic plasticity and learning and memory: (1) there is a paucity of research examining presynaptic plasticity mechanisms and presynaptic receptor functions; (2) synaptic dynamics are studied in behaving animals without consideration of the impact of endogenous factors, even though it looks to be clear that hormone signalling impacts upon synaptic processes: (3) An accurate assessment of synapse biology with respect to cognitive function can only arise from studies in living animals, an ambition that will require the development of new imaging tools. In this thesis I begin to address each of these points. First, using a combination of optical and electrophysiological tools I provide a functional framework for presynaptic NMDA receptor signalling that has been previously lacking. I show that the specific subunit expression at presynaptic terminals is important as it regulates Ca^{2+} dynamics. Second, I demonstrate that oestrogen, a neuromodulator, lowers the threshold of plasticity in several brain regions, emphasising how important it is to consider hormone status when studying synaptic dynamics. Finally, I implement several advances to a multimode fibre based minimally invasive system for high-resolution brain imaging, including the first examples of

two-photon MMF imaging of biological tissue and successive imaging cycles through a multimode fibre.

Table of contents

1. Prologue - Synaptic plasticity: new tools and perspectives

Learning and remembering shape our everyday lives. In the words of the neuroscientist Eric Kandel:

'Has it ever struck you ... that life is all memory, except for the one present moment that goes by you so quickly you hardly catch it going? It's really all memory ... except for each passing moment.'

In a time where artificial intelligence and learning algorithms impact our society more than ever, it is peculiar that the fundamental neurobiological processes defining physiological learning and memory remain undiscovered. Nonetheless, over the last decades, our understanding of learning and memory mechanisms has vastly increased. Numerous neuronal circuits and networks that contribute to learning and memory have been identified, and recently researchers have begun to localise and study the sites of memory formation and consolidation. The interest in synaptic plasticity and its relation to learning and memory remains great, partly related to the fact that altered synaptic plasticity mechanisms have been associated with memory loss and learning deficits both in age and in neurodegenerative diseases (van Spronsen and Hoogenraad, 2010). Due to the rapidly changing demographics of society, there is a pressing need to identify suitable treatments to alleviate such age-related cognitive impairments, and in order to develop such treatments a thorough understanding of synaptic plasticity processes and their role in learning and memory will be required.

A great many studies published over more than 60 years have identified in some detail various molecular players and regulatory mechanisms underlying synaptic transmission and plasticity. In more recent studies neuroscientists have begun to investigate synaptic plasticity in the context of behavioural paradigms *in vivo*. Even though the data obtained over the years leaves little doubt that synapse dynamics are important for cognitive functions, profound gaps in our knowledge persist. Some topics in synaptic research have been underrepresented, even though they are essential for a comprehensive understanding of synaptic transmission. This includes the regulation of synaptic plasticity specifically at the presynaptic compartment of the synapse. Moreover, although endogenous neuromodulators, such as hormones, have been shown to have strong regulatory effects on synaptic plasticity, their exact functions remain unclear. However, describing and understanding these effects is relevant, especially if synaptic dynamics are studied in intact organisms where endogenous neuromodulators are constantly active. Finally, studying synaptic transmission and plasticity *in vivo* has been extremely challenging, mostly due to a lack of suitable technologies that allow direct observation of synaptic dynamics in relevant brain structures in behaving animals.

The above presents the basis of my research motivation. More specifically, in the project presented in this thesis I focused on three extraordinary but important aspects in the context of synaptic plasticity research: understanding presynaptic transmission, the effects of endogenous neuromodulators and the development of new imaging tools. These individual advances contribute towards one overarching goal: to understand how synapses relate to learning and memory. Importantly, while I have alluded to both traditional models of

synaptic plasticity and recent advances establishing links between synaptic dynamics and learning and memory in the general introduction of this thesis for contextualization purposes, they do not feature as central components for the experiments presented in this work. As the title states, the goal of this project was to shed light on new perspectives of synaptic plasticity by studying some important plasticity components that have not been attended to in the past and by providing innovative ideas that might change the way we study synaptic plasticity in the future.

2. General Introduction

2.1. Synaptic plasticity in the hippocampus

A fundamental goal in neuroscience is to understand cognitive functions, especially learning and memory. The founder of modern neuroscience, Ramon y Cajal was first to demonstrate that neurones are connected and potentially communicate via small structures such as synapses (Ramón y Cajal, 1911). Some decades later, Donald Hebb proposed that synaptic connections and activity-dependent changes thereof lead to changes in the strength of synaptic transmission (Hebb, 1949). He suggested that if two cells fire together, the strength of their connections should increase and that these mechanisms represent the cellular substrate of learning and memory (Hebb, 1949). These initial ideas on synaptic plasticity have shaped and directed the research motivation of neuroscientists until today (Bi and Poo, 2001). Over the years, a tremendous amount of experimental as well as theoretical and computational work has been published investigating synaptic plasticity across the brain. It has become evident that there are multiple forms of synaptic plasticity, differentially

expressed in brain regions and cell types. Even at the subcellular level, different forms of synaptic plasticity have been described, varying between pre- and postsynaptic terminals.

2.1.1. The classic view on postsynaptic plasticity

The first direct experimental evidence for synaptic plasticity was the discovery of long-term potentiation (LTP) in the hippocampus (Bliss and Lømo, 1973; Lømo, 2003). Long-term depression (LTD) was later established as a counterpart for LTP, emphasising the neurone's potential for bidirectional plasticity (Collingridge et al., 2010; Malenka, 1994; Malenka and Bear, 2004). In traditional studies, both LTP and LTD depend on postsynaptic N-methyl-d-aspartate receptor (NMDAR) -mediated influx of Ca^{2+}. LTP is induced via strong depolarisation of the postsynaptic cell parallel to activation of postsynaptic glutamate receptors by presynaptic release (Bear and Malenka, 1994; Bliss and Collingridge, 1993; Malenka, 1995, 1994). The depolarisation causes relief of the Mg^{2+} block which, together with glutamate binding, results in strong Ca^{2+} influx into the postsynapse, triggering downstream signalling cascades (Lüscher and Malenka, 2012; Malenka, 1995; Malenka and Bear, 2004; Nicoll, 2017). LTD on the other hand is induced by low frequency stimulation resulting in a more moderate Ca^{2+} influx (Collingridge et al., 2010; Connor and Wang, 2015; Malenka and Bear, 2004). Thus, whether LTP or LTD is induced depends strongly on the amount of Ca^{2+} entering the cell (Lüscher and Malenka, 2012; Malenka, 1994). Downstream signalling molecules differ between LTP and LTD, as strong Ca^{2+} influx activates calcium/calmodulin-dependent kinase II (CaMKII), whereas moderate Ca^{2+} influx activates calcineurin and other phosphatases (Collingridge et al., 2010; Connor and Wang, 2015; Lüscher and

Malenka, 2012; Malenka and Bear, 2004; Malinow et al., 1989; Mulkey et al., 1993). CaMKII and calcineurin differentially affect AMPA receptors (AMPARs), either increasing or decreasing phosphorylation, respectively (Huganir and Nicoll, 2013; Lüscher and Malenka, 2012). Ultimately, dephosphorylation of AMPARs leads to their internalization and, thus, depression of synaptic strength (LTD), while phosphorylation increases channel conductance leading to long-lasting synaptic potentiation (LTP; Collingridge et al., 2010; Lüscher and Malenka, 2012).

Early on the question was raised as to whether LTP is a result of increased presynaptic neurotransmitter release or increased postsynaptic sensitivity to glutamate (Bliss and Collingridge, 2013, 1993; Huganir and Nicoll, 2013; Nicoll, 2017). Several facts support the idea that the expression of LTP is largely postsynaptic. It was originally proposed that postsynaptic NMDAR activation is essential for LTP induction (Bliss and Collingridge, 2013, 1993; Lüscher and Malenka, 2012; Nicoll, 2017). Moreover, experimental evidence emphasised the importance of postsynaptic AMPA receptors in LTP (Huganir and Nicoll, 2013; Kauer et al., 1988; Nicoll, 2017). It has been demonstrated that AMPAR expression is plastic, and LTD can lead to AMPAR endocytosis whereas LTP and synaptic strengthening cause AMPAR insertion; processes summarized as AMPAR trafficking (Ehlers, 2000; Huganir and Nicoll, 2013; Park, 2018; Shi et al., 1999). Convincing evidence for a postsynaptic expression mechanism came with studies using glutamate uncaging to specifically activate NMDARs at postsynaptic terminals to induce LTP (Harvey and Svoboda, 2007; Matsuzaki et al., 2004). Furthermore, uncaging experiments have shown that the activation

of postsynaptic signalling molecules such as CaMKII, is required for LTP induction (Lee et al., 2009).

2.1.2. Presynaptic plasticity

The traditional view of a postsynaptic expression of long-term plasticity was challenged shortly after the initial discovery of LTP. Dolphin and colleagues provided the first evidence for a presynaptic expression, showing that LTP is correlated with an increase in glutamate release (Dolphin et al., 1982). Optical quantal analysis provoked a major breakthrough towards studying presynaptic changes, as single synaptic events could be imaged, directly reflecting the probability of neurotransmitter release. Excitatory postsynaptic calcium transients (EPSCaTs) can be recorded at spines in response to single stimuli to calculate release probability (Emptage et al., 1999, 2003; Padamsey et al., 2019). Using this technique Emptage et al. demonstrated that following LTP induction, release probability is increased at most synapses. Other studies confirmed these results, supporting the idea that LTP is partially expressed via presynaptic changes (Bliss and Collingridge, 2013; Emptage et al., 2003; Enoki et al., 2009; McGuinness et al., 2010). Following years of intense research and debating, it is now agreed upon that NMDAR independent forms of LTP are expressed presynaptically (Citri and Malenka, 2008; Nicoll and Schmitz, 2005). Postsynaptic and presynaptic LTP are mechanistically different: while postsynaptic LTP depends on Ca^{2+} influx from NMDARs, presynaptic LTP relies on Ca^{2+} influx from L-type voltage-gated calcium channels (L-VGCCs; Citri and Malenka, 2008; Padamsey et al., 2017; Padamsey and Emptage, 2014).

Long-term plasticity can be divided into two phases: early-LTP lasts for a few hours and is followed by late-LTP that can last from hours to days (Abraham, 2003). Alongside long-lasting changes in synaptic strength, synapses undergo plasticity processes lasting from tens of milliseconds to several minutes. Known as short-term plasticity, synaptic strength can be enhanced (facilitation) or reduced (depression) within millisecond time scales or within minutes (augmentation and post-tetanic potentiation, PTP; Fioravante and Regehr, 2011; Regehr, 2012; Zucker and Regehr, 2002). From early recognition that synaptic transmission can be dynamically enhanced (Eccles et al., 1941) short-term plasticity was properly characterised in the late 90s (Abbott et al., 1997; Markram and Tsodyks, 1996a, 1996b; Stevens and Wang, 1995; Tsodyks and Markram, 1997; Varela et al., 1997).

Short-term plasticity

Short-term plasticity occurs if two (paired pulse) or more (burst) stimuli are delivered within a short time interval and is based on changes in the probability of transmitter release (p_r; Zucker and Regehr, 2002). Thus, short-term plasticity is almost exclusively a presynaptic phenomenon and short-term enhancement occurs without any changes in postsynaptic effectiveness (Fisher et al., 1997; Zucker and Regehr, 2002). While synapses with high initial transmitter release (high-p_r synapses) typically depress, low-p_r synapses tend to facilitate their response and thus raise p_r for subsequent stimuli (Citri and Malenka, 2008; Dobrunz and Stevens, 1997; Fioravante and Regehr, 2011; Regehr, 2012). During short-term synaptic enhancement, including facilitation, augmentation and PTP, p_r is increased due to either an increase in the probability that a

release site is occupied by a docked vesicle or increased probability of exocytosis of the vesicle (Zucker and Regehr, 2002). Both are directly affected by the accumulation of presynaptic calcium following stimulation (Neher and Sakaba, 2008). Presynaptic Ca^{2+} levels during bursts of stimuli comprise of Ca^{2+} build-up known as residual Ca^{2+} (Erulkar and Rahamimoff, 1978; Katz and Miledi, 1968), and Ca^{2+} that floods the terminal with each action potential, respectively (Zucker and Regehr, 2002). Subsequently, facilitation can be affected by numerous processes, all triggered by Ca^{2+}. For example, in conditions of high-Ca^{2+}, endogenous Ca^{2+} buffers such as calcium-binding proteins will be saturated, allowing more Ca^{2+} to reach release sites. Compared to such direct effects of Ca^{2+} on neurotransmitter release, presynaptic Ca^{2+} could also regulate the activity of other presynaptic proteins triggering downstream signalling cascades that ultimately modify Ca^{2+} levels and release (Greengard et al., 1993). Presynaptic Ca^{2+} can also be enhanced directly by an increased influx through P/Q-type Ca^{2+} channels in repeated APs (Brody and Yue, 2000). In contrast, the inactivation of voltage-dependent calcium channels can result in short-term depression (Forsythe et al., 1998; Xu and Wu, 2005), as reduced Ca^{2+} within the synapse slows processes that underlie the exocytosis of synaptic vesicles (Citri and Malenka, 2008; Fioravante and Regehr, 2011; Regehr, 2012; Zucker and Regehr, 2002). Besides a reduction in Ca^{2+} influx, short-term depression can be a result of vesicle depletion (Schneggenburger et al., 2002). Generally, a readily releasable pool (RRP) of vesicles determines the number of vesicles released during activity, and if firing frequency is faster than RRP replenishment, fewer vesicles will be released for each stimulus leading to synaptic depression (Fioravante and Regehr, 2011; Regehr, 2012; Rizzoli and

Betz, 2005). Alternatively, release sites can be inactivated due to ongoing vesicle fusion processes (Fioravante and Regehr, 2011; Hosoi et al., 2009; Neher and Sakaba, 2008; Regehr, 2012). Metabotropic and ionotropic autoreceptors have been assigned important roles in short-term plasticity, since the activation of such autoreceptors can provide feedback control often leading to homosynaptic inhibition and reduced p_r (Kwon and Castillo, 2008; MacDermott et al., 1999; McGuinness et al., 2010; Wu and Saggau, 1997). Fig. 1 summarizes important short-term plasticity processes.

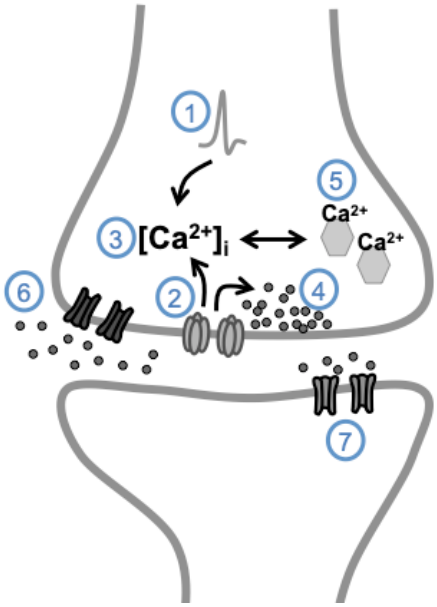

Fig. 1: Short-term plasticity mechanisms. Short-term plasticity is regulated at synaptic terminals involving the following mechanistic sites: (1) AP waveform (2) Ca^{2+} channel activation (3) internal Ca^{2+} concentration (4) readily releasable pool (5) Ca^{2+} binding proteins (6) metabotropic and ionotropic autoreceptors (7) postsynaptic receptor desensitization.

What are the functional consequences of short-term plasticity? Via short-term plasticity (STP), a presynaptic neurone influences the firing of its postsynaptic target, thus, STP plays an important role in the communication between neurones and how information is transmitted (Regehr and Abbott, 2004).

Traditionally, STP is seen as the presynapse' ability to act as a filter (Tong et al., 2020). Low-p_r facilitating synapses act as high-pass filters, which allows reliable transmission of high-frequency bursts. In contrast, high-p_r, depressing synapses more efficiently transmit low-frequency activity and therefore act as low-pass filters (Citri and Malenka, 2008; Fortune and Rose, 2001; Regehr and Abbott, 2004). Filtering properties of STP have been demonstrated in several experimental and theoretical studies in the cortex and hippocampus (Kandaswamy et al., 2010; MacLeod et al., 2007; Pan and Zucker, 2009; Tsodyks et al., 1998; Tsodyks and Markram, 1997). In hippocampal synapses, STP can act as adaptive filter during high-frequency natural spike patterns (Klyachko and Stevens, 2006). *In vivo* recordings have shown that short-term depression is important for adaptation during repeated sensory stimulation (Chung et al., 2002).

The individual forms of STP (facilitation, depression, augmentation) all play distinct roles in synaptic operations (Deng and Klyachko, 2011). On the behavioural level, facilitation serves as substrate for short-term memory and decision-making in the cortex (Deng and Klyachko, 2011). For example, Mongillo et al. have demonstrated that short-term synaptic facilitation mediated by increased residual calcium levels at presynaptic terminals serves as cellular substrate for transiently holding a memory. This mechanism provides an energy efficient option for short-term memory (Deng and Klyachko, 2011; Mongillo et al., 2008). In decision-making, short-term memory is relevant because two stimuli are compared at different times, requiring the first stimulus to be held in memory. Deco et al. have demonstrated that neurones can use synaptic facilitation to hold this memory, enabling comparison with the second stimulus

later in time (Deco et al., 2010; Deng and Klyachko, 2011). Moreover, STP is suggested to be involved in a number of other cognitive functions including sensory memory, attention and perceptual learning (Jääskeläinen et al., 2011). Although such models have yet to be confirmed *in vivo*, STP nonetheless appears to be much more than a theoretical approach for synaptic computation as it might underpin fundamental cognitive functions such as short-term memory and decision-making.

Interacting: pre- and postsynaptic plasticity mechanisms

New literature has taught us that the majority of plasticity processes are never exclusively pre- or postsynaptic, but most likely a combination of both (Bliss and Collingridge, 2013) and that unique plasticity rules for the pre- and postsynapse, respectively, are implemented to optimise their function (Tong et al., 2020). This was recently demonstrated by Padamsey and colleagues, showing that presynaptic long-term plasticity might not require glutamate signalling and therefore radically differs from traditional models of postsynaptic plasticity (Padamsey et al., 2017b). Experimental evidence for the coexistence of pre- and postsynaptic plasticity is available. For example, the discovery of silent synapses (Isaac et al., 1995; Liao et al., 1995) that are synapses that only express NMDARs but not AMPARs was presented as convincing evidence that LTP is expressed postsynaptically (Kerchner and Nicoll, 2008). Following LTP induction, these synapses undergo insertion of a population of AMPA receptors, turning them into ‘fully functional’ synapses (Kerchner and Nicoll, 2008). However, Ward et al. have demonstrated that although LTP-inducing stimulation caused an initial postsynaptic response without altering p_r via the

insertion of synaptic AMPA receptors, subsequent potentiation is expressed presynaptic by an increase in p_r (Bliss and Collingridge, 2013; Ward et al., 2006). Even in short-term plasticity, thought to be a presynaptic phenomenon, the postsynaptic terminal has shown to be involved, since the desensitization of postsynaptic receptors can lead to use-dependent decreases in synaptic strength (Jones and Westbrook, 1996; Zucker and Regehr, 2002; Fig.1). The interaction of pre- and postsynaptic plasticity processes appears even more evident when turning towards other forms of synaptic plasticity such as homeostatic plasticity. To avoid hyper- or hypoactivity within neural circuits, regulatory mechanisms are necessary to prevent saturation of synaptic strengths, termed “run-away”, or quiescence (Turrigiano, 2012; Turrigiano and Nelson, 2004). Pushing a neural network towards one of both extremes will compromise capacity for information storage and processing. Homeostatic plasticity is a collective term for mechanisms underlying the stabilization of neuronal activity (Turrigiano, 2012; Turrigiano and Nelson, 2004) and involves both pre- and postsynaptic mechanisms (Pozo and Goda, 2010). It has been shown that if network activity is suppressed pharmacologically with tetrodotoxin (TTX) or glutamate receptor blockers, readily releasable vesicles and thus p_r can be increased (Moulder et al., 2006; Murthy et al., 2001). While these experiments focussed on global homeostatic adjustments, it has also been demonstrated that p_r can be homeostatically adapted in a subset of synapses (Branco et al., 2008). Besides such presynaptic changes, postsynaptic strength is adjusted during homeostatic plasticity via trafficking and subunit combination of AMPA receptors (Bredt and Nicoll, 2003; Diering and Huganir, 2018; Fu et al., 2011; Pozo and Goda, 2010; Santos et al., 2009). It is still not fully

understood how exactly pre- and postsynaptic homeostatic plasticity interact and if, following specific triggers, one precedes the other.

2.1.3. Structural plasticity

One form of homeostatic plasticity at central synapses is synaptic scaling, a mechanism that occurs when network activity is manipulated for longer time periods (Turrigiano et al., 1998). A dramatic increase or decrease in network activity causes an adjustment of synaptic strength to compensate for the changes in excitability and maintain stable function (Turrigiano, 2008; Turrigiano et al., 1998). In synaptic scaling, one way of regulating synaptic strength is to increase or decrease the abundance of AMPARs and NMDARs in the postsynaptic membrane (reviewed in Turrigiano, 2012, 2008). The number of AMPA receptors at spines positively correlates with spine size (Matsuzaki et al., 2001), thus compensatory effects accompanying synaptic scaling are detectable as changes in activity as well as morphology. Indeed, following sensory deprivation by inducing retinal lesions, activity levels in the visual cortex are significantly decreased inducing synaptic scaling mechanisms including increases in spine size (Keck et al., 2013). Such morphological changes of synapses not only occur in homeostatic plasticity, but also in Hebbian plasticity and in response to many other protocols that alter synaptic activity. Collectively, structural rearrangements of synapses in response to stimuli, including synapse enlargement, shrinkage and elimination, can be summarized under the term structural plasticity. Structural plasticity can be induced at single spines using glutamate photolysis causing a rapid and selective enlargement of stimulated spines that can either be transient or long lasting (Matsuzaki et al., 2004). Besides glutamate uncaging, structural LTP has

been observed following conventional LTP protocols using electrophysiological (Yang et al., 2008) or chemical (Stewart et al., 2005) stimulation. To date, structural LTP and its counterpart, structural LTD, have both been identified and extensively studied at dendritic spines *in vitro* (Engert and Bonhoeffer, 1999; Lang et al., 2004; Nägerl et al., 2004; Popov et al., 2004; Sun et al., 2021; Wiegert and Oertner, 2013; Zhou et al., 2004) and *in vivo* (Grutzendler et al., 2002; Gu et al., 2014; Holtmaat et al., 2005; Noguchi et al., 2019, 2011; Poll and Fuhrmann, 2018; Trachtenberg et al., 2002; Zuo et al., 2005). Presynaptic morphological changes following potentiation have also been observed (Ash et al., 2018; Bailey and Chen, 1988; Becker et al., 2008; Böhme et al., 2019; De Paola et al., 2006; Qiao et al., 2016) and presynaptic remodelling has been shown to trigger the formation of new postsynaptic densities following plasticity induction (Nikonenko et al., 2003).

What are the underlying mechanisms of postsynaptic structural plasticity? Long lasting increases in spine size are accompanied by actin cytoskeleton remodelling and the translocation of specific proteins such as cofilin and postsynaptic density (PSD) proteins to the spine (Bosch et al., 2014). Following plasticity induction, increases in spine size, PSD and presynaptic bouton size closely correlate (Meyer et al., 2014). The underlying molecular mechanisms of structural plasticity are complex, as depicted in Figure 2. Broadly, these mechanisms can be divided in three classes: second messenger mechanisms, local regulation of protein synthesis, and actin cytoskeleton remodelling (Caroni et al., 2012; Lai and Ip, 2013; Lüscher et al., 2000; Patterson and Yasuda, 2011). One group of second messengers involved in structural plasticity are Rho GTPases and their inhibition negatively affects sustained spine growth

(Hedrick and Yasuda, 2017; Murakoshi et al., 2011; Patterson and Yasuda, 2011).

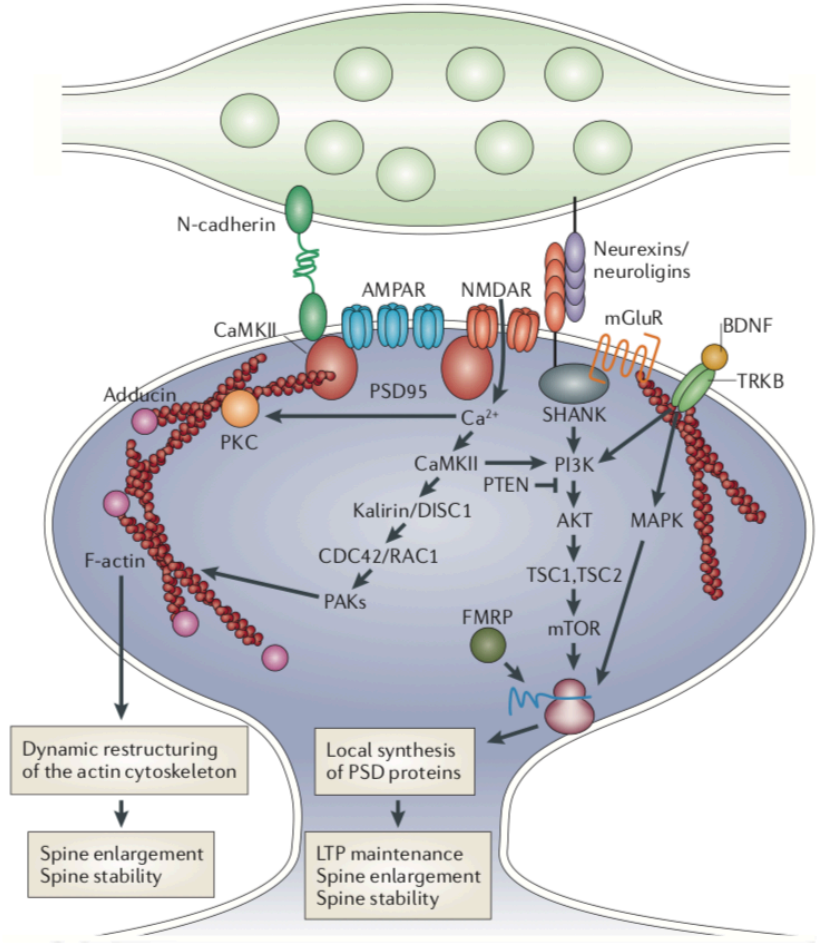

Fig. 2: Molecular mechanisms involved in structural plasticity. Structural plasticity at postsynaptic terminals is associated with an enlargement of the spine and an increase in synaptic efficacy accompanied by changes in protein expression of PSD95 (postsynaptic density protein of 95 kDa), SHANKs (SH3 and multiple ankyrin repeat domains proteins), neuroligins, N-cadherins, AMPA receptors (AMPARs) and NMDA receptors (NMDARs). Other signalling molecules contributing to spine enlargement, stability and LTP maintenance are kinases such as PKC (protein kinase C) and CaMKII (calcium/ calmodulin protein kinase II). Such signalling molecules affect the actin cytoskeleton (F-actin). In addition, local protein synthesis (for example of BDNF (brain-derived neurotrophic factor), TRKB (tyrosine kinase B), MAPK (mitogen-activated protein kinase) are important for some forms of structural plasticity. *Adapted from Caroni et al., 2012.*

The Ca^{2+} influx through NMDA receptors activates multiple other signalling molecules, including kinases such as CaMKII. In transgenic mice lacking CaMKII activity structural LTP is impaired suggesting that CaMKII is necessary for spine enlargement (Yamagata et al., 2009). Studies using CaMKII inhibitors confirmed that CaMKII plays a key role in structural plasticity (Harvey et al., 2008; Lee et al., 2009; Matsuzaki et al., 2004) especially since it binds and modifies actin filaments (Borovac et al., 2018). Actin is highly enriched in synaptic terminals and represents the major cytoskeletal component that regulates structural plasticity (Borovac et al., 2018). Inhibition of actin regulatory proteins such as cofilin impairs structural LTP (Bosch et al., 2014).

Studies over the years have concluded, that local protein synthesis in synaptic terminals is required for many forms of long-term plasticity (reviewed in Sutton and Schuman, 2006). This includes certain forms of structural LTP, as persistent increases in spine size could be blocked by application of protein synthesis inhibitors anisomycin or cyclohexamide (Yang et al., 2008). Furthermore, bath application of brain-derived neurotrophic factor (BDNF) parallel to glutamate uncaging can trigger protein synthesis dependent spine potentiation (Tanaka et al., 2008). Although most studies focused on the structural plasticity of the postsynapse, some research has been conducted focusing on presynaptic plasticity mechanisms. Similar to postsynaptic densities, presynaptic structural plasticity can manifest in either growth of presynaptic terminals or maturation and remodelling of existing boutons (Rekart et al., 2007). Thereby, presynaptic potentiation can be modulated by recruiting active zones or by generating new boutons (Reiff et al., 2002). A recent study by Chéreau et al. using superresolution microscopy, demonstrated that

following high-frequency AP firing, synaptic boutons are subject to rapid and transient enlargement followed by delayed axon shaft widening, providing a structural plasticity mechanism for fine-tuning AP conduction velocity (Chéreau et al., 2017). On the molecular level, the presynaptic growth protein GAP-43 might play a key role in presynaptic structural plasticity, as it regulates actin dynamics (Holahan, 2017; Laux et al., 2000). Downregulation of GAP-43 caused a decrease in synaptic bouton count (Grasselli et al., 2011). It has also been reported that the positioning of mitochondria within presynaptic terminals influences bouton stability (Lees et al., 2020). The previous sections present only a small overview of structural plasticity mechanisms and many more have been identified. For example, recent studies have shown that structural LTP at postsynaptic terminals is regulated by neurotrophins such as BDNF (Harward et al., 2016; Hedrick and Yasuda, 2017). Moreover, BDNF is involved in the structural plasticity of axons and boutons (Andreska et al., 2014; Lalo et al., 2018; Lowenstein and Arsenault, 1996).

2.1.4. Relevance of studying the presynaptic terminal

As described in the foregoing chapters, multiple forms of plasticity are expressed at both pre- and postsynaptic terminals. Generally speaking, synapses within the central nervous system (CNS) exhibit a great diversity in functional responses to activity – some synapses depress and some facilitate, thereby creating individual response patterns to stimuli (Andreae and Burrone, 2014). This synapse individuality is important for information processing (Regehr and Abbott, 2004), which becomes evident if one considers information transfer in neuronal networks: a single neurone communicates with a large

number of other neurones, all involved in different neural circuits within different parts of the brain. How can a single input be diversified into multiple specified outputs? Given the stochastic nature of neurotransmitter release, further modified by short-term plasticity processes, a neurone's output consists of a large variety of synapse-specific signals, thus expanding the range of communication. This is important if a neurone connects with two different cell types, such as interneurones and other excitatory neurones, necessitating differential signals and connections (Andreae and Burrone, 2014; Pala and Petersen, 2015). Indeed, studies have demonstrated that the presynaptic properties of hippocampal synapses differ according to the type of target cell (Scanziani et al., 1998; Schinder et al., 2000). In this scenario, the postsynaptic terminal belonging to the follower cell provides retrograde information, strongly influencing synaptic transmission at these terminals. However, individual synapses of a single neurone connecting with the same follower cell can also elicit different postsynaptic responses, indicating that in this second scenario, presynaptic properties determine the specification of each synapse (Atwood and Karunanithi, 2002; Markram et al., 1998a, 1998b; Thomson, 2000). Thus, basic signal transmission is affected by a number of both pre- and postsynaptic factors, however, a great part of synaptic diversity can be ascribed to presynaptic features.

Differential synaptic transmission was originally studied in large synaptic terminals that are experimentally accessible such as the vertebrate and crustacean neuromuscular junction (NMJ), the giant synapse of the squid, and later the calyx of Held, shaping our understanding of neural transmission and the role of Ca^{2+} in neurotransmitter release. These early studies already pointed

towards the importance of the presynaptic terminal in the regulation of synaptic transmission and plasticity (Bollmann et al., 2000; Del Castillo and Katz, 1954; Dudel and Kuffler, 1961; Fatt and Katz, 1952; Forsythe, 1994; Katz and Miledi, 1968; Schneggenburger and Neher, 2000; Thomson, 2000). But it was not until the 1990s that properties of individual synaptic transmission were thoroughly studied in small mammalian synapses, and the idea of synaptic individuality was supported by experimental evidence (Markram et al., 1998a; Thomson, 2000). Following several experimental studies, it was proposed that synapses in the hippocampus exhibit unique sets of synaptic parameters, even if they arise from the same axon, fundamentally increasing the computational power for neural information processing (Markram et al., 1998a). Biologically, these parameters include differences in p_r and diversity in receptor expression (Murthy et al., 1997; Shigemoto et al., 1997), both influenced by presynaptic mechanisms (Atwood and Karunanithi, 2002).

The importance of the presynaptic terminal for basic transmission and functional diversity as well as its key role in many plasticity processes has been demonstrated for years, as pointed out above and by others (Atwood and Karunanithi, 2002; Citri and Malenka, 2008; Padamsey et al., 2017b; Regehr and Abbott, 2004; Tong et al., 2020; Zucker and Regehr, 2002). Nevertheless, there is still a significant lack in studies investigating the functional outcomes of presynaptic plasticity mechanisms, its regulation at individual terminals and how presynaptic structural and molecular differentiation direct synaptic diversity. It has been challenging to close these gaps, for a number of reasons: firstly, compared to the size of the dendritic tree, the axon is thin and it is difficult to identify boutons that are suitable for studies (Fig. 3). Even with today's

advances in microscopy, it is still challenging to identify and image presynaptic terminals, mainly because of the physiological properties of the axon. The axon travels far, through multiple layers of tissue leaving superficial boutons that are suitable for experiments to be located a significant distance away from the neurone under study (Debanne et al., 2011; McGuinness et al., 2010).

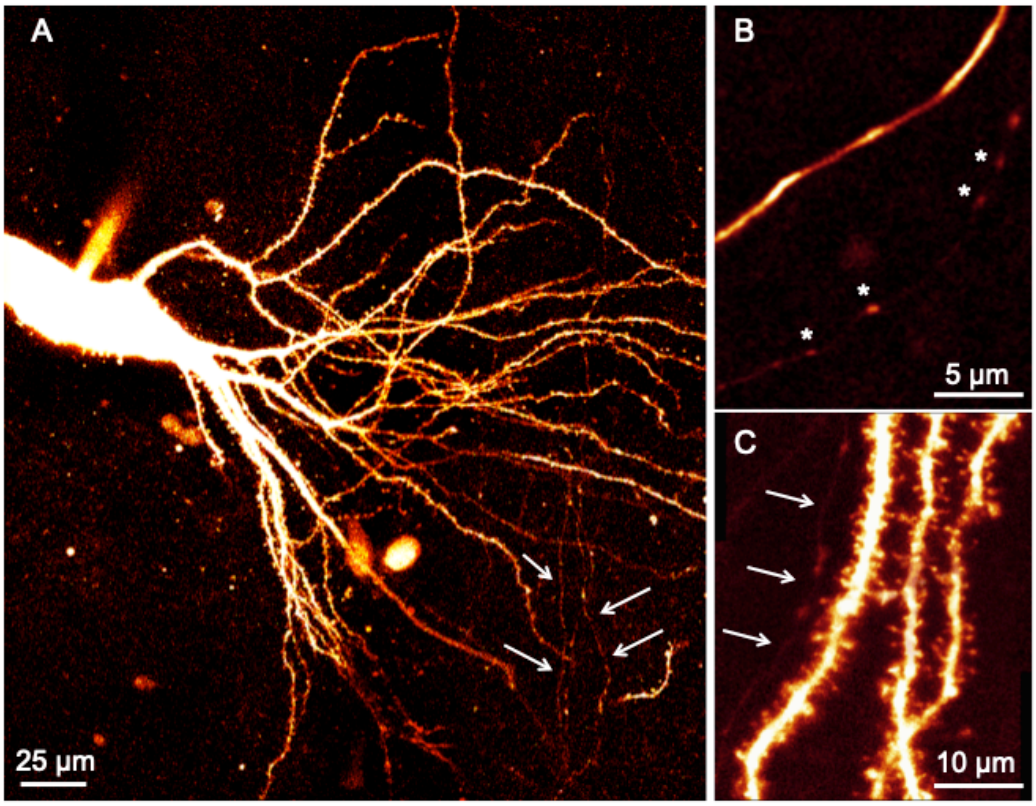

Fig. 3: Hippocampal pyramidal neurone: axon and bouton morphology. Images of a CA3 pyramidal neurone labelled with fluorescent dye via patch-clamp technique. The arrows indicate the position of the axon. (A) The axon is thin and harder to track compared to the brightness and size of the dendritic tree. (B) Once the axon is identified, thinner and superficial branches must be located to identify boutons for experiments (indicated with asterisks). (C) Emphasises the morphological differences of the axon (indicated with arrows) with individual boutons compared to much brighter and thicker dendrites with a large number of spines clearly visible.

Secondly, in experimental set-ups studying synaptic plasticity, it is challenging to dissect pre- from postsynaptic plasticity and thus it is difficult to investigate its

individual functional impact in experiments. Finally, the molecular composition at synaptic terminals is extremely complex and we have only started to identify receptor types and signalling molecules that direct synaptic mechanisms. New technologies such as superresolution microscopy are generally focused on postsynaptic terminals, identifying dynamics of small molecules during synaptic transmission and plasticity (Hruska et al., 2018; Inavalli et al., 2019; Nägerl et al., 2008; Nägerl and Bonhoeffer, 2010; Pfeiffer et al., 2018; Steffens et al., 2021; Tønnesen et al., 2014; Wegner et al., 2018 but see Chéreau et al., 2017; Tønnesen et al., 2011; Willig et al., 2006). There is an abundance of studies, characterising and labelling postsynaptic receptors, such as AMPARs, and their dynamics *in vitro* as well as *in vivo* (Inavalli et al., 2019; Ju et al., 2004; MacGillavry et al., 2013; Nair et al., 2013; Petrini et al., 2009; Roth et al., 2020; Tardin et al., 2003; Zhang et al., 2015). Few such studies exist for the presynaptic terminal; hence individual regulatory mechanisms thereof remain largely unexplored. Partially, reasons for this relate to the enhanced difficulty of labelling receptor types that are presynaptically expressed, such as NMDARs, compared to well established staining protocols for postsynaptic AMPARs (Kellermayer et al., 2018). Labelling techniques for postsynaptic AMPARs have developed ahead of those for NMDARs, and today endogenous AMPAR dynamics on hundreds of thousands of synapses can be tracked in behaving mice (Graves et al., 2021). In comparison, studies tracking NMDAR receptor dynamics are still performed *in vitro* (Ferreira et al., 2017; Kellermayer et al., 2018; Yong et al., 2021). Most high-resolution studies at the presynapse use electron microscopy for direct visualisation of vesicles and transmitter release in fixed preparations (Ultanir et al., 2007; Zuber and Lučić, 2019) and some

progress has been made visualising synaptic vesicle recycling using STED (Willig et al., 2006). Multiple studies consider presynaptic molecules but only investigate them in relation to the postsynaptic terminal, rather than their individual regulations and functions (Hruska et al., 2018; Inavalli et al., 2019).

The fact that synaptic performance is specifically regulated depending on the respective neural pathway emphasises the importance of synaptic regulation for neural transmission. For example, it was shown that the capacity for individual synapse dynamics, generating pathway-specific synaptic responses, enable temporal coding of correlated multisensory inputs by single neurones (Chabrol et al., 2015). Since the presynaptic terminal profoundly impacts synaptic signalling, for instance via the regulation of p_r, Ca^{2+} dynamics, and short-term plasticity, it is essential to study presynaptic regulatory mechanisms. Only then we can understand information transmission and processing in the brain, which underlies all cognitive functions. Understanding the basic principles of synaptic transmission, meaning how neurones communicate with each other, before we study these effects *in vivo* allows us to design more specific studies investigating how exactly synaptic and neuronal signalling relate to behaviour.

2.1.5. Synaptic plasticity as substrate for learning and memory

The preceding chapters hint at the complexity of plasticity at synapses and the sheer extent of plasticity mechanisms that have been investigated in different study designs. The scope of experimental studies ranges from presynaptic versus postsynaptic plasticity mechanisms or both combined occurring on different timescales including long- and short term, through plasticity induced alterations in synaptic activity and molecular signalling, up to plasticity induced

morphological changes. This is not to mention the large variety of experimental systems and technologies used to study these mechanisms, including electrophysiological, imaging and behavioural studies with *in vitro* as well as *in vivo* set-ups. Yet, the core motivation for all studies on synaptic plasticity has remained the same over the years: we want to understand the brains' ability to learn, remember and forget – cognitive functions that, as Hebb originally proposed over 70 years ago, are driven by experience-dependent synaptic changes (Hebb, 1949).

In the 1990s, hippocampal long-term plasticity (LTP and LTD) was excessively studied and resembled the dominant model of activity-dependent synaptic plasticity in the mammalian brain (Bliss and Collingridge, 1993). Early studies linking LTP to learning and memory used pharmacological or genetic inhibition of key players in synaptic plasticity, such as NMDA receptors or CaMKII, which blocked not only LTP but also the animal's ability to learn and memorise in behavioural tasks (Giese et al., 1998; Grant et al., 1992; Morris et al., 1986; Silva et al., 1992). Moreover, overexpression of NMDARs in the forebrains of transgenic mice has been shown to not only enhance synaptic potentiation but also increase ability in learning and memory in these animals in various behavioural tests (Tang et al., 1999). Thus, this positive correlation between long-term synaptic plasticity and learning provided compelling evidence for synaptic alterations as substrates for learning and memory.

The SPM hypothesis

These early studies laid the foundation for the synaptic plasticity and memory (SPM) hypothesis, an idea that has been developed, advanced, and debated

until today (Martin and Morris, 2002). Like many other theories, the SPM hypothesis experienced several setbacks over the years. Some studies reported normal spatial learning despite inhibition of NMDA receptor dependent LTP (Bannerman et al., 1995; Nosten-Bertrand et al., 1996; Saucier and Cain, 1995 but see Bannerman et al., 2012). Thus, it became apparent that establishing a relationship between synaptic plasticity and behaviour is far more complex than showing that some types of learning are impaired following NMDA receptor blockade (Goda and Stevens, 1996; Stevens, 1998). There are important factors that need to be considered when studying synaptic plasticity in relation to learning and memory: (1) There are many different forms of learning and memory broadly separated into explicit (declarative) memory, for facts and events, people, places, and objects; and implicit (nondeclarative) memory, for perceptual and motor skills (Kandel et al., 2014). Explicit and implicit memory is further divided into numerous subgroups ranging from fear conditioning through spatial memory up to motor learning. (2) Learning and memory consist of several interacting processes including encoding of new information, short-term memory, consolidation and maintenance of long-term memory, memory retrieval and expanding a given memory with other memories (Gallistel and Matzel, 2013; Kandel et al., 2014). Thus, the terms ‚learning' and ‚memory' must be defined carefully in experimental studies. (3) Learning and memory are never confined to individual but involve multiple brain regions, and mechanisms will differ depending on the respective structure under investigation. For example, fear conditioning and memory occur in various brain sites including amygdala, hippocampus, cortex and cerebellum (Kim and Jung, 2006). To avoid getting lost in the complexity of synaptic plasticity and memory memory a

consistent approach using simple and robust criteria should be applied to test the SPM hypothesis regardless of the system of study (Martin et al., 2000; Martin and Morris, 2002; Takeuchi et al., 2014). To this end, a number of criteria have been proposed, that are relevant for the assessment of the SPM hypothesis: (1) detectability of changes in synaptic efficacy following learning and memory; (2) anterograde intervention to prevent synaptic changes during learning should impair the animals' learning and memory behaviour; (3) retrograde intervention; changes in synaptic efficacy that have been detected following a learning experience are modified which should affect the animals' memory; and (4) mimicry, artificially inducing known changes in synaptic efficacy for a given memory should display this memory in a naive animal without previous experience (Martin et al., 2000; Martin and Morris, 2002; Takeuchi et al., 2014). Over the last 30 years, exciting discoveries have been made in each of those categories. New imaging techniques and *in vivo* approaches allow detection and investigation of small molecule dynamics during learning, such as AMPA receptor trafficking, which confirmed a critical role for AMPA receptors in learning as originally proposed in slices (Matsuo et al., 2008; Mitsushima et al., 2011; Penn et al., 2017; Roth et al., 2020; Zhang et al., 2015). The study from Penn et al. also fulfils the second criterion of anterograde intervention, as immobilizing AMPA receptors prevented plasticity and learning (Penn et al., 2017). Following early studies manipulating NMDAR signalling (Morris et al., 1986) inhibition or knockout of NMDA receptors has emerged as powerful tool for anterograde intervention to investigate synaptic plasticity and memory (Nakazawa et al., 2003, 2002), although these studies must be carefully interpreted given the existence of NMDAR independent forms

of synaptic plasticity. Mutating genes of downstream signalling molecules allows manipulation of other proteins such as PSD proteins or kinases and phosphates (Takeuchi et al., 2014). The best way of using retrograde intervention mechanisms is to tag and subsequently manipulate synapses that have undergone plasticity during a specific learning task. This has been demonstrated in an elegant study by Hayashi-Takagi et al. in which recently potentiated spines were specifically labelled with an optoprobe and then selectively shrunken which disrupted motor learning (Hayashi-Takagi et al., 2015). To realize the idea of mimicry, to artificially alter synaptic strength thereby inducing a ‚memory' without previous experience, would provide particularly strong evidence for synaptic plasticity as basis for learning and memory. Some forms of mimicry have been demonstrated, for example, during fear conditioning where a foot shock is usually combined with tone delivery to induce fear learning and memory, optogenetic stimulation of specific neurones during tone delivery can generate an artificial fear memory without the actual foot shock (Johansen et al., 2010). Recently, ‚artificial memories' of odours have been created in mice by optogenetic stimulation of specific olfactory glomeruli and optogenetic stimulation of distinct inputs into the ventral tegmental area that mediate either aversion or reward (Vetere et al., 2019). As a result, mice either approached or avoided an odour that they had never experienced before, purely based on the stimulation protocol induced by the researchers (Vetere et al., 2019).

Engram cells

The latter studies use optogenetic activation of subsets of neurones that are considered as cellular substrates for specific memories. These ‘engram cells'

are populations of neurones that are activated and modified by a learning experience and subsequent reactivation of those cells, either naturally or artificially, leads to memory retrieval of that experience (Josselyn and Tonegawa, 2020; Ryan et al., 2021; Tonegawa et al., 2018). In other words, the memory engram, as representation of a past experience, can manifest within neuronal assemblies providing biophysical conditions through which memories are stored in the brain (Josselyn and Tonegawa, 2020). To identify neurones that have been active during a specific memory task later on they must be marked. Several methods identifying cellular tags have been developed, for example, the first demonstration of engram cells made use of the fact that neurones expressing higher levels of cyclic adenosine monophosphate response element-binding protein (CREB) are preferentially activated by fear memory expression. Specifically ablating these neurones robustly blocked expression of that fear memory (Han et al., 2009). Such loss-of-function studies were followed by gain-of-function studies, in which memory retrieval was induced artificially by activating engram cells in absence of natural cues, through optogenetics (Cowansage et al., 2014; Lacagnina et al., 2019; Liu et al., 2012; Redondo et al., 2014). Most of those studies use cFos-tetracycline transactivator protein (tTA) transgenic mouse lines to label neurones that are active during specific experiences (Reijmers et al., 2007; Tanaka et al., 2018). Engram cells have been identified and their functions have been studied in the context of various forms of memories across multiple brain regions (extensively reviewed in Josselyn and Tonegawa, 2020) ranging from the location of social memory storage (Okuyama et al., 2016) and the recovery of "lost" infant memories (Guskjolen et al., 2018) to the identification of a "cocaine-engram"

(Hsiang et al., 2014). Some place cells, CA1 hippocampal neurones that fire location-specifically (O'Keefe and Dostrovsky, 1971), function as engram cells providing context information during memory recall (Tanaka et al., 2018).

The role of synapses in learning and memory has been complicated by the emergence of the cellular engram paradigm (Abraham et al., 2019). If memories can be generated, simply by activating neuronal ensembles, then what is the role of the synapse and how does synaptic plasticity fit into the picture (Han et al., 2021)? We do not have precise answers to this question yet, mainly related to the fact that studying engram cells in memory is a relatively new phenomenon and it will take time to integrate previous research on synaptic plasticity into engram cell studies. Several theories have been proposed which establish different roles for synapses in learning and memory: for example, Tonegawa et al. reported that while synaptic plasticity matters for normal memory function, engram cells can retain memory information even in the absence of synaptic plasticity, following protein synthesis inhibition (Ryan et al., 2015). Based on this data, they suggest that memories are not stored in synapse dynamics per se, but rather in specific connectivity patterns between engram cells, which can be modified by synaptic plasticity mechanisms (Tonegawa et al., 2015b, 2015a). The concept of this new theory can be traced back to old suggestions questioning the SPM theory by proposing that synaptic plasticity processes set the conditions for learning and memory instead of actually encoding and storing memories (Shors and Matzel, 1997). The concept of cell-intrinsic memory storage has been supported by others (Gallistel and Matzel, 2013; Johansson et al., 2014; Langille and Gallistel, 2020).

Synaptic tagging

Even though there is still some confusion about the role of synaptic plasticity in learning and memory, an interesting role has been proposed for synapses in the memory ‘consolidation’ process that follows initial experience and memory encoding. In laboratory settings, learning and memory formation are strongly simplified, often related to one individual experience and its outcome as linear events in time. However, in reality memorable experiences happen simultaneously and the memorability of an experience will be affected by previous and future experiences (Redondo and Morris, 2011). Thereby, each memory can potentially be consolidated into long-term memory, however some memories fade. The fate of each memory is not decided at the time of encoding, since that would require enormous computational power; initially encoded memories rather manifest as ‘synaptic tags’ (Frey and Morris, 1997; Martin and Kosik, 2002; Redondo and Morris, 2011; Rogerson et al., 2014). Synapses that have been stimulated during memory encoding can be tagged via local molecular changes, such as increased AMPAR trafficking and release sites, independent of protein synthesis (Redondo and Morris, 2011; Shires et al., 2012). Later on, these tagged synapses can capture plasticity-related proteins to maintain synapse potentiation over longer time periods underpinned by structural and functional changes (Frey and Morris, 1998; Martin and Kosik, 2002; Redondo and Morris, 2011; Rogerson et al., 2014). Synaptic tagging provides a temporal buffer, extending the time course and flexibility for long-term memory formation (Redondo and Morris, 2011). In other words, synaptic tagging is a potential mechanism to ‚prepare’ synapses for potential long-term stabilizing plasticity processes underlying memory consolidation. The fact that

memories can be recalled by optogenetic stimulation of engram neurones even under protein synthesis inhibition (as demonstrated by Ryan et al., 2015) does not necessarily exclude the possibility that synapses are important for memory storage after all. The results of Ryan et al. are reminiscent of studies investigating synaptic tags and capture, where LTP can be induced in synapses even in conditions of protein synthesis inhibition (Redondo and Morris, 2011; Shires et al., 2012). One could speculate that optogenetic stimulation induces the capture process within synapses that have been tagged by the initial memory experience, and that this mechanism, which is indeed protein synthesis independent, underlies memory storage.

Structural plasticity in learning and memory

The fact that structural changes occur during the capture process following synaptic tagging touches a whole other field linking synaptic dynamics to learning and memory. Structural plasticity of synapses (see 2.1.3.) correlates with learning, and the formation of new synapses occurs during experience and repeated training (Bailey et al., 2015; Caroni et al., 2012; Holtmaat and Caroni, 2016; Lamprecht and LeDoux, 2004; Tropea et al., 2010; Xu et al., 2009; Yang et al., 2008). During motor learning and memory, new spines are formed (Fu et al., 2012; Xu et al., 2009) and sleep following motor learning tasks promotes the generation of new spines on individual neurones (Yang et al., 2014). A standard method to assess synapse dynamics is to measure synapse turnover, meaning how many boutons or spines are newly formed, stable, or eliminated (Holtmaat and Caroni, 2016; Holtmaat et al., 2005; Trachtenberg et al., 2002). As shown by Roberts et al. enhanced spine turnover lead to greater capacity for

subsequent learning, expressed as spine stabilization, accumulation, and enlargement (Roberts et al., 2010). Following environmental enrichment, synapse turnover and density was increased and this effect has been linked to improved learning (Bednarek and Caroni, 2011). A more causal link between structural plasticity and memory was reported recently, as specific shrinkage of spines that have been potentiated during motor learning impaired memory function (Hayashi-Takagi et al., 2015). While structural plasticity of synapses most likely contributes to memory formation and consolidation, exact mechanisms remain unclear. It will be important to unravel, how synapse turnover processes relate to network functions, as studies have already indicated that synapse formation does not occur randomly, but in a location-specific manner (De Paola et al., 2006; Hofer et al., 2009; Holtmaat and Caroni, 2016; Lai et al., 2012). Recent ’engram’ studies provide other progress in this field, showing that learning can trigger synaptic potentiation and increase synapse density in engram cells (Choi et al., 2018; Kim and Cho, 2017; Roy et al., 2017) that correlates with memory strength (Choi et al., 2018). Abdou et al. emphasise the role of synapses by demonstrating that the identity of individual memories is represented by synapse-specific plasticity (Abdou et al., 2018).

In conclusion, there is overwhelming evidence that changes in synaptic efficacy, manifested as activity alterations, morphological changes and dynamics of the synaptic molecular equipment, play important roles in learning and memory. However, as exciting as the generation of ‚artificial memories’ (Vetere et al., 2019) may seem, we are still far from understanding how exactly learning and memory work and how synaptic plasticity relates to these cognitive functions (Rao-Ruiz et al., 2021). This is mostly due to the difficulty of study design, as in

most cases only a correlation of synaptic plasticity and certain forms of behaviour can be established but no causation. This is further complicated by the broad complexity of synaptic plasticity and memory mechanisms, acting on multiple scales and to different degrees in several brain regions, from molecular modifications at individual synapses to network dynamics, from plasticity forms expressed at individual terminals to large-scale homeostatic plasticity mechanisms. Moreover, most studies, investigating learning and memory *in vivo*, utilize a fear conditioning task, a valuable model system to investigate the neurobiological mechanisms parallel to behaviour and an easy learning paradigm for rodents (Kim and Jung, 2006). However, for a more comprehensive understanding of learning and memory it will be important to turn towards other, more complex forms of memory demanding the development of new experimental designs and techniques (Humeau and Choquet, 2019). Moreover, experimental outcomes in living organisms are generally very difficult to interpret, as interventions of synaptic plasticity via genetic mutations or inhibitors exhibit effects within the CNS that go beyond changes specifically assigned to synaptic plasticity. The precise structural substrate of memory remains elusive and the precise role of synaptic plasticity in learning and memory will be subject to many more years of research, especially since experimental evidence indicates that synaptic plasticity in behaviour might significantly differ from the well-established Hebbian plasticity models (Bittner et al., 2017).

2.2. Synaptic plasticity and Hormones

2.2.1. Sex hormones in neuroscience

Recent studies investigating the regulation of neurones and synapses in a memory context use experimental techniques that combine *in vivo* brain imaging with behavioural tasks. Studying synaptic plasticity mechanisms *in vitro* differs significantly from *in vivo* approaches, as brain structures in an intact organism are subject to endogenous, physiological processes such as hormone signalling. The interaction between the CNS and endocrine system, in other words how the brain regulates hormonal activity and vice versa, has led to a vast body of research compiled under the term neuroendocrinology. Several classes of hormones have been identified and assigned distinct roles within the CNS, including to regulate synaptic plasticity processes. Amongst them are stress hormones, hormones that underlie the circadian cycle, hormones that regulate the fluid and electrolyte balance, and hormones of the reproductive system (Al-Mana et al., 2008). Naturally, hormones carry out essential functions in synaptic transmission, as catecholamines such as dopamine and noradrenaline are neurotransmitters and their roles in synaptic plasticity and learning and memory have been thoroughly studied (Huang and Kandel, 1995; Kempadoo et al., 2016; Lisman and Grace, 2005; Murchison et al., 2004; Sajikumar and Frey, 2004; Tang and Dani, 2009). High levels of glucocorticoids accumulate in the hippocampus and cortex and increase synaptic plasticity and cognition in physiological conditions, whereas chronically elevated glucocorticoid levels, following stress, impair plasticity processes and decrease spine density (McEwen and Magarinos, 2001; Sorrells et al., 2009). Whole-

organism responses as induced by chronic stress also lead to interactions between functional hormone groups, for example, glucocorticoids and noradrenaline can both regulate synaptic function either alone or in synergy (Krugers et al., 2012). Effects of hormones regulating the circadian cycle such as melatonin have also been described, affecting long-term plasticity processes and performance in cognitive tasks (Frank, 2016).

The neuroscience community has shown particular interest in the relation of CNS and sex hormones, specifically androgens and oestrogen, as prominent sex differences appear in basic sensory experiences such as pain perception (Aloisi and Bonifazi, 2006). The range of sex hormone functions is immense and starts as early as during development to permanently restructure male and female brains (Arnold, 2009; McEwen and Milner, 2017). Generally, male brains are found to be larger than in females, with increased sizes of amygdala, putamen and globus pallidus, whereas female brains have larger hippocampi (Goldstein et al., 2001; Paus, 2010). Additionally, relative differences between brain hemispheres, known as functional cerebral asymmetries (FCAs) in many cognitive domains, differ between men and women indicating that sex hormones play a role in the regulation of the brains' functional connectivity (Hausmann, 2017). Besides such large-scale differences in brain organisation, androgens and oestrogen modify ongoing dynamics of the CNS, partially by modulating neurotransmitter receptors and ion channels (McEwen and Milner, 2017; Rupprecht et al., 2001; Rupprecht and Holsboer, 1999). Testosterone, the most prominent androgen, acts in the CNS via androgen receptors (ARs), which have been located in various brain regions including the amygdala, cerebellum, cortex and hippocampus (Mhaouty-Kodja, 2018). Blockade of ARs

in the hippocampus impaired cognitive performance (Edinger and Frye, 2007), while treatment with testosterone alleviated castration induced spatial memory defects (Moghadami et al., 2016). In AR knockout animals, temporal information processing is downgraded and hippocampal glutamatergic synaptic transmission is decreased due to a reduction in NMDAR activity resulting in decreased LTP (Picot et al., 2016). Besides effects on long-term plasticity, androgens impact structural synaptic plasticity by increasing spine density and in castrated rodents can even restore spine density to wildtype levels (Hatanaka et al., 2009; Ishii et al., 2007; Leranth et al., 2003; Mhaouty-Kodja, 2018). Androgens are converted to oestradiol via aromatization (Lephart, 1996) suggesting that even though some of the above effects are mediated via ARs, effects of androgens in experimental studies might actually be related to oestradiol (Aloisi and Bonifazi, 2006; Kawata, 1995). Compared to androgens, much more is known about oestrogens in the CNS, as elaborated in the following chapters.

2.2.2. Oestrogen as a neuromodulator and its effects on synaptic plasticity

Historically, it has been shown that oestrogens influence behaviours aside from sexual behaviour such as motor control, pain sensitivity, seizure susceptibility, mood and cognitive functions (McEwen and Alves, 1999; Van Hartesveldt and Joyce, 1986). Accordingly, sites of oestrogen actions are widely spread across the brain and can be detected in the brainstem, cerebellum, hypothalamus, prefrontal cortex, and hippocampus (McEwen and Milner, 2017). Importantly, oestrogens have neuroprotective effects against cell apoptosis, excitotoxicity, β-amyloid, oxidative stress and inflammation seizures demonstrating their relevance in pathological conditions such as stroke and neurodegenerative

diseases (Engler-Chiurazzi et al., 2016; Fiocchetti et al., 2012; McEwen and Alves, 1999; Petrovska et al., 2012; Spence and Voskuhl, 2012). Oestrogen receptors (ERs) are universally expressed in the CNS including the hippocampus and prefrontal cortex (Cui et al., 2012; Rossetti et al., 2016), brain regions that are considered relevant for learning and memory (Bird and Burgess, 2008; Euston et al., 2012; Preston and Eichenbaum, 2013; Shen et al., 1994). Studies indicating that oestrogen treatment modifies spatial and declarative memory in animals and humans led to detailed investigations as to how oestrogen affects cellular and subcellular processes, with special focus on synaptic transmission and plasticity in the hippocampus and prefrontal cortex (Becker et al., 1987, 1982; Luine et al., 1998; McEwen and Alves, 1999; Taxier et al., 2020; Zurkovsky et al., 2007). Research from the early 2000s delivered a plot twist, demonstrating that androgens and oestrogens are locally synthesised in adult brains, by neurones and astrocytes (Cui et al., 2013; Hojo et al., 2008, 2004; Ishii et al., 2007; Kawato et al., 2002; Rune and Frotscher, 2005; Fig. 4). Oestrogen is synthesised even in the absence of the ovaries (Kato et al., 2013), strongly supporting the idea that oestrogen can function as a neuromodulator and its effects in the CNS might differ from those of oestrogen produced in the ovaries. Overall, there are three major forms of physiological oestrogens: oestrone (E1), oestradiol (E2, or 17b-estradiol), and oestriol (E3), of which E2 is the most prominent form and represents the brain-synthesised oestrogen. Therefore, I will refer to oestrogen as E2 for the remainder of this thesis (Cui et al., 2012). Although various effects of E2 on synaptic plasticity have been demonstrated, little is known about those of brain-synthesised E2 and its relation to circulating E2 levels produced by the ovaries.

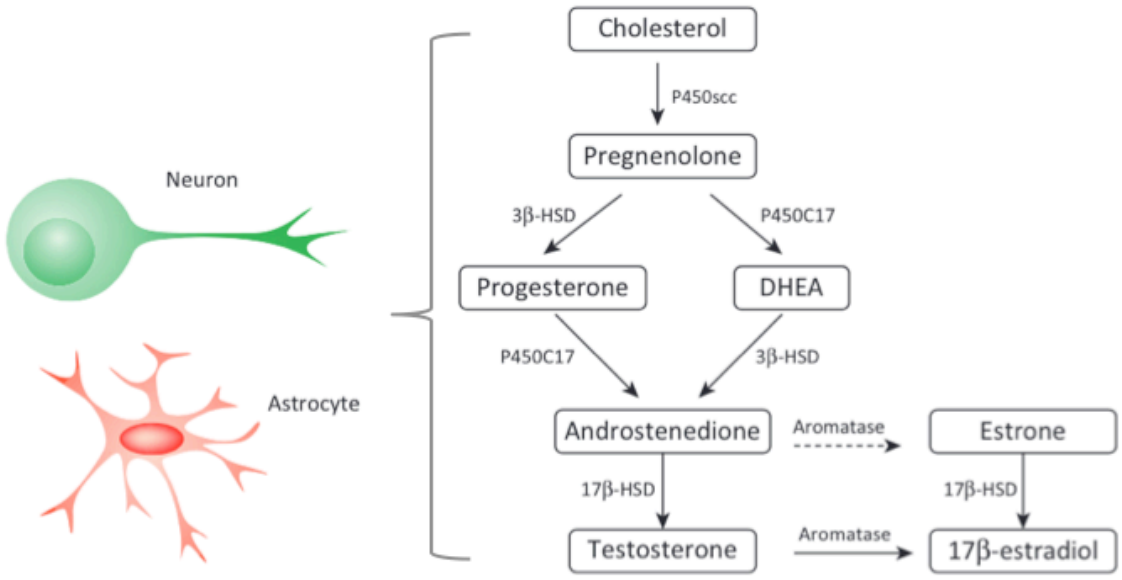

Fig. 4: Oestrogen synthesis in the brain. *Adapted from Cui et al., 2013.*

Brain E2 levels decrease in the brains of postmenopausal women and E2 levels in the hippocampus are substantially higher during proestrus, suggesting that brain E2 levels mirror those of circulating E2 (Kato et al., 2013; Rosario et al., 2011). However, it has also been shown that brain E2 levels can significantly differ from circulating ones as they are subject to brain-specific metabolic processes directed by neurosteroidogenesis, sex hormone-binding globulins, and steroid-converting enzymes in the brain (Cui et al., 2012; Rosario et al., 2011). Moreover, the fact that E2 is produced in male and female brains alike (Hojo et al., 2004) implies potential separate roles for E2 produced locally in neurones.

Circulating as well as brain-derived oestrogen modulate both functional and structural plasticity (Brinton, 2009; Ishii et al., 2007; MacLusky et al., 2006; Woolley, 1998). Both LTP and LTD are sensitive to endogenous and externally

induced fluctuations of oestrogen levels (Córdoba Montoya and Carrer, 1997; Good et al., 1999; Hojo et al., 2008; Ishii et al., 2007; Mukai et al., 2007; Warren et al., 1995; Woolley, 1998). Generally, elevated levels of E2 enhance the magnitude of LTP (Córdoba Montoya and Carrer, 1997; Warren et al., 1995; Woolley, 1998) and synthesis of androgens and E2 plays a role in determining the direction of synaptic long-term effects (Di Mauro et al., 2015). The effects of oestrogen on long-term plasticity are thought to be mediated by increased NMDAR and AMPAR transmission (Foy et al., 1999; Woolley, 2007) facilitating the magnitude of LTP (Smith and McMahon, 2006).

A series of studies have pointed out that spine density within the hippocampus fluctuates dependent on the stage of the oestrus cycle (Woolley, 1998; Woolley et al., 1990). Spine density is elevated during the proestrus phase, when E2 levels are highest, compared to oestrus and dioestrus (Sheppard et al., 2019), in other words, spine density positively correlates with E2 levels. Furthermore, these studies reported that ovariectomy caused a decrease in spine density at CA1 hippocampal pyramidal cells, which can be prevented and rescued with supplying E2 (Gould et al., 1990; Woolley and McEwen, 1993). Thus, it was proposed that oestrogen could induce spinogenesis, which was extensively tested both *in vitro* and *in vivo* (see Sheppard et al., 2019). Exogenous application of E2, either delivered subcutaneously or via direct injection into hippocampi, increases spine density in the hippocampus, and these effects can be observed on different timescales (Jacome et al., 2016; MacLusky et al., 2005; Phan et al., 2015, 2012, 2011; Sheppard et al., 2019). For these studies, E2 was injected at doses in the range of 45 µg/kg, resulting in circulating E2 levels higher than during any stage of the oestrus cycle, thus raising E2

concentrations to a non-physiological level (MacLusky et al., 2005). Notably, lower doses of E2 (1.5, 2, or 3 µg/kg) were sufficient to produce an increase in spine density (MacLusky et al., 2005; Sheppard et al., 2019). Little is known about the effects of oestrogen on presynaptic plasticity, although one study proposed that oestrogen can trigger the formation of new synaptic connections, as oestrogen promotes contacts from individual presynaptic boutons to multiple postsynaptic CA1 pyramidal cells (Yankova et al., 2001). The above results were primarily obtained from female rodents, which raises the question to what extend oestrogens influence synapse dynamics in male brains. Experimental evidence reveals that testosterone, although aromatized to E2 in brain tissue, affects spine density independent from oestrogens (Leranth et al., 2003; MacLusky et al., 2004). Notably, E2 treatment caused an increase in spine density in female animals and also in hippocampal slices obtained from male animals (Jacome et al., 2016; Mukai et al., 2007; Murakami et al., 2006; Tsurugizawa et al., 2005). The effects of E2 on structural plasticity are not restricted to the hippocampus (Brinton, 2009) but have been intensively studied in the prefrontal cortex (Shanmugan and Epperson, 2014). Similar to the hippocampus, decreases in PFC dendritic spine density caused by ovariectomy could be reversed by E2 administration (Chen et al., 2009; Hao et al., 2007; Rapp et al., 2003; Shansky et al., 2010; Tang et al., 2004). E2 treatment increased spine number in the PFC of male rodents (Hajszan et al., 2007). Apart from the effects of E2 on PFC synapses, it has been shown that E2 improves performance in behavioural tasks that are known to be PFC dependent (Keenan et al., 2001; Krug et al., 2006; Rapp et al., 2003).

What are the molecular pathways that underlie oestrogen mediated effects on neurones? Oestrogen receptors (ERs) can be divided into two subclasses: intracellular nuclear receptors ERα and ERβ, and membrane receptors represented by G protein-coupled oestrogen receptors (GPERs; Cui et al., 2013). Oestrogens can directly enter the cell since they are small, carbon-rich molecules built from cholesterol to target intracellular receptors and modify gene transcription. Alternatively, E2 can trigger signalling cascades via binding to membrane receptors (McEwen and Milner, 2017). Not only the application of E2 increases spine density, but similar effects have been described for ERα and GPER agonists (Gabor et al., 2015; Mukai et al., 2007; Phan et al., 2015, 2011). To what extent each receptor contributes to the regulation of synaptic plasticity is unclear, but distribution patterns differ and there seem to be brain region specific preferences in receptor function and expression (Österlund et al., 2000; Sheppard et al., 2019). While ERα and GPERs facilitate E2 effects in the hippocampus, ERβ signalling might dominate in other brain regions (Lymer et al., 2018). A variety of downstream signalling cascades triggered by E2 impact two critical factors that are known to drive changes in synapse morphology: the actin cytoskeleton and protein synthesis (see 2.1.3.). Accordingly, the effects of oestrogen have been categorized in 'genomic' and 'nongenomic' mechanisms, acting on different time scales to mediate long-term and rapid effects of E2 (McEwen and Alves, 1999; Taxier et al., 2020). E2 influences actin remodelling by stimulating RhoA kinase (RhoA/ROCK) and Rac/p21-activated kinase (PAK) which subsequently trigger the inactivation of the depolymerization factor cofilin by LIM domain kinase 1 (LIMK1)-mediated

phosphorylation enabling actin elongation and synapse growth (Briz and Baudry, 2014; Kramár et al., 2009; Yuen et al., 2011).

Genomic actions of E2 result from ER dimerization and subsequent binding of oestrogen response elements on target genes to regulate gene transcription and protein synthesis (Cui et al., 2012). The effects of E2 on protein synthesis are driven by signal molecules such as protein kinase B (Akt) and activated extracellular signal-regulated kinase (ERK), that induce the translation of proteins relevant for plasticity (Akama and McEwen, 2003; Briz and Baudry, 2014; Sarkar et al., 2010). Notably, the effects of E2 on translation might not be somatic but rather modulated locally in dendrites (Sarkar et al., 2010), suggesting a specific role for E2 in modulating synapses. In addition, E2 stimulates mTOR (mammalian target of rapamycin) activity via the activation of tropomyosin receptor kinase B (TrkB) ultimately inducing protein synthesis similar to BDNF (Briz and Baudry, 2014; Panja and Bramham, 2014). E2 and BDNF not only act via the same signalling molecules, a large range of similar actions on excitatory transmission and synapse morphology has been described, which suggests that BDNF might be a downstream target of E2 signalling (reviewed in Scharfman and MacLusky, 2005). However, recent experimental evidence emphasised the potential for E2 to independently regulate TrkB signalling and to promote memory consolidation (Gross et al., 2021).

2.2.3. Oestrogen in cognition and fear

Cognitive improvements in rodents (Dohanich, 2003, 2002) and humans (Sherwin, 2007) have been reported in relation to oestrogen administration

especially during states where endogenous oestrogen levels are low, such as post ovariectomy or post menopause (Koebele et al., 2021). Both female and male rodents show increased performance in conditioning and spatial memory tasks following oestrogen treatment (Daniel, 2006; Daniel et al., 1997; Koebele et al., 2021; Luine et al., 1998). In rodent models, the positive effects of E2 on learning and memory functions are largely consistent, whereas variability can be detected in human studies (Brinton, 2009). Rodent studies suggest that oestrogen therapy could promote neurological health and reduce the risk of neurodegenerative diseases. However, disparities in the beneficial effects of oestrogen in clinical trials exist, probably due to differences in the basic physiology of humans and rodents, different routes of E2 administration and preconditions such as age and health status (Brinton, 2005). How exactly oestrogen facilitates learning and memory, and if the latter relies on additive or synergistic interactions with downstream targets such as BDNF (Luine and Frankfurt, 2013), remains unknown. As argued in detail in Chapter 2.1.5., structural plasticity is generally considered to play a role in cognitive functions, learning, and memory. Given the effects of E2 on structural plasticity, one might speculate that effects of oestrogens on behaviour are partially mediated by the regulation of structural plasticity. Indeed, correlation studies reveal an association of E2 induced spinogenesis and memory performance in rodents (Sandstrom and Williams, 2001) and monkeys (Rapp et al., 2003). Moreover, decreased spine density in the PFC as a result of ovariectomy was followed by impaired object recognition and memory tasks (Wallace et al., 2006). Notably, the effects of E2 on spine changes match the timeline of cognitive improvements, and similar doses of E2 and ER agonists to the ones that

enhance spine density also facilitated learning and memory (Sheppard et al., 2019). Whether oestrogen induced structural plasticity of synapses is the underlying cause of oestrogen mediated differences in learning and memory remains to be elucidated – a challenging task as the precise contribution of synaptic plasticity to cognition is still unknown (see Chapter 2). Nevertheless, the fact that oestrogen affects several different types of behaviour and cognitive functions is undeniable.

To study the effects of oestrogen on different forms of learning and memory, various behavioural paradigms are included in experimental studies (Taxier et al., 2020). E2 administration in ovariectomized animals improved performance in the morris water maze (Sandstrom and Williams, 2001). Similarly, systemic administration of E2 immediately after training can improve spatial memory in object placement and object recognition tasks (Gresack and Frick, 2006; Inagaki et al., 2010; Luine et al., 2003). Neuroendocrine mechanisms can affect social discrimination, thus effects of E2 on social cognition have been proposed (Taxier et al., 2020). Indeed, the ability for long-term social recognition seems to change in line with the oestrus cycle (Sánchez-Andrade and Kendrick, 2011) and external administration of E2 positively regulates social memory (Spiteri and Ågmo, 2009; Tang et al., 2005). Male ERβ knockout animals showed altered social and mood-related behaviours, suggesting a role for E2 signalling in these types of behaviours (Dombret et al., 2020). The underlying molecular mechanisms that drive the effects of E2 on such broad range of cognitive functions are complex and might differ between female and male animals, but likely involve a combination of both short (membrane receptor signalling) and

long-term (genomic) actions of oestrogen, mediated by differential activation of the different types of ERs (Taxier et al., 2020).

Oestrogen signalling was allocated a special role in modulating the acquisition, consolidation, and extinction of fear memory (Pearson and Lewis, 2005; Taxier et al., 2020). While some studies showed enhanced fear conditioning in ovariectomized animals (Jasnow et al., 2006; Morgan and Pfaff, 2001), other studies emphasised that higher levels of E2 impair fear memory (Barha et al., 2010; Gupta et al., 2001; Markus and Zecevic, 1997) and facilitate extinction learning (Chang et al., 2009; Milad et al., 2009). Similarly, ER blockade and reducing E2 levels via contraceptives impairs extinction recall (Graham and Milad, 2013; Milad et al., 2009). Moreover, E2 might reduce fear responses via promoting infralimbic cortex-driven activation of a neural circuit inhibiting fear behaviour related processes in the amygdala (Taxier et al., 2020). Accordingly, neuroimaging studies have indicated that amygdala activity is enhanced during low oestrogen states and vice versa, proposing interactive effects between oestrogen and amygdala activity (Goldstein et al., 2010). Physiological states of low E2, such as during low oestradiol phases of the oestrus cycle or as a result of ovariectomy, facilitates encoding of threat memories (Frye and Walf, 2004; Hiroi and Neumaier, 2006). This leads to the intriguing thought, that oestrogen exhibits protective effects against the encoding of traumatic memories (Maddox et al., 2019). Findings from studies with human subjects support this idea, since low levels of oestrogen promote the long-term encoding of fear and trauma memories and impair fear extinction (Glover et al., 2013, 2012; Graham and Milad, 2013). Another study proposed that women with lower levels of E2 display stronger intrusive memories (conditioned emotional reactions to trauma

triggers), following a conditioned paradigm where they have been shown short violent film clips (Wegerer et al., 2014).

2.2.4. Oestrogen signalling as a therapeutic target

The finding that higher levels of E2 might reduce the encoding of threat and fear memory encourages to consider the potential utility of oestrogen signalling - related pharmacological targets as potential therapeutics in diseases triggered by trauma. Especially in the context of posttraumatic stress disorder (PTSD) where fear extinction is impaired, oestrogen-based therapies might be promising (Glover et al., 2015, 2012; Lebron-Milad and Milad, 2012). Based on this, a study has been conducted investigating the effects of E2 given orally within 48 hours following experiences of sexual assault (Ferree et al., 2012). Reduced rates of PTSD symptoms were detected in individuals that have undergone oestrogen therapy, as assessed in a 6-month follow-up (Ferree et al., 2012).

Other indications for oestrogen therapies might include psychiatric disorders (Hwang et al., 2021). It has been demonstrated that oestradiol administration can alleviate symptoms of depression in women (de Novaes Soares et al., 2001; Grigoriadis and Kennedy, 2002; Schmidt et al., 2000). Considering the interactive relationship between E2 and BDNF signalling, patients suffering from Alzheimer's and depression might benefit from E2 administration, as the downregulated levels of BDNF could potentially be reversed via oestrogen-dependent stimulation (Scharfman and MacLusky, 2006, 2005). Evidence that elevated levels of oestrogen can improve cognitive abilities in humans (Krug et al., 2006) suggests oestrogen signalling as a potential general therapeutic

target in diseases where memory functions are impaired as in the case of Alzheimer's, vascular dementia, and Parkinson's (Honjo et al., 1998; Uddin et al., 2020). Critically, proving the clinical relevance of oestrogen treatments requires more detailed studies including the characterisation of effects arising from other hormones and their complex interplay with oestrogen (Garcia et al., 2018). Moreover, side effects of prolonged oestrogen therapy must be considered, as long-term oestrogen administration might enhance the risk for ovarian and breast cancer (Beral et al., 2015; Greiser et al., 2005).

2.3. Imaging synaptic plasticity

2.3.1. Electrophysiological versus optical approaches

Traditionally, synaptic transmission and plasticity have been studied using electrophysiological techniques. Originally developed by Sakmann and Neher in the late 1970s and early 1980s, the patch clamp technique has been extensively used to record and manipulate ionic currents flowing through single ion channels or across the whole plasma membrane of a cell (Neher and Sakmann, 1976; Sakmann and Neher, 1984). In neuroscience, the patch clamp technique has been used for decades and besides the conventional whole-cell patching of neuronal somas, even direct recordings from dendrites (Davie et al., 2006) and boutons (Vandael et al., 2021) have been achieved. Thus, using electrophysiology one can directly measure a neurone's synaptic input and output and even simultaneously record from connected pairs of presynaptic and postsynaptic neurones. However, patching synaptic terminals is far from being a standard laboratory technique, as it is extremely challenging to visualise and manually target small synaptic structures with a patch pipette.

Compared to electrophysiology, using light to study synaptic signalling does not require actual physical contact with the cell or structure under investigation (Scanziani and Häusser, 2009). Thus, using imaging approaches is a much more convenient solution to investigate small synaptic terminals, specifically dendritic spines and boutons. Importantly, while with electrophysiology only signals from single structures, or in the case of field recordings an unidentified mixture of population signals, can be recorded, a large number of synaptic terminals can be observed independently and in parallel using imaging approaches. Moreover, structural changes of synaptic structures, for example structural LTP (Caroni et al., 2012; Lamprecht and LeDoux, 2004) can only directly be tracked using imaging techniques.

Overall, choosing the optimal technique to study synaptic dynamics will always depend on the type of neuroscientific question and in a vast number of experiments, imaging and electrophysiology are closely linked and used concomitantly. For the goal to understand the subcellular substrates of learning and memory it is inevitable to use imaging tools to investigate synaptic transmission and plasticity, regarding the importance of synapses as described in previous Chapters. Thus, observing the dynamics of populations of synapses and specific manipulations thereof are necessary – tasks that, right now, can only be achieved using light.

2.3.2. Fluorescent tools and transgenic mouse lines

In order to use imaging approaches to investigate neuronal processes and dynamics, a reporter is required that converts biological signals into optical signals. Fluorescent probes have been used in a wide array of neuroimaging

applications and have led to major discoveries and new methods changing our approach to study the nervous system (Scanziani and Häusser, 2009; Yuste, 2005). For example, fluorescent Ca^{2+} indicators can be used to overcome the difficulty of measuring transmitter release in intact tissue (Emptage et al., 1999, 2003; Padamsey et al., 2019). Since the initial development of fluorescent Ca^{2+} dyes (Grynkiewicz et al., 1985; Tsien, 1989), numerous studies have improved and used fluorescent Ca^{2+} indicators to measure subcellular Ca^{2+} dynamics (Bootman et al., 2013; Lock et al., 2015). However, the kinetics of Ca^{2+} dyes are slow and in order to measure subthreshold membrane depolarisations at synaptic terminals, voltage dyes have emerged as prime candidates, allowing the capture of even small voltage changes (Liu et al., 2021; Rowan et al., 2016, 2014; Wu et al., 1998).

Functional imaging, *in vitro* as well as *in vivo*, using Ca^{2+} and voltage indicators gives important information about states of activity and transmission at central synapses. Synaptic structures are plastic and change morphologically based on the level of activity, shaped via inputs from the neuronal network (see Chapter 2.1.3.). Studying structural changes including changes in synapse size during behaviour is necessary to gain insights about the relationship between spine dynamics and higher cognitive functions such as learning and memory (Lamprecht and LeDoux, 2004; Martin and Morris, 2002; Takeuchi et al., 2014). For this purpose, structural dyes are required that reliably label processes of interest. Several methods to label neurones and synapses are available for *in vitro* as well as *in vivo* applications. In a common *in vitro* approach, namely brain slices, Alexa dyes can be injected into the soma to visualise neurones and synapses (Padamsey et al., 2017a) or fluorescent probes can be genetically

expressed induced by viral transfection, bearing the advantage of specific cellular subtype labelling. *In vivo*, viral injections are commonly used to target cell populations in specific brain regions using stereotactic coordinates. Alternatively, fluorescent probes can be expressed in transgenic mouselines, offering the advantage of avoiding invasive surgical procedures for injections.

Transgenic animals expressing fluorescent proteins were developed in the 1990s including the first transgenic mice expressing green fluorescent protein (GFP; Ikawa et al., 1995; Okabe et al., 1997). Traditionally, these transgenic mice are generated by injecting fertilized eggs with DNA fragments containing the GFP coding sequence (Ebihara et al., 2003; Ikawa et al., 1995; Okabe et al., 1997). While a large variety of mouse colonies expressing fluorescent proteins from all colour spectra is available today, transgenic animals expressing GFP and its derivatives remain the most commonly used for structural synaptic imaging labelling axons, dendrites, and synaptic terminals over long distances (Attardo et al., 2015; Barretto et al., 2011; Ebihara et al., 2003; Feng et al., 2000; Nägerl et al., 2004; Pfeiffer et al., 2018). This is mainly due to their unique physical properties (Prasher, 1995). GFP is an extremely stable protein with a highly fluorescent chromophore, thus when expressed *in vivo*, the brightness of GFP can generate a large signal-to-background ratio ideal for imaging (Chudakov et al., 2005; Hua et al., 2005; Prasher, 1995; Rasse et al., 2005; Yuste, 2005). Importantly, the expression of GFP in the brains of transgenic animals is not detectably toxic (Feng et al., 2000; Lipták et al., 2019).

One significant advantage of GFP is that it can be mutated and several derivatives with altered spectral properties and thermostability have been

developed (Feng et al., 2000). These variants include red-shifted variants such as enhanced GFP (EGFP), which fluoresces approximately 30- to 40-fold more brightly than GFP, making them ideal candidates for labelling neuronal processes *in vivo*, where signal loss occurs due to scattering of light (Feng et al., 2000; Hadjantonakis and Nagy, 2001; Van Den Brandt et al., 2004). EGFP was originally developed in 1996 by Cormack et al. and EGFP transgenic mice have been widely used since in all fields of neuroscience (Jin et al., 2016; Margrie et al., 2003; Niclou et al., 2008; Okabe et al., 1997; Vasquez-Lopez et al., 2018).

Gene promoters allow for the regulation of the spatial and temporal expression patterns of a fluorescent protein (Haruyama et al., 2009), which is important to specifically label different subsets of neurones amongst the large diversity of cell types in the CNS (Masland, 2003). A variety of promoters has been reported that allow tissue-specific and cell type-specific expression of fluorescent reporters (Haruyama et al., 2009). The Thy1 promoter can be used to label neuronal processes and synaptic terminals of principal neurones (Barnes et al., 2017; Chen et al., 2012) specifically expressing fluorescent proteins in projection neurones (Caroni, 1997; Chen et al., 2012; Feng et al., 2000; Jósvay et al., 2014; Stefaniuk et al., 2016) for observing synapse dynamics. Thy1 (CD90) is a cell surface glycoprotein, expressed not only in neurones but also in T cells and thymocytes and its physiological properties include the promotion of T cell activation and inhibition of neurite outgrowth (Furlong et al., 2018; Haeryfar and Hoskin, 2004; Pont, 1987). Studies have shown, that due to strong transgenic position-effect variegation, transgenic animals that express proteins under the Thy1 promoter differ in levels and

patterns of expression (Chen et al., 2012; Feng et al., 2000). However, it has been reported that Thy1-lines display a heritable pattern of expression resulting in similar and consistent expression levels among offspring (Feng et al., 2000). Thy1-EGFP mice have been used in a wide range of studies observing synapse dynamics *in vivo* (Attardo et al., 2015; Barnes et al., 2017; Chen et al., 2012; Frank et al., 2018; Vasquez-Lopez et al., 2018), including in this work.

Using transgenic animals to genetically express fluorescent proteins offers several advantages compared to animals that have been injected with viruses. First, injecting animals with viruses requires a surgical procedure including a craniotomy and insertion of an injection needle (Lowery and Majewska, 2010). Even though this technique causes little damage to surrounding tissue, as the micropipette is small, some inflammation will occur and because the brain has been exposed there is a risk of infections (Lowery and Majewska, 2010). Second, it is more challenging to titrate the level of expression when fluorescent proteins are expressed following viral injections. Third, the deeper the brain region of interest, the deeper the injecting needle needs to be inserted, causing larger brain lesions that can drive tissue alterations and change the physiology of the network (Gonzalez-Perez et al., 2010). Although recently, micropipettes with lumen of only 50-µm have been developed (Gonzalez-Perez et al., 2010), in transgenic animals deep brain regions can be labelled without any surgical procedures at all.

2.3.3. Imaging synaptic plasticity *in vitro* versus *in vivo*

Accessibility of deeper brain regions such as the hippocampus or the amygdala is one of the major obstacles in brain imaging, especially for investigations on

synaptic plasticity that require high-resolution imaging. This is problematic given that the hippocampus is the most relevant structure regarding learning and memory processes (Bird and Burgess, 2008). Thus, to understand synaptic plasticity processes and how they link to learning and memory, studying synapse dynamics in the hippocampus is essential. For this reason, hippocampal slices have become the gold standard model system, as it is much more convenient to image synaptic plasticity in *in vitro* preparations. Acute or organotypic hippocampal slices are widely used to image synaptic plasticity, because neurones of interest are located superficially providing ideal conditions for light- and confocal microscopy. Moreover, due to the flat and thin structure of slices, electrophysiological techniques such as patch-clamp can be coupled to imaging at hippocampal synapses, which is not possible in *in vivo* situations. An obvious difference between studying slices or the respective brain structure *in vivo* is that it was removed from the overall brain network. Even though in hippocampal slices the cytoarchitecture and DG-CA3-CA1 synaptic circuits are preserved (Lein et al., 2011), neuronal projections to other brain regions are cut off. Thus, the effects of contextual information from the remaining brain are missing in experimental settings.

In vitro preparations have helped us to significantly advance our understanding of synaptic plasticity in deeper brain structures such as the hippocampus. However, considering the goal to understand how synaptic dynamics correlate with learning and memory, these structures must ultimately be imaged *in vivo.* It is necessary to observe synaptic dynamics, while animals are performing learning and memory tasks. Moreover, since learning and memory are processes happening over longer time spans, it is important to study synaptic

structures over weeks or months. Chronic synapse imaging of deep brain regions in behaving animals is a challenging task but will bring significant advances in the field.

2.3.4. Deep-brain imaging: challenges and advances in microscopy

Why is high-resolution brain imaging in subcortical structures difficult? With increasing imaging depths, image quality degrades due to optical aberrations caused by tissue heterogeneities and refractive index mismatches (Beuthan et al., 1996; Ji et al., 2012). Given that the brain consists of many different cell types and structures, a large heterogeneity of refractive indices exists causing optical scattering (Jacques, 2013; Tuchin, 2015, 1997). Thus, when light propagates through tissue and interfaces, light refraction occurs, reducing the overall imaging performance and resolution (Al-Juboori et al., 2013; Azimipour et al., 2014). Light scattering is another important, limiting factor. When light is scattered, its contribution to signal generation at the focus is lost which causes the excitation to decrease exponentially with imaging depth (Helmchen and Denk, 2005). This in turn limits the amount of fluorescent signal that can be generated by the fluorophore. Moreover, light scattering also generates out-of-focus fluorescence, which increases background signal thereby decreasing the signal-to-background ratio while imaging. For biological fluorescence imaging and depending on the modality chosen, these factors are important to consider for both light that is sent into the tissue to excite fluorophores and for the collection of light that is emitted.

All of the above constitute the fundamental obstacles of deep-brain imaging. While for slice imaging only superficial penetration depths in the µm range are

required, imaging the hippocampus *in vivo* requires depths beyond 1 mm. In a mouse brain, the CA1 region of the hippocampus is located around 1.5 mm deep, the CA3 region even deeper (Cetin et al., 2007). Several solutions have been proposed and implemented to allow greater imaging depths. Traditional confocal microscopy systems use linear (one-photon) absorption processes. However, using nonlinear optical microscopy techniques such as two-photon (2P) or three-photon (3P) microscopy offer multiple advantages over linear approaches making them less sensitive to scattering (Helmchen and Denk, 2005; Wang and Xu, 2020). With the idea originally developed in 1931 (Göppert-Mayer, 2009), 2P laser scanning microscopy has been widely used in neuroscience since the 1990s (Denk et al., 1990). The most important feature of multiphoton excitation laser scanning microscopy is optical sectioning as a result of the nonlinear dependence of the absorption rate on the photon concentration (Denk and Svoboda, 1997). In multiphoton microscopy, two or three infrared photons are simultaneously absorbed by a single fluorophore. In 2P microscopy, special near-infrared (IR) femtosecond laser sources, such as Ti:sapphire lasers are used to generate pulses delivering excitation photons in short intervals. Given the fact that photon concentration, and therefore the probability of two or three photons to collide, is only high enough in the focal volume, excitation is limited to this position. Thus, no out-of-focus fluorescence is generated and all photons that are emitted should be collected as they contribute useful signal (Denk and Svoboda, 1997; Williams et al., 2001; Zipfel et al., 2003). Importantly, photodamage and photobleaching are also restricted to the focal volume, rendering multiphoton microscopy less harmful to tissue (Stelzer et al., 1994; Williams et al., 2001; Zipfel et al., 2003). The use of longer

excitation wavelengths, between 800 and 1000 nm in 2P microscopy enables imaging deeper in tissue (Helmchen and Denk, 2005; Theer and Denk, 2006). This is mainly due to the fact that the average power on the sample surface dictates the maximum imaging depth in a logarithmic manner (Kobat et al., 2009) and that scattering is significantly reduced (Xu et al., 1996). Another reason for greater imaging depth is that with longer wavelengths, the attenuation of excitation light caused by absorption by structures within the tissue, as for example blood vessels, is reduced (Kobat et al., 2009; Williams et al., 2001; Yaroslavsky et al., 2002). This is of particular relevance for deep brain imaging, as the brain is highly vascularised. 2P fluorescence microscopy has been reported in various studies imaging synapses in the cortex (Grillo et al., 2013; Ishii et al., 2018; Körber and Stein, 2016; Sammons et al., 2018; Svoboda et al., 1997) revealing new insights into spine dynamics (Frank et al., 2018) and the relationship between spines and memory (Hayashi-Takagi et al., 2015). For such studies, cranial windows are the standard technique to directly observe neurones and synapses in specific cortical regions (Holtmaat et al., 2009; Yang et al., 2010). These cranial windows are created by replacing small pieces of skull by a cover glass, giving access to the tissue below. However, 2P microscopy can also be used with endoscopic tools, allowing superficial single spine imaging in freely behaving animals (Zong et al., 2017). Besides experiments focussed on cortical regions, imaging synapses in the hippocampus with 2P microscopy has also been achieved (Attardo et al., 2015; Gu et al., 2014; Mizrahi et al., 2004; Pfeiffer et al., 2018), although it generally necessitates cortical aspiration, i.e. the removal of cortical tissue to gain access to the hippocampus (Dombeck et al., 2010).

Advances in microscopy: 3P imaging and adaptive optics

3P microscopy (Hell et al., 1996) with wavelengths of more than 1300 nm has recently shifted into focus for deep tissue imaging. Even though it was originally believed that side effects such as tissue heating and the need of higher excitation pulse energy make 3P excitation unsuitable for microscopy systems, studies since 2010 have created new interest in 3PM (Denk and Svoboda, 1997; Wang and Xu, 2020). Using even longer wavelengths than for 2P excitation will help to increase maximum imaging depth as it helps to reduce scattering (Balu et al., 2009; Kobat et al., 2009; Xu et al., 1996). Moreover, out–of-focus fluorescence is even more reduced, significantly improving the signal-to-background ratio compared to 2P excitation (Horton et al., 2013; Xu et al., 1996). Importantly, 3P excitation is optimal for a range of fluorescent indicators to be excited at the 1700 nm spectral window that matches a one-photon excitation of 560 nm (Horton et al., 2013; Wang and Xu, 2020). 3P microscopy has been reported for *in vivo* deep brain imaging at cellular resolution in intact mouse brains down to 1.3 mm (Horton et al., 2013; Klioutchnikov et al., 2020; Ouzounov et al., 2017). Recently, advances have been made in using 3P microscopy for high-resolution deep-brain imaging. Streich et al. have demonstrated imaging of deep cortical spines down to 1.4 mm, the edge of the mouse hippocampus (Streich et al., 2021). This was achieved, by implementing adaptive optics (AO) into the 3P microscopy system. Indeed, adaptive optics coupled to multiphoton excitation or other imaging techniques can dramatically increase resolution and imaging performance (Booth, 2014, 2007; Débarre et al., 2009; Hampson et al., 2021; Ji, 2017; Ji et al., 2012, 2010; Liu et al., 2019; Marsh et al., 2003; Qin et al., 2020; Sinefeld et al., 2015). For example, spines

in deep cortical layers of the mouse brain *in vivo*, originally invisible, could be resolved using AO (Rodríguez et al., 2021). The working principle of AO is straightforward. Light properties such as amplitude, phase, and polarisation can be perturbed when travelling through tissue due to many changes in refractive indices, and tissue structures. Thus, aberrations occur, and the performance of the imaging system is degraded because imaging instruments are designed for specific optical properties and are challenged by complex samples (Booth, 2014; Girkin et al., 2009; Hampson et al., 2021; Ji, 2017). As previously pointed out, in scanning microscopy the excitation light is subject to aberrations until it reaches the focal plane, ultimately decreasing resolution and signal-to-background ratio. Besides sample-induced aberrations, optical systems might be affected by intrinsic system aberrations, further impairing image quality. Adaptive optics, using either electro-optical or computational methods, can be used to compensate for aberrations, by actively manipulating the wavefront, thus affecting the phase of light (Booth, 2014; Girkin et al., 2009; Hampson et al., 2021; Ji, 2017). AO is particularly effective in deep-brain imaging, as focusing light deeper into tissue leads to larger and more complex aberrations (Booth, 2014; Girkin et al., 2009; Hampson et al., 2021; Ji, 2017). Moreover, maximizing resolution is more relevant in brain areas such as the hippocampus, as synapses are more densely packed which introduces the risk of adjacent spines to be merged together in images (Attardo et al., 2015). Besides adaptive optics, recent advances in increasing resolution have also been made using superresolution microscopy. Hippocampal synapses were imaged *in vivo* over longer time periods using STED microscopy (Pfeiffer et al., 2018). STED substantially improved spatial resolution compared to conventional 2P

microscopy and a two times higher spine density was reported emphasising the possibility that individual spines appear as merged in 2P images (Pfeiffer et al., 2018).

2.3.5. Fibre optic imaging and micro-endoscopy

Even though modern technologies including multiphoton or superresolution fluorescence microscopy and adaptive optics have enabled high resolution imaging of deep cortical layers and beyond, both technologies represent only an extension of the depth ranges accessible for optical microscopy. Until today, *in vivo* high-resolution imaging of deeper brain structures such as the DG of the hippocampus or the amygdala could not be demonstrated – structures that play important roles in many types of behaviours and their synaptic dynamics are thought to underpin learning and memory (Eichenbaum et al., 1992; Girardeau et al., 2017; Jarrard, 1993; Maren and Fanselow, 1995; Richardson et al., 2004; Vazdarjanova and McGaugh, 1999). One promising solution to the accessibility problem was provided, by introducing endoscopic devices, which can be inserted into the brain at any depth.

Such devices are typically based on fibre optic fluorescence imaging. Optical fibres can transmit and collect light; hence they are ideal for fluorescence imaging as they can deliver excitation light as well as collect the emitted signal. Light is guided through the fibre by a process named total internal reflection, resulting from the fact that optical fibres are typically step-index fibres with differing refractive indices in the fibre core and cladding, respectively (Addanki et al., 2018). Early ideas for fibre optic in vivo imaging emerged in the 1980s (Mayevsky and Chance, 1982) and have since been advanced to visualise

physiological processes in many fields. In neuroscience, fibre optic devices provide a number of useful applications for *in vivo* imaging. Since fibres are flexible, they can be used to image in freely moving animals (Helmchen et al., 2001). Furthermore, fibre based devices can be implanted within the brain for longitudinal observations of cellular and subcellular dynamics (Attardo et al., 2015) and they bear the potential to access deep neuronal processes in a minimally invasive manner (Turtaev et al., 2018; Vasquez-Lopez et al., 2018). Different classes of optical fibres have been used in a variety of designs for fluorescence imaging in the brain. In optical fibres, light is guided in the form of spatial modes. Single-mode optical fibres (SMFs) guide only a single mode whereas multimode fibres (MMFs) guide several spatial modes. A third class of optical fibres, known as gradient refractive index (GRIN) fibres are MMFs with a gradually declining refractive index in the fibre core. All three classes of fibres have been implemented for fluorescence endoscopy, serving a variety of purposes. SMFs can deliver light for optical stimulation, however, since they can only guide one mode of light, the ability to collect information is fairly low. Thus, MMFs are generally more suitable for fluorescence imaging since they can guide more modes and have greater numerical apertures (NA) enabling higher resolution and the collection of more signal. Often, MMFs are coupled to SMFs and following implantation into the brain, used for optogenetics to stimulate specific neurones (Adamantidis et al., 2007; Aravanis et al., 2007; Deisseroth, 2011; Delaney et al., 1994; Fenno et al., 2011; Zhang et al., 2010). SMFs and MMFs can also be inserted as fibre bundles and have been used to image cerebellar neurones in anaesthetised and freely behaving mice (Flusberg et al., 2008, 2005; Szabo et al., 2014). However, to reach sufficient resolution *in*

vivo fibre bundles are commonly combined with micro-objectives (Szabo et al., 2014), requiring increased diameters of over 500 µm of these optical probes. This in turn increases invasiveness in *in vivo* applications. Although low-diameter fibre bundles exist (Vincent et al., 2006), lateral and axial resolutions strongly depend on the number of fibres included in the bundle.

Using fibre based endoscopes to study synapses in deep brain structures *in vivo* coheres with several important factors. First, the resolution of the set-up must be high enough to resolve synaptic structures. Second, the optical probe should be suitable for imaging at any given depth in the brain. And third, synaptic dynamics of deep brain structures should be studied in the most physiological way, meaning as minimally invasive as possible which directly relates to the size of the optical probe. Compared to the complex and limited design of fibre bundles, micro-endoscopes can be designed involving one single MMF within optical probes with total diameters between 0.12 - 1 mm (Flusberg et al., 2005; Jung et al., 2004; Jung and Schnitzer, 2003; Levene et al., 2003; Turtaev et al., 2018; Vasquez-Lopez et al., 2018). Over the last two decades, GRIN fibres have been reported as central components of micro-endoscopes, as they can be cut to specific lengths and used as lenses for fluorescence imaging. Experimental set-ups including GRIN lenses for deep-brain imaging typically mirror the layout of conventional one- or multiphoton laser-scanning microscopes, with the GRIN lens as the optical head of the system (Jung et al., 2004). One end of the GRIN lens probe is thereby inserted inside the brain (Levene et al., 2004). GRIN - based micro-endoscopes consist of doublet or triplet arrangements of different types of optical lenses, at diameters between 350 – 1000 µm (Jung et al., 2004). For multiphoton

fluorescence endoscopy, GRIN-lens optical probes comprise an objective lens, a relay lens, and a coupling lens that translate an image plane from outside the coupling lens to the focal plane within a sample (Jung and Schnitzer, 2003). Thus, the GRIN lens refocuses excitation light at a certain distance from the distal end inside the specimen and fluorescent light is subsequently collected back through the GRIN lens (Levene et al., 2004). Relay lenses are used to provide sufficient length of the micro-endoscope for insertion into deep tissue (Jung et al., 2004). Using GRIN-lens based optical probes for minimally invasive imaging *in vivo* has been reported at cellular resolution (Jung et al., 2004; Levene et al., 2004, 2003) for imaging in deep brain regions down to the hypothalamus (Betley et al., 2015; Jennings et al., 2015; Resendez et al., 2016). GRIN lenses have also been used combined with fibre bundles as epifluorescence microscopes at cellular resolution in freely moving mice enabling imaging depths down to the hippocampus (Flusberg et al., 2008). Even though GRIN lenses were successfully used to study neuronal activity deep within the brain, imaging synaptic dynamics adds another layer of complexity to the experimental design, as resolutions at the cellular level are not sufficient to resolve fine synaptic terminals. Indeed, GRIN lenses have been used for high-resolution imaging in the hippocampus (Barretto et al., 2011) and to study spine dynamics (Attardo et al., 2015). However, this was only possible with cortical aspiration meaning the removal of significant amounts of tissue. One could argue that the study performed by Attardo et al. does not require the use of GRIN-lens based micro-endoscopes. Importantly, even though similar, or even higher (Pfeiffer et al., 2018), resolutions were achieved for deep-brain synaptic imaging with conventional microscope systems and hippocampal

windows (Gu et al., 2014; Mizrahi et al., 2004), micro-endoscopes including GRIN-lenses or other types of fibres can be used in freely behaving animals. This is a crucial point; because to study correlations between synapses and behaviour, synaptic dynamics must be observed while an animal is performing behavioural tasks.

Regarding the suitability for GRIN lenses as part of micro-endoscopes to study synapses in deep brain structures *in vivo* the axial and lateral resolution is high enough to identify and track synaptic structures over several days (Attardo et al., 2015). GRIN-lens based imaging has also been shown combined with other methodologies such as adaptive optics (Qin et al., 2020) or Bessel-beam design (Meng et al., 2019), further increasing resolution and imaging volume, thus allowing long-term tracking of synapses. As for the imaging depth, GRIN lenses could theoretically be implanted at any given depth in a mouse brain and are commercially available in lengths of up to several tens of centimetres. However, current approaches to image synaptic structures at the depth of the hippocampus require the aspiration of cortical tissue, with or without GRIN-lenses (Barretto et al., 2011; Gu et al., 2014; Mizrahi et al., 2004; Pfeiffer et al., 2018).

Why do effects of tissue damage matter? Following the implantation of a micro-endoscope, side effects such as neuroinflammation, cellular death and haemorrhage will occur post-operative to varying degrees (Travis et al., 2019). These processes might further trigger secondary pathways leading to long-term alterations in tissue. For example, neuroinflammation can induce the onset of a biological process called cellular senescence, characterised by a permanent state of cell cycle arrest affecting the function of tissues (Martínez-Cué and

Rueda, 2020). Neuroinflammation is complex, and it is difficult to evaluate the effects of cytokines and chemokines on neuronal health and synaptic signalling (Kokkas, 2010). Inflammation in the brain following tissue damage can involve extrinsic cells that cross the blood-brain barrier including neutrophils and macrophages, or CNS resident cells with inflammatory capacity such as microglia and astrocytes (Cederberg and Siesjö, 2010).

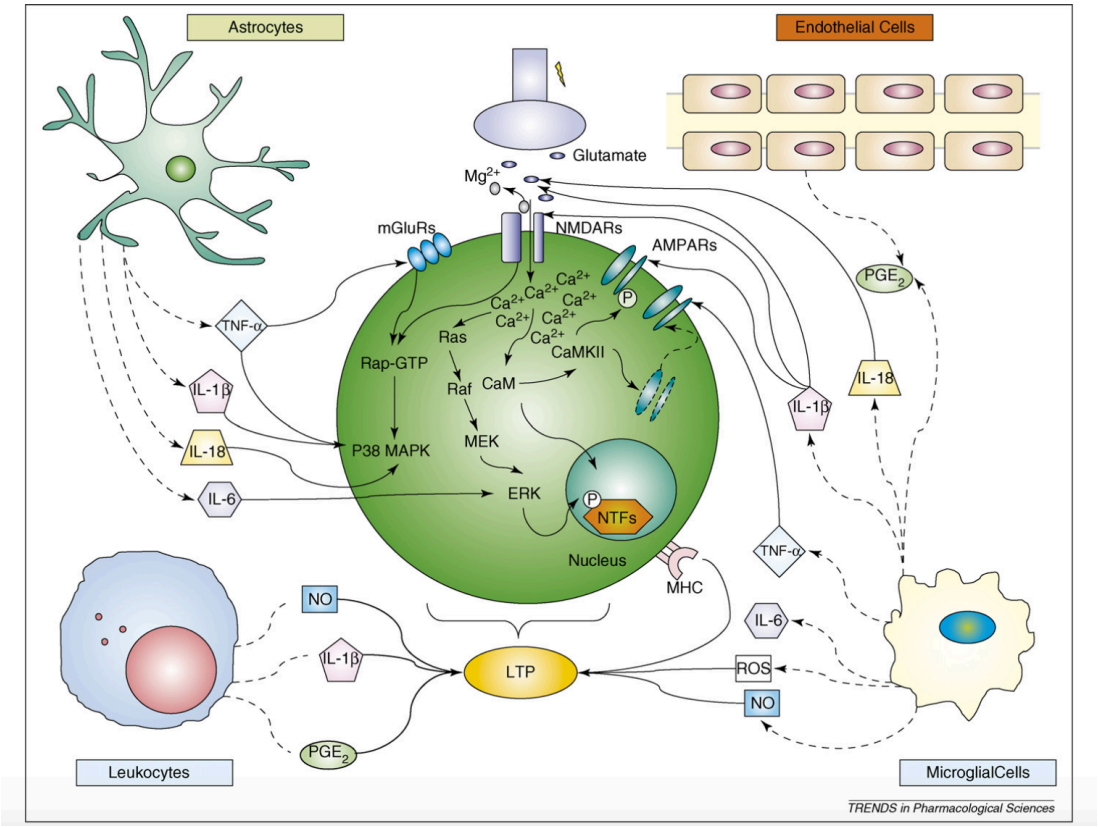

Fig. 5: Multiple effects of immune molecules on synaptic transmission and plasticity. Cytokines and other molecules influence neurotransmitter release, post-receptor signal transduction mechanisms and the ability of the synapse to undergo LTP, during neuroinflammatory processes. LTP induction requires activation of postNMDARs and several signal transduction systems. Glutamate release through AMPA and NMDA receptors is influenced by cytokines (IL1-b, TNF-α, IL-18). During neuroinflammation, reactive oxygen species (ROSs), prostaglandin E2 (PGE2) and nitric oxide (NO) are overexpressed affecting the induction of LTP. *Adapted from Di Filippo et al., 2008.*

These cell types secrete cytokines and express inflammatory mediators including TNF-alpha, interferon-y and IL-6 in response to tissue damage (Cederberg and Siesjö, 2010). The release of such pro-inflammatory cytokines has been shown to affect synaptic plasticity and synaptic scaling in multiple brain areas including the cortex, striatum and hippocampus (Rizzo et al., 2018). Some cytokines, such as interleukin-1β and others are consequently expressed in the healthy brain to maintain synaptic plasticity but start to exert noxious effects on synaptic transmission in pathological situations (Rizzo et al., 2018; Schneider et al., 1998). Such effects include altered neurotransmitter release and receptor signalling at synapses which ultimately affect the synapse' ability to undergo different forms of plasticity (Di Filippo et al., 2008; Fig. 5).

The hippocampus is particularly prone to the effects of pro-inflammatory cytokines on plasticity (Costello et al., 2011; Min et al., 2009) and it has been shown that long-term plasticity is impaired during inflammatory processes (Di Filippo et al., 2013, 2008). Considering the close relationship between plasticity and cognitive functions, the effects of CNS inflammatory processes on synaptic plasticity induced by tissue damage might have significant downstream effects on cognitive functions such as learning and memory (Di Filippo et al., 2008).

Even though it is difficult to study the direct effects of neuroinflammation on synaptic plasticity in relation to changes in cognitive abilities, since we are still struggling to close that gap in physiological conditions, clear evidence for inflammation induced tissue alterations and synaptic dysfunction is provided. Thus, tissue damage induced by using larger micro-endoscopes will have effects on synaptic processes, and over longer time periods as during chronic

imaging will cause downstream events. Therefore, to study synaptic dynamics and plasticity *in vivo*, the most minimally invasive approach should be chosen, since neuroinflammation and other effects of tissue damage will affect exactly the synaptic processes under investigation.

Multimode fibre based imaging

The research on the effects of inflammatory processes on synaptic plasticity has encouraged the development of minimally invasive micro-endoscopes for high-resolution deep-brain imaging *in vivo*. Substantial progress has been made in using single MMFs for fluorescence micro-endoscopy. Compared to GRIN lenses (350-1000 μm) and fibre bundles, single MMFs can be used with core diameters of only 50 μm and total diameters of around 100 μm (Turtaev et al., 2015). Moreover, surgical preparations of GRIN-lens based micro-endoscopes require the removal of tissue or implantation of larger (600-1000 μm) guide cannulas (Barretto et al., 2011; Bocarsly et al., 2015; Levene et al., 2004). The insertion of MMF micro-endoscopes however, necessitates only a small craniotomy and tissue damage is significantly reduced following brain insertion (Turtaev et al., 2018; Vasquez-Lopez et al., 2018). As light propagates through MMFs by total internal reflection, unpredictable phase delays and coupling occur between the modes causing the output intensity profile from a Gaussian input to have a speckle-like appearance. Wavefront control can be used to fully describe the light-field propagation through the MMF allowing the transferral of images across a single MMF (Čižmár and Dholakia, 2011; Di Leonardo and Bianchi, 2011; Papadopoulos et al., 2012). Wavefront shaping devices such as spatial light modulators (SLMs) have been used for a number of applications in neuroscience. For example, using SLMs different patterns of illumination can be

generated, allowing individual and selective photostimulation of neurones based on their specific functional properties (Packer et al., 2015, 2013, 2012). Besides, SLMs can be used to determine and shape the light-field propagation through MMFs (Vasquez-Lopez et al., 2018). To use MMF micro-endoscopes for fluorescence imaging with point scanning, the light propagation through the MMF is characterised in a calibration procedure. In this calibration procedure, a transmission matrix is acquired describing the complex light-field transformation between the fibre input and output (Popoff et al., 2010). Then, the SLM is used to shape the light travelling through the MMF to produce a focus at the fibre output, that can be scanned across the field-of-view (Turtaev et al., 2015). In contrast to SMFs, MMFs can guide a considerable number of spatial modes in a relatively small core diameter. Therefore, MMF-based endoscopes offer imaging resolutions down to the diffraction limit, which is necessary to observe synaptic dynamics (Caravaca-Aguirre and Piestun, 2017; Turtaev et al., 2015). Indeed, MMFs have been recently used for deep-brain *in vivo* imaging of spines (Vasquez-Lopez et al., 2018). Despite their small diameter, MMFs can be used at relatively high NAs, which also improves imaging performance.

Owing to their small size MMFs can be inserted into the brain at any given depth. Moreover, MMF micro-endoscope technologies feature all requirements that are needed to combine their experimental set-up with multiphoton excitation, superresolution microscopy and AO to increase resolution and image quality. Contrary to GRIN-lens applications, MMF micro-endoscopes provide a powerful tool for multisite imaging. Since MMFs are thin, multiple endoscopes could be inserted in different areas of the brain, for instance, studying synaptic dynamics of connected brain structures that are relevant for certain behaviours.

With this methodology, the hippocampus and amygdala could be studied simultaneously, as they have both been shown to be relevant in learning and memory behaviour. Thus, MMFs serve as ideal candidates for minimally invasive high-resolution imaging to study synaptic plasticity and dynamics at any given depths within tissue. In chronic applications, synaptic dynamics could be observed over longer time periods and, ultimately, in freely moving animals, due to the flexibility of MMFs. It is therefore desirable to advance current MMF designs (Turtaev et al., 2018; Vasquez-Lopez et al., 2018) and optimise them for *in vivo* deep-brain imaging.

2.4. The hippocampus as model system

2.4.1. Organisation of the hippocampus

A substantial part of this thesis focuses on plasticity processes (Chapters 4 and 5, parts of Chapter 6) and synaptic transmission at Schaffer collateral - CA1 synapses (Chapters 4 and 5) in the hippocampus. The hippocampus plays an important role in memory, as demonstrated by early studies showing that damage to the hippocampus produces amnesia (Zola-Morgan et al., 1986). Subsequent electrophysiological and imaging experiments demonstrated that hippocampal function is especially relevant for the formation of episodic, declarative, and spatial memories (Bird and Burgess, 2008; Neves et al., 2012). Information storage in the hippocampus is thought to depend on activity-dependent modifications in the efficacy of synaptic transmission, summarized as synaptic plasticity (Malenka, 1994). The hippocampus consists of three major subregions: The dentate gyrus (DG), which receives sensory input from

the entorhinal cortex (EC) via the perforant path, the cornu ammonis regions (CA1, CA2, CA3) and the subiculum (Neves et al., 2012; Fig. 6).

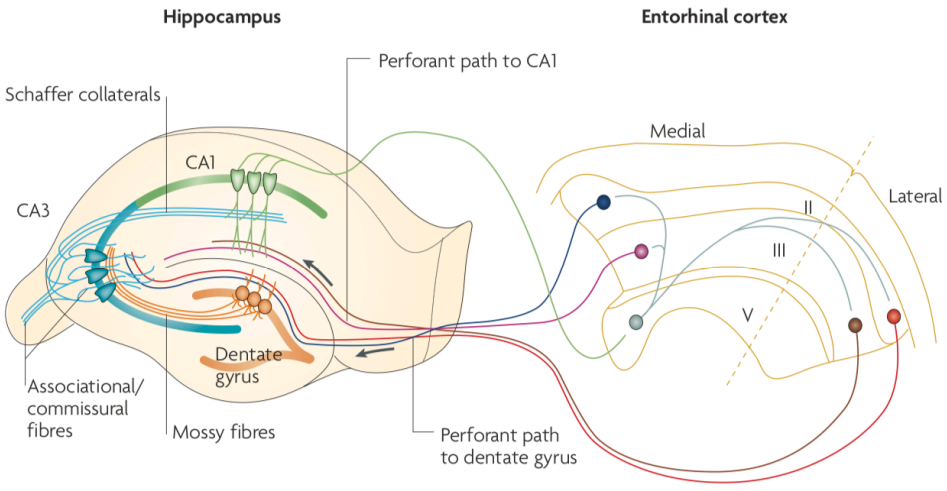

Fig. 6: Hippocampal tri-synaptic pathway. Schematic of a coronal hippocampal section illustrating the simplified information flow within the hippocampus. The entorhinal cortex (EC) projects to the dentate gyrus (DG) via the perforant path. Axons from DG neurones project as mossy fibres to CA3 pyramidal cells. Schaffer collaterals from CA3 neurones connect with the apical dendrites of CA1 pyramidal cells in the stratum radiatum. Additionally, CA1 and CA3 neurones receive direct inputs from the EC. *Adapted from Neves et al., 2012.*

Classically, information flow within the hippocampus is represented as a tri-synaptic feedforward circuit (in short: EC -> DG-> CA3 -> CA1). Fibres of the entorhinal cortex innervate DG neurones (granule cells), which in turn project to the CA3 region via the mossy fibres. CA3 pyramidal neurones form connections with CA1 neurones via the Schaffer collaterals and further project to contralateral CA3 and CA1 pyramidal neurones through comissural connections (Knierim, 2015; Neves et al., 2012). CA1 cells send output back to the EC but also to various other brain regions including the prefrontal cortex and amygdala (Orsini et al., 2011; Thierry et al., 2000; van Strien et al., 2009). The basic

model denoting the hippocampal formation as a tri-synaptic feedforward circuit does not capture the full connectivity of the hippocampus. Several other projections are involved in hippocampal function, including direct projections from the EC to CA3 and CA1 regions (van Strien et al., 2009). Importantly, CA3 axons not only project to CA1 neurones but also to other CA3 neurones, thus forming a recurrent pathway that has been described as an autoassociative network (Le Duigou et al., 2014). Within DG, CA1, and CA3 areas, different layers can be distinguished describing the topology of the projections in more detail. The EC projections innervate the superficial layer of the DG, which is called stratum moleculare while neurones of the DG (granule cells) send out mossy fibres to proximal apical dendrites of CA3 neurones in the stratum lucidum. CA3 neurones in turn project to the superficial layer of CA1 called stratum radiatum via the Schaffer collaterals. Additionally, Schaffer collaterals innervate basal dendrites of CA1 neurones, located in stratum oriens (van Strien et al., 2009). CA2 neurones, receiving inputs from the EC, directly connect with CA1 neurones in stratum oriens and their activity has been reported to affect information flow within the hippocampal formation (Chevaleyre and Siegelbaum, 2010).

In the hippocampus, a wide range of cell types can be found (Zeisel et al., 2015). Most intensively studied are the tightly arranged glutamatergic pyramidal neurones within CA1 and CA3 and it has been suggested that pyramidal neurones themselves display a large heterogeneity (Cembrowski and Spruston, 2019). Other glutamatergic cell types such as mossy cells located in the hilus of the DG have been described (Scharfman, 2016). Besides such glutamatergic neurones, the hippocampus hosts a variety of GABAergic cell types including

amongst others somatostatin- and parvalbumin- expressing interneurones (Pelkey et al., 2017; Zeisel et al., 2015). In addition, various glia cell types, including astrocytes and microglia, regulate the neuronal microenvironment and synaptic transmission within the hippocampus (Hertz et al., 2016; Keyser and Pellmar, 1994).

The Schaffer collateral - CA1 synapses, formed between CA3 and CA1 pyramidal cells, have been subject of many electrophysiological and imaging studies, because the highly ordered and isolated nature of the axonal fibre bundles that project along the stratum radiatum make them particularly accessible for experimental interventions. Schaffer collateral – CA1 synapses comprise of *en passant* boutons, formed as varicosities on Schaffer collaterals. The physiology of these synapses has been intensely investigated in the context of long-term plasticity (Bashir and Collingridge, 1994; Karpova et al., 2006; Lin et al., 2008; Malenka and Nicoll, 1993; O'Riordan et al., 2018; Zhang et al., 2008). Moreover, short-term plasticity mechanisms are commonly studied at the Schaffer collateral - CA1 synapse (Lee et al., 2020; Meighan et al., 2007; Speed and Dobrunz, 2009), verifying its suitability as model system for this thesis.

2.4.2. Hippocampal slice preparations

Two types of hippocampal slice preparations are commonly used for electrophysiology and imaging studies: acute hippocampal slices (Lein et al., 2011; Shetty et al., 2015) and organotypic hippocampal slice cultures (Bahr, 1995; Gogolla et al., 2006; Humpel, 2015). Besides retaining the hippocampal circuitry, both exhibit distinct features that must be considered when designing

experiments. Organotypic slice cultures show increased spontaneous activity, due to enhanced connectivity that develops as a result of constraining the cellular network into a two-dimensional tissue piece. Furthermore, organotypic slices are prepared from young animals (P7) and subsequently develop *in vitro* which results in reorganisations of connections and morphological changes such as increased dendritic branching (Collin et al., 1997; De Simoni et al., 2003; Gähwiler et al., 1997). In organotypic slices, dead cells and tissue are removed after 1-2 weeks *in vitro* providing excellent optical access, which is the biggest advantage in using organotypic slice cultures to study synaptic plasticity (Gähwiler, 1981; Lein et al., 2011). Acute hippocampal slices are prepared from adult rodents and used on the day of slicing, thus their physiology might be closer to the actual *'in vivo'* state of the brain at the time of harvest (Lein et al., 2011). However, imaging quality degrades in acute compared to organotypic slices, and drug delivery is easier in organotypic slices. Processes such as structural plasticity should be studied in acute slices, as cell and synapse morphology are altered in organotypic slices. Acute hippocampal slices can be prepared from transgenic animals, preserving the genetic modification (Mathis et al., 2011), but providing better optical access than *in vivo* settings, an approach that has been used in this project.

2.5. Thesis aims

Copious research has been conducted to reveal the mechanisms of synaptic plasticity and how they relate to memory formation and learning. *In vitro* as well as *in vivo* studies have investigated synaptic plasticity and its regulation on different timescales, in various brain regions and in the context of varying behavioural paradigms. The wide range of studies has expanded our knowledge about functional as well as structural changes at synapses, and molecular components of these processes have been intensively studied using different experimental settings such as electrophysiology, imaging, pharmacological manipulations and behavioural tests. However, a direct link between synaptic changes and phases of learning or memory is challenging to establish due to a) the complexity of synaptic plasticity mechanisms and b) a lack of tools that can be used to observe and manipulate synaptic plasticity *in vivo* without affecting basal neurotransmission. In the project presented in this thesis, I intended to explore important components involved in synaptic plasticity, whose functional consequences might have been underestimated previously. Furthermore, I contributed to the development of a minimally invasive, high resolution imaging method suitable for *in vivo* deep-brain imaging. The work presented in this thesis is divided in three parts as followed:

(1) In chapters 4 and 5, I present work on presynaptic transmission and plasticity, specifically presynaptic NMDA receptors (preNMDARs) at hippocampal Schaffer collateral terminals. While postsynaptic NMDA receptors have been intensively studied and assigned an extensive range of functions, the role of preNMDARs remains largely unexplored. Importantly, the literature

presents several inconsistencies with regards to preNMDAR signalling and function. I sought to unravel NMDAR signalling mechanisms at presynaptic terminals, that might explain controversial results in the field. Therefore, I asked several questions: Does glutamate release trigger preNMDAR activation and lead to autocrine feedback signals within presynaptic terminals? If so, how are Ca^{2+} dynamics in boutons driven by such preNMDAR mediated feedback? What are the functional consequences of preNMDAR signalling in the context of short-term plasticity? The goal was to build a framework for presynaptic NMDA receptor function that is currently lacking.

(2) Chapter 6 concerns the regulation of synaptic plasicity processes by endogenous factors such as hormones. Specifically, I studied the effects of oestrogen on structural plasticity, since it has been shown that higher levels of oestrogen result in increased postsynaptic densities. The influences of oestrogen on dendritic spines have been associated with differential performances in learning and memory tasks. Thus, studying oestrogen signalling in the context of plasticity is of relevance to understand modulations of cognitive functions. I therefore asked: Does oestrogen promote spine density in acute settings? Are there any differences concerning the effects of oestrogen with regards to different brain areas? I have also explored potential functions of oestrogen-mediated effects on spine plasticity in the context of network activity.

(3) Finally, in chapters 7 and 8 I sought to improve a multimode fibre (MMF) -based imaging device for minimally invasive deep-brain imaging of synapses, previously developed by the Emptage lab (Vasquez-Lopez et al., 2018). Several technical advances could be implemented into the system to enhance imaging quality and applicability for *in vivo* imaging. MMF-based imaging devices require

a calibration procedure prior to imaging, to characterise the light propagation and create a focus that can be scanned across a fluorescent sample. Because of the sensitivity of this calibration procedure, repeated high-resolution imaging through MMFs is currently impossible. Therefore, firstly, I explored potential effects of refractive index mismatches between the medium the calibration was performed in and the subsequent imaging medium. Secondly, I investigated potential advantages of the implementation of multiphoton imaging into the MMF system. Thirdly, I proposed a solution to overcome the challenges of repeated imaging, and aim for it to allow repeated high-resolution fluorescence imaging through a MMF. I would like to mention that even though myself collected all presented data in these Chapters, Dr. Raphaël Turcotte has accompanied all projects as engineer and contributed to the programming and installation of the technological advances. Details about contributions can be found at the end of this thesis.

The overall goal of this work was to expand our knowledge of synaptic function, how it relates to neuronal networks and ultimately learning and memory, and how to effectively study such relationships with suitable imaging techniques. Notably, the interest of understanding synaptic function, underpinning learning and memory processes, goes beyond basic physiology, since impaired synaptic plasticity and synapse loss have been documented in the context of a variety of neurodegenerative diseases associated with memory loss and cognitive impairments.

Some results from this project have been published or are currently under review, as indicated in the following list:

Schmidt, CC., Turcotte, R., Booth, MJ., Emptage, NJ. Repeated imaging through a multimode optical fiber using adaptive optics. Biomedical Optics Express 13 (2) 662-675. (2022)

Schmidt, CC., Tong, R., Emptage, NJ. Homeostatic regulation of presynaptic NMDA receptor subunit composition modulates action potential driven Ca^{2+} influx into boutons setting the bandwidth for information transfer. biorxiv, doi:10.1101/2021.09.19.460978. (2021) *currently under review.*

Turcotte, R., Schmidt, CC., Booth, MJ., Emptage, NJ. Volumetric two-photon fluorescence imaging of live neurons using a multimode optical fiber. Optics Letters 45 (24) 6599-6602. (2020)

Turcotte, R., Schmidt, CC., Emptage, NJ., Booth, MJ. Focusing light in biological tissue through a multimode optical fiber: refractive index matching. Optics Letters 44 (10) 2386-2389. (2019)

3. Materials and Methods

3.1. Preparation of hippocampal slices

3.1.1. Preparation of acute hippocampal slices

Acute hippocampal slices were prepared from 8-12 week-old Thy1-EGFP transgenic mice or P14-21 Wistar rats (Harlan UK). Animals were sacrificed by cervical dislocation and decapitation, subsequently the brain was extracted and covered in ice-cold dissection media (in mM: 65 sucrose, 85 NaCl, 2.5 KCl, 25 $NaHCO_3$, 1.25 NaH_2PO_4, 10 D-glucose, 7 $MgCl_2$, and 0.2 $CaCl_2$) which was bubbled with 95% O_2 and 5% CO_2 for 30 minutes prior to dissection. Afterwards, the brain was transferred to a petri dish constantly submerged in ice-cold solution and the cerebellum was detached with a razor blade. Then, the brain was glued onto the vibratome plate next to a 4% agar square, to stabilize it during the cutting procedure. Using a Leica VT1000 S Vibrating blade Microtome, 350 µm coronal slices were cut and hemispheres were separated. Subsequently, slices were transferred to a recovery chamber containing standard artificial cerebral spinal fluid (aCSF; in mM: 120 NaCl, 2.5 KCl, 26 $NaHCO_3$, 1.2 NaH_2PO_4, 11 glucose, 1$MgCl_2$, and 2 $CaCl_2$) constantly bubbled with 95% O_2 and 5% CO_2. Slices were then placed in a water heating bath (37 °C) for 10 min to flatten the slice surface before keeping them at room temperature for 1.5 hours prior to experiments. To ensure slice health, slices were maintained at room temperature for no more than 5 hours.

3.1.2. Preparation of organotypic hippocampal slices

Transverse 350 µm organotypic hippocampal slices were prepared from male

P6-P8 Wistar rats (Harlan UK, Nihon SLC) using a McIlwain tissue chopper (Mickle Laboratory Engineering Co. Ltd. and Cavey Laboratory Engineering Co. Ltd.), as previously described (Emptage et al., 2003; Stoppini et al., 1991). In brief, rats were sacrificed by cervical dislocation and decapitation. Dissected brains were then incubated in ice-cold Earle's Balanced Salt solution (EBSS)-based dissection buffer with additional 21 mM Hepes and 27.8 mM D-glucose (pH-corrected with 5 mM NaOH). After dissection, slices were cultured on Millicell CM membranes (0.4 µm pore size, Merk Millipore) and maintained in culture media at 37°C and 5% CO_2 for 7-14 days prior to use. Culture media comprised of 78.8% Minimum Essential Media, GlutaMAX (Gibco), 20% heat-inactivated horse serum, 30 mM HEPES, 26 mM D-glucose, 5.8 mM $NaHCO_3$, 1 mM $CaCl_2$, 2 mM $MgSO_4$ and 1% B-27 Plus Supplement (Gibco). The media was replaced every 2-3 days to ensure optimal and constant conditions for the slices.

3.1.3. Preparation of fixed brain slices

At the end of experiments, Thy1-EGFP transgenic mice were overdosed with sodium pentobarbital (240 mg/kg). Subsequently, transcardial perfusion with phosphate buffered saline (PBS) then 4% paraformaldehyde was performed to fix brains. Afterwards, fixed brains were extracted and kept in PBS for 1-2 weeks. Fixed brains were sectioned into 60 µm thick slices with a Vibratome designated for fixed tissue. Slices were then mounted on a coverglass and covered with a coverslip prior to imaging. Images of fixed slices were obtained with an Olympus BX40 microscope.

3.2. Electrophysiology

3.2.1. Electrophysiological recordings in organotypic slices

Cultured slices on their supporting membranes were transferred to a recording chamber and fixed with vacuum grease (glisseal® HV, Borer). During the experiments slices were constantly perfused with oxygenated (95% O_2 and 5% CO_2) artificial cerebrospinal fluid (aCSF; composition in mM: 145 NaCl, 2.5 KCl, 1 $MgCl_2$, 3 $CaCl_2$, 1.2 NaH_2PO_4, 16 NaH_2CO_3, 11 glucose) heated to near-physiological temperature (33-35˚C) using a custom made heater. Ascorbic acid (0.2 mM) and Trolox (1 mM, Sigma Aldrich) were further added to minimize photodynamic damage. The aCSF also contained 200 nM NBQX (Abcam) to avoid unwanted spiking in the network.

Electrophysiological data was recorded in whole-cell patch clamp mode with WinWCP (Strathclyde Electrophysiology Software). Patch pipettes (3-5 MΩ) were prepared with a horizontal micropipette puller (Sutter Instrument Co.) and filled with standard internal solution (in mM: 135 K-Gluconate, 10 KCl, 10 mM HEPES, 1-2 $MgCl_2$, 2 mM Na_2ATP, and 0.4 Na_3GTP, pH 7.2-7.4). Data was collected with an an Axoclamp 2B amplifier and WinWCP software (Strathclyde Electrophysiology Software). To adjust the resting membrane potential to -70 mV, current was injected and cells were clamped at -70 mV in voltage clamp experiments. To monitor the quality of the patch, access conductance and membrane capacitance were regularly checked throughout experiments. Generally, a minimum access conductance of Ga ≥ 25 nS was required for all experiments.

In organotypic slices, neurones were stimulated using a monopolar tungsten electrode encased in a glass pipette filled with NaCl solution.

3.2.2. Electrophysiological recordings in acute slices

Acute slices were transferred to the recording chamber and fixed with a “harp” (Warner Instruments), constantly perfused with heated and bubbled aCSF (95% O_2 and 5% CO_2) and 100 μM picrotoxin (Sigma Aldrich) to block inhibitory synaptic transmission. CA1 neurones in deeper cell layers were chosen for recordings, to ensure cell health throughout experiments. In acute slices, neurones were stimulated using a monopolar tungsten electrode placed directly into the tissue.

3.2.3. Action potential burst stimulation

CA1 neurones were patched with low-resistance patch-pipettes (3-5 MΩ) and clamped at -70 mV for voltage clamp experiments. For all experiments, 1 mM MK-801 was added to the internal solution within patch-pipettes, to inhibit postsynaptic NMDARs. For extracellular stimulation of CA1 neurones, the electrode was placed into the stratum radiatum, targeting Schaffer collaterals of CA3 neurones. At the beginning of each experiment, blockade of postsynaptic NMDARs was initiated by stimulating neurones at low frequency (0.06 Hz) for 8-10 min. This also allowed stabilization of cellular responses. CA1 neurones were then stimulated with 5-10 APs at 50 or 200 Hz to elicit short-term facilitation. In experiments for Chapter 5, 50 Hz stimulation was followed by a single pulse given 100 ms from the end of burst. For each experiment, stimulation was repeated 5-10 times at 0.06 Hz. To block NMDARs, 50 μM AP5 and Ro - 25 6981 (1 μM) were washed in after recording the control dataset to

block preNMDAR receptors. Alternatively, aCSF was washed in during vehicle experiments.

3.2.4. Analysis of the EPSC and short-term plasticity

Electrophysiological traces were analysed in Clampfit (Version 10.6.2.2, Molecular Devices). The slope of the EPSC was analysed, due to polysynaptic connections in organotypic slices, but when EPSC amplitude was used instead no qualitative differences in experimental outcomes could be detected. The slope was calculated for a time window of 2-3 ms.

The slope of the EPSC to each stimulation pulse was used to analyse the course of short-term plasticity during burst stimulation. Since burst stimulation caused strong after-hyperpolarisation, the baseline was manually adjusted. EPSC slope was normalised to the first pulse within each experiment. 5-10 traces were collected per experiment, and EPSC slopes of all pulses were normalised to pulse 1 for each trace before averaging.

3.3. Fluorescence confocal imaging

For Ca^{2+} imaging superficial CA3 pyramidal cells were patched with patch electrodes (3-5 MΩ) containing the Ca^{2+}- sensitive dye Oregon Green 488 BAPTA-1 (OGB-1; 1 mM) for 2-5 minutes. Afterwards, the patch electrode was slowly withdrawn to allow the cell membrane to re-seal. For optimal visualisation of the axons, the dye was allowed to diffuse for around 20-30 minutes. After successful identification of the axon and superficial boutons following specific criteria (Emptage et al., 2001), cells were re-patched for experiments. Only superficial boutons were selected to maximise optical

access. Electrodes for re-patching contained low OGB-1 concentration (0.05 mM) diluted in internal, to avoid cell damage caused by too intense changes in the concentration gradient. Cells were imaged with a LEICA DMLFSA microscope combined with a LEICA TCS SP2 confocal scan head and a 63x water-immersion objective (NA = 0.9, HCX APO L 63x/0.9W U-V-I, Leica) using the Leica Confocal Software (Version 2.61).

3.3.1. Presynaptic action potential-evoked Ca^{2+} transients and glutamate uncaging

Following re-patching, line scans through superficial boutons were performed and synchronised to intrasomatically stimulated APs triggered by injecting current (0.5–2.5 mA) with a stimulus duration of 10 ms to elicit presynaptic action potential-evoked Ca^{2+} transients (APCaTs). At least 10 line scans through the presynaptic terminal evoked at 20 s intervals were sampled for every condition.

After identification of superficial boutons, a glass pipette (3-5 MΩ) filled with 4-methoxy-7-nitroindolinyl-caged-l-glutamate (MNI-glutamate; 10 mM) diluted in Tyrodes (composition in mM: 120 NaCl, 2.5 KCl, 20 HEPES, 30 Glucose, 2 $CaCl_2$, 1 $MgCl_2$) was connected to a picospritzer and placed above the surface of the slice, close to the bouton to ensure focal delivery of the MNI-glutamate. For spot photolysis a 405 nm UV-laser was focused to a small spot and the location of the spot was marked on the computer screen. A movable stage was used to place the bouton exactly under the photolysis spot. A fast external shutter and a custom-built shutter control box enabled temporal control of the photolysis. Laser intensity was adjusted in the beginning to generate a visible

Ca^{2+} response in nearby dendritic spines to elicit Ca^{2+} transients in spines of 0.5-1 ΔF/F. Laser exposure was limited to a minimum (2 ms) and the UV-pulse was delivered 0.5 ms after the triggered action potential for each experiment to mimic physiological conditions. The timing was controlled and edited using TTL pulses programmed in a WinWCP (University of Strathclyde) stimulus protocol.

Experiments were excluded from analysis if the bouton lost responsiveness, showed signs of photodynamic damage including swelling or increased basal Ca^{2+} signal, or if the picospritzer was blocked after the experiment.

Ca^{2+} transients in boutons were analysed with ImageJ and Microsoft Excel and expressed as the fractional change in fluorescence (ΔF/F). To calculate the values, I used the following formula:

$$\Delta F/F = (F_{\text{total F over ROI}} - F_{\text{background}}) / (F_{\text{baseline}} - F_{\text{background}})$$

Peak APCaTs were then determined by taking the maximum value of signal in a 20 ms time window following the onset of the AP. For final analysis, peak APCaTs were averaged across 10-20 trials.

3.3.2. Induction of structural plasticity

Structural plasticity (sLTP) of spines was induced by local glutamate uncaging following available protocols (Harvey and Svoboda, 2007; Hedrick et al., 2016). MNI-glutamate was delivered and uncaged with a train of 4–6 ms, pulses (30 times at 0.5 Hz) near a spine of interest. Only small dendritic spines (< 1 µm) well separated from the dendritic branch and neighbouring spines were selected for experiments. All experiments were performed in Mg^{2+} free aCSF. Subthreshold stimuli (sub) were delivered similarly but using a train of 1 ms

pulses (30 times at 0.5 Hz). A maximum of 1-2 spines were stimulated per cell. Up to three cells from the same slice were used for sLTP and sub experiments.

Images of the dendrite containing the target and neighbouring spines were acquired with 512 x 512 resolution as a z-stack with a step size of 0.5 µm. Images were taken at -3, -2 and -1 to generate a baseline, and then at 0, 1, 5, 10, 15, 20, 25 and 30 minutes post glutamate uncaging protocol.

3.3.3. Analysis of spine morphology

Spine size was analysed in ImageJ and estimated as the background-subtracted integrated fluorescence intensity over an elliptic region of interest (ROI) around the dendritic spine. Fractional changes in fluorescence of the spine head were used to estimate fractional changes in spine size and calculated as % increase = 100 x $(F-F_{background})/(F_{initial}-F_{background})$. In graphs, changes in spine size were expressed as fractional changes with respect to the average size prior to experiments. For sLTP experiments, spine size changes at the end of the experiment were defined as the average change observed at 30 min.

For acute oestrogen incubation experiments, fractional changes in spine size displayed as Δ(%intensity) from the beginning to the end (post 30 minutes) of experiments were normalised by subtracting Δ(%intensity) of vehicle experiments without drug incubation expressed as Δ(Δ%intensity).

To evaluate whether the above analysis method is valid and qualitative results can be reproduced when choosing a different analysis method, for some experiments, the FWHM was calculated instead. For this purpose, line profiles

through spine heads were manually selected. Subsequently, line profiles were analysed and the FWHM calculated using a custom MATLAB script. This analysis yielded similar results to the above.

3.4. Pharmacology

3.4.1. Ion channel and receptor pharmacology

NMDARs were blocked by bath application of 50 μM D-AP5 (Abcam). Pre- or postsynaptic NMDARs were selectively blocked by including 1 mM MK-801 (Abcam) into the internal solution.

NMDAR subunits were blocked with bath application of specific subunit inhibitors and drug concentrations were maintained throughout imaging experiments. The GluN2B subunit was selectively blocked with 1 μM Ro - 25 6981. 100 nM PEAQX (Tocris) and 50 μM DQP 1105 (Tocris) were used to block the GluN2A and GluN2C/D subunits, respectively. During electrophysiology experiments, slices were perfused with Ro – 256981 (1 μM) for at least 10 minutes to ensure reliable block of GluN2B.

For SK-channel inhibition, slices were preincubated in 1 μM apamin (Sigma Aldrich) for 30 minutes, which was maintained throughout the experiment. To prevent Ca^{2+} release from intracellular stores, 15 μM CPA and 20 μM ryanodine (Sigma Aldrich) were included in the aCSF during experiments.

3.4.2. Induction of homeostatic plasticity

To induce homeostatic plasticity in organotypic slices for Chapter 5, global network activity was manipulated for 48 – 72 hours. Activity was increased with

1 μM gabazine (Tocris) and decreased with 10 μM NBQX (Tocris) and 50 μM AP5 (Abcam). Slices were incubated by directly adding drugs to the culture medium.

To decrease activity in acute slices as presented in Chapter 6, slices were incubated for >2 h in NBQX (10 μM) and AP5 (50 μM). Recordings were performed in aCSF containing the same drug concentrations.

3.4.3. Application of oestrogen

17β-estradiol (E2, Sigma Aldrich) was used to stimulate oestrogen signalling in acute slices. 100 nM E2 was bath-applied to acute slices for 30 minutes after control images were recorded. Vehicle experiments were performed, where only aCSF was perfused for 30 minutes.

For experiments where structural plasticity was induced by glutamate uncaging, slices were pre-incubated with 100 nM E2 for 30 minutes.

3.5. Thy1-EGFP transgenic mice

Transgenic Thy1-GFP-M mice (THYE colony, line 007788, Jackson Laboratories) expressing EGFP under the Thy1 promoter were used in this thesis for fibre imaging and oestrogen experiments. EGFP was expressed in a subset of neurones resulting in bright labelling of neurones and neuronal processes including dendritic spines.

3.6. Preparation of fluorescence beads samples

Beads samples were prepared using standard microscopy glass slides. Small amounts of Poly-D-Lysine were applied to the glass side and subsequently

covered with diluted fluorescent beads. Three different kinds of beads were used including 1.0 or 2.0 μm yellow-green fluorescent beads (FluoSpheres™ Carboxylate-Modified Microspheres, 1.0 μm or 2.0 μm, yellow-green fluorescent (505/515)) and 2.0 μm red fluorescent beads (FluoSpheres™ Carboxylate-Modified Microspheres, 2.0 μm, red fluorescent (580/605)). For some experiments in Chapter 8, fluorescent beads (FluoSpheres™ Carboxylate-Modified Microspheres, 2.0 μm, yellow-green fluorescent (505/515) were immersed in agar, simulating the properties of fluorescently tagged neurones in mouse brains. The agar dilution was 0.5% to roughly match the mechanical properties of brain tissue. Agar pieces of 1.5 × 1.5 cm were glued onto microscope glass slides and covered with the top part of a small petri dish, serving as an 'artificial skull'.

3.7. Multimode fibre imaging: Experimental system

The experimental system comprised four different units: a source unit, an imaging unit, a calibration unit and a sample unit (Vasquez-Lopez et al., 2018). A source unit distributes monochromatic, linearly polarised light beam (λ = 488 nm, CrystalLaser, DL488-020-S) which is split and coupled into two separate optical fibres: a polarisation maintaining single-mode fibre (PM-SMF, Thorlabs, P1-488PM-FC-2) and a custom SMF (C-SMF, Thorlabs, P1-405B-FC-5), cleaved with a 10º angle for power stability. The SMFs distribute light to the imaging unit (PM-SMF) and to the calibration unit (C-SMF).

Within the imaging unit, an achromatic doublet lens (f = 60 mm) is used to collimate the light exiting the PM-SMF and its polarisation aligns with the working polarisation of the LC-SLM (Meadowlark Optics, HSPDM512, 512 ×

512 pixels). The LC-SLM is used to modulate the phase of light in an off-axis regime and to Fourier transform it with a plano-convex (f = 100 mm) lens onto an iris that only transmits the first diffraction order. In the following, light is reflected by a dichroic mirror (Thorlabs, MD498) and circularly polarised by a quarter-wave plate to assure minimum coupling between polarisation states. The transmitted signal in the form of circularly polarised light then propagates through a telescope consisting of plano-convex (f = 50 mm) and aspheric (f = 8 mm) lenses coupling the light into a multimode fibre (MMF; standard fibre used: Thorlabs, FG050UGA, NA = 0.22).

For calibration procedures, the light exiting the MMF is coupled into the calibration unit and relayed by a microscope objective lens (Olympus 20×, RMS20X, NA = 0.4) and an achromatic doublet (f = 150 mm) onto a CCD camera (Basler pilot, piA640-210gm). Using a quarter-wave plate, the signal is converted back into the linear polarisation state between the lenses. A reference beam delivered by the C-SMF is then merged with the MMF output signal using a 50:50 non-polarising beam-splitter. In order to align the wavefront shaping module with the calibration unit, the distal facet of the MMF was imaged on the calibration camera. Subsequently, coupling of light into the MMF was optimised by axial and lateral translation of the lens located immediate before.

The sample unit contained a three-dimensional micro-positioning stage to navigate the MMF-implant towards biological or other fluorescent beads samples. Samples positioned below the MMF included living transgenic Thy1-EGFP mice, organotypic hippocampal slices and fluorescent beads.

3.8. Calibration procedure and Transmission matrix generation

Prior to imaging, a calibration procedure is used to describe the light propagation through the MMF by generating a transmission matrix (TM). Generally, the TM represents a linear relation between bases of input and ouput modes (Popoff et al., 2010). For this experimental set-up, the input modes are diffraction-limited focal points defined across an orthogonal grid (50×50) at the input facet of the MMF and the output modes are analogously defined as 120×120 across the plane of the MMF output facet or any other plane away from the fibre facet. In this thesis, calibrations were performed between 40-50 μm away from the fibre facet. Using the LC-SLM, input modes are sequentially generated, travelling through the MMF and exiting as a linear combination of output modes, subsequently interfering with the reference signal at the CCD camera. For different phase steps of each input mode an image is recorded (phase stepping), respectively, and the output modes are then analysed by fitting the phase dependency to find the input phase maximising each output mode by a corresponding number (120×120) of CCD camera pixels, thus resulting in one vector of the TM matrix. Finally, the TM can be used to design specific input fields and the corresponding LC-SLM modulation to generate invidual output modes represented as diffraction-limited foci at the MMF output plane.

The implementation of a GPU-accelerated toolbox for LC-SLM control allowed the acquisition of the full TM of a MMF in less than 10 minutes. Calibration time depended on the diameter and NA of the MMF, thus, the number of modes that had to be characterised. For a 50-μm-core MMF the TM could be generated in less than four minutes.

Calibrations in experiments where biological tissue was imaged were performed in different media. For imaging of organotypic slices, calibrations were performed in Tyrode's solution. For *in vivo* imaging, calibrations were performed in a 22% glucose solution.

3.9. Multimode fibre implants

In this thesis, three different types of MMFs were used. For most experiments, 50 µm-core fibres were used (Thorlabs, FG105UCA, cladding 75 µm, NA = 0.22). MMF implants consisted of fibres cut to a length of 2.0 cm and glued into a ferrule (Thorlabs, CF128-10). For some experiments, high-NA fibres were used, custom designed with a 170 µm glass/polyimide coating to generate rigid fibres that are less sensitive to fibre bending. Either 60 µm-core MMFs (doric lenses, MFC-ZF2.5, cladding 67 µm, NA = 0.37, length 1.5 cm) or 44 µm-core fibres (doric lenses, MFC-ZF1.25, cladding 50 µm, NA = 0.66, length, 2 cm) were used.

3.10. Multimode fibre imaging

Immediately after the calibration, imaging can be performed as MMF-based point-scanning fluorescence micro-endoscopy. The region of interest within a fluorescent sample is positioned on a three-dimensional micro-positioning stage below the MMF. The LC-SLM produces a linear superposition of input modes (50×50, modulated wave front of the light field) along the proximal fibre facet, which constructively interferes to generate a single, diffraction limited focal light-point at the MMF output plane. Diffraction limited focal light-points can then be digitally raster-scanned across the fluorescent sample. Notably, points can be scanned as a set of 120×120 points to generate full images, or arbitrary access

points can be chosen to only scan a portion of the field-of-view. The maximum LC-SLM refresh rate determines imaging speed and was 204 Hz in this set-up. While scanning, the emitted light is collected and passed back through the fibre and registered by a photo multiplier tube (PMT, Thorlabs, PMM02). The intensity of each raster scan position constitutes the pixel value in the final acquired image. The above numbers correspond to MMF with an NA of 0.22 (Thorlabs, FG105UCA). MMF having an increased NA (doric lenses, MFC-ZF2.5, 60 μm core, NA = 0.37 and MFC-ZF1.25, 44 μm core, NA = 0.66) required the adjustment of input modes. A total of 69×69 input modes were used for these fibres.

3.10.1. Imaging of fluorescent beads

Following the calibration procedure beads samples were mounted on a multi-axis stage below the MMF. Glass slides covered with diluted beads (1 μm) were attached to the stage with double-sided tape and then positioned approximately 100 μm below the tip of the MMF. While imaging, the sample was translated towards the MMF tip, until beads were in focus, evaluated by maximum signal.

For experiments in Chapter 8, an image was acquired at this plane, serving as ‘Original’. Subsequently, the beads sample was moved downwards, giving enough space to manually remove the MMF implant. The MMF implant was fully removed from the optical system and rotated and flipped several times (Step 1). Then, the MMF implant was reinserted into the system via attaching the magnets on the implant to the magnets within the optical system (Step 2). Afterwards, the beads sample on the stage was moved up to the same plane that was used to capture the ‘Original’ image. Fine axial positioning in

increments of 2 µm was performed, to determine the image plane that gives the highest signal. An image was taken at this plane, named ‘Reinsertion 1’ (Step 3). Sensorless optimisation was performed choosing ROIs in the centre of multiple beads. The image acquired was titled ‘Optimisation 1’ (Step 4). Steps 1-4 were repeated three times. For experiments in Fig. 48, a small hole (2 × 2 mm) was drilled into the petri dish covering the agar with immersed beads (2 µm). Subsequently, the sample was transferred to the multi-axis stage and moved upwards until the full length of the fibre was inserted into the agar. While imaging, one fluorescent bead was positioned into focus and an image was acquired (‘Original’, Pre attachment). Then, the MMF implant was attached to the sample. First, super glue was used to attach the headplate to the petri dish. Next, dental cement was carefully applied to firmly fix the MMF implant onto the petri dish. Once the dental cement was dry, an image was taken to assess any shifts occurring during the attachment process (Post attachment). If the attachment was successful, the full construct of sample + MMF implant was removed from the optical system. Then, sample + attached MMF implant were reinserted and an image was taken (‘Reinsertion’). Sensorless optimisation was performed choosing an ROI in the centre of the bead that was originally positioned in focus.

3.10.2. Imaging of organotypic hippocampal slices

Prior to imaging, brain slices were transferred to a recording chamber and individual hippocampal neurones in the CA1 or CA3 region were loaded with Alexa 488 (Thermo Fisher Scientific, 2 mM) or Alexa 594 (Thermo Fisher, Scientific, 2 mM) for 1 minute using whole cell patch-clamp technique. Slices were then transferred on a glass slide covered in Tyrode’s solution, and

positioned in the MMF system, onto the multi-axis stage. Imaging was performed in physiological Tyrode's solution to maintain slice health throughout the experiment. The hippocampal slice was positioned below the MMF, with the fibre tip directly above the CA3 region containing the neurones that have been filled with fluorescent dye. While imaging, cell soma, neuronal processes such as thin dendrites and synapses as dendritic spines were identified.

3.10.3. *In vivo* imaging

All experiments were approved by the local ethical review committee at the University of Oxford and licensed by the UK Home Office. Transgenic Thy1-GFP-M mice (line 007788, Jackson Laboratories) were used for MMF-based *in vivo* imaging. Animals aged 8–12 weeks were premedicated with intraperitoneal injections of dexamethasone (Dexadreson, 4 µg), atropine (Atrocare, 1 µg) and carprofen (Rimadyl, 0.15 µg). General anaesthesia was induced by an intraperitoneal injection of ketamine (Vetalar, 100 mg/kg) and medetomidine (Domitor, 0.14 mg/kg). Mice were then placed in a custom-designed holder. Depth of anaesthesia was monitored by pinching the tail and rear foot and by observation of the respiratory pattern. Body temperature was closely monitored throughout the procedure and kept constant at 37ºC by the use of a heating mat. Both eyes were covered with eye ointment (Maxitrol, Alcon). After assessing anaesthesia depth, the skin over the craniotomy site was shaved and an incision was made to expose the skull. Subsequently, a hole of 1 mm diameter was drilled (Foredom K.1070, Blackstone Industries, CT, USA). Generally, craniotomies were centred at 1.95 mm posterior and 1.6 mm lateral to bregma, to target the hippocampus according to the Allen Mouse Brain Atlas (https://mouse.brain-map.org/static/atlas).

The custom-made mouse holder could directly be transferred to the MMF system with the mouse' head securely fixed. Subsequently, the MMF was gradually lowered several mm into the brain tissue, targeting cortical or subcortical brain structures. The MMF was lowered in 10-20 μm steps until fluorescence from neuronal processes could be detected. Then, the structure of interest was approached in 2 μm steps until maximum signal was detected and the structure was in focus. For experiments in Fig. 35, the above process was reversed and instead of lowering the MMF into tissue, the mouse was moved towards the MMF.

3.11. Illumination characterisation

Analysis of illumination foci was performed in ImageJ and Excel. Generally, images (120×120 pixels) of the illumination foci were recorded with the distal CCD camera at the axial position at which the calibration was performed. Illumination foci were centred and a 15×15 pixel square region of interest (ROI) was selected and peak intensity was measured. Lateral width was measured by cropping line profiles through the peak of the illumination focus and analysed by a custom MATLAB script (by Raphaël Turcotte) using Gaussian fitting.

For index matching experiments in Chapter 7, the illumination focus was captured with four different illumination powers (optical densities from 0 to 3) to reconstruct high dynamic range images. Three metrics were used to characterise focus quality: the peak intensity, the intensity enhancement factor (IEF), and the lateral full width at half-maximum (FWHM). The IEF was defined as the peak intensity divided by the average intensity from all pixels within the central 50 μm diameter of the field imaged by the fibre.

For experiments in Chapter 8, to evaluate different quality metrics, a focus was formed with varying amount of tip, tilt or defocus coefficient without displacement of the implant. Images were captured at 49 lateral positions arranged as a uniformly spaced grid (7×7) for each coefficient and mode. For assessing the performance of sensorless AO during sequential removals/reinsertions, the optimisation was performed at location [45,60] and illumination images were acquired and analysed when focusing at 49 lateral positions arranged as a uniformly spaced grid (7×7). To analyse the spatial variance in AO improvements across the field-of-view (FoV), the optimisation was performed at pixel [45,60]. Illumination images were then acquired and analysed for the 10 locations of the 7×7 grid described above located in the fourth octant. To analyse the spatial dependence of AO, sensorless optimisation was performed at pixels [x,x], with x = {5 to 60 in increment of 5}. Illumination images were then acquired and analysed when focusing at pixels {[45,60], [60,45], [75,60], [60,75]}.

3.12. Multimode fibre: image analysis

Analysis of fluorescent images was performed in ImageJ and Excel. Peak intensity and lateral width analysis for fluorescent beads images were similar to analysis of illumination foci (see 3.11.). For beads, the peak intensity was set as the maximum value of the line profile drawn through the centre of the bead. The lateral width was evaluated as the FWHM of the profile and calculated using a MATLAB script. The profile was first linearly rescaled by a factor of 11 before removing the background and normalising it. Then, linear interpolation between the 2 points closest to 0.5 was performed on each side of the peak to find the

0.5-value positions. The difference between the 2 positions was the FWHM value.

The signal-to-background ratio was calculated as the peak signal in the image divided by a background. The background was obtained by selecting a 20×20 pixels region where no structures were visible and measuring the average value. Fourier transform images were generated using ImageJ.

3.13. Headplate and implant design for repeated multimode fibre imaging

Two different types of MMF were used: Low-NA MMF (Thorlabs, FG050UGA, core diameter 50 μm, NA 0.22, length 2 cm) glued inside a ferrule (Thorlabs, CF128-10) and high-NA MMF (Doric lenses, custom MFC-ZF2.5, core diameter 60 μm, NA = 0.37, length 1.5 cm) within a 170 μm glass/polyimide rigid coating and glued into a ferrule. Ferrules were glued into the custom head plate (Fig. 7) and this assembly positioned into the imaging system using magnets. Four magnets were attached to the headplate and within the system, respectively (First4Magnets, F321-N35-50, 2 mm diameter and 1 mm height, N35 Neodymium). The custom head plates were designed using AutoCAD software and 3D printed. They were made of MJF Nylon 12, a biocompatible material. The weight of the headplate with a MMF and magnets was of 3.5 g.

3.14. Sensorless adaptive optics optimisation

For sensorless adaptive optics, the distal intensity distribution was imaged with a camera and several metrics can be evaluated including signal intensity, background intensity and background autocorrelation. Fig. S8, Appendix shows how the metrics changed when tilt was incrementally changed while focusing at

different distal locations immediately after evaluating the TM (similar results were obtained for tip and defocus).

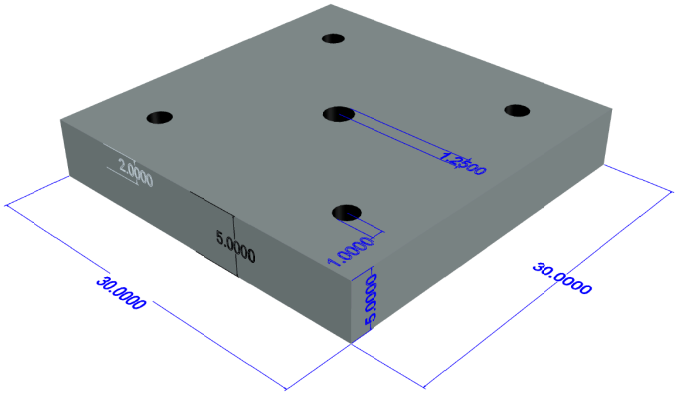

Fig. 7: 3D AutoCAD drawing of the headplate used for repeated MMF imaging.

The optimal tilt coefficient, here zero as there were no perturbations, could be correctly evaluated with all metrics. Critically, the SLM was sufficiently sensitive to impart wavefront modulations allowing for gradual changes in the metrics. The background intensity was minimal at the optimal tilt value, consistent with the fact that most of the intensity should reside in the focus when focusing optimal; however, the relative amplitude change was very limited (Fig. S8, Appendix). The background autocorrelation had a larger modulation but using this metric would not be compatible with endoscopic imaging without distal access (Fig. S8, Appendix). The peak signal intensity was maximal at the optimal tilt value, had the largest modulation and a minimal variance was observed across the different spatial locations (Fig. S8), thus the peak intensity appears to be the optimal metric for sensorless AO through a MMF.

Sensorless AO optimisation was performed using 1) images of the illumination as captured by the CCD camera in the distal plane, or 2) the fluorescence

signal detected by the proximal PMT. For both, illumination and fluorescence data, three aberration modes in the LC-SLM plane were tested in the following order: tip, tilt, and defocus. For each mode, 21 biases were sequentially superimposed on the wavefront dictated by the TM with an increment of 0.001π rad for tip and tilt and of $4\times10^{-6}\pi$ rad for defocus around zero bias (no aberrations). Next, the peak intensity was calculated and served as the quality metric, unless otherwise mentioned. A Gaussian fit was then performed on the quality metric to evaluate the optimal modal coefficient and the correction was immediately applied, before measuring the next mode. For the illumination case, the optimisation was conducted by capturing images of a focus at a single, specified distal location. For the fluorescence case, the optimisation was performed on the signal of a number of specified ROIs, in general between 1 and 6, taking advantage of the random-access capability of the system. Signals from the different ROIs were averaged together before Gaussian fitting. The time for sensing was less than 5 sec, when considering 6 ROIs.

3.15. Statistics

Statistical tests were performed using Graphpad Prism and the type of statistical test is explicitly stated where used. Mann-Whitney test and Unpaired t-test were used for comparisons of independent means and Wilcoxon signed rank test was used for dependent means. Kruskal-Wallis test followed by post hoc Dunn's test was used for multiple comparisons. Significance is denoted as follows: *: $p < 0.05$, **: $p < 0.01$, *** $p < 0.001$. In all tests, alpha = 0.05. Error bars represent ± standard error of the mean (SEM).

4. Mechanisms of presynaptic NMDA receptor signalling at Schaffer collateral boutons

4.1. Introduction

N-methyl-D-aspartate receptors (NMDARs) are glutamate-gated cation channels that have been extensively studied in the context of synaptic plasticity (Malenka and Nicoll, 1993). Investigating the physiology of NMDARs began as early as the 1970s, where most research in the field focussed on glutamate and other excitatory amino acid- induced responses in neurones (reviewed in Watkins and Jane, 2006). Using different classes of agonists including *N*-methyl-D-aspartic acid (NMDA) amongst others, Watkins and colleagues suggested that neurones expressed different classes of receptors, NMDA and non-NMDA receptors (Watkins and Evans, 1981). Subsequently, several antagonists were developed to competitively block the NMDARs' glutamate recognition site, first and foremost D-2-amino-5-phosphonopentanoate (AP5). Throughout the 1980s, such antagonists could be used to evaluate the contribution of NMDARs in synaptic transmission, and AP5 remains the most widely used substance to block NMDAR activity. Following these early studies, it soon became evident that NMDARs exhibit several unique features. Mayer et al demonstrated, that the activation of NMDARs requires the relief of a Mg^{2+} block by membrane depolarisation (Mayer et al., 1984). Other studies pointed out that NMDARs are not only activated by glutamate binding, but also by other agonists such as glycine (Johnson and Ascher, 1987). NMDARs are highly permeable for Ca^{2+} (MacDermott et al., 1986) substantiating their role in plasticity processes (Malenka and Nicoll, 1993). Ca^{2+} influx through NMDARs

triggers LTP and LTD (Malenka and Bear, 2004) and underlies various forms of homeostatic plasticity (Turrigiano, 2012). Moreover, repetitive activation of NMDARs can elicit a shift in plasticity thresholds without causing LTP or LTD, thus, NMDAR signalling is involved in processes referred to as metaplasticity (Huang et al., 1992; Wang and Wagner, 1999). Conventionally, research on NMDARs focuses on postsynaptically located NMDARs (postNMDARs). Generally in synaptic transmission, postNMDARs are seen as coincidence detectors, that contribute to the excitatory postsynaptic current (EPSC) once glutamate is released from the presynaptic terminal concurrent with postsynaptic depolarisation to remove the Mg^{2+} block (Bourne and Nicoll, 1993) and a detailed framework for postNMDAR signalling and functional outcomes has been built over the years. Recently, postsynaptic NMDA dependent plasticity has been demonstrated *in vivo* (Zhang et al., 2015). However, NMDARs are expressed at both post- and presynaptic terminals (Abrahamsson et al., 2017; Bouvier et al., 2018, 2015; Larsen et al., 2011; Lituma et al., 2021; McGuinness et al., 2010; Rebola et al., 2010). While the functional roles of postNMDARs are well-established (Lüscher and Malenka, 2012; Malenka and Nicoll, 1993), the repertoire of presynaptic NMDAR (preNMDAR) function remains largely unexplored despite clear evidence implicating preNMDARs in synaptic plasticity.

In the early 1990s, Pittaluga and Raiteri provided the first evidence of presynaptically located NMDARs on hippocampal axon terminals (Pittaluga and Raiteri, 1992, 1990). A presynaptic expression locus of NMDARs was further demonstrated by numerous studies using electron and fluorescence microscopy (Duguid and Smart, 2004; Janssen et al., 2005; Lituma et al., 2021;

McGuinness et al., 2010; Siegel et al., 1994). Time-lapse imaging displayed preNMDAR dynamics during formation of cortical synapses (Gill et al., 2015). Shortly after the first anatomical detections, physiological and functional evidence of preNMDARs in the CNS was presented. Berretta and Jones were first to suggest a functional role for preNMDARs in synaptic transmission, since the application of AP5, a potent NMDAR antagonist, decreased miniture excitatory postsynaptic currents (mEPSCs) even after previous postNMDAR blockade (Berretta and Jones, 1996). The possibility that preNMDARs enhance neurotransmitter release was confirmed in various brain regions including the cortex, hippocampus, spinal cord, and the cerebellum (Banerjee et al., 2016; Corlew et al., 2008; Madara and Levine, 2008; Rodríguez-Moreno and Paulsen, 2008; Woodhall et al., 2001). PreNMDARs modulate both spontaneous and evoked action potential-driven transmitter release (Banerjee et al., 2016) supposedly via distinct signalling pathways (Abrahamsson et al., 2017). The modulatory effects of preNMDARs on release strongly support the idea of preNMDARs as key players in synaptic plasticity processes. Indeed, preNMDARs are considered essential for the induction of spike timing-dependent long-term depression (t-LTD) at some synapses (Bender et al., 2006; Corlew et al., 2008, 2007; Gill et al., 2015; Larsen et al., 2011; Rodríguez-Moreno et al., 2010; Rodríguez-Moreno and Paulsen, 2008 but see Carter and Jahr, 2016). Moreover, preNMDARs are of relevance for long-term plasticity considering experiments indicating that glutamate release induces presynaptic LTD by acting on preNMDARs (Rodríguez-Moreno et al., 2013) thereby inhibiting presynaptic LTP (Padamsey et al., 2017b). Traditionally, preNMDARs are considered ionotropic receptors, however, some metabotropic

actions have been proposed (Abrahamsson et al., 2017; Dore et al., 2017) and other unconventional signalling regimes underlying preNMDAR activity might affect synaptic plasticity (Chung, 2013).

In short, preNMDAR function has been reported at both cortical (Buchanan et al., 2012; Rodríguez-Moreno et al., 2013; Sjöström et al., 2003) and hippocampal synapses (Abrahamsson et al., 2017; Bouvier et al., 2018; Janssen et al., 2005; Lituma et al., 2021; McGuinness et al., 2010; Padamsey et al., 2017b). However, the literature shows several inconsistencies in relation to preNMDAR function and regulation. Traditionally, Ca^{2+} sensitive dyes are used to detect Ca^{2+} influx through NMDARs and voltage-gated Ca^{2+} channels (Padamsey and Emptage, 2011). Over the years, experiments in axons using these dyes in combination with local NMDAR agonist application have shown mixed results. Presynaptic NMDAR dependent Ca^{2+} transients were demonstrated in cortical and hippocampal cells (Buchanan et al., 2012; Lituma et al., 2021; McGuinness et al., 2010), however, others could not detect any Ca^{2+} excursions (Christie and Jahr, 2009, 2008). Direct agonist delivery onto presynaptic boutons via 2P photolysis of MNI-glutamate did not elicit any NMDAR-mediated Ca^{2+} signals in the somatosensory cortex (Carter and Jahr, 2016). For some, these results appear to cast doubt on the existence of preNMDARs, but the overwhelming anatomical and functional evidence of preNMDARs rather suggests special signalling mechanisms for these receptors, that differ substantially from their postsynaptic counterparts. Notably, Buchanan and colleagues have shown that preNMDAR expression varies between individual synapses, highlighting the probable complexity of preNMDAR function (Buchanan et al., 2012).

Different versions of preNMDARs exist with regards to their subunit composition and expression locus. NMDARs are di-heteromers comprised of two GluN1 subunits and two GluN2 (GluN2A, GluN2B, GluN2C and GluN2D) or GluN3 (GluN3A and GluN3B) subunits (Paoletti et al., 2013) with GluN2A and GluN2B being the predominant subunits found in the mammalian forebrain (Cull-Candy et al., 2001; Paoletti, 2011). At the postsynaptic terminal, NMDAR subunit composition directs functional diversity through subunit specific differences in ion permeability, channel gating and conductance, and coupling to accessory regulatory proteins (Kutsuwada et al., 1992; Paoletti et al., 2013). NMDAR subunit composition can be linked to distinct parallel processing pathways often serving opposing roles at the postsynaptic terminal. For example, GluN2 subunits within hippocampal neurones selectively mediate the direction of plasticity through the regulation of Ca^{2+} influx (Fox et al., 2006; Shipton and Paulsen, 2014). The inhibition of NMDARs containing the GluN2B subunit prevents long-term depression whereas blockade of GluN2A-containing NMDARs inhibits long-term potentiation (Liu et al., 2004). Moreover, NMDAR deactivation times depend on the GluN2 subunit composition, which directly affects the decay time course of EPSCs. Therefore, NMDAR subunit diversity is relevant for the precise tuning of synaptic responses (Hansen et al., 2017; Monyer et al., 1994, 1992; Vicini et al., 1998). Even more functional NMDAR diversity results from their synaptic localisation, as they can be localised at synaptic as well as extrasynaptic sites (Köhr, 2006; Lozovaya et al., 2004; Paoletti et al., 2013; Sanz-Clemente et al., 2013; Thomas et al., 2006; Wyllie et al., 2013). Ca^{2+} influx through NMDARs can trigger differential internal signalling cascades dependent on extrasynaptic or synaptic activation (Kaufman et al.,

2012; Papouin et al., 2012).

Given the importance of preNMDARs in various plasticity processes, I intended to further explore the mechanisms of preNMDAR signalling, which are presently poorly understood. By imaging action potential – evoked Ca^{2+} transients (APCaTs) at Schaffer collateral - CA1 synapses coupled to focal glutamate uncaging at boutons of CA3 pyramidal neurones, I identified two functionally opposing presynaptic NMDAR populations. On the one hand, activation of preNMDARs containing the GluN2B subunit reduces Ca^{2+} influx into presynaptic terminals, while on the other hand, preNMDARs comprising the GluN2A subunit increase action potential – evoked Ca^{2+} influx. Furthermore, I show that this bidirectional modulation of bouton Ca^{2+} dynamics is driven by the activation of small conductance Ca^{2+}-activated K^+ channels (SK-channels).

4.2. Results

4.2.1. Activation of presynaptic NMDA receptors decreases AP-evoked Ca^{2+} influx at Schaffer collateral boutons

To examine the action of preNMDARs at the presynaptic terminal of the Schaffer collateral - CA1 synapse in the hippocampus, CA3 pyramidal cells were bolus loaded with the Ca^{2+} indicator dye Oregon green 488 BAPTA-1 (OGB-1; 1 mM). Organotypic slices prepared from male Wistar rats (age P6 – P8) were used for experiments. CA3 pyramidal cells were patch-filled with OGB-1 for 2-5 minutes. Subsequently, the axon was located and superficial presynaptic terminals at axonal arbours were identified as visually distinct varicosities (see Methods; Fig. 8A). Rapid line scan imaging through boutons was coupled to photolytic release of glutamate, supplied by local perfusion of

MNI-glutamate, to activate glutamate receptors specifically at the bouton (Fig. 8B). Glutamate photolysis was performed using a 405 nm UV-laser and titrated at spines located at a similar depth to elicit Ca^{2+} transients with similar magnitude as observed during endogenous evoked release of glutamate (Fig. 9A,B). Activation of postNMDARs typically requires AMPAR activation, since AMPAR activity contributes to membrane depolarisation necessary to relieve the voltage-dependent Mg^{2+}-block of NMDARs (Mayer et al., 1984; Nowak et al., 1984). This study focuses on preNMDARs, thus postNMDAR activation should be avoided. To prevent the activation of postNMDARs, AMPAR activity was inhibited (10 µM NBQX).

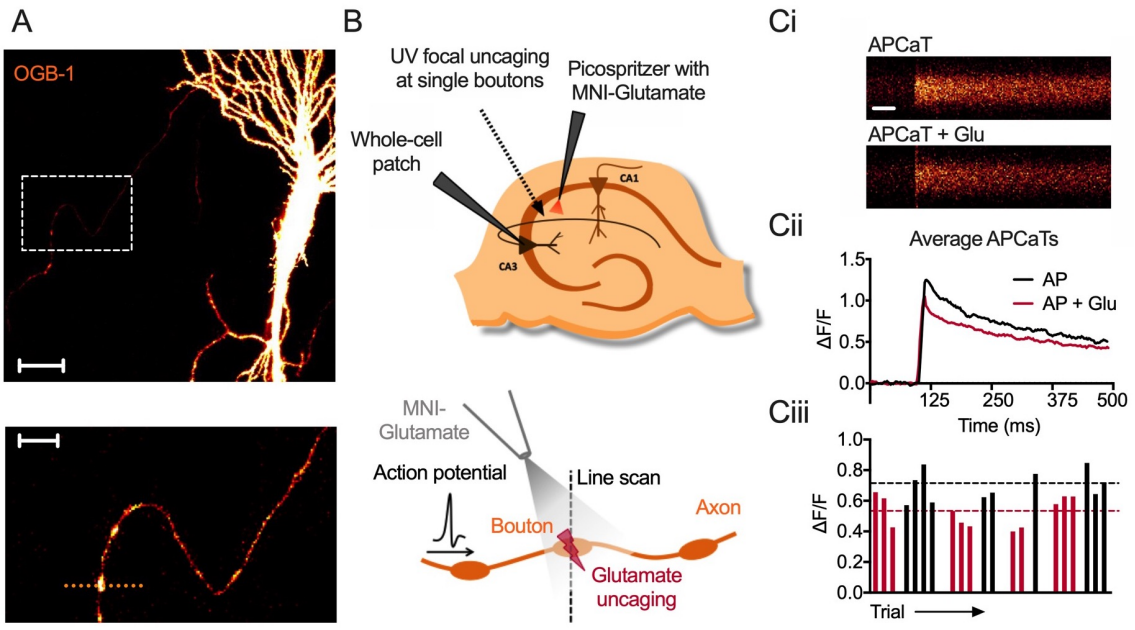

Fig. 8: Glutamate photolysis decreases AP-evoked Ca^{2+} influx at Schaffer collateral boutons. (A) Top, CA3 hippocampal neurone in an organotypic slice loaded with OGB-1. The white box indicates presynaptic varicosities (boutons) along the Schaffer collaterals. Scale bar = 20 µm. Bottom, Enlarged image of the axon with several superficial boutons. The dashed orange line indicates line scanning through the bouton. Scale bar = 5 µm. (B) Top, Experimental setup: CA3 neurones were patched in whole-cell mode to elicit action potentials via current injection. A glass pipette attached to a picospritzer enabled delivery of MNI-glutamate to Schaffer collateral boutons. Focal uncaging at individual boutons was performed with a 405 nm laser. Bottom,

Rapid line scan imaging of bouton Ca^{2+} dynamics was performed to detect AP – evoked Ca^{2+} transients (APCaTs) with simultaneous glutamate uncaging. (Ci) Line scans of AP – evoked Ca^{2+} transients (APCaTs) with or without glutamate photolysis. Scale bar = 50 ms. (Cii) Traces of average APCaTs. Without glutamate = black, with glutamate = red. (Ciii) Trial-by-trial peak APCaTs.

As previously described in cortical neurones (Carter and Jahr, 2016), glutamate photolysis did not cause a significant rise in Ca^{2+}, even in conditions of low Mg^{2+} (Fig. 9C,D). One possible explanation is that Ca^{2+} entry may require additional membrane depolarisation. For this purpose, glutamate photolysis was coupled to an AP, evoked by intrasomatic current injection via the patch pipette into the neurone under study (Fig. 8B). The photolysis pulse was set to occur 0.5-2.5 ms after an AP to consider the physiological delay of AP propagation through the axon (Südhof, 2013). APs evoked robust Ca^{2+} transients, which will be referred to as APCaTs for the remainder of this thesis (Methods 3.3; Fig. 8C).

Unexpectedly, peak APCaTs in response to an AP paired with glutamate release between 0.5-2.5 ms following the onset of the AP, were substantially decreased compared to controls without glutamate photolysis (N = 9 boutons from 8 cells / 6 animals, ΔAPCaT = -0.402 ± 0.091 $\Delta F/F$; Fig. 8C, Fig. 10A). Controls without glutamate photolysis are defined as APCaTs without local glutamate supply but including activation of the photolysis laser, to exclude the possibility that our results are biased by potential artifacts by the UV-light. The decrease in APCaTs was consistent over multiple trials (Fig. 8C). *(Note that this experimental design will be replicated throughout Chapter 4, under varying external conditions).*

Given the strong Ca^{2+} permeability of NMDARs, an obvious outcome of preNMDAR activation would have been an increase in peak APCaTs, elicited

by glutamate photolysis. Due to the data showing the opposite effect, control experiments were performed to determine that the observed reduction in APCaTs represents the outcome of a biological process and is not a result caused by the experimental set-up (Fig. S4, Appendix). Notably, no change in APCaTs could be detected following glutamate photolysis at axon collaterals (Bouton vs. Collateral, p = 0.004; Mann Whitney test; Fig. S4E, Appendix).

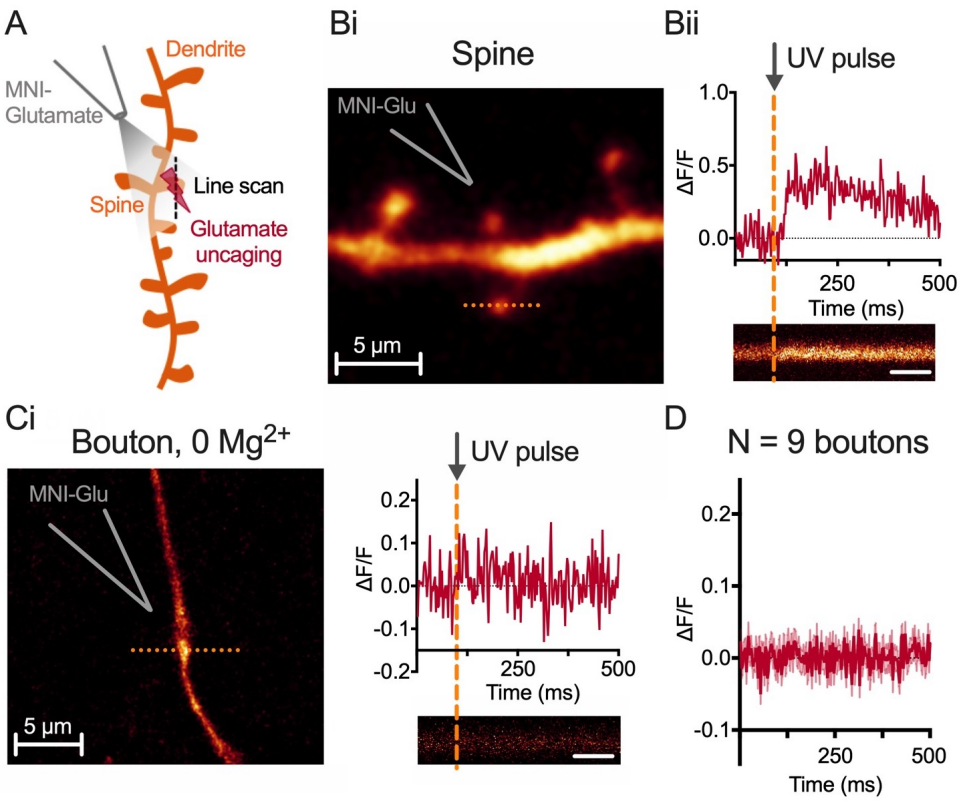

Fig. 9: Glutamate photolysis elicits Ca^{2+} transients in spines but not in boutons. (A) Schematic of glutamate photolysis and line scan imaging at dendritic spines of CA3 hippocampal neurones filled with OGB-1. (Bi) Example image of a dendrite from a CA3 neurone loaded with OGB-1. Scale bar = 5 µm. Orange dashed line indicates line scans through a spine at similar depth as boutons. (Bii) Line scan through a dendritic spine as indicated in Bi. Glutamate photolysis elicits postsynaptic Ca^{2+} transients. The UV uncaging laser was titrated at small spines to elicit a response of approximately 0.5 ΔF/F. Scale bar = 125 ms. (Ci) Left, Example image of a superficial bouton. Scale bar = 5 µm. Right, Example trace from a line scan through the bouton on the left. Scale bar = 125 ms. Glutamate photolysis in low Mg^{2+} did not elicit a Ca^{2+} response at Schaffer collateral boutons. (D) Average trace from 9 different boutons across three CA3 neurones.

To confirm that preNMDAR receptor activation by glutamate photolysis initiates the reduction in APCaTs, experiments were replicated with preNMDARs inhibited. AP5 is a selective NMDAR antagonist known to reliably block NMDAR signalling (McGuinness et al., 2010; Padamsey et al., 2017b). Bath application of AP5 (50 µM) completely abolished the decrease in APCaTs (N = 6 boutons from 4 cells / 3 animals, ΔAPCaT = -0.047 ± 0.024 ΔF/F; Fig. 10B,D).

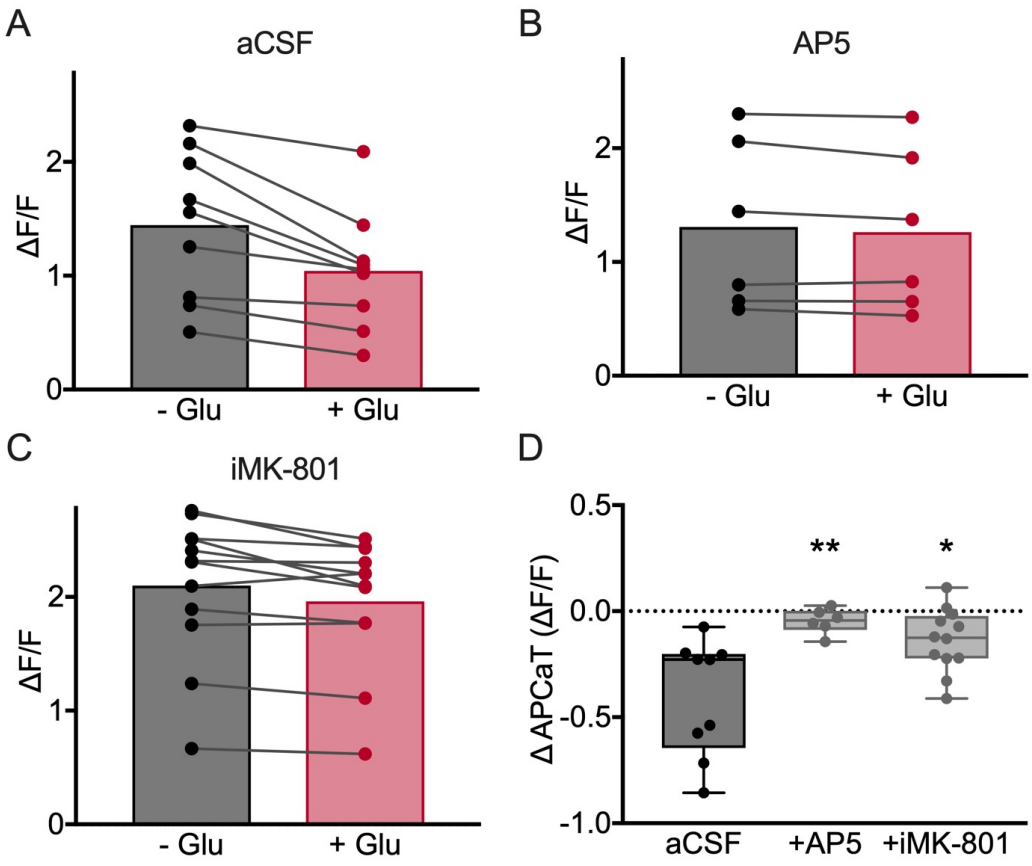

Fig. 10: Glutamate photolysis activates presynaptic NMDA receptors resulting in a reduction in AP-evoked Ca^{2+} influx at Schaffer collateral boutons. (A-C) Average peak APCaTs in aCSF, N = 9 (A) or in the presence of 50 µM AP5, N = 6 (B), 1 mM iMK801, N = 12 (C) to block preNMDARs. PreNMDAR inhibition diminished the reduction in APCaTs. (D) The difference in the peak amplitude between trials with and without glutamate (ΔAPCaT) is shown for control experiments in aCSF, experiments with 50 µM AP5 and 1 mM intracellular MK-801 ("iMK-801"). (AP5 vs. aCSF p = 0.003, N = 6; MK-801 vs. aCSF p = 0.037, N = 12; Kruskal-Wallis with post hoc Dunn's test). Error bars represent SEM.

Inhibition of neither metabotropic glutamate receptors (mGluRs) nor GABA receptors affected the reduction in APCaTs (Fig. S4, Appendix). MK-801, an open channel blocker of NMDARs, can be used to specifically block preNMDARs of the neurone under investigation, by loading the cell with MK-801 (1 mM) through the patch pipette (Nevian and Sakmann, 2006; Padamsey et al., 2017b). Thus, patch pipettes were filled with MK-801 (1 mM) in addition to OGB-1 diluted in internal solution (see Methods). Experiments conducted with intracellular MK-801 ("iMK-801", 1 mM) confirmed preNMDAR activation, and, consistent with the AP5 experiments the decrease in APCaTs was significantly blocked (N = 12 boutons from 8 cells / 5 animals, ΔAPCaT = -0.137 ± 0.043 ΔF/F; Fig. 10C,D).

In summary, AP-evoked Ca^{2+} entry into Schaffer collateral boutons was reduced when paired with glutamate photolysis. The application of AP5 to block NMDARs prevented the observed reduction. Furthermore, the presynaptic nature of NMDARs could be confirmed by using intracellular MK-801. Thus, the activation of presynaptic NMDA receptors decreases AP-evoked Ca^{2+} influx at Schaffer collateral boutons.

4.2.2. Presynaptic NMDA receptors and SK-channels form a negative feedback loop at Schaffer collateral boutons

How does the activation of preNMDARs lead to a reduction in AP-evoked Ca^{2+} transients? Small-conductance Ca^{2+}- activated K^+ channels (SK-channels) are known to form a Ca^{2+}-mediated negative feedback loop with NMDARs at postsynaptic terminals to reduce Ca^{2+} influx into spines (Faber, 2010; Griffith et al., 2016; Ngo-Anh et al., 2005). SK-channels are activated by NMDAR-

dependent Ca^{2+} influx and can, in turn, negatively regulate NMDAR activity which is why they are considered of relevance in synaptic plasticity processes (Faber, 2010; Griffith et al., 2016; Ngo-Anh et al., 2005). Moreover, SK-channels are well established as shaping the action potential wave form (Bond et al., 2005; Faber and Sah, 2007, 2002; Sah and Faber, 2002; Xia et al., 1998), impacting on the dynamics of presynaptic voltage-gated Ca^{2+} channels and ultimately p_r (Bean, 2007; Chéreau et al., 2017; Hoppa et al., 2014). Protein signalling motifs are commonly repurposed to serve different functional outcomes, thus, downstream targets of postsynaptic NMDARs may also exist at the presynaptic terminal. Notably, it has already been demonstrated that SK-channels and NMDARs are colocalised at the presynaptic terminal (Nanou et al., 2013; Ngo-Anh et al., 2005). Based on this evidence, I hypothesised that NMDAR/SK-channel interactions may also be present in Schaffer collateral presynaptic terminals to modulate the action potential evoked Ca^{2+} influx.

For this purpose, I repeated glutamate photolysis experiments following bath-application of the SK channel inhibitor apamin (1 µM; Fig. 11). Apamin is noted to selectively block the SK-channel subtypes SK2 and SK3 in neurones (Köhler et al., 1996; Lamy et al., 2010). Indeed, apamin (1 µM) application abolished the glutamate photolysis-induced decrease (N = 6 boutons, ΔAPCaT = -0.037 ± 0.041 ΔF/F; Fig. 11A-C). Control experiments in aCSF produced a significant reduction in Ca^{2+} transients which was prevented if SK-channels were previously blocked with apamin (apamin vs. aCSF, p = 0.003; Mann Whitney test; Fig. 11C).

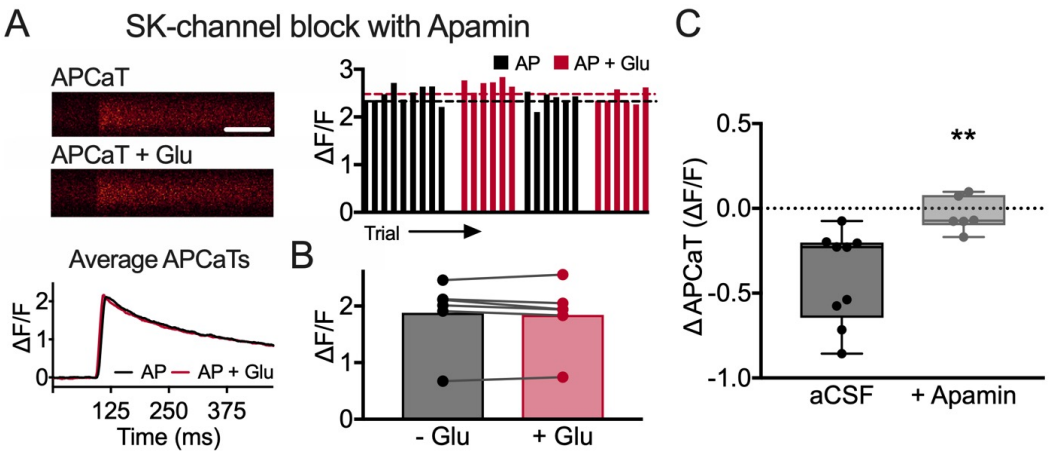

Fig. 11: PreNMDARs modulate AP-evoked Ca^{2+} influx via the activation of SK-channels. (A) Top, Left, Line scans of APCaTs following SK – channel inhibition with 1 µM apamin. Scale bar = 125 ms. Bottom, Left, Traces of average APCaTs. Without glutamate = black, with glutamate = red. Top, Right, Trial-by-trial peak APCaTs following pre-incubation with apamin. No difference in peak APCaTs can be observed with (red) or without (black) glutamate photolysis. (B) Average peak APCaTs in 1 µM apamin. The reduction in peak APCaTs was diminished after SK - channel inhibition, N = 6. (C) The difference in the peak amplitude of APCaTs is shown for experiments in aCSF, N = 9 (from Fig. 10) and experiments with 1 µM apamin (apamin vs. aCSF, p = 0.003; Mann Whitney test). Error bars represent SEM.

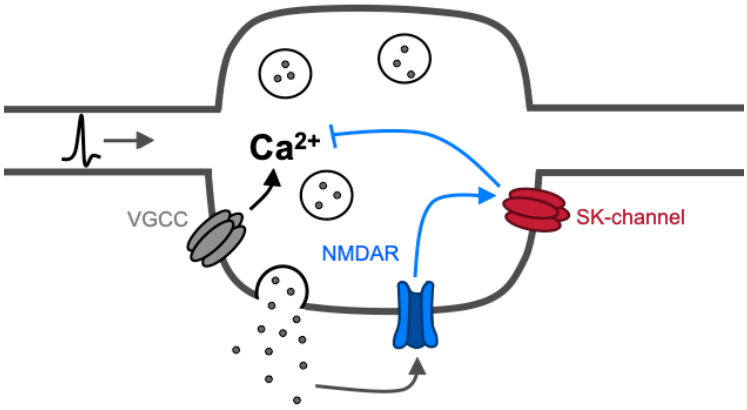

Fig. 12: SK channels and NMDA receptors form a negative feedback loop in Schaffer collateral boutons. Glutamate binds and activates presynaptic NMDARs which leads to local Ca^{2+} influx. The NMDAR-dependent Ca^{2+} influx activates SK-channels, likely accelerating the repolarisation of the membrane potential due to sharpening of the AP waveform. Subsequently, this leads to the closure of voltage-gated Ca^{2+} channels (VGCCs), thus, a reduction in Ca^{2+} influx into the bouton.

In summary, the data strongly support the idea that the activation of preNMDARs leads to the opening of SK-channels likely sharpening the action potential waveform, which in turn reduces the amount of Ca^{2+} entering the cell (Fig. 12). In other words, I have shown that preNMDARs and SK-channels form a Ca^{2+} mediated negative feedback loop at Schaffer collateral boutons (Fig. 12).

4.2.3. Activation of extrasynaptic presynaptic NMDA receptors causes a decrease in AP-evoked Ca^{2+} influx

The lack of direct Ca^{2+} entry following glutamate photolysis and the glutamate-induced decrease in APCaTs, are outcomes quite different to those seen for postsynaptic NMDARs, suggesting that preNMDARs are regulated and function in a different way than their postsynaptic relatives. It is already known that synaptic versus extrasynaptic NMDARs have different Ca^{2+} permeabilities and exert differential effects also on synaptic plasticity postsynaptically (Hardingham and Bading, 2010). Whether similar principles apply to preNMDARs is not known. Therefore, I asked whether extrasynaptic preNMDARs are coupled to SK-channels and mediate the decrease in bouton Ca^{2+} influx previously observed. For this purpose, I followed the protocol from Liu et al. using the NMDAR blocker MK-801 to silence synaptic preNMDARs (Liu et al., 2013; Fig. 13A). Synaptic preNMDARs were selectively blocked by preincubating slices with MK-801 (20 µM) for 20 minutes and subsequently delivering a short train of LFS (5 Hz/16 s) in the presence of MK-801 (Liu et al., 2013). Given that MK-801 is an open-channel blocker, only NMDARs that are active in the presence of MK-801 are blocked. Low-frequency stimulation preferably activates synaptic preNMDARs, thus, following complete MK-801 washout, synaptic preNMDARs are silenced while extrasynaptic preNMDARs remain active (Hardingham et al.,

2002; Liu et al., 2013). Next, I used glutamate photolysis to trigger the activation of the remaining population of preNMDARs (supposedly extrasynaptic) and examine its effect on boutonal Ca^{2+} by analysing APSCaTs (Fig. 13).

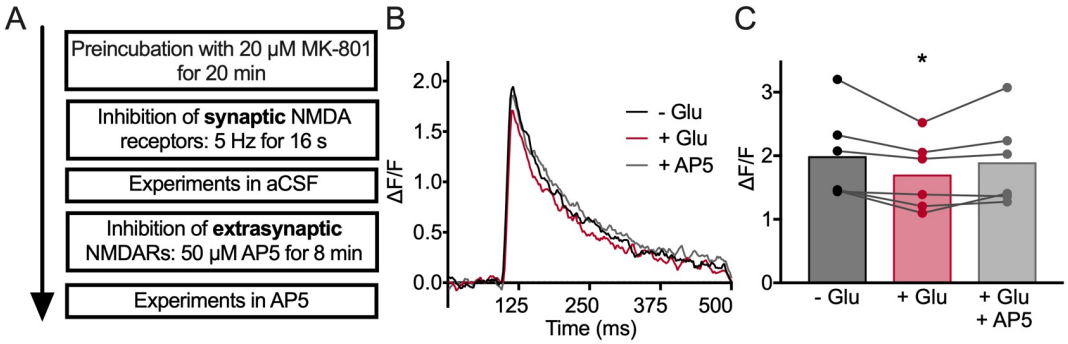

Fig. 13: Activation of extrasynaptic presynaptic NMDARs contributes to the decrease in AP-evoked Ca^{2+} transients induced by glutamate photolysis. (A) Experimental protocol to specifically silence preNMDAR populations. (B) Average APCaTs in CA3 boutons before (black and red trace) and after (grey trace) extrasynaptic preNMDARs have been blocked. Without glutamate = black trace, with glutamate = red trace and grey trace. (C) Average peak APCaTs following silencing of synaptic preNMDARs for control experiments with (+Glu) or without (-Glu) glutamate photolysis in aCSF and experiments in AP5 (50 µM). Significance was assesed with ANOVA followed by a post-hoc test (n = 6 cells).

As pointed out earlier, in control experiments, the photolysis laser was triggered but no MNI-glutamate was present. Following silencing of synaptic preNMDARs, a slight but significant reduction in Ca^{2+} transient could be observed when glutamate was uncaged compared to the control experiment without glutamate (N = 6 boutons from 6 cells / 2 animals, APCaT/control = 1.90 ± 0.30 ΔF/F; APCaT/+Glu = 1.60 ± 0.20 ΔF/F; p = 0.009; ANOVA followed by a post-hoc test; Fig. 13B,C). As a control, AP5 was bath applied (50 µM) to block all remaining preNMDARs including the extrasynaptic preNMDAR population. Notably, under these conditions peak APCaTs in response to AP stimulation paired with glutamate photolysis recovered almost back to baseline

(APCaT/+Glu+AP5 = 1.80 ± 0.30; p = 0.056; Fig. 13B,C). This data supports the idea that preNMDARs responsible for the reduction in bouton Ca^{2+} influx might be partially located at extrasynaptic sites.

4.2.4. Activation of GluN2B subunit containing presynaptic NMDA receptors decreases AP-evoked Ca^{2+} influx at Schaffer collateral boutons

Apart from synaptic versus extrasynaptic localisation, another source explaining the unexpected Ca^{2+} reduction mediated by preNMDARs could be the subunit composition of preNMDARs. To characterise the subunit composition of preNMDARs on Schaffer collaterals in the experimental system, I repeated the experiments from before with NMDAR antagonists that have a preferential affinity for specific subunits. I started with the well-established and highly specific GluN2B subunit antagonist Ro - 25 6981 (Fischer et al., 1997).

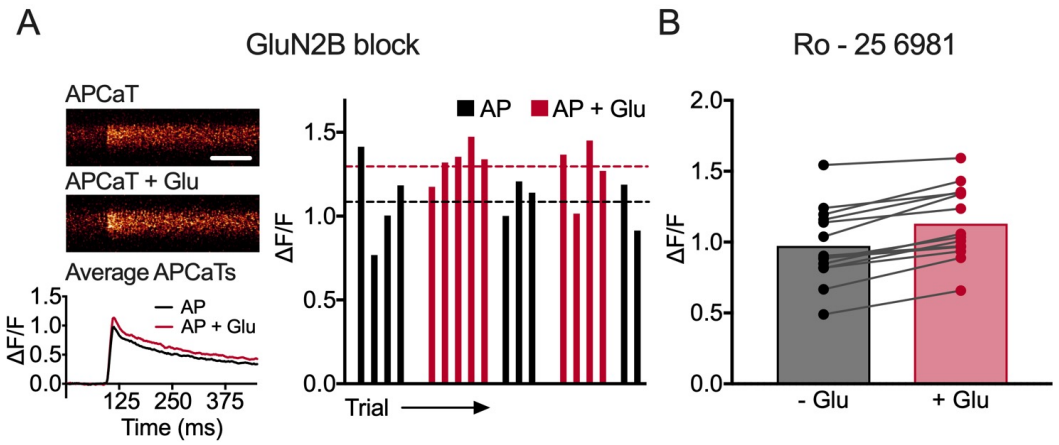

Fig. 14: The GluN2B subunit decreases AP-evoked Ca^{2+} influx at Schaffer collateral boutons. (A) Top left, Line scans of APCaTs following GluN2B inhibition with 1 µM Ro – 25 6981. Scale bar = 125 ms. Bottom left, Traces of average APCaTs. Without glutamate = black, with glutamate = red. Right, Trial-by-trial peak APCaTs following bath application of 1 µM Ro – 25 6981. (B) Average peak APCaTs in 1 µM Ro – 25 6981. GluN2B inhibition unmasks an increase in peak APCaTs, N = 14.

Bath application of Ro - 25 6981 (1 µM) not only prevented the previously described reduction Ca^{2+} influx but produced an increase in APCaTs (N = 14 boutons from 9 cells / 4 animals, ΔAPCaT = 0.157 ± 0.02 ΔF/F; Fig. 14). The increase in APCaTs was consistent over trials (Fig. 14A) and experiments (Fig. 14B). Thus, I have shown that the GluN2B subunit causes the preNMDAR/SK-channel mediated negative regulation of Ca^{2+} influx into Schaffer collateral boutons.

4.2.5. Activation of GluN2A subunit containing presynaptic NMDA receptors increases AP-evoked Ca^{2+} influx via SK-channels

The previous results motivated me to explore the idea, whether there is another population of preNMDARs mediating an increase in glutamate evoked AP-evoked Ca^{2+} influx at Schaffer collateral boutons. Therefore, I performed control experiments to test if the increase in AP-evoked Ca^{2+} influx is indeed preNMDAR mediated.

Firstly, I reproduced the glutamate photolysis experiments from 4.2.4. in aCSF unmasking an increase in AP-evoked Ca^{2+} influx when GluN2B was blocked with Ro – 25 6981 (1 µM). Next, I investigated the effects of several inhibitors, to characterise the origin of the increase in bouton Ca^{2+}. In paired experiments, where the NMDAR blocker AP5 was bath-applied at the end, the increase in APCaTs was abolished (N = 6 boutons from 6 cells / 2 animals, ΔAPCaT/+Glu = 0.148 ± 0.045 ΔF/F; ΔAPCaT/+Glu+AP5 = -0.054 ± 0.037 ΔF/F; Fig. 15A). Similar results were obtained if preNMDARs were blocked intracellularly with MK-801 (N = 6 boutons from 4 cells / 3 animals, ΔAPCaT = -0.074 ± 0.068 ΔF/F; Fig. 15B). I thought it important to assess whether intracellular Ca^{2+}

stores represented a potential source for the observed increase in Ca^{2+}. For this purpose, I used cyclopiazonic acid (CPA), a specific blocker of smooth endoplasmic reticulum Ca^{2+}/ ATPases and ryanodine, a specific blocker of the ryanodine receptor (RyR) Ca^{2+} channel (Emptage et al., 1999). Both drugs serve as inhibitors of calcium-induced calcium release (CICR).

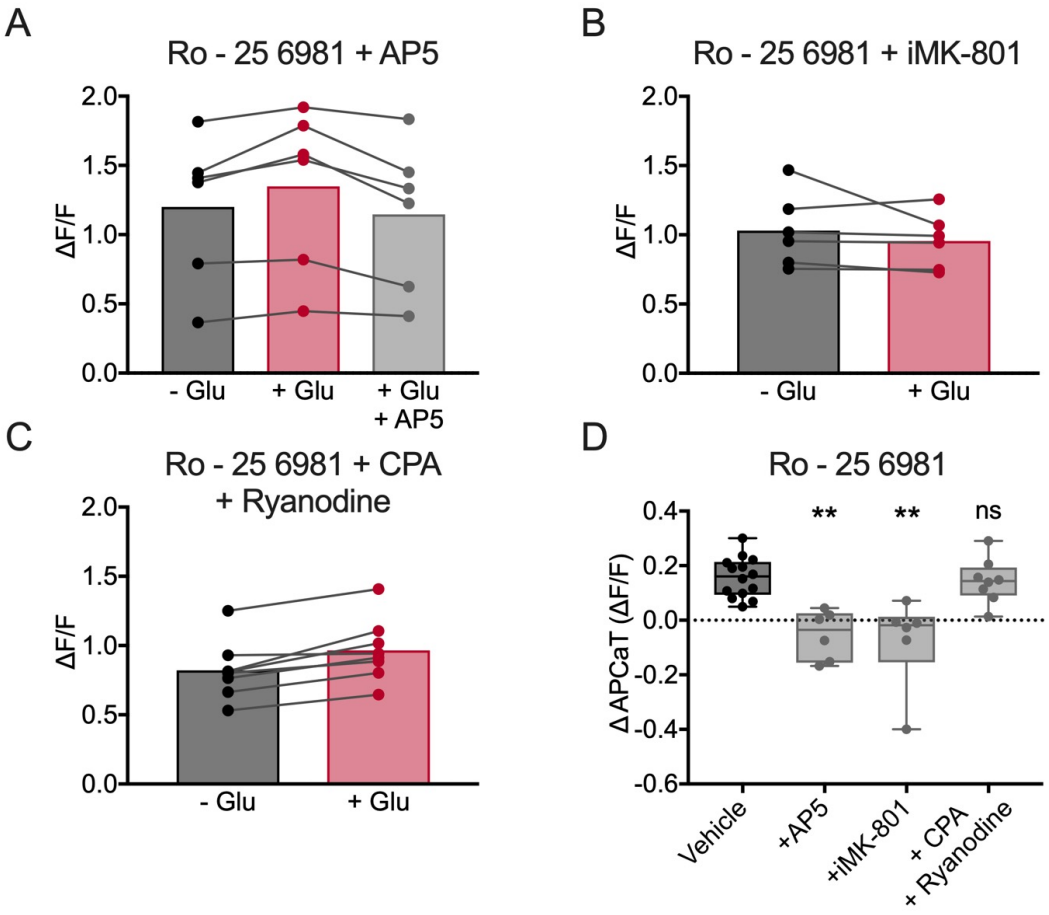

Fig. 15: The increase in AP-evoked Ca^{2+} influx following GluN2B inhibition is preNMDAR dependent. (A-C) Average peak APCaTs in 1 µM Ro – 25 6981 in the presence of 50 µM AP5, N = 6 (A) or 1 mM iMK801, N = 6 (B) to block preNMDARs and in the presence of CPA (15 µM) and ryanodine (20 µM) to block Ca^{2+} release from intracellular stores, N = 8 (C). PreNMDAR inhibition diminished the increase in APCaTs. Prevention of Ca^{2+} release from intracellular stores did not affect the increase in APCaTs. (D) The difference in the peak amplitude between trials with and without glutamate (ΔAPCaT) is shown for experiments in 1 µM Ro – 25 6981: vehicle experiments (from Fig. 14), experiments with 50 µM AP5, 1 mM intracellular MK-801 ("iMK-801") and 15 µM CPA/ 20 µM ryanodine. In Ro – 25 6981: AP5 vs. Vehicle p = 0.002, N = 6; MK-801 vs. Vehicle p = 0.002, N = 6; 15 µM CPA/ 20 µM ryanodine vs. Vehicle p > 0.99, N = 8; Kruskal-Wallis with post hoc Dunn's test. Error bars represent SEM.

Application of CPA (15 µM) and ryanodine (20 µM) did not affect the increase in APCaTs (N = 8 boutons from 6 cells / 3 animals, ΔAPCaT = 0.144 ± 0.029 ΔF/F; Fig. 15C,D). Thus, while preNMDAR inhibition fully blocked the increase in APCaTs, the prevention of CICR did not, suggesting a preNMDAR dependent but CICR independent mechanism (AP5 vs. Vehicle p = 0.002, N = 6; iMK801 vs. vehicle p = 0.002, N = 6; CPA/ryanodine vs. vehicle p > 0.99, N = 8; Kruskal-Wallis with post hoc Dunn's test; Fig. 15D).

Having established that a second population of preNMDARs is present at presynaptic terminals, that do not contain the GluN2B subunit, an obvious question arised: Which preNMDAR subunit mediates the glutamate triggered increase in APCaTs?

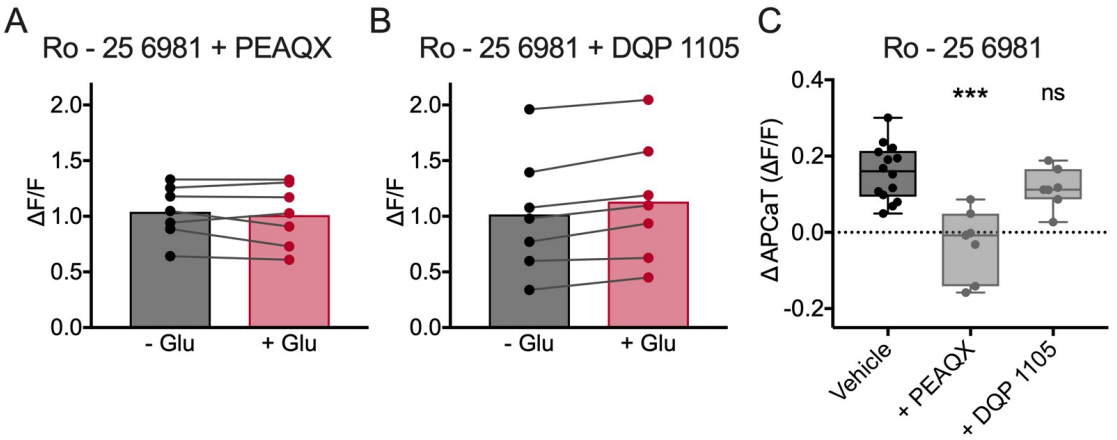

Fig. 16: The GluN2A subunit mediates the increase in AP-evoked Ca^{2+} influx following GluN2B inhibition. (A,B) Average peak APCaTs in 1 µM Ro – 25 6981 in the presence of 100 nM PEAQX, N = 7 (A) or 50 µM DQP 1105, N = 7 (B) to block preNMDAR subunits. GluN2A inhibition diminished the increase in APCaTs whereas GluN2C/D blockade did not. (C) ΔAPCaT is shown for experiments in 1 µM Ro – 25 6981: vehicle experiments (from Fig. 14), experiments with 100 nM PEAQX and 50 µM DQP 1105 (in Ro – 25 6981: PEAQX vs. Vehicle p < 0.001, N = 7; DQP 1105 vs. Vehicle p = 0.77, N = 7; Kruskal-Wallis with post hoc Dunn's test). Error bars represent SEM.

To investigate the subunit composition of the second preNMDAR population, I used the GluN2A subunit inhibitor PEAQX and the GluN2C/D inhibitor DQP 1105 (Fig. 16). I performed similar glutamate photolysis and Ca^{2+} imaging experiments as before and all experiments were performed in Ro – 25 6981 (1 µM), which produced increases in AP- evoked Ca^{2+} influx as previously shown. Inhibition of the GluN2A subunit using PEAQX (100 nM) completely abolished the increase (N = 7 boutons from 6 cells / 3 animals, ΔAPCaT = -0.029 ± 0.034 ΔF/F; Fig. 16A,C), whereas inhibition of the GluN2C/D subunits using DQP 1105 (50 µM) had no effect (N = 7 boutons from 5 cells / 3 animals, ΔAPCaT = 0.116 ± 0.02 ΔF/F; Fig. 16B,C). Notably, PEAQX application alone preserved the decrease in APCaTs (N = 10 boutons, ΔAPCaT = -0.10 ± 0.02 ΔF/F; Fig. 17).

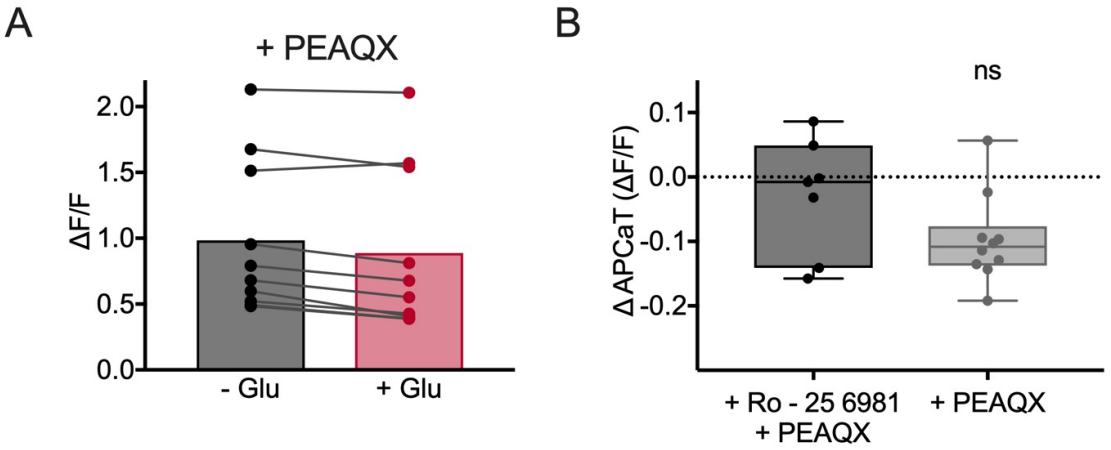

Fig. 17: GluN2A subunit inhibition preserves the decrease in AP-evoked Ca^{2+} influx in aCSF. (B) Average peak APCaTs in 100 nM PEAQX. A reduction in peak APCaTs can be observed following GluN2A inhibition in aCSF, N = 10. (C) The difference in the peak amplitude of APCaTs is shown for experiments in 100 nM PEAQX either in aCSF, N = 10 or following GluN2B inhibition with 1 µM Ro – 25 6981, N = 7 (PEAQX + Ro – 25 6981 vs. PEAQX alone, $p > 0.99$; Mann Whitney test). Error bars represent SEM.

I have already shown that the negative regulation of Ca^{2+} influx, caused by the GluN2B subunit, is mediated through SK-channels. Next, I examined whether the increase in Ca^{2+} influx resulting from the activation of GluN2A containing preNMDARs, also involves SK-channels. Hence, I used the SK-channel blocker apamin to test whether the increase in Ca^{2+} influx could be prevented by SK-channel blockade (Fig. 18). Indeed, apamin fully abolished the increase in APCaTs as mediated by Ro – 25 6981 (N = 9 boutons from 7 cells / 3 animals, ΔAPCaT = -0.029 ± 0.034 ΔF/F; Fig. 18A-C). This suggests that activation of the GluN2A containing preNMDAR population regulates bouton Ca^{2+} dynamics via downstream SK-channels (Fig. 18).

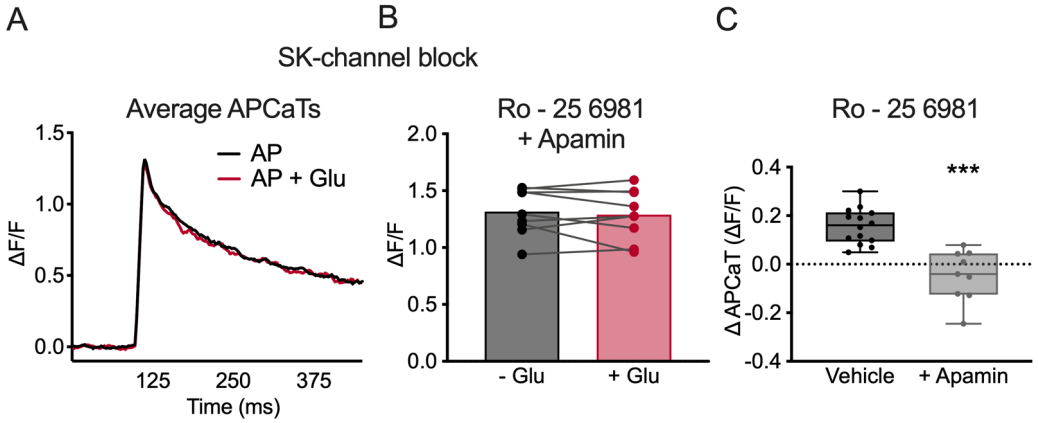

Fig. 18: The GluN2A subunit mediated increase in AP-evoked Ca^{2+} influx is mediated via SK-channels. (A) Average peak APCaTs in 1 µM Ro – 25 6981 and 1 µM apamin. (B) No difference in peak APCaTs with (red) or without (glutamate) can be observed following GluN2B and SK-channel inhibition, N = 9. (C) The difference in the peak amplitude of APCaTs is shown for experiments in 1 µM Ro – 25 6981 either with (grey, N = 9) or without (black, N = 12; from Fig. 14) apamin (Vehicle vs. apamin, $p < 0.001$; Mann Whitney test). Error bars represent SEM.

In summary, using Ca^{2+} imaging coupled to focal glutamate uncaging, I have identified two distinct populations of preNMDARs that bidirectionally modulate Ca^{2+} dynamics at Schaffer collateral boutons, containing either GluN2B or GluN2A subunits (Fig. 19). The acute activation of these preNMDARs either

decreased (GluN2B) or enhanced (GluN2A) action potential (AP)-evoked Ca^{2+} influx. Further I have shown that each preNMDAR population triggers a cascade of intracellular signalling events, which converge upon SK-channels (Fig. 19). Subsequently, SK-channel activation modulates the AP waveform and VGCC activity thereby affecting the amount of Ca^{2+} entering the bouton. Additionally, the data implies that extrasynaptically located preNMDARs partially drive these mechanisms.

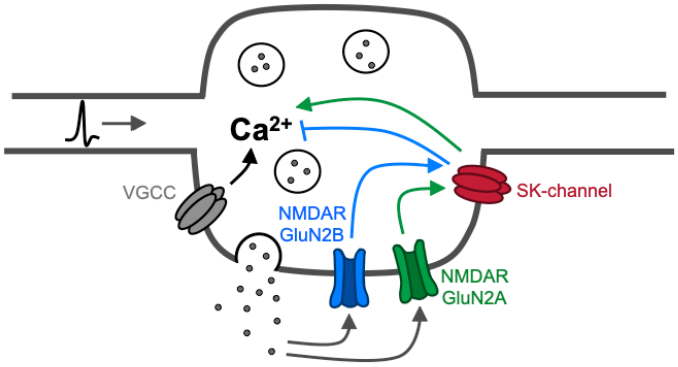

Fig. 19: Two preNMDAR sub-populations bidirectionally regulate Ca^{2+} dynamics at Schaffer collateral boutons. Glutamate binds and activates two distinct presynaptic NMDAR subpopulations containing either GluN2B or GluN2A subunits. Both subpopulations regulate Ca^{2+} dynamics via SK-channel activity. Depending on which population is activated, Ca^{2+} influx into the bouton is either decreased (GluN2B) or increased (GluN2A).

4.2.6. Glutamate photolysis-induced Ca^{2+} influx at Schaffer collateral boutons following GluN2B inhibition

The previous data showed that different preNMDAR subpopulations can exert opposing functional rules suggesting that preNMDAR signalling at boutons is more complex than initially anticipated. Similar to other studies, preNMDAR-dependent modulation of Ca^{2+} was investigated by pairing preNMDAR

activation with APs (Buchanan et al., 2012).

After unmasking an increase in Ca^{2+} transients by inhibiting the GluN2B subunit, I wondered whether a direct Ca^{2+} influx through preNMDARs elicited by glutamate photolysis could be detected in such conditions. Previously, glutamate photolysis even in low-Mg^{2+} did not produce any measurable Ca^{2+} transients at boutons (Fig. 9).

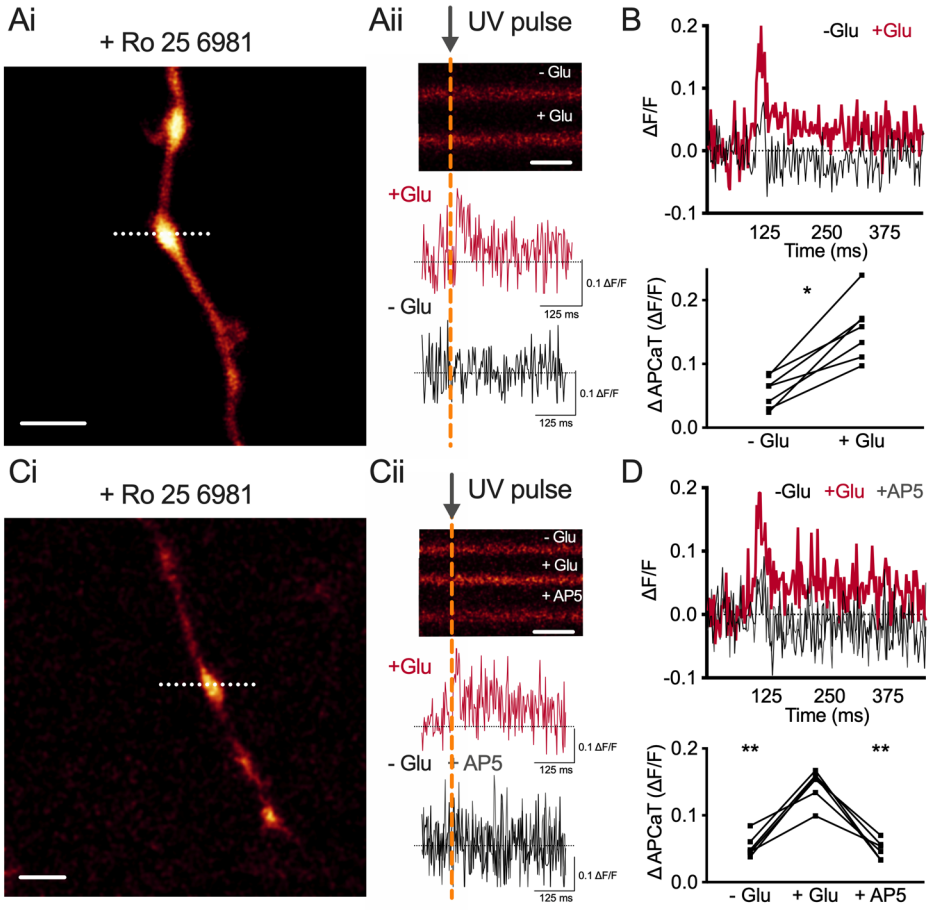

Fig. 20: Glutamate uncaging induced Ca^{2+} influx at Schaffer collateral boutons following GluN2B inhibition. (Ai) Line scans through boutons of CA3 neurones loaded with OGB-1. Scale bar = 5 µm. (Aii) Blockage of GluN2B subunits with 1 µM Ro – 25 6981 unmasked an increase in Ca^{2+} following glutamate uncaging in low Mg^{2+}, Scale bar = 50 ms. (B) Top, Average Ca^{2+} transient following glutamate uncaging (N = 7 boutons, p = 0.016; Wilcoxon signed rank test). Bottom, GluN2B inhibition unmasked an increase in Ca^{2+} influx at all boutons tested. (C,D) Application of AP5 blocked the Ca^{2+} increase (N = 6 boutons, -Glu vs +Glu: p = 0.009, +Glu vs AP5: p = 0.005; Kruskal-Wallis with post hoc Dunn's test).

Thus, I performed line scan imaging through boutons while uncaging glutamate at Schaffer collateral boutons (similar to Fig. 9) under the GluN2B inhibitor Ro – 25 6981 (1 µM; Fig. 20). Surprisingly, when isolating the GluN2A subunit, a small Ca^{2+} influx through the preNMDARs is unmasked (N = 7 boutons from 6 cells / 2 animals, ΔAPCaT = -0.098 ± 0.016 ΔF/F; Fig. 20A,B). This increase in Ca^{2+} was blocked by subsequent bath-application of AP5, confirming that the elevated Ca^{2+} levels within the bouton effectively stem from preNMDARs (N = 6 boutons from 4 cells / 2 animals, ΔAPCaT/+Glu = 0.092 ± 0.013 ΔF/F; ΔAPCaT/+Glu+AP5 = -0.005 ± 0.010 ΔF/F; Fig. 20C,D).

4.3. Discussion

I have shown that the activation of two different preNMDAR subunit populations at Schaffer collateral boutons bidirectionally regulates Ca^{2+} dynamics at presynaptic terminals. The activation of preNMDARs containing the GluN2B subunit, results in a negative feedback-loop via SK-channels and decreases Ca^{2+} influx into the cell. Signalling through preNMDARs with the GluN2A subunit causes an increase of Ca^{2+} influx into the bouton. In this study, preNMDAR receptors are activated by glutamate photolysis paired with an action potential. Some studies suggest, that preNMDAR activation requires additional membrane depolarisation or other co-agonists such as d-serine or glycine (Banerjee et al., 2016). The intrasomatically elicited action potentials in this study cause vesicle release of glutamate and, maybe, other co-agonists potentially facilitating preNMDAR activity. However, in final experiments, I was able to detect Ca^{2+} transients through preNMDARs simply by glutamate photolysis (Fig. 20). Notably, co-agonists could always be present extracellular in the synaptic cleft, and not dependent on vesicle release. Intriguingly, it has

been demonstrated that preNMDAR function requires glycine binding in the cortex, however, it was also suggested that the glycine site on preNMDARs might be saturated in physiological conditions (Corlew et al., 2008; Li and Han, 2007). Thus, if preNMDARs in this study are co-activated by additional agonists, perhaps by glycine, remains to be explored, potentially via caged-compounds of the latter (Klausen et al., 2019).

AP5 is a selective NMDAR antagonist known to block both ionotropic and metabotropic effects associated with NMDAR activation and is widely used to block NMDARs in the CNS (50 µM; McGuinness et al., 2010; Nabavi et al., 2013; Padamsey et al., 2017b). However, it might be possible that observed presynaptic effects are due to electrotonic spread or cross effects from postNMDARs (see Carter and Jahr, 2016). To prevent the activation of postNMDARs, AMPAR activity was inhibited (10 µM NBQX) in all experiments. Moreover, in this study two sets of experiments were generally performed, blocking NMDARs either with AP5 or MK-801. While bath-application of AP5 globally inhibits NMDARs, using MK-801 in the internal solution allows to specifically target preNMDARs. As it is cell-impermeable, MK-801 could be used in the patch electrode to block NMDARs terminals specifically from the cell under investigation. Therefore, a contribution from postsynaptic NMDARs can be excluded.

Within the hippocampus a large variety of NMDAR subunits and isoforms can be found, while the GluN2 subunit diversity mostly determines the receptor's functional identity (Paoletti, 2011; Paoletti et al., 2013). In this study, I focused on GluN2B and GluN2A as they are both predominantly expressed in the adult hippocampus. In contrast, GluN2C and GluN2D expression levels in the adult

brain are considerably lower and mostly present in the cerebellum and the brainstem, respectively (Monyer et al., 1994; Paoletti, 2011; Paoletti et al., 2013; Sanz-Clemente et al., 2013; Wyllie et al., 2013). This fits with the results obtained from experiments where I inhibited GluN2C/D, which had no effect on the preNMDAR-mediated modulation of Ca^{2+}. The vast majority of studies on preNMDAR subunit diversity focused on the postsynaptic terminal, however, both GluN2A and GluN2B signalling has been shown at presynaptic terminals (Bidoret et al., 2009; McGuinness et al., 2010). Biophysical and pharmacological receptor properties are strongly dependent on subunit profiles. While GluN2A and GluN2B show similar characteristics for Ca^{2+} permeability, sensitivity to Mg^{2+} blockade, and channel opening conductance, GluN2A-containing receptors deactivate much faster and show lower agonist sensitivity for glutamate and glycine (Paoletti, 2011; Paoletti et al., 2013). Diheteromeric NR1/NR2 receptors have been studied intensively, however, over the recent years more and more studies focus on triheteromeric NMDARs, indicating an even broader functional diversity. I cannot exclude the possibility that NR1/NR2A/NR2B triheteromers are activated in this study, as the literature indicates their expression and function at adult hippocampal postsynaptic and presynaptic terminals (Cull-Candy and Leszkiewicz, 2004; Dubois et al., 2016; Köhr, 2006; Paoletti and Neyton, 2007; Rauner and Köhr, 2011; Stroebel et al., 2018). Due to technical limitations it remains challenging to distinguish between distinct functions of triheteromeric and mixed diheteromeric NMDAR populations.

Data from this study can be interpreted to characterise preNMDAR function with regards to their localisation. As control experiments, I performed line scans

through several axon collaterals and could not detect any difference in Ca^{2+} signal induced by glutamate photolysis, compared to controls (McGuinness et al., 2010). This confirms that the observed Ca^{2+} regulatory effects derive from preNMDARs located at the bouton. However, the data provides some evidence that extrasynaptic preNMDARs mediate the Ca^{2+} dependent negative feedback loop into boutons. Differences between extrasynaptic and synaptic NMDA receptors have been extensively studied postsynaptically (Hardingham and Bading, 2010) and it is known that both GluN2B and GluN2A are localised at synaptic as well as extrasynaptic sites (Köhr, 2006; Lozovaya et al., 2004; Paoletti et al., 2013; Sanz-Clemente et al., 2013; Thomas et al., 2006; Wyllie et al., 2013). The uncaging spot in the experimental system is bigger than the bouton under investigation, which means that glutamate is also uncaged at extrasynaptic areas. Superresolution microscopy revealed, that receptors are typically arranged in clusters at synaptic terminals (MacGillavry et al., 2013). Thus, it could be hypothesised that the preNMDAR population containing the GluN2B subunit and mediating the decrease in Ca^{2+} influx is preferably localised extrasynaptically, while preNMDARs comprising GluN2A positively regulating Ca^{2+} dynamics are localised synaptically. Further experiments confirming the extrasynaptic nature of preNMDARs in our system are needed, but are difficult to execute. Mostly because there are no suitable techniques to fully separate synaptic from extrasynaptic preNMDARs. Even with the protocol used in this study and by others (Liu et al., 2013), a clear separation of synaptic and extrasynaptic function is not ensured. One possibility could be to improve the experimental set-up and use two-photon instead of one-photon uncaging (Tong et al., 2021), increasing precision of the uncaging laser which may give

clearer results about the exact localisation of the preNMDARs involved.

Whether the preNMDARs investigated in this work are of triheteromeric or diheteromeric, synaptic or extrasynaptic nature is unknown. Even though some effort has been made to image preNMDAR dynamics with confocal imaging (Gill et al., 2015), visualising specific receptor subunits, their dynamics, and distribution at presynaptic terminals requires higher resolutions. Superresolution microscopy techniques such as PALM or STORM have been used to investigate nanodomain organisations on synaptic terminals (Dani et al., 2010; MacGillavry et al., 2013). Notably, results from such studies indicate that the distribution of receptors shows a broad heterogeneity between individual synapses including perisynaptic and synaptic clustering (Dani et al., 2010). Such single-molecule imaging studies are typically performed in dissociated hippocampal neurones, since autofluorescence background is limited in cell cultures, while prominent in slices.

During my DPhil, I was able to participate in the *Frontiers in Neurophotonics Summer School* in Quebec. During a mini project, I tried superresolution imaging of preNMDARs using a STED microscope. Even labelling preNMDARs in fixed neurones was challenging, as the NMDAR antibodies created a lot of unspecific labelling background (see Fig. 21). Nevertheless, I could detect some GluN2B enrichment at boutons (Fig. 21) and new NMDAR labelling methods are constantly being developed (Neubert et al., 2018). In the future, improved labelling and microscopy techniques will enable imaging of preNMDAR subunits in slices or even *in vivo* and enormously advance our understanding about preNMDAR localisation, arrangement and function.

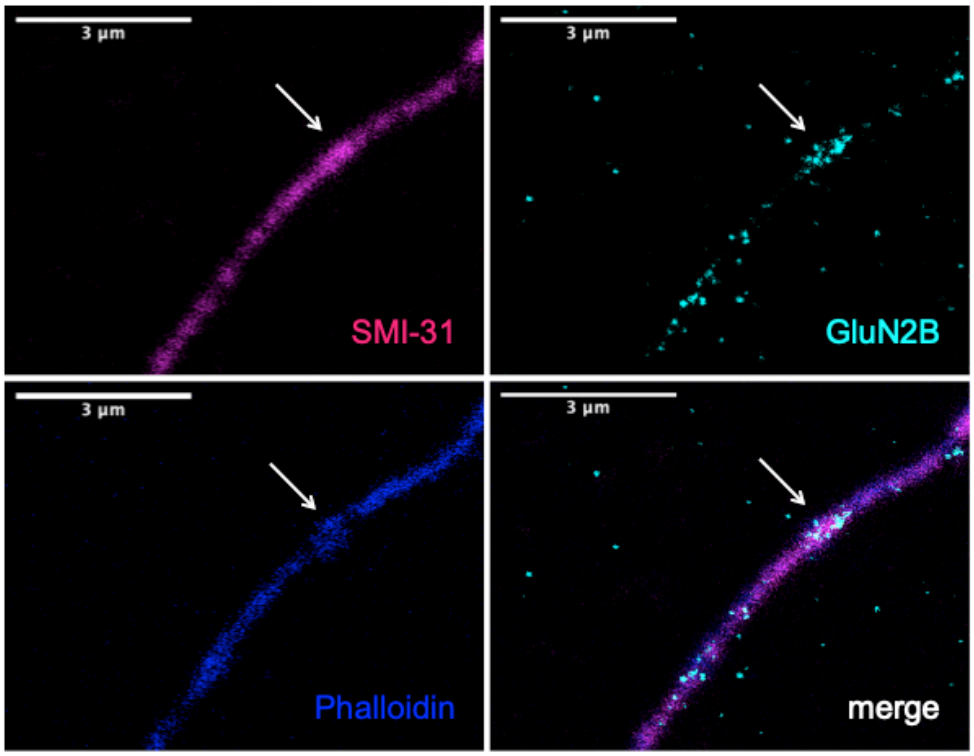

Fig. 21: STED imaging of preNMDARs in fixed hippocampal neurones. STED images were recorded during the *Frontiers in Neurophotonics Summer School* with help from Theresa Wiesner, Andréanne Deschênes and Flavie Lavoie-Cardinal from the CERVO Brain Research Centre, Québec. GluN2B puncta representing preNMDARs are accumulated in boutons. However, the attempt to label preNMDARs for STED imaging resulted in a lot of unspecific background labelling. Antibodies targeted SMI-31 = anti Neurofilament expressed predominantly in axons, GluN2B, and phalloidin = f-actin binding.

Superresolution microscopy could also improve our understanding of how individual subunit expression varies from bouton to bouton. It has been argued that cortical preNMDARs are only expressed in a subset of axonal boutons (Buchanan et al., 2012), however, in this study preNMDAR function could be recorded at all examined boutons. Notably, the relative expression of preNMDAR subpopulations in individual boutons may vary, as different effect sizes could be recorded in different boutons. Alternative experiments with different system equipment could be performed where glutamate is simultaneously uncaged at different boutons, as it was already done on spines

(Tong et al., 2021). Thereby, mechanistic differences of individual boutons located on the same axon could be thoroughly investigated.

It is well known that SK-channels are activated by Ca^{2+} influx through NMDARs (Faber et al., 2005; Lin et al., 2008; Shah and Haylett, 2002) resulting in hyperpolarisation, which subsequently reduces Ca^{2+} influx through VGCCs (Bond et al., 2005; Faber and Sah, 2007; Griffith et al., 2016). This negative feedback relationship between NMDARs and SK channels has been intensively studied at postsynaptic terminals (Faber, 2010; Griffith et al., 2016; Narasimhan, 2005; Ngo-Anh et al., 2005), while SK-channels and NMDARs are also colocalised at presynaptic terminals (Nanou et al., 2013; Ngo-Anh et al., 2005). In this study, I confirmed this negative feedback interaction and related it to the GluN2B subunit. In addition, I showed that the GluN2A subunit forms a positive feedback loop with SK-channels. Such a bidirectional subunit dependent regulation at the synapse is a common theme, considering the fact that postsynaptic NMDAR subunit populations can cause opposing effects on plasticity in the hippocampus (Fox et al., 2006; Liu et al., 2004; Massey et al., 2004; Shipton and Paulsen, 2014).

Both mechanisms act via different downstream proteins to enhance or reduce SK-channel activity. SK-channels are part of larger protein complexes and co-assembled with protein kinase CK2 and phosphatase PP2A, with opposing effects on SK-channel activity (Allen et al., 2007; Bildl et al., 2004; Luján et al., 2009). While CK2 phosphorylates SK-bound Calmodulin (CaM) resulting in faster channel deactivation and reduced Ca^{2+} sensitivity, PP2A dephosphorylates CaM causing enhanced Ca^{2+} sensitivity (Luján et al., 2009). Both CK2 and PP2A differentially impact NMDAR activity dependent on which

NMDAR subunits are expressed. CK2 only phosphorylates the GluN2B subunit resulting in an upregulation of GluN2A expression (Sanz-Clemente et al., 2013, 2010; Zhang and Luo, 2013). One possible explanation for my results is that the activation of GluN2A receptors causes an increase in CK2 activity within the bouton leading to an inhibition of SK-channels resulting in greater membrane depolarisation and Ca^{2+} influx (Griffith et al., 2016; Ngo-Anh et al., 2005). It is well known that NMDARs can increase CK2 as well as PP2A activity, but a direct link between different NMDAR subunit populations and these proteins at presynaptic terminals remains to be elucidated.

Ca^{2+} sensitive dyes have been used for decades to study neuronal and synaptic activity (Padamsey and Emptage, 2011). However, recently a new class of indicators has received much attention (Loew, 2015; Miller, 2016; Peterka et al., 2011). Using voltage-sensitive dyes, one can directly image membrane potential dynamics at synaptic terminals and even demonstrate voltage compartmentalization in spines *in vivo* (Cornejo et al., 2021). The implementation of voltage sensitive dyes in my experimental system would provide benefits including the possibility to directly study the effects of SK-channel activity. Most likely, in this study, SK-channels, activated by Ca^{2+} influx through preNMDARs, act on the action-potential waveform (Bond et al., 2005; Faber and Sah, 2007, 2003; Sah and Faber, 2002; Xia et al., 1998), but whether this is actually the case remains to be proven experimentally, potentially by using voltage sensitive dyes.

I have shown that GluN2A containing preNMDARs mediate an increase in Ca^{2+} influx into boutons. For this purpose, I used the GluN2A subunit inhibitor

PEAQX to specifically block GluN2A subunits which abolished the increase in Ca^{2+} influx previously unmasked by application of Ro – 25 6981. Notably, application of PEAQX alone preserved the decrease in APCaTs (Fig. 17), however, to a more modest extent than observed in aCSF. Most likely, this results from the lower specificity of PEAQX, as it has been shown that it partially inhibits the GluN2B subunit as well (Auberson et al., 2002; Feng et al., 2004). Thus, the negative regulation of Ca^{2+} will be reduced under PEAQX, as it inhibits some of the GluN2B containing preNMDARs that mediate the decrease in Ca^{2+}. Pharmacological manipulations remain the gold-standard when studying receptor functions. However, other technologies, especially genetic knock-outs are useful if antagonists do not provide sufficient selectivity (Docherty, 2007). Indeed, NMDAR knock-outs have been used to study synaptic plasticity (Padamsey et al., 2017b). Thus, future experiments could include knock-out models to eliminate specific NMDAR subunits, even though this technique represents a longer and more significant disruption of receptor function and would prohibit physiological subunit interactions.

Last and importantly, the differential expression patterns of preNMDAR subunits might account for inconsistencies in the literature that are commonly observed when studying NMDARs at presynaptic terminals. Functional and anatomical evidence for preNMDARs has been demonstrated since the 1990s (Duguid and Smart, 2004; Janssen et al., 2005; McGuinness et al., 2010; Pittaluga and Raiteri, 1992, 1990; Siegel et al., 1994). However, direct proof of NMDAR activation has been challenged as some studies demonstrated Ca^{2+} transients in axons (Buchanan et al., 2012; McGuinness et al., 2010) whereas others could not detect any Ca^{2+} influx (Carter and Jahr, 2016; Christie and Jahr, 2009,

2008). This study offers an explanation for these discrepancies, as it emphasises the importance of specific preNMDAR subunit expression at individual synapses. Subunit expression will vary between model systems, and an observation of preNMDAR activity will be difficult if the overall outcome is a negative regulation of Ca^{2+} influx into the cell, as it is for the activation of the GluN2B subunit. Curiously, I could only detect a direct Ca^{2+} transient through preNMDARs with GluN2B inhibition. Several explanations could account for this observation. For example, there might be specific subunit-subunit interactions causing a direct inhibition of GluN2A induced by GluN2B. An alternative explanation could lay in subunit localisation, if GluN2B receptors are effectively expressed extrasynaptically, as pointed out above. Following inhibition of the GluN2B subunit, I could detect a Ca^{2+} transient triggered by glutamate photolysis, potentially as GluN2A receptors are clustered at synaptic sites. Nevertheless, I have demonstrated direct Ca^{2+} influx through preNMDARs, and provided a possible explanation why this has been previously unsuccessful in our lab.

What might be the physiological function of opposing feedback loops mediated by different preNMDAR subpopulations? The coupling of SK channels to Ca^{2+} sources such as preNMDARs most likely acts as a mechanism to regulate p_r and shape synaptic transmission. Another role for the GluN2B/SK-channel feedback could be protection from NMDAR-mediated excitotoxicity. It is generally believed that NMDARs due to their high Ca^{2+} permeability play a major role in mediating glutamate dependent excitotoxic neuronal cell death (Sattler and Tymianski, 2001). As excitotoxicity is in general known to be a key contributor to neuronal injury in several acute and chronic neurodegenerative

disorders (Dong et al., 2009), negative feedback loops might represent possible protection mechanisms. These mechanisms may take effect only when very high glutamate levels are present as it is the case in my experiments, due to the AP-induced glutamate release and the additional glutamate uncaging.

5. Presynaptic NMDA receptor sub-populations modulate short-term plasticity at boutons setting the bandwidth for information transfer

5.1. Introduction

In Chapter 4, I described how distinct preNMDAR sub-populations bidirectionally modulate Ca^{2+} dynamics in boutons. Next, I wanted to explore the physiological role of this mechanism. Changes in presynaptic Ca^{2+} signalling regulate synaptic transmission predominantly impacting on neurotransmitter release (p_r) and short-term plasticity (STP). In particular, the temporal profile of the Ca^{2+} concentration within the bouton is linked to the expression of short-term facilitation (Zucker and Regehr, 2002). STP describes the phenomenon that synapses are regulated by their past activity on timescales of milliseconds. It is generally believed that STP plays a crucial role to optimise information transmission specifically for short high-frequency bursts (Dobrunz et al., 1997; Dobrunz and Stevens, 1997; Jackman and Regehr, 2017; Regehr and Abbott, 2004; Rotman et al., 2011). Hippocampal pyramidal cells commonly fire in a characteristic pattern including high-frequency trains of APs i.e., brief bursts of two to nine action potentials with interspike intervals ranging from 2 to 10 msec (Buzsáki and da Silva, 2012; Dobrunz et al., 1997; Hablitz and Johnston, 1981; Kandel and Spencer, 1961; Suzuki and Smith, 1985). Specifically, CA3 pyramidal neurones are known to generate high-frequency complex spike bursts (Balind et al., 2019; Harris et al., 2001; Mizuseki et al., 2012). These AP bursts play an important role in hippocampal function and are thought to represent an information rich signal important for

reliable neurotransmission (Balind et al., 2019; Lisman, 1997). During high-frequency AP firing, a relatively large amount of glutamate accumulates at the synapse. The experimental design in Chapter 4, including glutamate photolysis at boutons paired with APs mimics such high levels of glutamate, suggesting that the functional outcomes of preNMDAR/SK-channel interactions can be examined during burst firing.

PreNMDARs are known to regulate STP at cortical synapses via frequency-dependent facilitation of evoked glutamate release (Chamberlain et al., 2008). Alternatively, preNMDARs have been shown to modulate downstream intracellular signalling cascades (Banerjee et al., 2016; Pinheiro and Mulle, 2008). More recently, it has been shown that preNMDARs selectively enhance BDNF release and STP at hippocampal mossy fibre synapses (Lituma et al., 2021). Less is known about the effects of preNMDAR subunit composition on STP. Previous efforts to investigate the effects of preNMDAR subunit compositions suggest that preNMDARs containing the GluN2B or GluN2C/D subunits at hippocampal CA3 – CA1 synapses can enhance glutamate release (Prius-Mengual et al., 2019), though no mechanistic details are provided. Similarly, in cortical neurones, the GluN2B subunit exhibits a tonic facilitatory effect on spontaneous glutamate release (Chamberlain et al., 2008).

Based on this evidence, I hypothesised that the preNMDAR-mediated bidirectional modulation of Ca^{2+} influx acts to modify short-term plasticity on Schaffer collateral boutons. Using electrophysiological recordings at Schaffer collateral - CA1 synapses, I show that the preNMDAR subunit composition impacts on short-term facilitation in a use-dependent manner during bursts of action potentials. This allows for fine adjustment of the presynaptic integration

time window and thus the bandwidth of information transfer. Finally, using Ca^{2+} imaging coupled to focal glutamate photolysis at boutons of CA3 pyramidal neurones, I demonstrate that the preNMDAR populations are plastic and can homeostatically adapt to changes in network activity.

5.2. Results

5.2.1. Presynaptic NMDA receptors modulate short-term plasticity of action potential bursts via SK-channels

To investigate the effects of preNMDAR activation on STP, I recorded current responses from CA1 neurones in organotypic hippocampal slices during high frequency stimulation (10 pulses at 200 Hz) of Schaffer collateral inputs (Fig. 22). Experiments were performed in voltage clamp at -70 mV. In order to isolate preNMDAR function, 1 mM MK-801 was included in the patch electrode and synapses were stimulated at low-frequency (0.06 Hz) for 5-10 min before commencing experiments, which blocked postsynaptic NMDARs.

First, I examined the effect of application of the NMDAR antagonist AP5 (50 µM) on STP. High frequency AP trains elicited short-term facilitation, followed by a slow decline (Fig. 22A,B), indicating short-term depression caused by the depletion of neurotransmitter vesicles (Dobrunz and Stevens, 1997; Fioravante and Regehr, 2011; Schneggenburger et al., 2002). Wash-on of AP5 significantly increased short-term facilitation (N = 10, 2^{nd} pulse: 2.78 ± 0.24 to 3.63 ± 0.46, p = 0.037; 3^{rd} pulse: 2.03 ± 0.29 to 2.86 ± 0.50, p = 0.012; 4^{th} pulse: 1.31 ± 0.21 to 1.91 ± 0.33, p = 0.022; Wilcoxon signed rank test; Fig. 22A; S5.1, Appendix). Note that in some experiments experiments, AP5 was applied at the start of the experiment and washed out instead. If the inhibitory effect of preNMDARs is

due to the activation of SK channels, as suggested for the GluN2B negative feedback loop, inhibition of SK channels should occlude an AP5-induced increase in short-term facilitation. Therefore, I performed experiments where SK-channels were inhibited with apamin (1 µM), before adding AP5 (Fig. 22B).

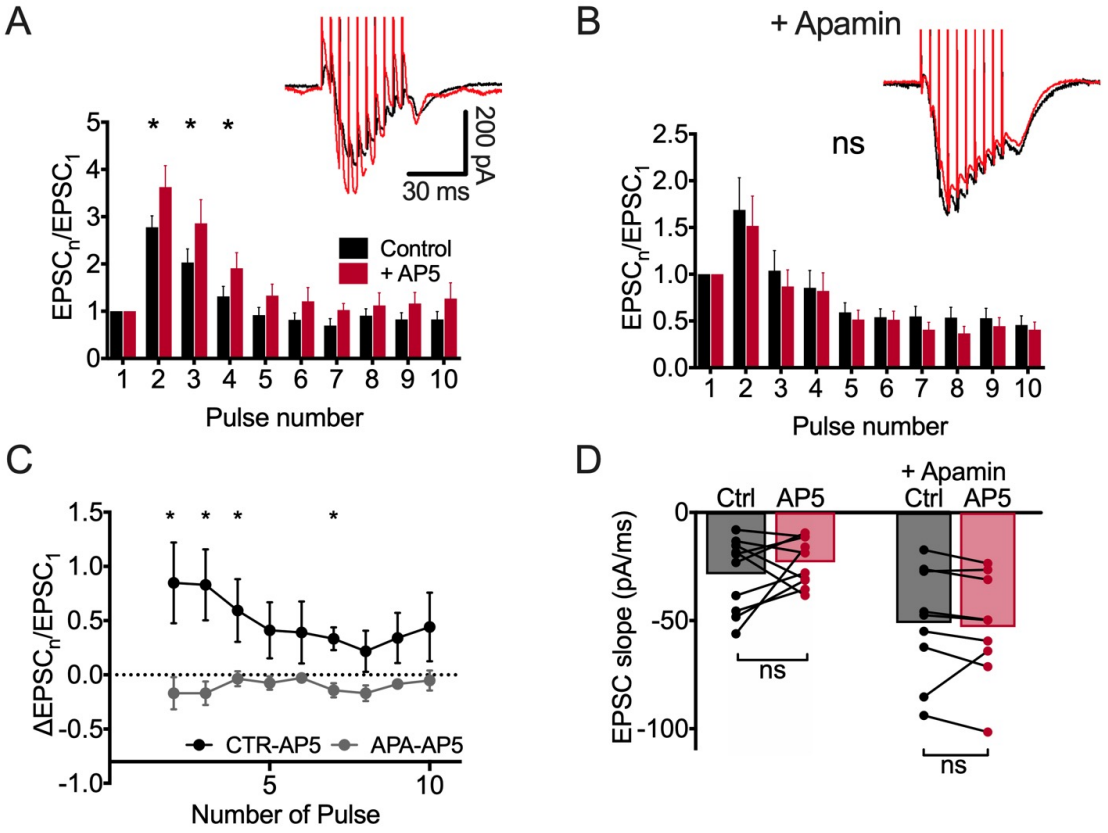

Fig. 22: Inhibition of preNMDARs increases short-term facilitation of high-frequency bursts in organotypic slices. (A) Top, Sample traces of burst stimulation (10 APs at 200 Hz) before (black) and after (red) the addition of 50 µM AP5 to block preNMDARs. Bottom, Average normalised slope of the EPSC during burst stimulation before and after the addition of AP5. Application of AP5 significantly increased the magnitude of short-term facilitation (N = 10 cells; $p < 0.05$ for pulses 2-4; Wilcoxon signed rank test). (B) Inhibition of SK-channel function with 1 µM apamin occludes the AP5-induced increase in short-term facilitation. (N = 9 cells; ns; Wilcoxon signed rank tests). (C) The difference in the normalised EPSC slope of pulse 1-10 before and after the addition of AP5 with (grey trace) or without (black trace) SK-channel inhibition (N = 10 cells (control), 9 cells (apamin); $p < 0.05$ for pulses 2-4, 7; Mann-Whitney U test). (D) The initial EPSC slope does not change during the experiments (N = 10 cells (control), $p = 0.38$; N = 9 cells (apamin), $p = 0.16$; Wilcoxon signed rank tests). Error bars represent SEM.

Notably, the facilitatory effect of preNMDAR inhibition on STP was abolished under SK-channel blockade (N = 10 cells (control), 9 cells (apamin); $p < 0.05$ for pulses 2-4,7; Mann-Whitney U test; Fig. 22B,C). Since STP depends strongly on the initial p_r of the synapse, the facilitatory effect of AP5 might be caused by a decrease in the basal p_r. However, this appears unlikely as the magnitude of the EPSC slope of the first pulse did not change with AP5, and apamin did not cause a change in the magnitude of the basal response (N = 10 cells (control), $p = 0.38$; N = 9 cells (apamin), $p = 0.16$; Wilcoxon signed rank test; Fig. 22D). When repeated in acute hippocampal slices under $GABA_A$- and $GABA_B$-receptor blockade with Picrotoxin (30 µM) and CGP55845 (5 µM), application of AP5 (50 µM) also led to an increase in short-term facilitation (N = 7 cells; 3rd pulse: 1.68 ± 0.23 to 1.98 ± 0.24, $p = 0.046$; Wilcoxon signed rank test; Fig. S5.1, Appendix). However, the effects of AP5 on STP were less prominent in acute slices, than in organotypic slices (Fig. S5.1, Appendix; Fig. 23).

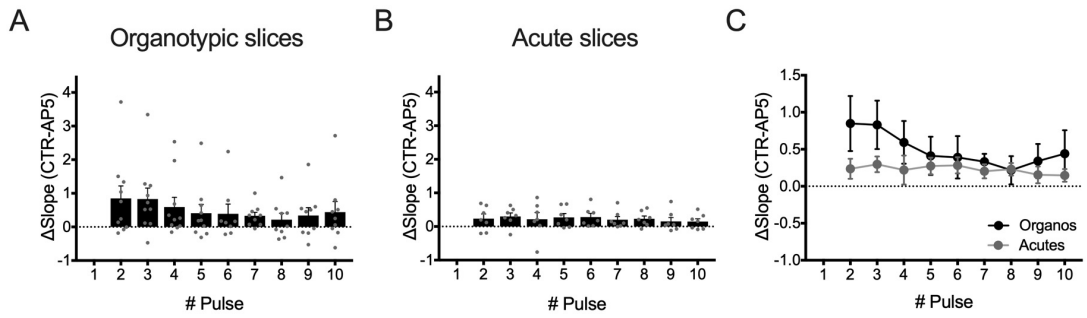

Fig. 23: Increases in short-term facilitation mediated by preNMDAR blockade is more pronounced in organotypic than acute hippocampal slices. Individual data points showing the difference in the normalised EPSC slope of pulse 1-10 before and after the addition of AP5 for experiments in organotypic (A) and acute (B) hippocampal slices. (C) The difference in the normalised EPSC slope of pulse 1-10 before and after the addition of AP5 in organotypic (black trace) or acute (grey trace) hippocampal slices.

5.2.2. Subunit composition of presynaptic NMDA receptors regulates short-term plasticity to adjust the presynaptic integration time window

Following this initial evidence supporting the hypothesis that preNMDARs regulate STP, I seeked to explore the effects of differential preNMDAR subunits in this context, as I have previously shown that two distinct preNMDAR sub-populations bidirectionally regulate Ca^{2+} dynamics at boutons. To investigate whether these preNMDAR subunit populations also differentially regulate short-term facilitation, I recorded from CA1 neurones in response to bursts of APs (5 pulses at 50 Hz) elicited at the Schaffer collateral inputs. Additionally, a single recovery pulse 100 ms after the burst was included in experiments (Fig 24B, top), to examine the speed of recovery from short-term depression. Again, 1 mM MK-801 was included in the patch electrode to block postsynaptic NMDARs.

Similar to experiments with 200 Hz stimulation, AP trains at 50 Hz elicited short-term facilitation, followed by a slow decline (Fig. 24A-D) as previously reported for Schaffer collateral – CA1 synapses (Bartley and Dobrunz, 2015; Dobrunz et al., 1997; James et al., 2006; Stevens and Wang, 1995; Sun and Dobrunz, 2006). In order to inhibit the GluN2B subunit, the specific antagonist Ro - 25 6981 (1 μM) was applied. Application of Ro - 25 6981 significantly increased short-term facilitation of the second pulse (N = 15 cells; $p = 0.001$ for pulse 2; Wilcoxon signed rank test) and enhanced short-term depression of subsequent pulses (N = 15 cells; $p < 0.05$ for pulse 3-5; Wilcoxon signed rank test; Fig. 24A,B).

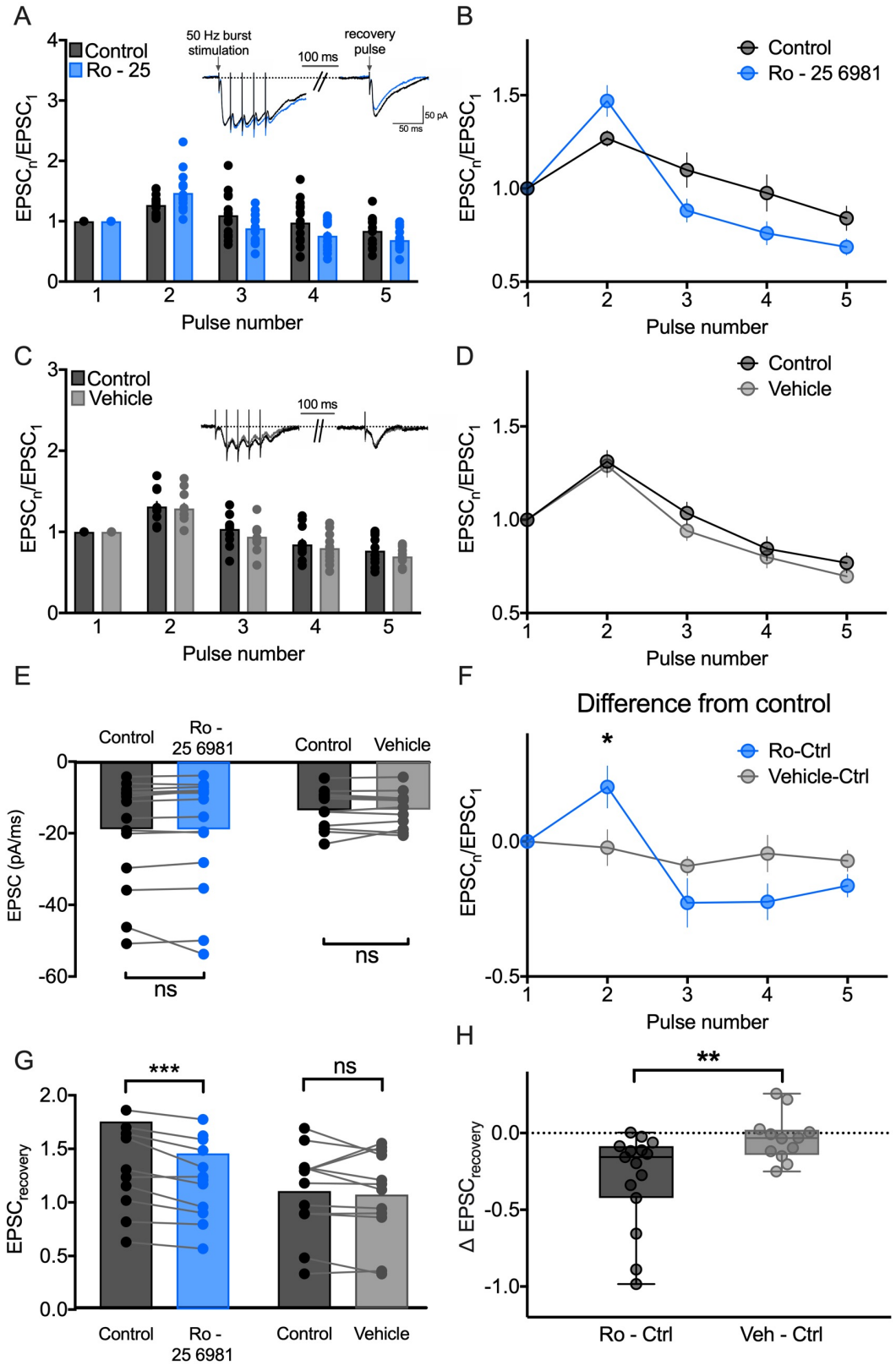

Fig. 24: PreNMDAR modulation of AP-evoked Ca^{2+} influx results in use-dependent modulation of short-term facilitation. (A) Top, Sample traces of burst stimulation (5 APs at 50 Hz) before (black) and after the addition of 1 µM Ro – 25 6981 (blue) to block GluN2B containing preNMDARs. Bottom, the normalised EPSC slope

during burst stimulation before and after the addition of Ro – 25 6981 is shown for all experiments. (B) Average normalised slope of the EPSC during burst stimulation before and after the addition of Ro – 25 6981. Application of Ro – 25 6981 significantly increased the magnitude of short-term facilitation (N = 15 cells; p = 0.001 for pulse 2; Wilcoxon signed rank test) and enhanced the magnitude of short-term depression (N = 15 cells; p < 0.05 for pulse 3-5; Wilcoxon signed rank test). (C,D) Same as (A,B) for Vehicle (aCSF alone, N = 11 cells). (E) The initial EPSC slope does not change during the experiment (N = 15 cells (control), p = 0.08; N = 11 cells (Vehicle), p > 0.99; Wilcoxon signed rank test). (F) The difference in the normalised EPSC slope of pulse 1-5 before and after the addition of Ro - 25 6981 (from B) or in control experiments (from C) (p < 0.05 for pulse 2; Mann-Whitney test). (G,H) The magnitude of the recovery pulse given 100 ms after the burst was significantly decreased when GluN2B activity was inhibited with Ro - 25 6981 but not in control experiments (Ro - 25 6981: p < 0.001; Vehicle: p = 0.34; Wilcoxon signed rank test; Ro vs vehicle: p < 0.01, Mann Whitney test).

I performed control experiments to determine potential effects of the drug wash-on procedure, caused by the perfusion system, since Ro - 25 6981 cannot be used in wash-out experiments such as AP5. In these vehicle experiments, if aCSF alone was perfused, short-term plasticity remained unchanged (N = 11 cells; ns; Wilcoxon signed rank test; Fig. 24C,D). To rule out the possibility that application of Ro - 25 6981 caused a change in p_r, I compared the magnitude of the first pulse in each burst (Ro - 25 6981: N = 15 cells, p = 0.09; Vehicle: N = 11 cells, p > 0.99; Wilcoxon signed rank test; Fig. 24E) and could not find a significant difference.

Short-term plasticity during high-frequency firing modulates synaptic performance during subsequent stimulations. If GluN2B inhibition affects short-term facilitation and depression, correspondent changes should be detectable in a subsequent recovery-pulse. Thus, next I evaluated the recovery from short-term depression. Indeed, the magnitude of a single recovery pulse given 100 ms after the burst was significantly decreased when GluN2B activity was inhibited with Ro - 25 6981 (Ro - 25 6981: N = 15 cells, p < 0.001; Vehicle: N =

11 cells, p = 0.34; Wilcoxon signed rank test; Fig. 24G). No such changes could be detected in control vehicle experiments (Ro - 25 6981 vs. Vehicle: p = 0.01; Mann-Whitney U test; Fig. 24H).

In conclusion, I have shown that the preNMDAR-mediated modulation of Ca^{2+} influx, established in Chapter 4, serves to modify short-term facilitation. This modulation is use-dependent, in other words, conditioned by the recent history of release events, as proven by the fact that the activation of preNMDARs requires glutamate (Chapter 4). Potential outcomes of this use-dependent modulation of short-term facilitation affect synaptic transmission, specifically the adjustment of the presynaptic integration time window. The data indicate that activation of the GluN2B dominant pathway forms a negative feedback loop that restricts the increase in p_r during bursts of APs (Fig. 25). Importantly, glutamate release must first occur to stimulate this pathway, ensuring that some neurotransmitter is always released. Thus, the GluN2B dominant pathway functions as use-dependent ‘clamping’ of short-term facilitation, preventing excessive vesicle depletion (i.e. short-term depression). This is necessary to reset the synapse for subsequent AP trains. Effectively, such a mechanism will enhance information transfer within short integration time windows (Fig. 25). The other pathway, predominantly activating preNMDARs containing the GluN2A subunit forms a positive feedback loop within presynaptic terminals. In a use-dependent manner, i.e. following glutamate release, p_r is increased over the course of the AP burst (Fig. 25). This mechanism ensures that multiple release events occur for an AP burst, which extends the impact of the burst in time. Thereby, the postsynaptic neurone is given more time to integrate

information, hence, activation of the GluN2A pathway augments the robustness of information transmission (Fig. 25).

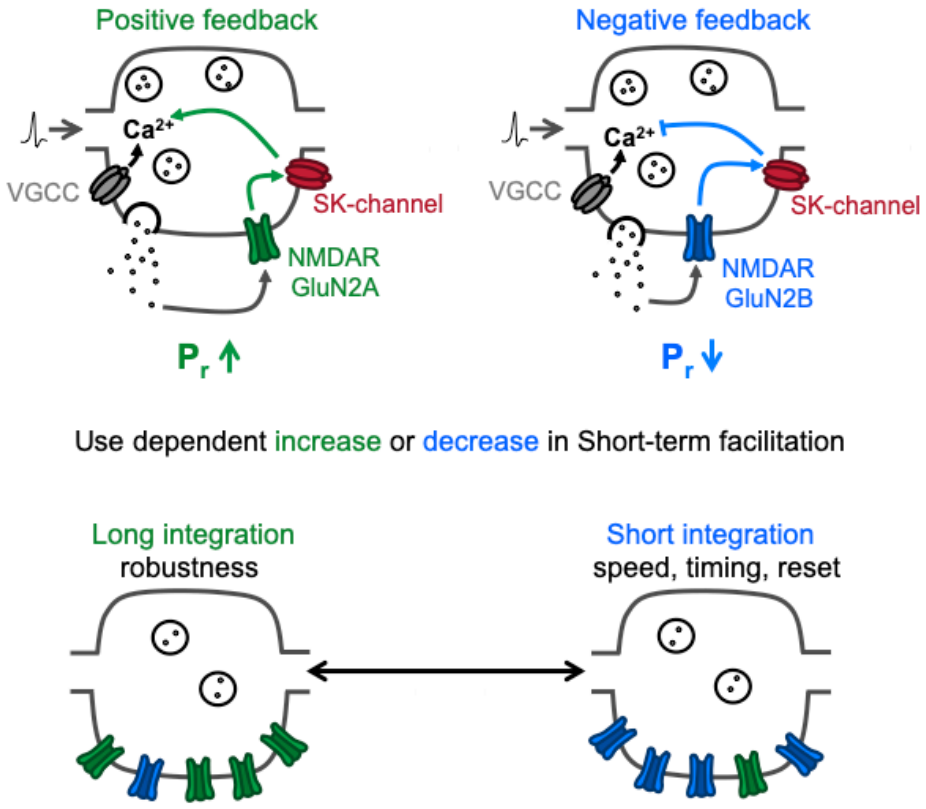

Fig. 25: Functional outcomes of presynaptic NMDAR sub-population dependent modulation of Ca^{2+} dynamics at Schaffer collateral boutons.

5.2.3. The relative contribution of presynaptic NMDA receptor subpopulations adapts to global network activity

My results suggest that the balance between GluN2A and GluN2B subpopulations regulates the presynaptic integration time window and thus the bandwidth of information transfer. Ideally, this balance should be adjustable with respect to network activity (Fig. 25, bottom). During states of sparse activity, robust transmission should be favoured to reliably transmit information.

If network activity is high, information transfer occurs within short integration time windows, thus excessive vesicle depletion should be prevented to ensure that the synapse can transmit subsequent activity. Therefore, I wondered whether manipulating network activity can be used to change the contribution of each preNMDAR subpopulation, with states of high activity favouring the GluN2B subunit and states of low activity stimulating GluN2A (Fig. 26).

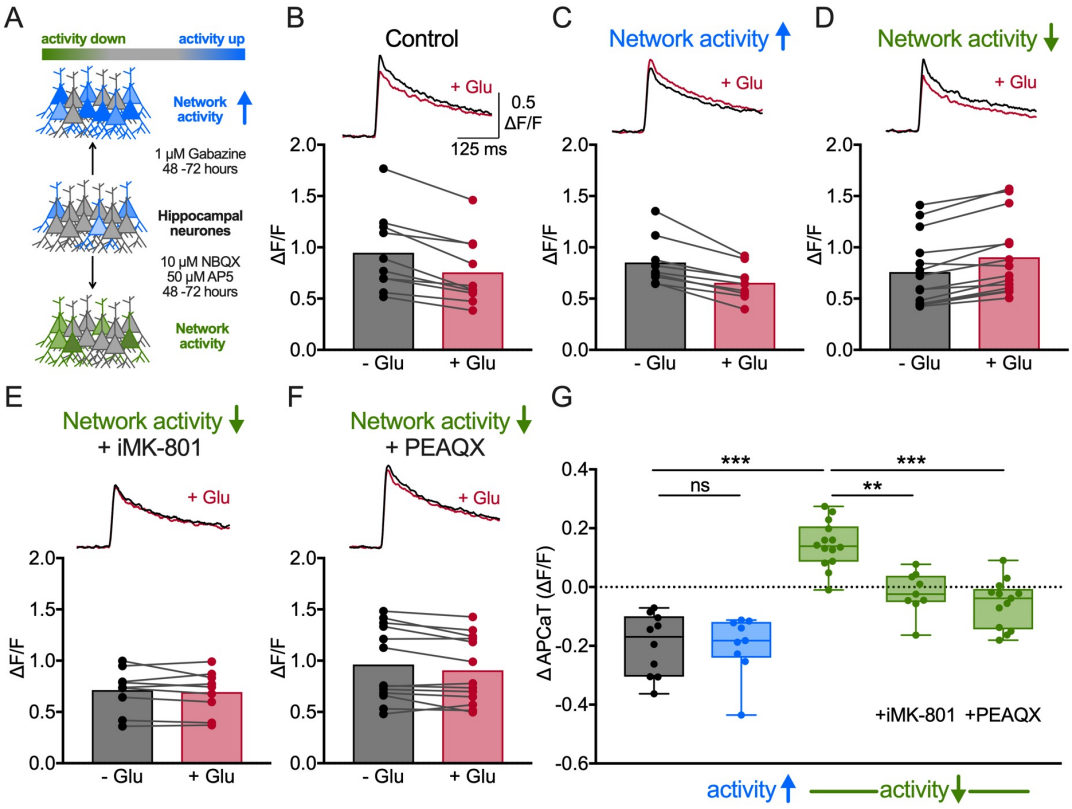

Fig. 26: Network activity shifts the balance between GluN2A and GluN2B subpopulations. (A) Schematic of the experimental conditions. Network activity was either increased or decreased via application of 1 µM gabazine or 10 µM NBQX and 50 µM AP5 for 48-72 hours, respectively. (B-D) Peak APCaTs in control conditions, N = 10 (B) and after increasing, N = 9 (C) or decreasing, N = 14 (D) network activity. Decreasing network activity led to an increase in peak APCaTs (D). This increase was abolished with intracellular MK-801, N = 9 and PEAQX, N = 13 (E,F). (G) Summary of the regulation of subpopulation balance by network activity ($Vehicle_{low\ activity}$ vs. Control $p < 0.001$, $Vehicle_{lowactivity}$ vs. iMK-801 $p = 0.002$, $Vehicle_{lowactivity}$ vs. PEAQX $p < 0.001$; Kruskal-Wallis with post hoc Dunn's test). Error bars represent SEM.

To test this hypothesis, I used an established protocol to induce homeostatic plasticity (Turrigiano, 2012). Network activity was either globally increased (1 µM gabazine) or decreased (10 µM NBQX and 50 µM AP5) for 48-72 hours (Fig. 26A). For subsequent investigations on subunit-dependent Ca^{2+} dynamics, I returned to Ca^{2+} imaging coupled to glutamate photolysis experiments in organotypic slices, similar to those in Chapter 4, and measured the modulation of APCaTs induced by network dynamics. Increased network activity with gabazine resulted in an overall decrease in the peak amplitude of APCaTs (N = 9 boutons, ΔAPCaT = -0.2 ± 0.034 ΔF/F; Fig. 26C) which was not significantly different from control experiments (Gabazine vs. CTR $p > 0.99$; Kruskal-Wallis with post hoc Dunn's test; Fig. 26B,C,G). In contrast, decreasing network activity with NBQX and AP5 resulted in a substantial increase in APCaTs (N = 14 boutons, ΔAPCaT = 0.144 ± 0.021 ΔF/F; Fig. 26D) following photolysis of glutamate (AP5/NBQX vs. CTR $p < 0.001$; Kruskal-Wallis with post hoc Dunn's test; Fig. 26G). This increase is caused by enhanced activity of GluN2A containing preNMDARs, as confirmed by the application of intracellular MK-801 (N = 9 boutons, ΔAPCaT = -0.019 ± 0.024 ΔF/F; Fig. 26E,G) and the specific GluN2A inhibitor PEAQX (N = 13 boutons, ΔAPCaT = -0.057 ± 0.023 ΔF/F; Fig. 26F,G). Notably, the application of PEAQX did not unmask a decrease in APCaTs (Fig. 26G). No difference in effect depending on the duration of drug incubation (48 or 72 hours) could be observed and homeostatic plasticity protocols did not affect slice health (Fig. S5.3, Appendix).

5.3. Discussion

I have shown that the activation of two preNMDAR populations with distinct subunit composition bidirectionally regulate Ca^{2+} dynamics and STP at Schaffer

collateral boutons. In summary, the activation of preNMDARs containing the GluN2B subunit form a negative feedback-loop via SK-channels, that decrease the Ca^{2+} influx that occurs during an action potential leading to a reduction of short-term facilitation during high frequency firing. Activation of preNMDARs containing the GluN2A subunit increase the action potential driven Ca^{2+} influx into the bouton, which results in the reinforcement of short-term facilitation during burst firing.

Further, I have demonstrated that the GluN2B pathway is predominant in conditions of high network activity, as commonly observed in hippocampal slice preparations (De Simoni et al., 2003), whereas GluN2A signalling dominates when network activity is low. Hence, the data support the idea that synaptic terminals flexibly adjust the balance between GluN2A and GluN2B subpopulations depending on the activity state of the network. Such alterations in subunit composition have been demonstrated for postsynaptic terminals in different forms of plasticity. For example, during Hebbian LTP synaptic NMDARs switch from GluN2B containing towards GluN2A containing NMDARs (Bellone and Nicoll, 2007). But even during homeostatic plasticity, if network activity was silenced with tetrodotoxin (TTX), GluN2A containing receptors were upregulated on postsynaptic terminals (Soares et al., 2013). In this study I show, that preNMDAR subunit dynamics are regulated in a similar fashion in response to changes in network activity.

As pointed out above, I was able to detect preNMDAR function at all investigated boutons, however, effect sizes varied suggesting that the relative expression of preNMDAR subpopulations in individual boutons may differ. Indeed, individual expression patterns of preNMDARs at synapses from the

same neurone have been reported (Buchanan et al., 2012). Synapse-specific regulation of the GluN2B/GluN2A balance could be responsive to local activity, meaning the unique pre- and postsynaptic activity patterns experienced by each individual synapse. This would endow the presynaptic terminal with exceptional computational flexibility suggesting that bidirectional preNMDAR signalling mediated via different subunits plays an essential role for information processing in neuronal networks. To illustrate the significance of such regulatory processes at presynaptic terminals one should consider how information is actually transmitted at synapses (see a recently proposed model for presynaptic computation by Tong et al., 2020). Many studies have focussed on this central question and it is now generally believed that both the onset as well as the average frequency of burst firing conveys information (Krahe and Gabbiani, 2004). Imagine neurone A receiving a burst input containing information for neurone B. Short-term plasticity, differentially expressed from synapse to synapse of neurone A, is used to define whether to transmit information related to the timing of presynaptic bursts or to the average burst frequency (Markram et al., 1998b, 1998a). Various studies have shown that boutons from the same axon can give rise to facilitating synapses as well as to depressing synapses depending on the target neurones (Regehr and Abbott, 2004). The bidirectional functional outcomes of subunit specific preNMDAR/SK-channel interactions demonstrated in this study represent a mechanism as to how this short-term plasticity can be regulated on the molecular level. If conveying the precise timing of presynaptic bursts is important, the GluN2B pathway will be up-tuned to clamp neurotransmitter release ensuring the reliable transmission of activity onsets. In contrast, if burst frequency contains

relevant information, increasing short-term facilitation and upregulating release via the GluN2A subunit is favourable to enable neurone B to sense every stimulus during the burst during low-activity states (Dittman et al., 2000; Tsodyks and Markram, 1997). Via short-term plasticity, information can be differentially distributed by the same neurone, specifically shaped to transmit to postsynaptic neurones engaged in different neural pathways (Markram et al., 1998a, 1998b; Markram and Tsodyks, 1997; Regehr, 2012). If we consider that neurone A will also be engaged in different contexts, the synapse-specific regulation of the GluN2B/GluN2A balance in response to network activity is beneficial. Thus, if short-term plasticity represents the mechanism by which neurone A shapes its output to neurone B, identifying mechanisms that modulate this short-term plasticity, such as the one discovered in this study, adds another layer of flexibility to synaptic processing. Differential expression of preNMDARs dependent on the functional identity of the synapse has been previously demonstrated (Buchanan et al., 2012). I show that specific expression of preNMDAR subunit populations can regulate p_r during high-frequency firing. This flexible adjustment of p_r via differential expression of preNMDAR subunits allows individual synapses to efficiently transmit the bandwidth of presynaptic firing frequencies that are most informative for the postsynaptic neurone (Tong et al., 2020). In summary, I have given evidence that preNMDARs containing either the GluN2B or the GluN2A subunit compete at presynaptic terminals regulating the synapse' specific output.

Apart from increasing the potential for synaptic computation at the presynaptic terminal, other physiological consequences of the described feedback loops are worth to be considered. The negative feedback loop involving the GluN2B

subunit could provide a homeostatic control of the amount of glutamate released. This might be useful in minimising the metabolic cost of the synapse. If information were encoded in the onset of an AP burst, only a single release event would be required to transfer the information about the occurrence of a burst, rendering all subsequent release events redundant. This redundancy can be reduced by clamping neurotransmitter release for subsequent release events.

The extent of functional impact from both preNMDAR sub-populations can be flexibly adjusted as shown by the upregulation of GluN2A containing preNMDARs during phases of low network activity. The exact mechanisms driving this flexibility remain to be investigated but such homeostatic effects probably fall in three different categories. Option one includes the stimulation of preNMDAR membrane trafficking to upregulate the expression of either preNMDAR sub-population (Aoki et al., 2003; Barria, 2007; Lau and Zukin, 2007). Another possibility could be to upregulate respective pathways via local protein translation (Holt et al., 2019; Holt and Schuman, 2013). Lastly, increased activation of either GluN2A or GluN2B could be independent of receptor expression and simply result from functional upregulation potentially by activity shifts of downstream signalling proteins. Perhaps synaptic adjustments include a combination of all three mechanisms. Notably, as shown in the last Figure (Fig. 26), application of PEAQX inhibited the increase in APCaTs but did not unmask a decrease in APCaTs. This suggests, that the extensive silencing of network activity has caused a shift in the dominant subpopulation expression such that far few GluN2B containing receptors remained. Although trafficking and functional upregulation provide the most obvious and least energy

consuming solutions, protein synthesis could play a role in long-term adjustments of synaptic strength. To explore this possibility, the GluN2A/GluN2B flexibility should be studied on different time scales.

I provided initial evidence for the involvement of preNMDARs and SK-channels in STP by investigating the effects of AP5 and apamin on short-term facilitation. The data support the idea that preNMDARs influence short-term facilitation probably via SK-channels. However, detailed analysis showed that facilitation was generally decreased by apamin (Fig. S5.2, Appendix), potentially impacting on results. Notably, these experiments were performed in organotypic as well as acute hippocampal slices, showing stronger changes in short-term plasticity following burst stimulation in organotypic slices compared to acutes. The activity within organotypic slices is strongly enhanced (De Simoni et al., 2003) and our data show that increasing network activity with gabazine caused no stronger decrease in Ca^{2+} influx. This suggests that the effect of the GluN2B pathway is already at maximum in our control conditions. Accordingly, when we inhibit all preNMDARs in organotypic slices with AP5, an increase in short-term facilitation can be observed, resulting from alleviation of the negative regulatory GluN2B pathway. In acute slices, inhibition of preNMDARs with AP5 also resulted in an increase in short-term facilitation, however to a much smaller extend. Thus, the GluN2B dominant pathway is more impactful in organotypic slices, where network activity is enhanced, than in acute slices, where activity is generally lower.

At this point, it is also worth to return to the possibility of an extrasynaptic nature of preNMDARs containing GluN2B, as proposed in Chapter 4. Considering the observed effects of preNMDARs during AP bursts, a contribution of

extrasynaptic preNMDAR activity is likely in our experiments, since stronger extrasynaptic GluN2B activity has been demonstrated during high-frequency trains (Brickley et al., 2003; Köhr, 2006; Lozovaya et al., 2004). Given that preNMDARs with GluN2B are preferentially active during high states of network activity, an extrasynaptic localisation of this population of preNMDARs could declare them as sensors for high amounts of glutamate during increased activity. Thereby, GluN2B preNMDARs could sense both locally released glutamate and spillover from neighbouring synapses, serving as a trigger to preferentially activate the negative feedback loop with SK-channels.

In conclusion, inconsistencies in preNMDAR signalling and functional outcomes as indicated in the literature, together with what I presented in Chapters 4 and 5 emphasises the following: Future studies on preNMDARs should consider to identify which subunits are expressed and that their activation is plastic dependent on several factors such as network activity. Importantly, besides the relevance of NMDAR signalling for synaptic transmission, understanding NMDAR regulation and functional outcomes is clinically valuable, since NMDAR dysfunction is associated with psychosis, epilepsy, memory and learning impairments and even with excitotoxic brain injury (Cull-Candy et al., 2001; Newcomer et al., 2000; Yang et al., 2006; Zhou and Sheng, 2013).

6. Effects of oestrogen on structural plasticity of spines

6.1. Introduction

The effects of oestrogen and the oestrous cycle on synapses, specifically dendritic spines, have been characterised since the 1990s (Sheppard et al., 2019; Woolley and McEwen, 1993). Not only has it been shown that spine density fluctuates by approximately 30% across the oestrous cycle (Woolley et al., 1990), but also exogenous delivery of oestradiol benzoate (EB) or oestradiol (E2) via injections increased spine density (Jacome et al., 2016; MacLusky et al., 2005; Woolley and McEwen, 1993, 1992). Despite well-established differences in spine number and density, less research has been conducted to characterise spine morphology changes in response to oestrogen (Brinton, 2009). E2 treatment resulted in no changes with regards to spine length (Phan et al., 2015). However, the application of an oestrogen receptor agonist enhanced the number of larger 'mushroom' type of spines in the hippocampus, indicating that E2 signalling affects spine size (Li et al., 2004; Liu et al., 2008).

The majority of experimental studies investigating the effects of oestrogen on spines build on exogenous treatments, where animals are injected either directly with E2, or with substances that stimulate E2 signalling (Jacome et al., 2016; Li et al., 2004; MacLusky et al., 2005; Woolley and McEwen, 1993, 1992). Subsequently, animals are sacrificed and brains are cut into slices to visualise neurones and dendrites with Golgi staining (Jacome et al., 2016; Tuscher et al., 2016). In other studies, acute slices are prepared first and incubated with E2 or E2 receptor agonists prior to fixation with paraformaldehyde and subsequent labelling (Mukai et al., 2007; Murakami et

al., 2006; Phan et al., 2015; Tsurugizawa et al., 2005). Overall, in studies reporting E2 induced changes, these effects have been measured in fixed tissue. Results may significantly differ in acute experiments in which structures would be observed in real-time before and after the application of oestrogen.

Recently, *in vivo* two-photon imaging was used to study the effects of fluctuating oestrogen levels on cortical spine plasticity (Alexander et al., 2018). Alexander and colleagues have performed a longitudinal examination of spines from L5 pyramidal neurones in the somatosensory cortex (SSC) of naturally cycling female and male mice. Contrary to the traditional framework of oestrogen functions, spine density was constant across the oestrous cycle and overall similar compared to male animals (Alexander et al., 2018). However, structural plasticity evoked by sensory stimulation differed with regards to the stage of the oestrus cycle, respectively, showing more pronounced spine dynamics during proestrus and oestrus phases where oestrogen levels are enhanced (Alexander et al., 2018).

These results support the idea, that oestrogen modulates the synaptic network thereby affecting subsequent plasticity events. Indeed, such a two-step mechanism for oestrogen signalling has been proposed suggesting that E2 increases synaptic connectivity (Step 1) and subsequently stimulation or plasticity mechanisms (Step 2) cause these synapses to undergo long-term potentiation (Sheppard et al., 2019; Srivastava et al., 2008). Thus, the level of ongoing plasticity processes in different brain regions probably influences the effects of oestrogen on synapses. The SSC can exhibit various forms of plasticity, including structural plasticity, however, mostly in response to sensory stimulation such as peripheral lesions, passive sensory experience, and training

on sensory tasks (Feldman and Brecht, 2005). In contrast, the hippocampus as part of the limbic system is involved in ongoing plasticity regulating emotional behaviours, learning and memory. The prefrontal cortex (PFC) is tightly connected to the limbic system and evidence points towards specific roles for the PFC, distinguishing it from other cortical regions such as the SSC (Kolb and Gibb, 2015). For example, the acquisition, consolidation, and extinction of fear memory involves interactions between the PFC and hippocampus (Pearson and Lewis, 2005; Taxier et al., 2020).

Oestrogen exerts strong effects on structural plasticity in highly plastic brain regions such as the hippocampus and PFC (see 2.3.3., Sheppard et al., 2019; Wallace et al., 2006) and in the SSC the induction of plasticity via sensory stimulation may be needed to reveal oestrogen-induced effects on spine dynamics (Alexander et al., 2018 but see Ye et al., 2019). This together with the fact that a two-step regulatory mechanism of oestrogen signalling has been proposed (Srivastava et al., 2008) led me to the following hypothesis: oestrogen as a neuromodulator lowers the threshold of plasticity, affecting spine dynamics and related experimental observations in different brain regions. Here, I test this hypothesis using acute slices from the hippocampus, SSC, and PFC of transgenic Thy1-EGFP mice expressing sparse labelling of projecting neurones. Note that in this Chapter, oestradiol (E2) is the oestrogen variant under study. Thus, effects of oestrogen in this case are equated with effects of oestradiol (E2). First, I demonstrate that the acute application of E2 for 30 minutes has no effects on the number of spines. Next, I show that E2 incubation significantly increases spine size in the hippocampus and PFC of female and male animals, but not in the SSC. Using a subthreshold glutamate uncaging protocol, I provide

evidence that oestrogen lowers the threshold for plasticity in the hippocampus, PFC and SSC. Finally, I demonstrate that the detectability of oestrogen-induced effects on spine size depend on the basal level of neuronal activity.

6.2. Results

6.2.1. Spine number in acute hippocampal slices is not significantly altered by oestrogen application

The literature states that oestrogen induces rapid structural changes increasing spine density by 25–50% within 15–40 min of hormone application (Jacome et al., 2016; Phan et al., 2015, 2012, 2011; Srivastava et al., 2008). Specifically in the hippocampus, dendritic spine density increased within the stratum oriens and stratum radiatum after 20–30 min of treatment with E2 (Phan et al., 2015). In order to investigate acute effects of E2 on spines, I applied 100 nM of E2 onto acute brain slices from 8-12 week old Thy1-EGFP transgenic mice (Fig. 27), a concentration that is commonly used to investigate acute effects of oestrogen (Chang et al., 2013; Ye et al., 2019). Two different sets of experiments were performed, and images of spines were taken before and after 30 minutes of incubation. In control experiments, slices were incubated in aCSF without drug application. In a second set of experiments, slices were incubated with E2 (100 nM) for 30 minutes. Subsequently, the effects of oestrogen on spine dynamics were examined by evaluating changes in spine number and spine size.

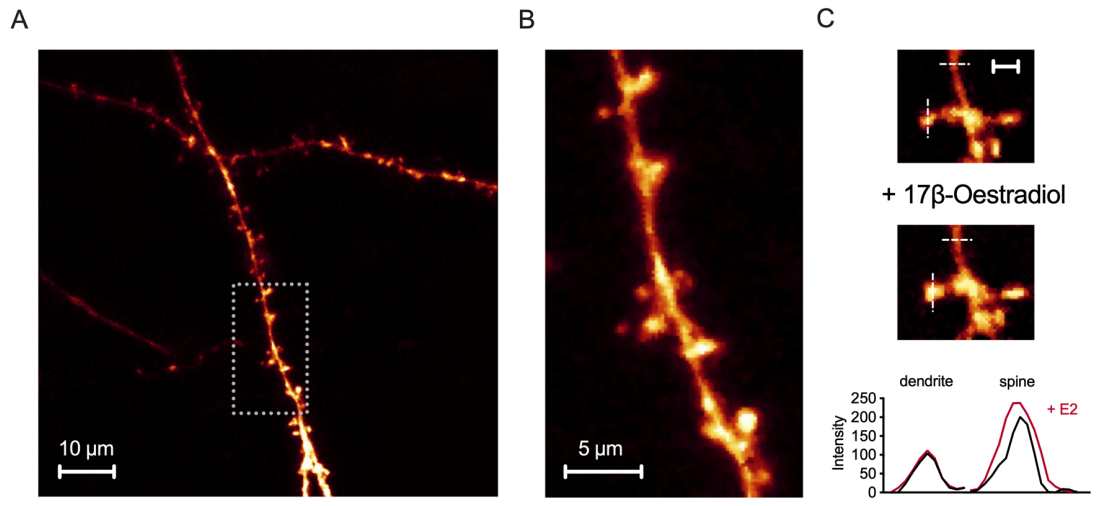

Fig. 27: Experimental set up: acute brain slices from Thy1-EGFP transgenic mice. (A) Dendrites in acute hippocampal slices from Thy1-EGFP transgenic mice. (B) Enhanced image of the box from (A) displaying spines along the dendritic branch. (C) The effects of the acute application of oestradiol (E2, 100 nM) to acute brain slices. Line profiles demonstrate, that while the spine head increases in size, the corresponding dendrite diameter is not affected by E2. Scale bar: 2 µm.

Dendritic branches with up to 40 spines each (a total of 300-400 µm of dendrites per experimental group) were analysed in acute slices from the hippocampus, the prefrontal cortex (PFC), and the somatosensory cortex (SSC; Fig. 28). To investigate the effects of E2 application on spine dynamics, the number of new and lost spines per 10 µm of dendritic branch was analysed in both control experiments and experiments with oestrogen incubation (Fig. 28). Overall, spine dynamics were extremely low in both conditions, with on average less than one lost or newly formed spine per 10 µm over 30 minutes (Fig. 28A,B). No significant differences could be detected between oestrogen and control experiments (N, dendrite branches; control = 5 (hippo female), 6 (hippo male), 6 (PFC), 7, (SSC); N, dendrite branches; oestrogen: 8 (hippo female), 6 (hippo male), 11 (PFC), 11 (SSC); Mann-Whitney test, ns; Fig. 28A,B).

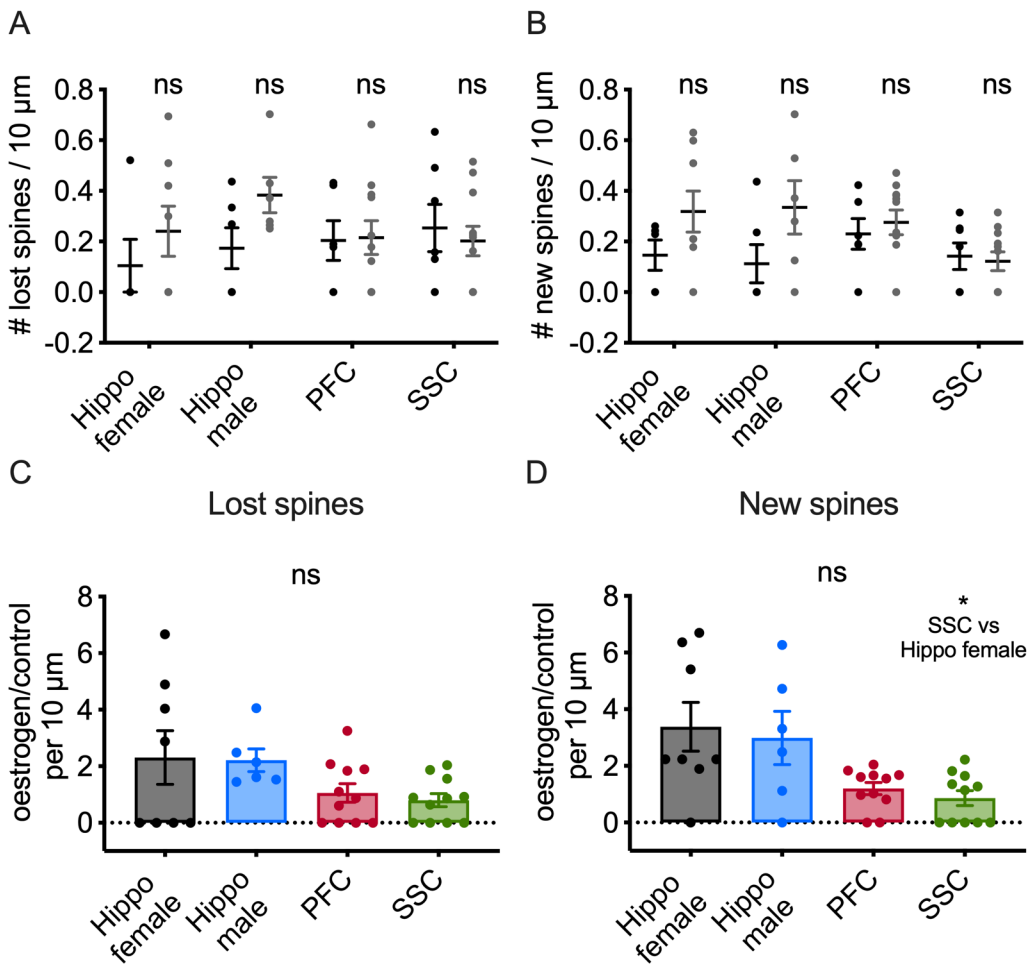

Fig. 28: Dendritic spine turnover rate in acute hippocampal slices is not significantly altered by oestrogen application. (A,B) The number of lost (A) and new (B) spines over 30 minutes in control experiments (black) and following the application of 100 nM E2 (grey). Slices from Thy1-EGFP transgenic mice were prepared from the hippocampus, the prefrontal cortex (PFC) and the somatosensory cortex (SSC). Sample number represents the average number of lost or new spines per 10 µm for individual dendritic branches. No enhanced spine dynamics could be observed following E2 incubation. (C,D) The number of lost (C) and new (D) spines normalised to control experiments for the female and male hippocampus, the PFC and the SSC. No significant differences in E2-induced spine dynamics could be detected between brain regions when compared to the female hippocampus. The only exception was the number of new spines in the SSC, which was smaller compared to the female hippocampus (All ns except SSC vs. female hippo p = 0.015; Kruskal-Wallis with post hoc Dunn's test). Error bars represent SEM.

When normalising spine dynamics of oestrogen experiments to control experiments, it became evident that in acute slices from the hippocampus the

number of new and lost spines was slightly higher compared to the PFC and SSC (Fig. 28C,D). However, because numbers were extremely low in general, no significant differences could be detected in E2-induced spine dynamics between different brain regions (Fig. 28C,D). The only exception was a slightly decreased number of new spines in the SSC compared to the female hippocampus (SSC vs. female hippo $p = 0.015$; Kruskal-Wallis with post hoc Dunn's test; Fig. 28D). Taken together, this data suggests that the acute application of oestrogen for 30 minutes produces only minor changes in spine dynamics, but potentially exhibiting stronger effects in the hippocampus than in cortical brain regions.

6.2.2. Oestrogen potentiates spine size in acute brain slices from hippocampus and prefrontal cortex but not somatosensory cortex

Having found that the effects of oestrogen on spine number were minimal, I analysed the effects of oestrogen on spine size. Indeed, the application of E2 onto acute slices from the hippocampus substantially increased spine size (Fig. 27). I quantified spine size changes in control experiments and experiments where E2 (100 nM) was applied by analysing the same spines at the beginning of each experiment and after 30 minutes. Fig. 29 displays the relative changes in spine size, estimated by changes in the integrated fluorescence intensity measured after 30 minutes (Δ % intensity). Then, I compared oestrogen experiments to control experiments within different brain regions including the hippocampus, PFC, and SSC.

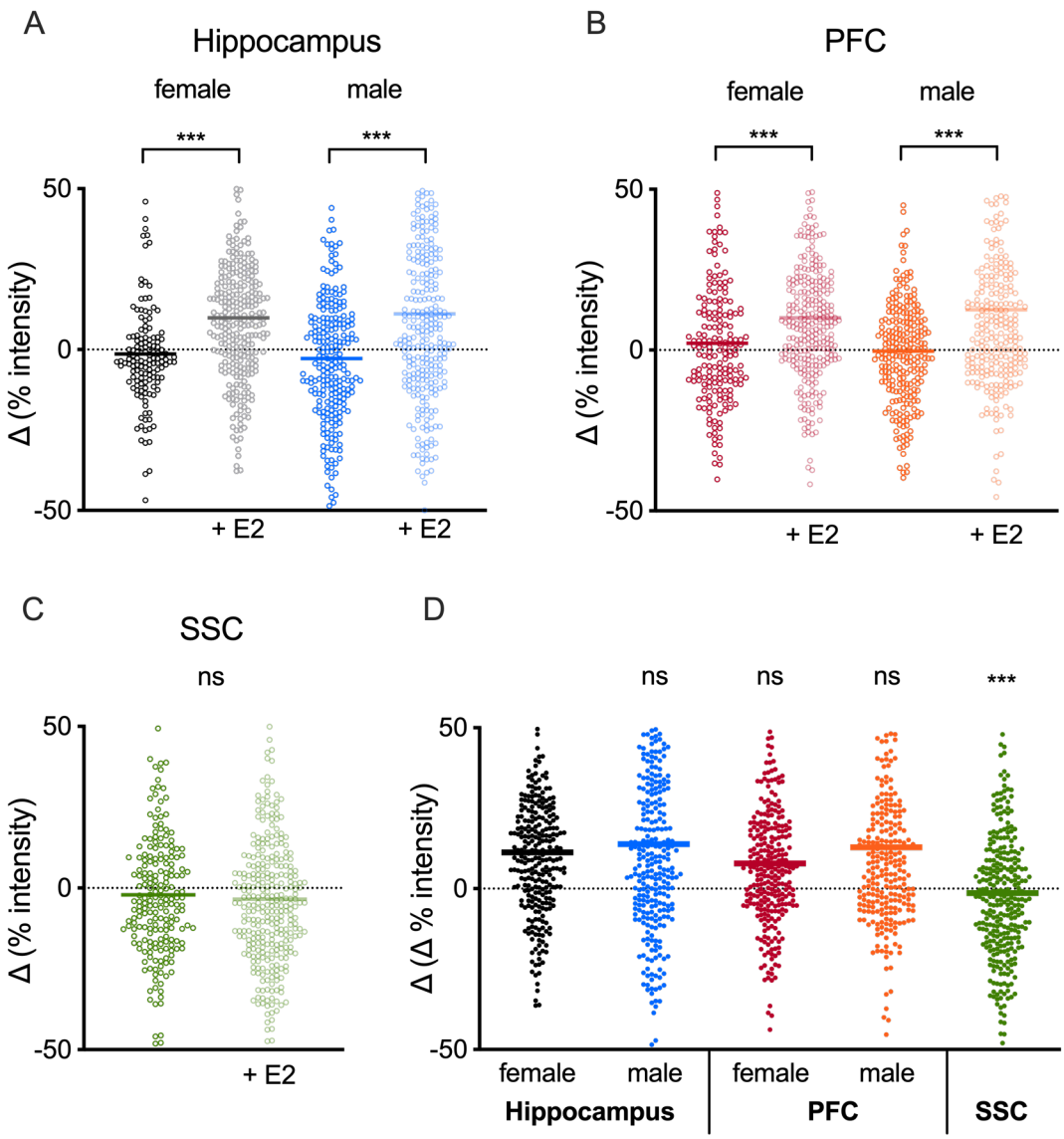

Fig. 29: The application of Oestrogen increases spine size in acute brain slices from hippocampus and prefrontal cortex but not somatosensory cortex. (A) The difference in mean fluorescence signal of spines before and after 30 minutes for control experiments (black, dark blue) and experiments where 100 nM E2 was applied (grey, light blue) to slices from the female and male hippocampus. The difference in mean fluorescence signal is expressed as percentage change of intensity relative to the intensity before the 30 minutes of incubation. (B) Same as (A) but for the prefrontal cortex (PFC). (C) Same as (A,B) for control experiments (dark green) and experiments where 100 nM E2 was applied (light green) to slices from the female somatosensory cortex (SSC). An increase in signal intensity was detected following E2 application for the female and male hippocampus and PFC, but not in control experiments without E2 incubation (A,B). No such changes could be detected for the SSC (C). (D) Summary figure of (A-C). Δ(Δ % intensity) was calculated by normalising oestrogen to control experiments. E2 incubation of acute slices from the female hippocampus potentiated spine size. Similar effects were observed for the male hippocampus and the female and male prefrontal cortex. However, the E2-induced increase in spine size was not detectable in the somatosensory cortex (Hippo male (N = 295), PFC female/male (N =

297/261) vs Hippo female (N = 282) all ns, SSC (N = 315) vs. Hippo female $p < 0.001$; Kruskal-Wallis with post hoc Dunn's test).

As indicated by the relative increase in integrated fluorescence signal, spine size increased in response to E2 treatment in both the hippocampus and prefrontal cortex (Hippo female: control, -1.37 ± 1.61 %, N = 140 spines / 3 slices / 3 animals; oestrogen, 9.86 ± 1.22 %, N = 282 spines / 5 slices / 3 animals; Unpaired t-test, $p < 0.001$; PFC female: control, 2.13 ± 1.45 %, N = 182 spines from 4 slices / 3 animals; oestrogen, 10.03 ± 1.47 %, N = 297 spines from 6 slices / 3 animals; Unpaired t-test, $p < 0.001$; Fig. 29A,B,D). Notably, this was the case for slices obtained from female as well as male animals (Hippo male: control, -2.79 ± 1.61 %, N = 239 spines from 4 slices / 2 animals; oestrogen, 11.06 ± 1.80 %, N = 295 spines from 4 slices / 3 animals; Unpaired t-test, $p < 0.001$; PFC male: control, -0.36 ± 1.20 %, N = 252 spines from 7 slices / 3 animals; oestrogen, 12.53 ± 1.73 %, N = 261 spines from 6 slices / 3 animals; Unpaired t-test, $p < 0.001$; Fig. 29A,B,D). However, no such effects of E2 application on spine size could be detected in acute slices from the SSC (SSC: control, -2.10 ± 1.51 %, N = 206; oestrogen, -3.47 ± 1.42 %, N = 315; Unpaired t-test, $p = 0.521$; Fig. 29C,D).

6.2.3. Oestrogen decreases the threshold for structural potentiation of spines in acute brain slices

Sensitivity to oestrogen signalling has been demonstrated in the SSC as lower levels of E2 during the oestrus cycle or following ovariectomy surgery correlated with a significant decrease in spine density in SSC neurones (Chen et al., 2009; Ye et al., 2019). Moreover, oestrogen receptors are expressed throughout the

SSC of Thy1-EGFP transgenic mice (Alexander et al., 2018). Therefore, I considered it important to carefully interpret the negative results obtained from the SSC. I hypothesised that there may be another reason as to why no changes in spine size could be detected in the SSC. Alexander and colleagues have shown that differences in spine changes related to oestrogen signalling were only detectable in the SSC when plasticity was induced externally (Alexander et al., 2018). This raises the possibility that oestrogen lowers the threshold of plasticity and provides a potential explanation for the results observed in my study.

The hippocampus and PFC are both highly plastic brain regions, involved in cognitive functions and emotional behaviour differing significantly from the functions of the SSC. If the application of oestrogen to the hippocampus and PFC lowers the threshold for plasticity, spine potentiation will be detected as a result of high levels of ongoing activity in these brain regions, but not in the SSC where plasticity-related activity is low without external stimuli.

To test this hypothesis, I used acute slices from 8-12 week old Thy1-EGFP transgenic mice and externally stimulated spines with local glutamate photolysis, driving them to express structural potentiation (Fig. 30). I used an established structural plasticity protocol (sLTP) which produced robust increases in spine size in stimulated but not in neighbouring spines in acute hippocampal slices (Harvey and Svoboda, 2007; Hedrick et al., 2016; Fig 30A,B). Next, some spines were stimulated with a subthreshold protocol (sub; Harvey and Svoboda, 2007; Hedrick et al., 2016) that did not produce any increases in spine size (Fig. 30C,D). However, if slices were pre-incubated in

E2 (100 nM, for 30 minutes) the subthreshold protocol (sub + E2) induced spine potentiation similar in magnitude to the one observed with the sLTP protocol (ΔSpine size at 30 min (% baseline): sLTP: N = 6, 28.90 ± 6.79; sub: N = 5, -5.98 ± 4.13; sub + E: N = 6, 22.32 ± 3.33; sLTP vs sub p = 0.007, sLTP vs sub + E p > 0.99; Kruskal-Wallis with post hoc Dunn's test; Fig. 30C,D).

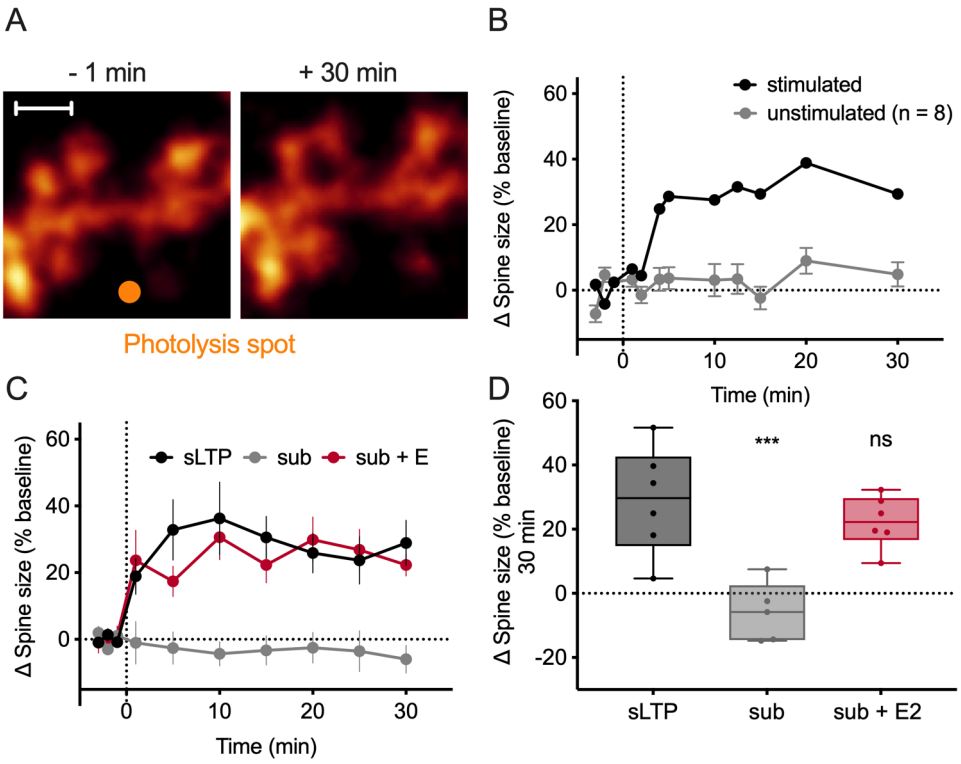

Fig. 30: Oestrogen lowers the threshold for potentiation of spines in acute hippocampal brain slices. (A) Example image of a dendrite with spines from the hippocampus of a Thy1-EGFP transgenic mouse. Glutamate photolysis was performed to induce structural plasticity at small, dim spines. 30 minutes following glutamate photolysis, spines were significantly potentiated. Scale bar: 2.5 µm. (B) Following the structural plasticity protocol based on glutamate photolysis, stimulated spines increased in size, whereas unstimulated neighbouring spines did not. (C) Besides the protocol to induce structural plasticity (sLTP), two other protocols were used. Some spines were stimulated with a subthreshold plasticity protocol (sub) without or with 30 minutes pre-incubation in E2 (sub + E). Spines stimulated with the subthreshold protocol did not change in size. If spines were pre-incubated with E2, the subthreshold protocol produced increases in spine size similar to the ones observed with the sLTP protocol. (D) The increase in spine size compared to baseline is shown after 30 minutes for all three protocols (from C). The structural potentiation effect was absent following subthreshold stimulation but could be reproduced following pre-incubation

with E2 (ΔSpine size at 30 min (% baseline): sLTP: N = 6, 28.90 ± 6.79; sub: N = 5, -5.98 ± 4.13; sub + E: N = 6, 22.32 ± 3.33; sLTP vs sub p = 0.007, sLTP vs sub + E p > 0.99; Kruskal-Wallis with post hoc Dunn's test). Error bars represent SEM.

Having shown that E2 incubation can lower the threshold for structural plasticity induction in acute hippocampal slices, experiments were replicated in the PFC and SSC. Similarly to the hippocampus, robust increases in spine size could be observed following sLTP induction in the PFC and SSC (Fig. 31A,B). Additionally, while the subthreshold protocol did not trigger increases in spine size in control conditions, pre-incubation in E2 (100 nM, for 30 minutes) followed by the subthreshold protocol elicited spine growth in both the PFC (ΔSpine size at 30 min (% baseline): sLTP: N = 8, 22.81 ± 8.94; sub: N = 5, -1.37 ± 4.38; sub + E: N = 5, 21.44 ± 3.96; sLTP vs sub p = 0.026, sLTP vs sub + E p > 0.99; Kruskal-Wallis with post hoc Dunn's test; Fig. 31A,C) and the SSC (ΔSpine size at 30 min (% baseline): sLTP: N = 10, 24.91 ± 4.41; sub: N = 6, 0.68 ± 6.12; sub + E: N = 9, 17.53 ± 6.56; sLTP vs sub p = 0.020, sLTP vs sub + E p = 0.87; Kruskal-Wallis with post hoc Dunn's test; Fig. 31B,C).

In conclusion, this data proves that the SSC is sensitive to oestrogen signalling and incubation of acute brain slices in E2 decreases the threshold of plasticity in the hippocampus, PFC and SSC.

6.2.4. The effects of oestrogen on structural plasticity depend on the basal level of activity

E2 lowers the threshold of plasticity, thus, in highly plastic brain regions such as the PFC and hippocampus, increases in spine size can be detected following E2 application. In the SSC, overall activity and basal plasticity levels are lower,

thus, the application of oestrogen does not produce detectable effects on spine morphology (see 6.2.2.).

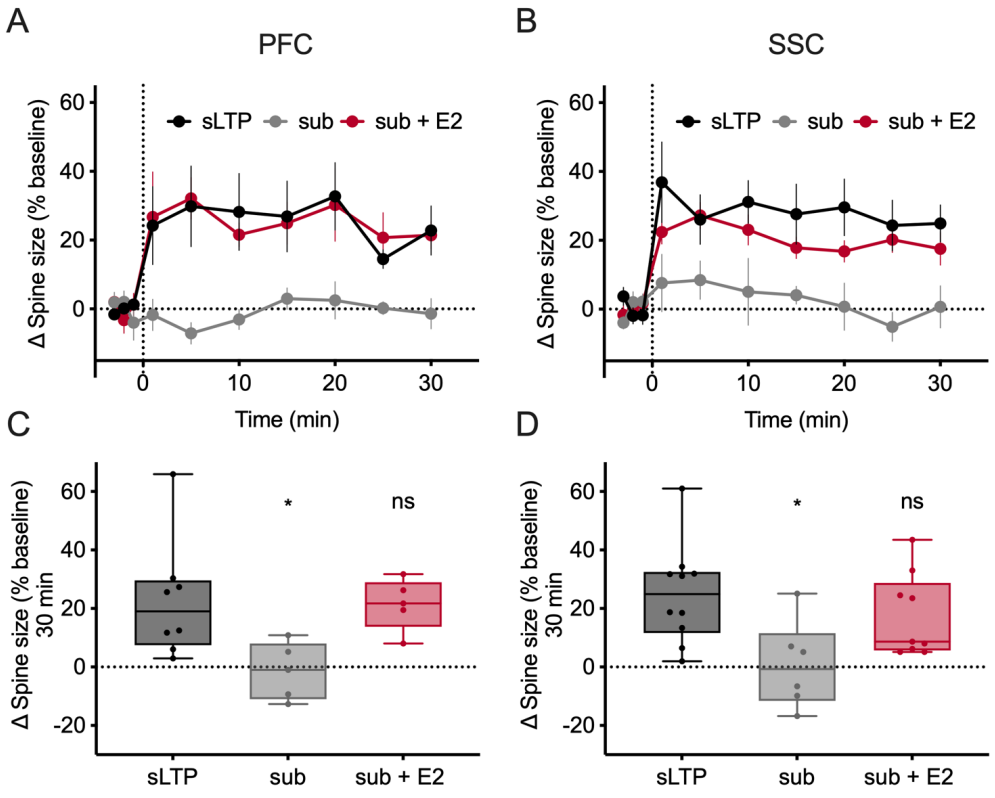

Fig. 31: Oestrogen lowers the threshold for potentiation of spines in acute cortical brain slices. (A,B) Acute slices from the prefrontal cortex (PFC, A) and the somatosensory cortex (B, SSC) of Thy1-EGFP transgenic mice were used for the same experiments as shown in Fig. 30. Spines were stimulated with one of the three protocols: structural plasticity (sLTP), subthreshold plasticity (sub) or subthreshold plasticity with 30 minutes pre-incubation in E2 (sub + E). Similar to the hippocampus, spines stimulated with the subthreshold protocol did not change in size. If spines were pre-incubated with E2, the subthreshold protocol produced robust increases in spine size similar in magnitude to the ones observed with the sLTP protocol. (C,D) The increase in spine size compared to baseline is shown after 30 minutes for the three protocols. No structural potentiation could be detected in spines following subthreshold stimulation but pre-incubation with E2 could rescue the effect in both the PFC (ΔSpine size at 30 min (% baseline): sLTP: N = 8, 22.81 ± 8.94; sub: N = 5, -1.37 ± 4.38; sub + E: N = 5, 21.44 ± 3.96; sLTP vs sub p = 0.026, sLTP vs sub + E p > 0.99; Kruskal-Wallis with post hoc Dunn's test; C) and the SSC (ΔSpine size at 30 min (% baseline): sLTP: N = 10, 24.91 ± 4.41; sub: N = 6, 0.68 ± 6.12; sub + E: N = 9, 17.53 ± 6.56; sLTP vs sub p = 0.020, sLTP vs sub + E p = 0.87; Kruskal-Wallis with post hoc Dunn's test; D). Error bars represent SEM.

To confirm that the lower levels of basal activity in slices from the SSC are the underlying cause why no effects of acute E2 application could be detected, I replicated the initial experiments in acute hippocampal slices from 8-12 week old transgenic mice. Importantly, for these experiments network activity in hippocampal slices was substantially reduced by incubating slices in AP5 and NBQX for several hours (Fig. 32).

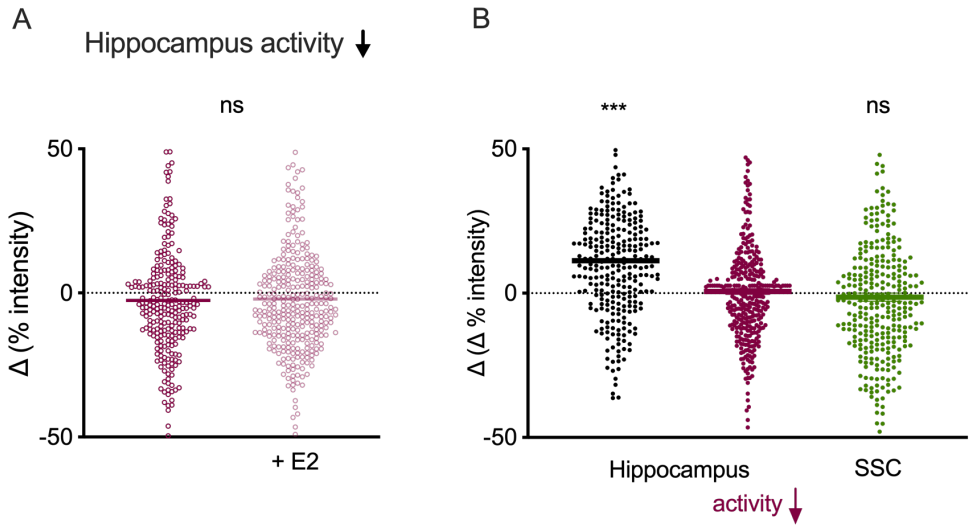

Fig. 32: The application of oestrogen shows no effect on spine size in acute brain slices from hippocampus if network activity was decreased. (A) The difference in fluorescence intensity of spines before and after 30 minutes for control experiments (dark purple) and experiments where 100 nM E2 was applied (light purple) to hippocampal slices, in which global network activity was decreased with AP5 (50 µM) and NBQX (10 µM). The difference in mean fluorescence signal is expressed as percentage change of intensity relative to the intensity before the 30 minutes of incubation. (B) Normalised oestrogen experiments are shown for experiments in hippocampal slices without any treatment (black, from Fig. 29), hippocampal slices where global activity was decreased (purple), and slices from the somatosensory cortex (green, from Fig. 29). E2 incubation of acute slices from the hippocampus potentiated spine size, but this effect was abolished if hippocampal slices were incubated with AP5 and NBQX to decrease activity. In conditions of low activity, no E2-induced changes in spine size were detectable in hippocampal slices, similar as observed for the SSC.

As expected, when activity was suppressed, no effects of E2 on spine size in hippocampal slices were detectable anymore (Hippo low activity: control, -2.59 ± 1.17 %, N = 261 spines from 6 slices / 3 animals; oestrogen, -2.15 ± 1.05 %,

N = 324 spines from 6 slices / 3 animals; Unpaired t-test, p = 0.778; Fig. 32A), yielding similar results as experiments performed in slices from SSC (Hippo female (N = 295) vs Hippo low activity (N = 324) p < 0.001; SSC (N = 315) vs. Hippo low activity (N = 324) p = 0.403; Kruskal-Wallis with post hoc Dunn's test; Fig. 32B).

In conclusion, rather than directly inducing plasticity itself, I show that oestrogen acts as a neuromodulator to lower the threshold of plasticity. Therefore, in states of low activity and few ongoing plasticity processes, no effects on synapse size are detectable as experimental outcomes, as shown for slices from the SSC or hippocampal slices where activity was decreased.

6.3. Discussion

In this Chapter, I have shown that contrary to the conventional view, acute application of E2 does not affect spine number, but increases spine size in the hippocampus and PFC. This effect was reported for acute slices from male as well as female animals but could not be detected in slices from the SSC. I show that the latter result can be explained by oestrogen lowering the threshold of plasticity in hippocampus, PFC, and SSC. The reason why acute effects of oestrogen on spines can only be detected in hippocampus and PFC depends on the overall activity and plasticity occurring inside the network. Even though the SSC is sensitive to oestrogen signalling, the acute application to slices from this brain region does not produce any effects, since the overall activity is low. I have confirmed this hypothesis by showing that if activity is reduced in hippocampal slices, the originally described effect of E2 on spine size is absent. In summary, these data support the idea that oestrogen lowers the threshold of

plasticity, in other words, ‘primes’ the system for subsequent plasticity events. Similar theories were proposed by others, suggesting that oestrogen signalling contributes to a two-step plasticity mechanism (see 6.1., Sheppard et al., 2019; Srivastava et al., 2008). Further experimental evidence supporting this idea implies that E2, following an initial induction of plasticity (Step 1), enhances the magnitude of subsequent LTP (Step 2) elicited by a second high-frequency stimulation (Nebieridze et al., 2012). This mechanism is also known as metaplasticity (Abraham, 2008; Abraham and Bear, 1996). Here, I have provided further evidence for an oestrogen-dependent regulation of metaplasticity and show that this can explain differential results of oestrogen-induced effects on spine morphology detected in different brain areas.

Traditionally, the facilitating effects of E2 on learning and memory have been studied in the PFC and hippocampus (Sheppard et al., 2019; Wallace et al., 2006), with few studies reporting effects in the SSC (Chen et al., 2009). With the development of *in vivo* imaging, recent studies have focused on investigating the effects of oestrogen on spines in longitudinal studies, performed exclusively in the SSC, due to difficulties to implant cranial windows above the hippocampus and PFC (Alexander et al., 2018; Wang et al., 2018; Ye et al., 2019). In the latter studies, oestrogen signalling was either manipulated by external agonist application (Wang et al., 2018; Ye et al., 2019), or the effects of endogenous oestrogen fluctuations during the oestrus cycle have been studied. Effects of oestrogen signalling are consistently reported, however, the impact on spine number varies, potentially due to an incomplete understanding of oestrogen signalling mechanisms with regards to plasticity. Here, I provide evidence that can explain differential results because rather

than directly impacting on synaptic plasticity, oestrogen modulates the state of the synaptic network thereby setting the conditions and threshold for future plasticity actions. Given that activity states and plasticity processes differ between brain regions and even networks, the effects of oestrogen must be discriminated and interpreted more carefully.

A large body of literature supports the fact that oestrogen signalling affects spine number in various brain regions (Sheppard et al., 2019; Ye et al., 2019). By contrast, my findings do not reveal significant effects of acute E2 application on spine number. One possible explanation could be, that the number of dendritic branches analysed was too low to detect an effect, although this seems unlikely as the sample numbers in this study matched other studies were substantial effects were reported (Jacome et al., 2016). Moreover, the literature indicates that oestrogen facilitates spine density by 25–50% (Jacome et al., 2016; Phan et al., 2015, 2012, 2011; Srivastava et al., 2008) and with approximately 25-40 spines analysed per experiment I would expect an increase in spine number of 7-20 new spines per dendrite. Such obvious changes in spine number oppose the overall extremely low number of new and lost spines reported in this work and only subtle differences in spine dynamics triggered by oestrogen could be reported for the hippocampus.

In this study, significant effects of oestrogen application were reported for spine size instead of spine number, which may provide slightly different insights. As reported by some, the generation of new spines following stimulation of oestrogen signalling are immature, ‘silent’ synapses (Phan et al., 2015). In contrast, 30 minutes after E2 application I observed significant changes in spine size that generally correlate with increased AMPA and NMDA receptor numbers

and increased synapse strength (Holtmaat and Svoboda, 2009; Patterson and Yasuda, 2011). My data aligns with the results from other studies, showing that the stimulation of oestrogen signalling has no effect on the overall spine density and number, but enhances the number of larger, 'mushroom' spines (Li et al., 2004; Liu et al., 2008). Importantly, my work suggests that the increase in spine size while induced by oestrogen application, is ultimately caused by ongoing plasticity dynamics within the network. Thus, for the studies published by Li and Liu and colleagues, it may be that activating oestrogen signalling lowers the threshold of plasticity thereby turning smaller, immature spines into larger spines reflecting the higher number of 'mushroom' type spines. Notably, it could still be true that in my experiments, oestrogen induces the formation of new small, silent synapses that cannot be detected as protrusions, potentially due to lack of resolution. Generally, it should be considered, that besides generating new spines, oestrogen induces effects on pre-existing spines emphasising that oestrogen signalling exerts multiple, differentially regulated effects on spine morphology.

Systemic injections of oestradiol correlate with enhanced spine density (Jacome et al., 2016; MacLusky et al., 2005; Woolley and McEwen, 1993, 1992). Such systemic effects differ from the acute experiments presented in this study, since when introduced via subcutaneous injections, oestrogen will trigger other signalling cascades potentially affecting different signalling cascades in the brain. In contrast, the acute application of E2 onto brain slices focuses on the direct effects of oestrogen as a neuromodulator. Overall, it is generally challenging to pin down whether observed effects are due to cycling oestrogen or oestrogen locally synthesised in the brain (Cui et al., 2012; Hojo et al., 2004;

Ishii et al., 2007; Kawato et al., 2002; Rune and Frotscher, 2005). In this work, an effect of cycling oestrogen cannot be excluded, given that acute brain slices were prepared from female animals. It may be that slices were prepared from animals undergoing the high-oestrogen proestrus phase, causing oestrogen signalling to be generally enhanced within the slice. Though the effects of cycling oestrogen are most likely not saturated, since I could detect increases in spine size for all experiments. Importantly, effects could also be detected in slices from male animals at a similar magnitude, indicating that cycling oestrogen plays only a minor role for my results. There are other methods to distinguish the effects from cycling to brain-derived oestrogen, first and foremost the removal of gonadal oestrogen by ovariectomy surgery. Preventing the production of oestrogen with the aromatase inhibitor letrozole affects the hippocampus of ovariectomized animals (Vierk et al., 2015; Zhou et al., 2010), pointing to the relevance of brain-derived oestradiol in synaptic plasticity. Moreover, specific transgenic animals have been generated such as a forebrain-neurone-specific aromatase knock-out (FBN-ARO-KO) mouse model to specifically deplete neurone-derived E2, determining key roles for brain-derived E2 in regulating synaptic plasticity and cognitive function in both female and male animals (Lu et al., 2019). Future studies could include these approaches, to study the effects of oestrogen with regards to different brain regions and its role in metaplasticity.

Here I have shown, that oestrogen as a neuromodulator affects the dynamics and overall state of the synaptic network, by lowering the threshold of plasticity. Moreover, I showed that such effects can be found in the brains of female as well as male animals emphasising its importance as a general neuromodulator.

We only begin to understand the functional consequences of oestrogen signalling in the brain and besides its effects on synaptic plasticity the oestrous cycle impacts many other mechanisms. For example, its effects on cortical inhibition have recently been demonstrated (Clemens et al., 2019). Finally, the data presented in this Chapter supports the notion that the effects of oestrogen on synapses are more complex than originally believed, differentially affecting several brain regions in both female and male animals. In conclusion, oestrogen as a neuromodulator must be considered when studying plasticity processes in order to understand learning and memory.

7. Improving imaging with multimode fibre based micro-endoscopes for monitoring synaptic plasticity

7.1. Introduction

As pointed out throughout this Thesis, subcortical structures such as amygdala or hippocampus are of especial interest, given their central role in cognitive processes including learning and memory. Imaging these structures in living animals represents a crucial step towards a complete understanding of the underlying cellular and subcellular processes of cognitive functions and how they are altered in neurodegenerative diseases. However, scattering and optical aberrations introduced by the heterogenous refractive index distribution within brain tissue hinder fluorescence imaging of structures deeper than 1 mm. To overcome these difficulties, diverse optical strategies have been developed to access deep brain regions. For example, cortical tissue can be aspirated to image hippocampal synapses (Barretto et al., 2011; Dombeck et al., 2010; Gu et al., 2014; Mizrahi et al., 2004; Pfeiffer et al., 2018). Over the years, incorporating fibre optics into imaging tools led to the development of micro-endoscopes for *in vivo* imaging. Gradient refractive index (GRIN) lenses or fibre bundles are commonly used to enable high-resolution imaging of synapse dynamics in *in vivo* applications (Attardo et al., 2015; Szabo et al., 2014).

Recently, multimode fibre (MMF) based micro-endoscopes have been developed, significally reducing the device footprint within the brain (Turtaev et al., 2018; Vasquez-Lopez et al., 2018). These systems allow minimally-invasive high-resolution imaging of subcortical brain regions (Vasquez-Lopez et al., 2018). Compared to conventional deep-brain imaging techniques, the MMF

system developed by our lab causes significantly less tissue damage, which may compromise the physiology of neuronal networks. This is due to the small size of MMF-based endoscopes, with total diameters of less than 150 µm (Fig. 33B).

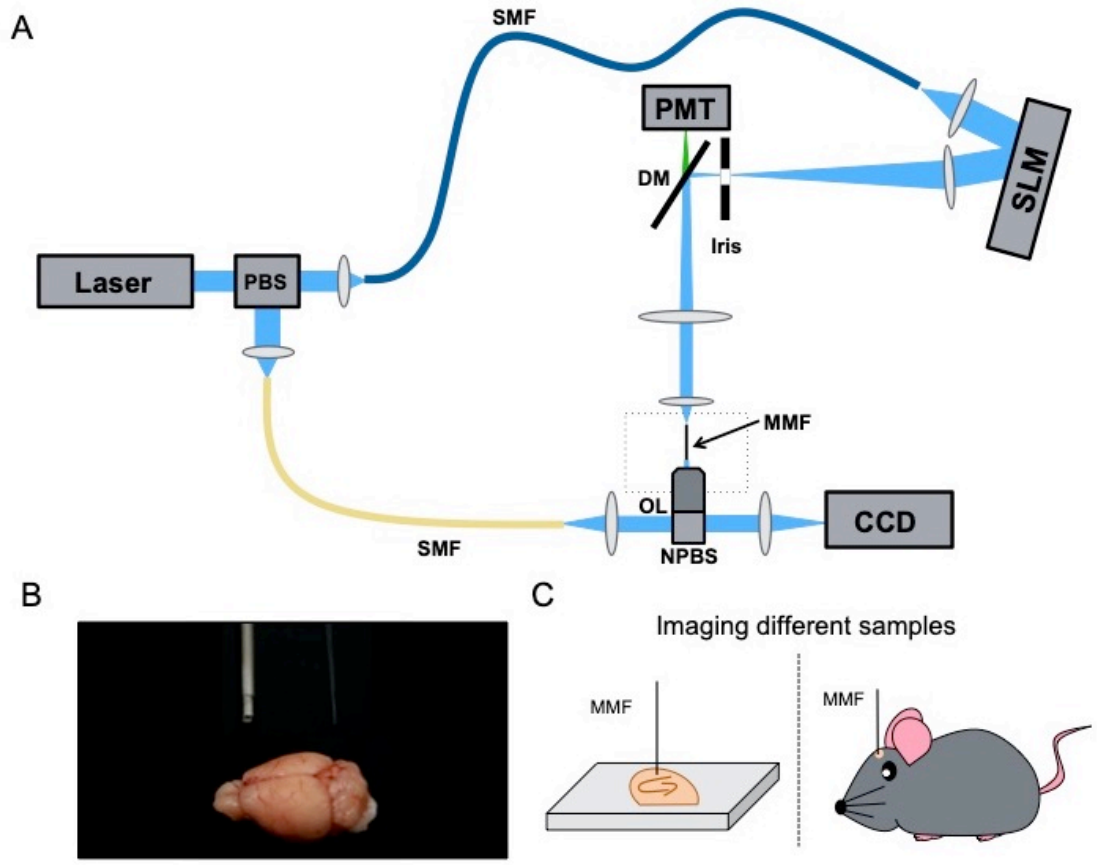

Fig. 33: MMF imaging system. (A) Schematic of the experimental system: A 488 nm light beam is split and coupled into two separate single mode optical fibres (SMF). Wavefront shaping of light is achieved using a LC-SLM. The light is transformed onto an iris that only transmits the first diffraction order. The transmitted signal is then reflected by a dichroic mirror and coupled into a multimode fibre. During the calibration the output of the MMF is imaged by a microscope objective lens and, together with a reference beam delivered by a SMF, imaged onto a CCD camera. PBS polarising beam splitter, SMF single mode fibre, PMT photo multiplier tube, SLM spatial light modulator, MO microscope objective, MMF multimode fibre, NPBS non polarising beam splitter, CS coverslip, DM dichroic mirror. (B) Picture of a mouse brain with optical components for in vivo imaging: a GRIN lens (left), and a 50-µm-core 0.22 NA MMF (right). (C) For imaging, the objective lens together with the whole calibration unit was replaced by a sample. Either by organotypic hippocampal slices or by an anaesthetised Thy1-EGFP mouse.

Generally, MMFs guide light by total internal reflection. As light propagates through the fibre, unpredictable phase delays and coupling occur between modes causing the output intensity profile from a uniform input to have a speckle-like appearance. In order to fully describe the light-field propagation through the MMF we use a liquid-crystal spatial light modulator (LC-SLM) to manipulate the propagating light field (Fig. 33A). Prior to imaging, the LC-SLM is used in a calibration procedure to determine the light-field propagation through the MMF in form of a transmission matrix (TM; see Methods). The goal of the calibration procedure is to use the TM to generate a high intensity spot of laser light after the fibre that can be scanned across the sample to excite fluorophores, just like a standard point-scanning confocal microscope.

Generally, the calibration procedure involves distal optical components, however, the impact of distal optical aberrations present during calibration versus imaging is not known. Traditionally, the TM is frequently evaluated with the distal facet of the MMF in air. For imaging of biological structures, fibres are inserted in other milieus than air, such as in different biological tissues. This causes a refractive index mismatch between the biological and calibration media, probably affecting imaging performance. For example, the index of refraction in air is $n_{air} = 1.00$, which greatly differs from brain tissue, where $n_{brain} = 1.37$ (Binding et al., 2011). Thus, this type of mismatch is commonly encountered in neuroscience applications, as calibrations are routinely performed in air, while imaging is performed in brain tissue (Turtaev et al., 2018; Vasquez-Lopez et al., 2018).

A common goal when developing new imaging tools is to implement multiphoton techniques, given the numerous image quality-enhancing features

provided by multiphoton versus single-photon imaging (see 2.3.4.). Multiphoton imaging through MMFs has been previously demonstrated, but only with bead samples, CHO cells in vitro, and fixed cochlear hair cell samples (Kakkava et al., 2019; Morales-Delgado et al., 2015b; Pikálek et al., 2019; Sivankutty et al., 2016). Implementing multiphoton imaging into MMF systems offers unique advantages for brain imaging besides enhancing image quality. For example, volumetric two-photon fluorescence imaging methods based on axially extended foci are particularly well-suited to monitor neuronal dynamics occurring on the millisecond timescale (Ji et al., 2016; Lu et al., 2017; Thériault et al., 2014).

In the following Chapters, my overall goal was to further the development of the next-generation MMF based micro-endoscopes specifically in the context of improving monitoring of synaptic plasticity. First, I present MMF-based high-resolution images of dendrites and spines *in vitro* and *in vivo*. Next, I have characterised the effects of a refractive index mismatch between the biological and calibration media on focus formation in the context of brain imaging using one-photon fluorescence point-scanning microscopy through MMF. My results showed that the effects of refractive index matching on fluorescence imaging were substantial and should be considered when using MMF-based systems for biological imaging (*published in* Turcotte et al., 2019). Finally, I have demonstrated two-photon fluorescence imaging with an axially extended focus through a MMF. By considering the wavelength-dependent axial shift caused by the limited bandwidth of step-index MMFs, an extended focus could be generated through chromatic dispersion. I showed that this focus can be used for volumetric imaging of beads and neurones in living rat brain slices

(*published in* Turcotte et al., 2020a). Overall, I present several important advancements of MMF-based endoscopic applications, to increase imaging performance and image quality of neuronal structures with these devices.

7.2. Results

7.2.1. *In vitro* and *in vivo* imaging of synapses using a multimode optical fibre

To assess the imaging performance of the MMF-based system I began by imaging neuronal structures in ex vivo brain slices and in transgenic animals with particular focus on synaptic terminals (Fig. 34). The MMF used in these experiments had a total diameter of 125 µm, with a 50 µm core and a NA of 0.22 (Thorlabs, FG050UGA). Prior to imaging, the LC-SLM was used to determine a transmission matrix (TM), describing the light propagation through the MMF (see Methods). Using this TM, the light field could be modulated to produce a diffraction-limited spot at specific locations across the fibre output plane, thus serving as the basis for MMF-based point-scanning fluorescence micro-endoscopy. Notably, foci can be generated at an arbitrary distance from the distal fibre facet (see Methods). For experiments in Figure 34, data were acquired 50 µm away from the distal facet. A three-dimensional micro-positioing stage was used to align the MMF during calibrations as well as to navigate the MMF probe into brain tissue. As previously described the MMF-micro-endoscope achieves diffraction-limited performance with a FWHM of the excitation PSF of 1.27 ± 0.01 µm laterally and 20.2 ± 1.4 µm axially (Vasquez-Lopez et al., 2018).

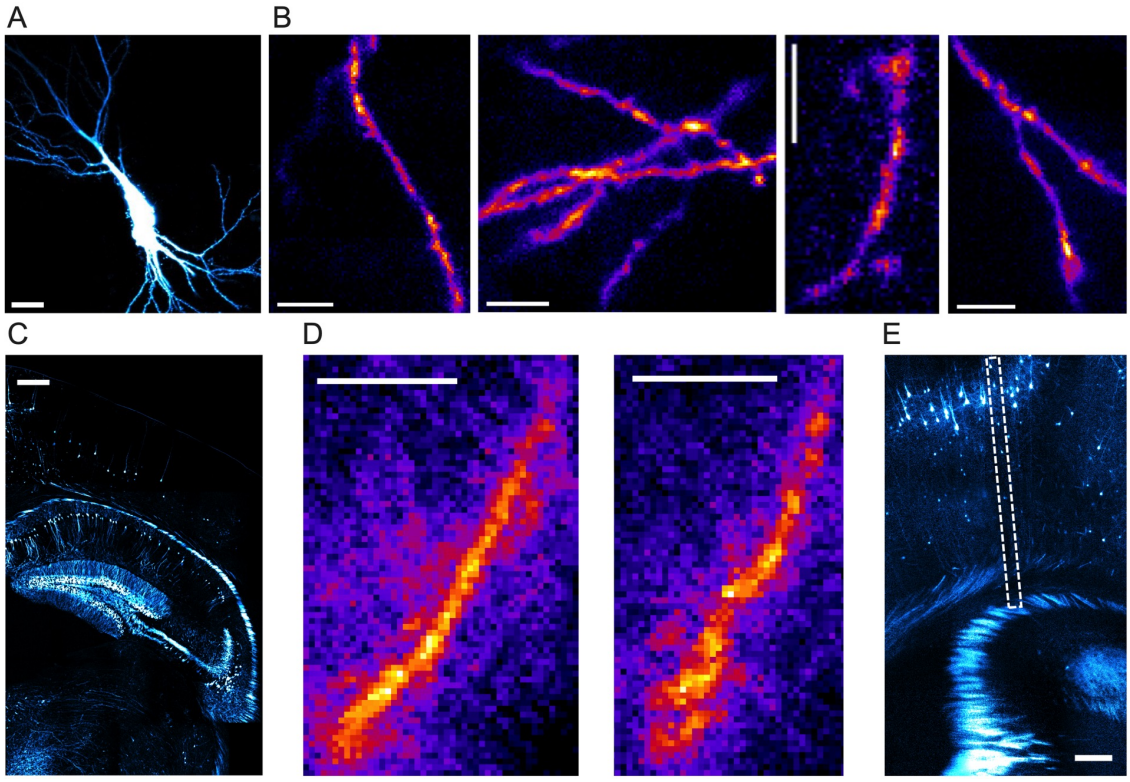

Fig. 34: MMF imaging of live neurones *in vitro* and *in vivo.* (A) Confocal image of a hippocampal neurone in a rat brain slice filled with structural dye (Alexa Fluor 488) before imaging with the MMF. Scale bar: 20 µm. (B) Structural images through a MMF reveal dendrites, on which spines could be clearly identified Scale bars: 10 µm. (C) Imaging was performed by inserting a MMF 1.7 mm into the brain of an anesthetized Thy1-EGFP mouse. Thy1-EGFP mice showed sparse labelling of neurones and dendrites in the cortex and dense labelling of the hippocampus, as demonstrated by this image of a fixed slice obtained from these animals. Scale bar: 200 µm. (D) Structural images through a MMF in an anesthetized Thy1-EGFP mouse. Dendritic spines are visable. Scale bars: 10 µm. (E) Post-mortem histological section of the mouse brain imaged in (D) showing the path of the fibre through the cortex. Scale bar: 100 µm.

For imaging in hippocampal slices, two to three CA3 pyramidal neurones in organotypic hippocampal slices were filled with the structural dye Alexa Fluor 488 (2 mM) via patch-clamp technique (Fig. 34A). To ensure slice health, imaging of hippocampal slices was performed in physiological Tyrode's solution. Indeed, when imaging dendritic processes with the MMF-based system spines could be identified (Fig. 34B). To explore imaging performance *in vivo*, I sought to image neuronal processes in the intact brain of live mice. For

this purpose, I used transgenic Thy1-EGFP mice in which neurones are sparsely but brightly labelled throughout the nervous system (Fig. 34C). Mice were anaesthetised and a small craniotomy was performed which was sufficient to directly insert the fibre into the brain. Subsequently, the fibre was advanced slowly through the tissue until a target structure was identified. Figure 34 shows images of fluorescent neuronal processes imaged after lowering a fibre 1.7 mm into the brain of an anesthetized Thy1-EGFP mouse. Processes could be identified as dendrites, with dendritic spines clearly visible (Fig. 34D). Post-mortem histological analysis confirmed the trajectory of the fibre through the cortex down to deeper brain structures (Fig. 34E).

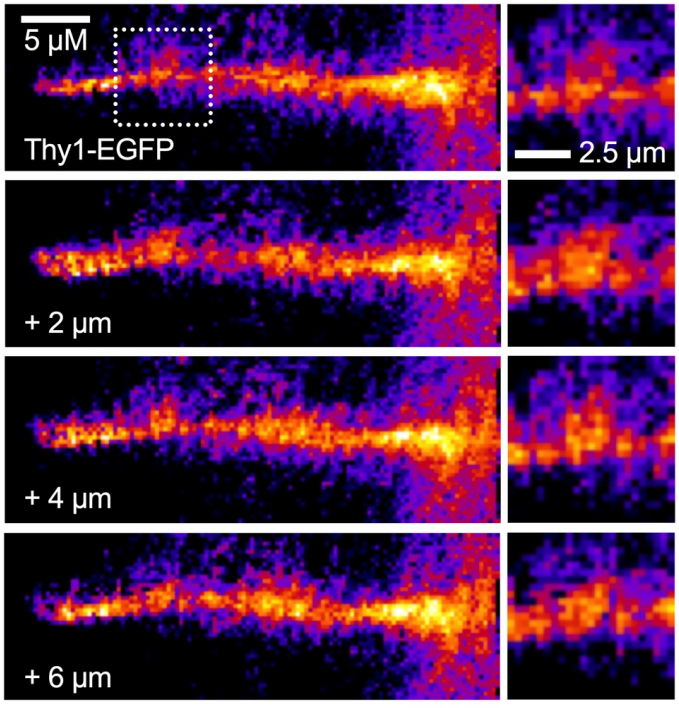

Fig. 35: MMF imaging of spines *in vivo.* Left, imaging was performed in a Thy1-EGFP mouse at a depth of 1.6 mm. A neuronal process was observed at different depths in 2 µm increments. The process could be identified as a dendrite with spines. Right, The three dimensional structure of one prominent spine (indicated by the white dashed box) became visible when changing imaging depth.

Figure 35 displays images of a dendritic branch *in vivo* recorded with the MMF-based system at a depth of 1.6 mm. Specifically, when lowering the fibre in 2 µm steps into the brain, the three-dimensional structure of dendritic spines can be observed (Fig. 35). Thus, I have confirmed that the MMF-based system is suitable for structural imaging imaging of neuronal processes and synapses in living neuronal tissue *ex vivo* as well as *in vivo*. In the following, I seeked to explore potential strategies to further improve image quality.

7.2.2. Enhancing image quality by increasing the numerical aperture of the multimode fibre

In the previous experiments, MMFs with a NA of 0.22 were used. However, MMFs can be designed and fabricated with varying NAs. Generally, a light ray's angle of incidence determines if it will be coupled into the fibre's core. The limit of this angle, in other words the 'cutoff angle' represents the maximum acceptance angle in which light rays will be coupled into the fibre and thus propagate through the fibre via total internal reflection. The maximum acceptance angle is directly related to the NA and thus the NA of the MMF determines the amount of light brought into the fibre. The NA is a critical factor regarding the resolution limit when imaging through multi-mode fibres (Mahalati et al., 2013). Hypothetically, increasing the NA of the fibre should increase the information content that can be collected, and therefore increase the quality of the image. To evaluate the effects of increasing the NA of the MMF in our system, I conducted imaging trials with two different types of MMFs with either a NA of 0.22 (Thorlabs, FG050UGA, 50 µm core) or 0.66 (doric lenses, MFC-ZF1.25, 44 µm core). Neurones in organotypic hippocampal slices were filled with Alexa 488 using patch-clamp electrophysiology. Subsequently, the brain

slice was positioned below the fibre and image acquisition started. High-resolution images of dendrites and dendritic spines were recorded (Fig. 36).

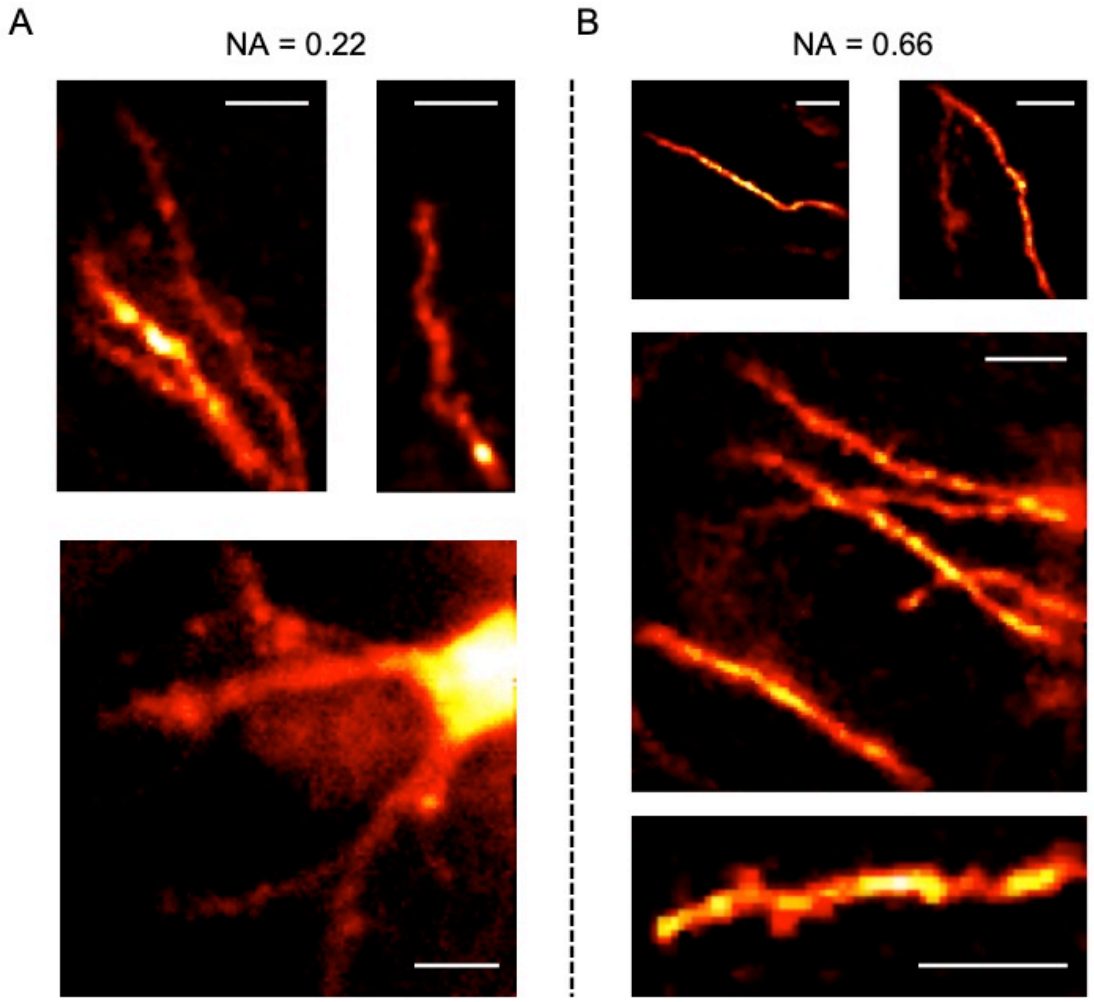

Fig. 36: MMF in vitro imaging of neurones. (A-B) Structural images of CA3 pyramidal neurones in organotypic hippocampal slices through a MMF with either a NA of (A) 0.22 or (B) 0.66. Cell somas, neuronal processes and dendritic spines can be identified. Scale bars: 10 µm.

As expected, image quality was increased with the 0.66 NA fibre compared to the 0.22, with improved resolution and a higher signal-to-noise ratio (Fig. 36). Thus, when imaging small synaptic structures with MMF, using a higher NA

MMF may be beneficial as increased resolutions are necessary to properly monitor synapses.

7.2.3. Focusing light in biological tissue through a multimode optical fibre: refractive index matching

Besides basic features of the MMF fabrication such as the NA, the calibration procedure significantly affects imaging performance. Typically, calibrations are performed in air, while the actual imaging is performed in biological tissue, such as brain structures. Thus, a refractive index mismatch emerges between the calibration and imaging media. Notably, the impact of such distal optical aberrations present during calibration versus imaging has not been characterised before and thus was explored here.

Fig. 37 depicts the experimental set-up of the study. A 50 μm core fibre (Thorlabs, FG050UGA; NA = 0.22) was used and data were acquired 50 μm away from the distal facet. Two different calibrations were acquired with a media present between the MMF distal facet and the coverglass, either air (Fig. 37b) or a 22% glucose solution (Fig. 37c), which will be referred to as the air and glucose calibration for the remainder of this Thesis. Then, focusing and imaging quality was evaluated with the distal end of MMF submerged in a solution of 22% glucose, having a similar refractive index to brain tissue (n_{brain} = 1.37, $n_{glu,22\%}$ = 1.37; Binding et al., 2011; Turcotte et al., 2019).

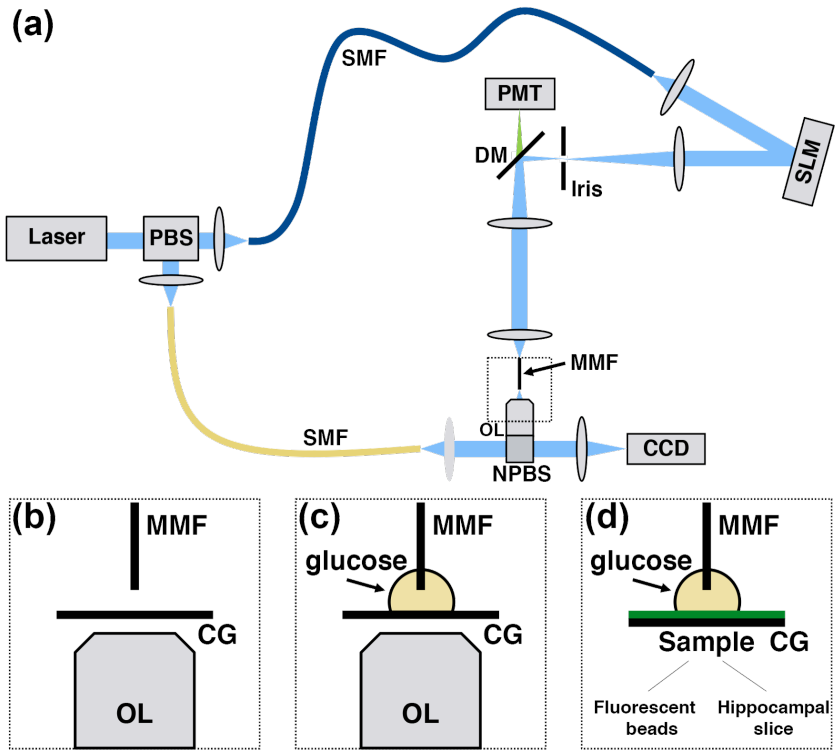

Fig. 37: Experimental set-up. (a) Simplified schematic of the optical system (SMF, single mode optical fibre; PBS, polarising beam splitter; PMT, photomultiplier tube; DM, dichroic mirror; SLM, spatial-light modulator; NPBS, non-polarising beam splitter; MMF, CCD, charge-coupled device; multimode fibre; and OL, objective lens). (b–d) Schematics of the experimental setup: (b) for air calibration, (c) for glucose (refractive index matching) calibration, and (d) for imaging (CG, coverglass). *Published in Turcotte et al., 2019, Optics Letters, Vol. 44, No. 10*

First, the effect of a refractive index mismatch between the calibration and imaging media on the illumination focus was assessed. Three metrics were used to characterise focus quality: the peak intensity, the intensity enhancement factor (IEF), and the lateral full width at half-maximum (FWHM). The FWHM and IEF of the illumination focal volume was assessed when the distal end of MMF were submerged in glucose, for both prior calibrations performed in air or glucose. At the centre of the imaged field, the peak intensity and IEF were 20 ± 11% and 11 ± 10% larger, respectively, when using the calibration acquired in a 22% glucose solution over the one acquired in air (n =

6, one-sided paired Wilcoxon signed rank test, p = 0.016; Fig. 38a). Similarly, the FWHM decreased from 1.28 ± 0.05 µm with the air calibration to 1.24 ± 0.05 µm with the 22% glucose one (n = 6, one-sided paired Wilcoxon signed rank test, p = 0.03; Fig. 38b). By analysing the variation in peak intensity and FWHM as a function of the distance from the centre of the fibre, it became evident that the peak intensity and FWHM were constant over a larger radius in the index-matched condition, thus providing a more uniform field-of-view (Fig. 38c,d).

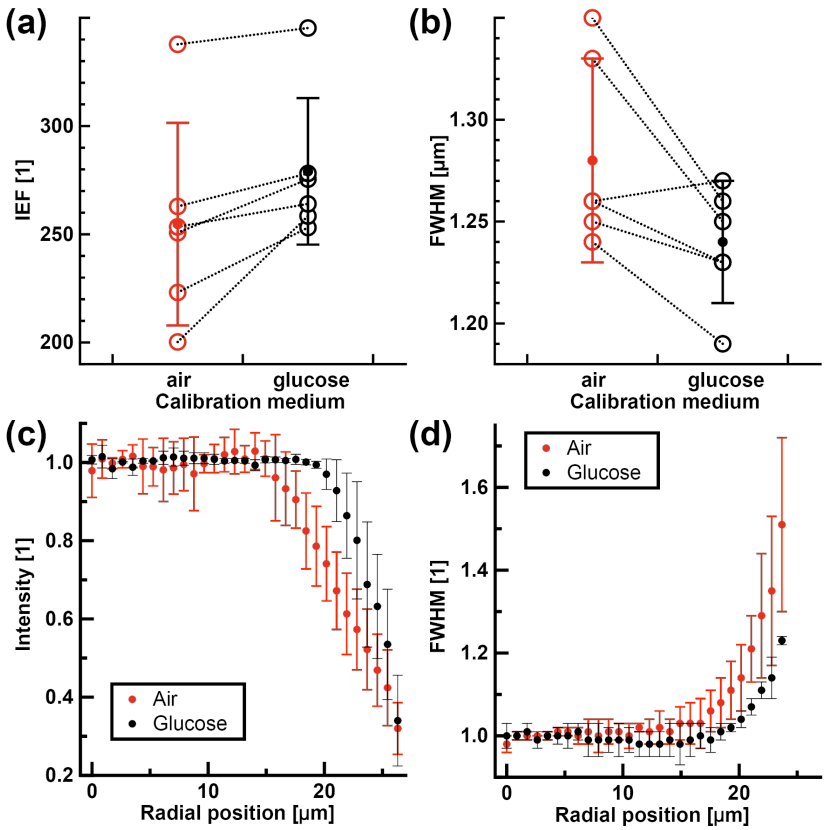

Fig. 38: Characterisation of the illumination focal volume through an MMF in a 22% glucose solution. (a, b) Focal volume at the centre of the MMF, characterised by (a) the IEF and (b) FWHM as a function of the calibration medium (n = 6 fibre segments, open circles represent individual measurements). (c, d) Radial variation in (c) peak intensity and (d) FWHM of the focal volume for a calibration done in air and in a 22% glucose solution (n = 3 fibre segments). Full circles are average values, and error bars represent the standard deviation. *Published in Turcotte et al., 2019, Optics Letters, Vol. 44, No. 10.*

These results indicate that matching the refractive index of the calbration and imaging media will improve the signal-to-background ratio and the lateral width of the illumination focus and improving focus formation at the outer regions of the fibre facet.

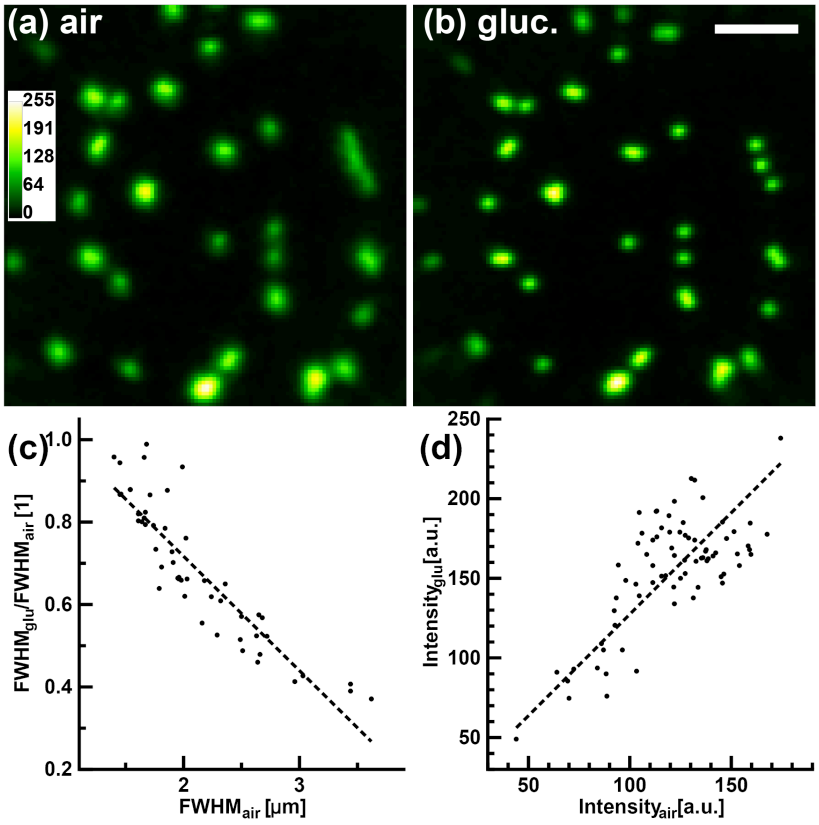

Fig. 39: Imaging of fluorescent beads through an MMF. (a, b) Images of 1.0-µm beads acquired with the TM determined from a calibration in (a) air and in (b) a 22% glucose solution. Scale bar: 10 µm. Images were normalised to the peak intensity in (b). (c) Graph of the FWHM ratio for individual beads from images acquired with the glucose TM over that of the air TM as a function of the FWHM measured from images acquired with the air TM (n = 51, for individual beads from images acquired with the glucose calibration slope = − 0.3 µm^{-1}, R^2 = 0.81). (d) Graph of the peak intensity as a function of the peak intensity measured from images acquired with the air calibration (n = 75, slope = 1.3, R^2 = 0.47). *Published in Turcotte et al., 2019, Optics Letters, Vol. 44, No. 10.*

Next, a number of fluorescent samples were used in order to test how a refractive index mismatch between calibration and imaging media impacts imaging performance. Fluorescent beads samples (1.0 µm, yellow-green fluorescent (505/515)) were prepared and imaged in a 22% glucose solution, while images were acquired with both an air (Fig. 39a) and a glucose calibration (Fig. 39b) at their respective optimal focal plane.

Comparing the two conditions revealed that individual beads had a circular profile in images acquired with the glucose calibration (0.91 ± 0.05), whereas the bead shape was less symmetric for the air calibration (0.79 ± 0.11, circularity: n = 36, one-sided paired Wilcoxon signed rank test, $p = 2.1 \times 10^{-6}$; Fig. 39). Circularity was calculated after fitting an ellipse to individual beads and calculating the ratio of the minor to major axis. When measuring the FWHM of single beads the ratio between the glucose and air calibration was 0.69 ± 0.17 (n = 51, Δ35%, one-sided paired Wilcoxon signed rank test, $p = 3 \times 10^{-9}$; Fig. 39c). Most of the variability originated from the FWHM measured with the air calibration (2.1 ± 0.5 µm), while the FWHM with the glucose calibration was more consistent between beads (1.37 ± 0.13 µm). This observation is in line with a more uniform illumination being achieved with the glucose calibration. Notably, the significant gain in peak intensity, a factor of 1.3 ± 0.2 (n = 75, one-sided paired Wilcoxon signed rank test, $p = 1.0 \times 10^{-13}$; Fig. 39d), was larger than that achieved for the illumination peak intensity.

How does refractive index matching of the calibration and imaging media affect imaging in biological samples? To explore the latter, CA1 pyramidal neurones from organotypic hippocampal slices were patch-filled with Alexa Fluor 488 (0.5 - 1 mM; Fig. 40). To maintain slice health, imaging of hippocampal slices was

performed in physiological Tyrode's solution. Two calibrations were performed: in air and in Tyrode's solution, respectively. With the air calibration, no synaptic specialisations (dendritic spines) were visible (Fig. 40a). In contrast, spines were clearly visible with the Tyrode's calibration (Fig. 40b).

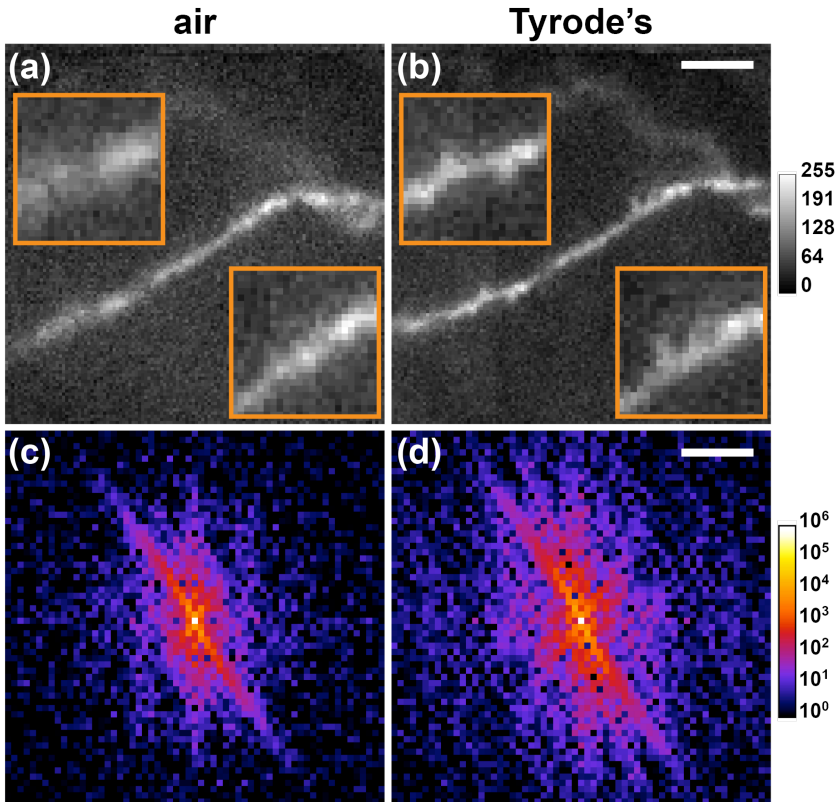

Fig. 40: Imaging of live neurones through an MMF in organotypic slices. (a, b) Images of a dendrite labelled with Alexa Fluor 488, acquired with the TM determined from a calibration in (a) air and in (b) a Tyrode's solution. Scale bar and inset width: 10 µm. Images were normalised to the peak intensity in (b). (c, d) Power frequency spectra of the images shown in (a, b), respectively. Scale bar: 0.22 μm^{-1}. *Published in Turcotte et al., 2019, Optics Letters, Vol. 44, No. 10.*

This improvement in spatial resolution and signal-to-background ratio was also apparent in the Fourier transform images (Fig. 40c,d), revealing the larger spatial frequency bandwidth accessible with the Tyrode's calibration. Additionally, with the air calibration the shape of the dendrite was distorted,

appearing tilted with respect to the focal plane. Thus, refractive index matching of the calibration and imaging media significantly improves image quality in live brain tissue, highlighted by the fact that fine neuronal structures such as synapses could only be detected when both the calibration and imaging were performed in Tyrode's.

7.2.4. Volumetric two-photon fluorescence imaging of beads and live neurones using a multimode optical fibre

Having characterised several aspects as to improve image quality mainly focussing on conditions pre-imaging, i.e. choosing a higher NA fibre and matching the refractive index of the calibration and imaging medium, potential system-integrated technologies facilitating imaging performance should be considered. So far, the MMF-based micro-endoscope system for fluorescence imaging was based on a continuous wave (CW) laser producing 488 nm excitation light. However, volumetric two-photon fluorescence imaging methods based on axially extended focus are particularly well suited to monitor neuronal dynamics. Moreover, multiphoton imaging in neuroscience applications is beneficial over one-photon imaging, offering lower background signal and less phototoxicity.

Therefore, we implemented a dual-source laser (Mira Optima 900-F V5XW, coherent, 830 nm, 76 MHz, mode: CW or femtosecond pulses (pulsed)) into the MMF-based system (Fig. S7.1, Appendix). We employed a step-index MMF offering a relatively high NA of 0.37 and a total diameter of 75 µm, which are optimal in terms of maximizing lateral resolution and minimizing invasiveness, respectively. The TM was evaluated with the laser source in CW mode, as

described earlier. For all data, the calibration was performed 40 µm from the distal facet. After the calibration, the laser was switched to pulsed mode allowing transverse spatial focusing of femtosecond laser pulses through a MMF (Fig. S7.2, Appendix). After confirming that uniform illumination with multiphoton excitation can be achieved across the field-of-view (Fig. S7.2, Appendix), the axial properties of the illumination focus were evaluated. By taking advantage of the wavelength-dependent axial shift we could generate an extended focus through chromatic dispersion, thereby the lateral FWHM was maintained below 1.5 µm over a distance of 40 µm (Fig. S7.3, Appendix).

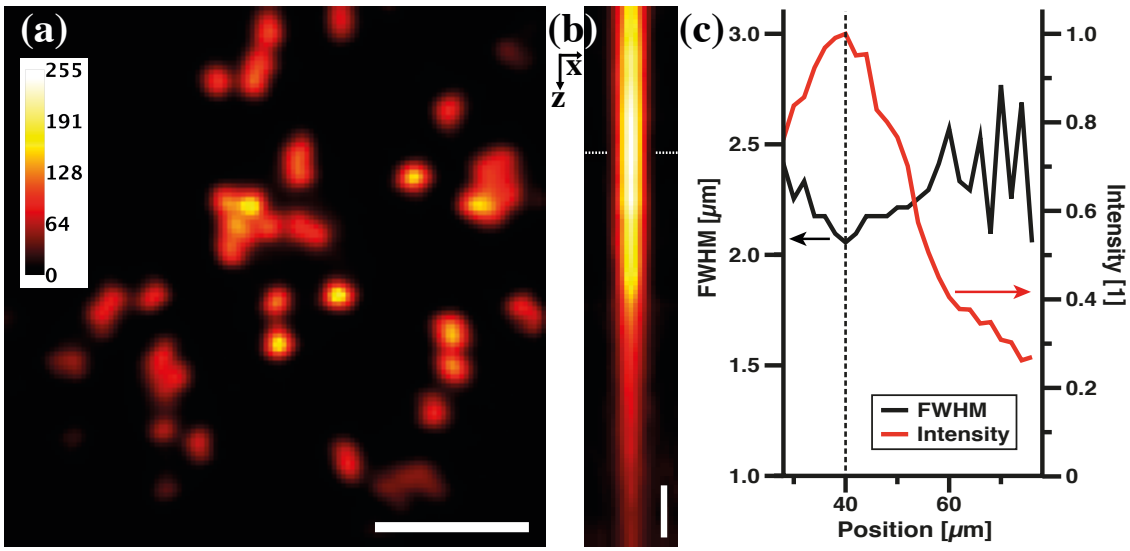

Fig. 41: MMF volumetric two-photon fluorescence imaging of beads. (a) Image of beads located at the calibration plane (40 µm from the MMF facet). Scale bar: 15 µm. (b) Averaged axial (z)-lateral (x) profile from five beads. Images were acquired by translating the sample in steps of 2 µm. Scale bar: 5 µm. (c) Intensity profile and FWHM as a function of the distance between the distal facet and sample for the data shown in (b-c) Dashed lines indicate the calibration plane. *Published in Turcotte et al., 2020, Optics Letters, Vol. 45, No. 24.*

Once the TM was generated and the system performance was characterised, the calibration module was removed, and fluorescent samples were positioned at the distal end of the fibre for two-photon volumetric imaging through a MMF. Note that to increase stability, the original system described by Vasquez-Lopez and colleagues was adjusted, so that instead of lowering the fibre, the sample was positioned on a 3D stage and moved while the MMF remained fixed. Using 2 μm red fluorescent beads (580/605) images were acquired displaying an excellent signal-to-noise ratio (SNR= 6.0 ± 0.6) with a total incident power at the sample of 10 mW (Fig. 41a). Figure 41b shows an axial-lateral profile of single beads recorded by translating the sample in steps of 2 μm. This profile reveals the extended focus along the axial dimension, as the signal was detectable even when the sample was located 30 μm away from the calibration plane. The lateral FWHM of a single bead was relatively constant (2.2 ± 0.1 μm) in the 30 μm around the calibration plane (Fig. 41c).

As the design of the MMF-system is optimised for imaging in live tissue, I assessed its performance by imaging Alexa Fluor 594 labelled CA3 pyramidal neurones in living brain slices from the rat hippocampus. Organotypic hippocampal slices were imaged in physiological Tyrode's solution at room temperature. Fluorescent structures were readily located and could be identified as neuronal cell soma (Fig. 42a). Pyramidal cell apical dendrites were also clearly visibly projecting from the soma. In an attempt to visualise smaller features, the apical dendrite was followed away from the cell body. Subsequently, secondary dendritic branching from the primary apical dendrite could be detected (Fig. 42b).

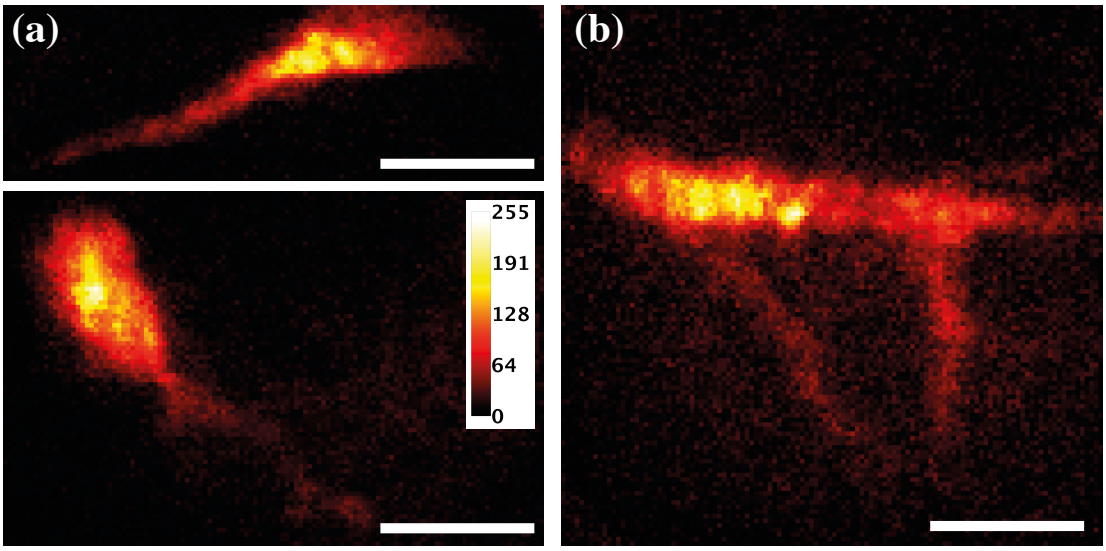

Fig. 42: MMF volumetric two-photon fluorescence imaging in live brain tissue from the rat hippocampus. (a) neuronal cell bodies and apical dendrites (b) smaller dendrites branching off from an apical dendrite, after labelling CA3 neurones with 5 mM of Alexa Fluor 594 using whole-cell patch electrophysiology. Scale bar: 15µm. *Published in Turcotte et al., 2020, Optics Letters, Vol. 45, No. 24.*

7.3. Discussion

Visualising synapses within live tissue is the main application of MMF-based imaging systems, as they are optimised for high-resolution live brain imaging through compactness, stability, and mobility (Vasquez-Lopez et al., 2018). Given that this technique is relatively new, I have demonstrated various technical advances that are useful to enhance imaging performance with MMF-based systems. These include basic properties of the MMF such as the NA, refractive index matching of the calibration and imaging media and the implementation of two-photon volumetric imaging.

I have shown, that using MMF with higher NA provides increased spatial resolution and higher signal-to-background ratio. Importantly, using fibres with higher NA is desirable as they have been linked to a decreased sensitivity to

bend translation, which is important especially for *in vivo* applications (Bianchi et al., 2013; Loterie et al., 2017). Notably, increasing the NA of a MMF will have substantial impacts on other aspects presented in this Chapter. For example, increasing the NA will most likely increase the aberrations originating from a mismatch in the refractive index between the calibration medium and the sample. Moreover, for two-photon fluorescence MMF-based imaging, high-NA fibres are essential as two-photon fluorescence efficiency increases nonlinearly with the NA (Morales-Delgado et al., 2015b, 2015a). Generally, increasing the NA affects the number of modes propagating through the MMF, more precisely, the number of modes scales with the square of the NA (Loterie et al., 2017). Thus, increasing the NA necessitates higher computational power, and the more modes are characterised the longer the calibration procedure takes. A similar relationship is known with regards to the diameter of the MMF. One current limitation is the field-of-view (FoV) of the system, which corresponds to the core diameter of the MMF (50 or 60 μm in this Chapter). Wider FoVs can be achieved using MMF with larger core diameters (Vasquez-Lopez et al., 2018). However, using such large-diameter MMF would require a different wavefront-shaping device with increased pixel capacity to allow for the larger number of modes guided by such MMF. Moreover, this comes at the cost of increased invasiveness, and might not be necessary for imaging synapses that are only 1-2 μm in diameter. Conclusively, increasing the NA and diameter of the fibre significantly will enhance spatial resolution and increase the field-of-view but there is a trade-off in calibration speed and new wavefront-shaping devices are most likely required to implement such changes. Nevertheless, the implementation of a different wavefront-shaping device would be desirable,

since our current MMF-system is also limited in imaging speed depending on the refresh rate of the LC-SLM. Alternatively, digital micro-mirror devices could be incorporated in the system, achieving update-rate orders of magnitude larger than LC-SLM (Conkey et al., 2012; Mitchell et al., 2016; Turtaev et al., 2017). Increasing the imaging speed would be essential for functional imaging, i.e. using Ca^{2+} and voltage-dyes, but are not necessarily required for structural imaging of synapses.

A fibre-specific calibration is required to shape light through MMF prior to imaging. It is well known that such calibration will compensate not only distortions occurring inside the fibre, but proximal aberrations as well. However, the data presented here indicate that this is not true for distal aberrations. Indeed, the ability to resolve subcellular, synaptic structures is substantially improved when one takes account of the refractive index of brain tissue during the calibration. Even when focusing light at 488 nm through only 50 μm of tissue, a significant difference was measured, both in terms of focus quality and uniformity across the FoV. The aberrations present when performing the calibration in air are akin to spherical aberrations. They nevertheless differ in that the light field at the distal facet, the interface where the refractive index changes, is not uniform and varies between fibres. Accordingly, the aberrated focal profile will be fibre dependent, depending on the spatial intensity and phase variations at the interface. It is also interesting to note that the lateral extent of the focus deteriorated when a mismatch was present, while spherical aberrations typically have a limited effect on this parameter (Turcotte et al., 2017).

Moreover, the results obtained from the refractive index matching experiments point to the importance of assessing the performance of MMF-based imaging systems using the signal of interest. Indeed, the effects of refractive index matching on fluorescence imaging were substantial, while the improvements in illumination focus were moderate, most likely resulting from the detected fluorescence signal being a lateral and axial integration within the illumination focus. Thus, the results with respect to the fluorescence imaging experiments correspond more closely to the actual improvement that will be achieved in images of biological samples. Overall, this suggests that it might not be sufficient to look exclusively at the illumination, as is commonly done for MMF-based imaging systems, to characterise the impact on imaging performance. Importantly, I found that under the impact of a refractive index mismatch between the calibration and the imaging medium, neuronal structures appeared tilted towards the edges. This observation has previously been assumed to reflect the actual position of the dendrite (Vasquez-Lopez et al., 2018), however, this is clearly erroneous as the dendrite lay within the focal plane of the Tyrode's image. In fact, it was the reduced uniformity in focusing ability with the air calibration that generated less resolved structures, appearing out-of-focus, at the circumference of the image. While here the significance of the observations related to refractive index matching are emphasised for biological imaging, the ultimate conclusion stating the importance of considering distal aberrations, applies to all applications requiring focusing light at the distal end of a MMF.

Matching the refractive index of the calibration and imaging media enhanced the signal-to-noise ratio when imaging fluorescent samples with a MMF.

Generally, the fluorescence background from the focal plane has been a limiting factor for attaining high dynamic range imaging with linear fluorescence. When imaging with the MMF-based system, the background fluorescence from bright out-of-focus objects can easily overwhelm the signal from a dim in-focus object, considering that the fluorescence background is integrated over a relatively large volume. Thus, suppression of the in-focus background from the non-linearity of two-photon fluorescence is beneficial for increasing the dynamic range of the imaging system. Indeed, in our system, we obtained an enhancement factor, evaluated as the ratio of the peak to average intensity, of 383 ± 34 in the CW mode and 63 ± 6 in the pulsed mode. The calculated enhancement factor for the pulsed squared was of 914 ± 114. The large enhancement factor for pulsed squared is consistent with the minimal background present while performing two-photon fluorescence imaging. Furthermore, implementing two-photon imaging into MMF-based applications is beneficial for *in vivo* micro-endoscopy. When inserting the fibre into a living brain it will hit blood vessels and micro bleedings inside the tissue might occur despite the small size of the fibre. While one-photon light is absorbed by blood, using multiphoton excitation can overcome this issue. I have for the first time demonstrated volumetric multiphoton imaging of neuronal soma and associated dendrites in living brain tissue using wavefront control through a MMF. This demonstration was accomplished by integrating a dual CW/pulsed laser source into a micro-endoscopic system. The use of a CW laser for the calibration had the added benefit of allowing a design employing removable distal optics, an important advantage for biological imaging applications. Finally, while the non-linearity of the multiphoton process decreased the background, it exacerbated

some spatial non-uniformities in the illumination, which make the focus elliptical on the edges of the FoV. Notably, these non-uniformities are independent of the calibration method, as they arise intrinsically from the fibre geometry and could be alleviated, by performing spatially variant deconvolution in order to regularize the spatial response (Turcotte et al., 2020b).

In conclusion, I have presented several improvements for the MMF-based imaging system originally described by our lab (Vasquez-Lopez et al., 2018). The data provided in this Chapter supports the idea that selecting higher-NA fibres and taking the refractive index of the imaging sample into account together with technological advances such as multiphoton imaging will as a whole significantly improve imaging performance of MMF-based systems. Such improvements, initially demonstrated in brain slices, are crucial to advance the system for subsequent *in vivo* applications.

8. Repeated imaging through a multimode optical fibre

8.1. Introduction

Assessing the role of synapses in normal brain function, or their role in neurological disease, can be achieved by direct observation of their form and function in the living brain. Ideally, such observations should be made for different brain regions, including deep within the brain, and across long time periods to track synapse dynamics. In other words, to dissect mechanisms underlying neural function and circuit plasticity, thus learning and memory, chronic imaging of synaptic structures and their dynamics is necessary. In the best case, such observations should be feasible in conditions where animals behave naturally or perform certain learning tasks.

Studying synaptic connectivity and plasticity deep within living brains over longer time-periods requires the development of systems capable of repeated imaging. Micro-endoscopic approaches are ideal for this purpose, not only do they provide subcellular spatial resolution for synapse visualisation but they are also compatible with imaging applications in freely behaving animals. To date, endo-microscopes for chronic deep-brain high-resolution imaging commonly comprise gradient refractive index (GRIN) lenses (Barretto et al., 2011; Barretto and Schnitzer, 2012a, 2012b). Using GRIN lenses and time-lapse two-photon micro-endoscopy, spine dynamics of CA1 pyramidal neurones have been tracked over several months (Attardo et al., 2015). The implantation of these probes necessitates the removal of cortical tissue or the use of guide cannulas, which are often between 0.8 and 2 mm in diameter (Attardo et al., 2015; Barretto et al., 2011). Hence, these imaging tools cause substantial damage to

brain tissue, which is accompanied by inflammation and is thought to negatively affect neuronal network function (Bocarsly et al., 2015; Di Filippo et al., 2013).

Micro-endoscopic approaches should ideally offer unlimited imaging depth, cause minimal damage to the surrounding tissue and disruption of the neuronal network, provide subcellular spatial resolution for synapse visualisation, and be compatible with imaging applications in freely behaving animals. Multimode optical fibres (MMF) unite all these points, owing to their small size and imaging capabilities down to the diffraction limit (Ohayon et al., 2018; Turtaev et al., 2018, 2015; Vasquez-Lopez et al., 2018). In order to investigate physiological synaptic processes and plasticity, that are minimally altered by tissue damage, the development of minimally invasive MMF-based endo-microscopes suitable for longitudinal *in vivo* studies is desirable.

As pointed out earlier, wavefront control is typically used to shape the light travelling through the MMF in order to compensate for perturbations in light propagation occurring inside the MMF (Čižmár and Dholakia, 2011; Di Leonardo and Bianchi, 2011; Papadopoulos et al., 2012). For fluorescence imaging with point-scanning in the sample, the light propagation through the fibre is characterised by performing a calibration procedure consisting of the acquisition of the transmission matrix (TM, see Methods). However, the calibration, and thus the wavefront used for imaging, is highly sensitive to the relative position between the wavefront shaping device and the MMF. Any change in their relative positions will lead to a substantial degradation in the quality of the illumination focus and to an equivalent decrease in image quality. Repeated imaging with a MMF-based micro-endoscope involves removing and reinserting a MMF implant into the system between each imaging session. This

task is challenging since it is necessary to manually reposition the MMF into the optical system multiple times with sufficient (sub-micrometric) accuracy to preserve focus quality (peak intensity and spatial extent). This is complicated by the fact that it is not possible to recalibrate the light propagation through the MMF, as for *in vivo* chronic imaging the MMF will be implanted into an animal's brain, which restricts the access to the distal end of the fibre impeding the measurement of light output from the MMF.

I therefore set out to develop a method allowing repeated imaging using MMF. Here, I present a two-step solution to overcome the difficulties described above. First, a custom three-dimensional (3D) printed headplate was designed, allowing precise reinsertion of the MMF implant into the optical system. This mechanical optimisation step allowed the creation of low-quality foci in the sample. Then, sensorless AO was implemented to correct for any remaining translational shift in the MMF position with respect to the wavefront shaping device in order to recover optimal focusing performance. Furthermore, I demonstrate the feasibility of the proposed method by characterising illumination foci and fluorescent bead images following multiple MMF removals and reinsertions. Moreover, I evaluated the effects of sensorless AO on imaging performance in living brain tissue.

8.2. Results

8.2.1. Mechanical and sensorless optimisation

The proximal MMF facet, the facet closest to the laser source, was located at a conjugated Fourier plane from the wavefront-shaping device (LC-SLM; Fig. 43A). During the calibration procedure, the TM was measured to determine the

wavefronts required to create high-quality foci in the sample for high-resolution imaging (Fig. 43A,B). Generally, the TM is considered to describe light propagation through complex media, such as the MMF itself, however, light propagation between the LC-SLM and the proximal facet must also be considered in the TM. Indeed, the relative position of the MMF to the LC-SLM, and any optical element in-between, is critical for focus generation. Any displacement, even if the fibre remains straight and no bending occurs, will have a deleterious impact on the quality of the focus being formed in the sample. Removal and reinsertion of the MMF implant cause such positional changes between the wavefront shaping device and the MMF. These are typically so significant and the calibration so sensitive to any perturbation that no focus can be formed at the distal output of the MMF using standard approaches (Turtaev et al., 2018; Vasquez-Lopez et al., 2018; Fig. 43A,B).

To enable repeated imaging, a custom 3D printed headplate was designed to attach the MMF implant onto the animal and connect it to the optical system. The MMF was fixed in the centre of the headplate and circled by 4 magnets as depicted in Fig. 43C. The counterparts of those magnets were fixed into to the optical system, enabling repositioning after the MMF implant had been removed. This mechanical optimisation procedure allowed for accurate reinsertions of the MMF implant sufficiently close to its original position such that a low-quality focus could be formed at the distal fibre facet (Fig. 43B,C). Further optimisation of the focus quality was performed using sensorless adaptive optics (AO). Sensorless AO is based on the optimisation of an image quality metric for different modes representing the optical aberrations present in the system. The 3D shift between the MMF and the LC-SLM was considered

and, thus, optimisation was performed for tip, tilt, and defocus at the LC-SLM plane (Fig. 43B,D). Each of these modes was sequentially corrected by applying different biases, finding the optima, and then superimposing the correction onto the shaped wavefront. The peak intensity was used as metric for sensorless AO through a MMF (see Methods; Fig. S8, Appendix).

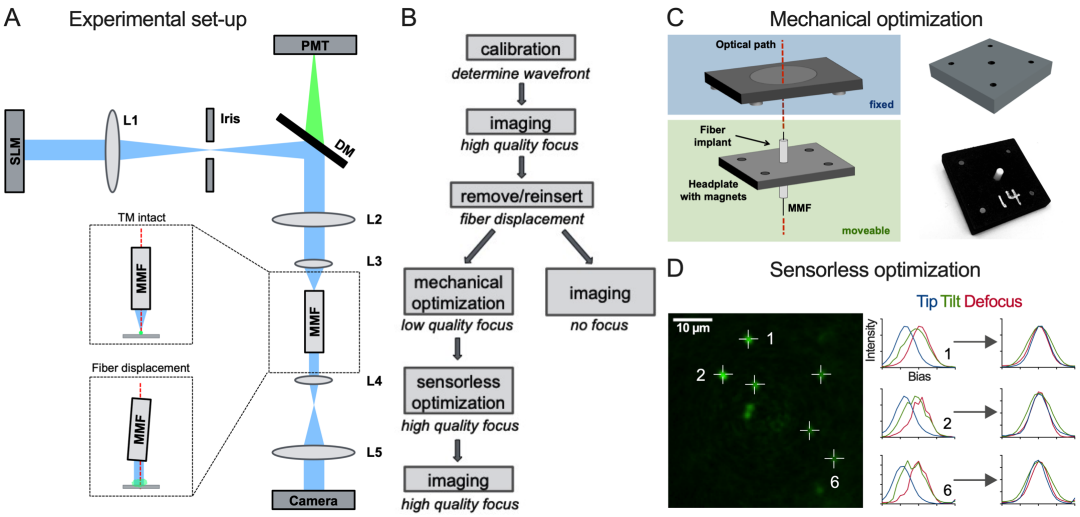

Fig. 43: Two-step approach for repeated imaging with a MMF. (A) Schematic of the experimental set-up. Top inset shows focusing immediately after calibration and bottom inset shows loss of focusing capability if the MMF is displaced. (B) Flowchart of the two-step approach. (C) Schematic of the magnetic implant for mechanical optimisation. (D) Illustration of sensorless adaptive optics (AO).

8.2.2. Focus formation for repeated imaging using sensorless adaptive optics

To assess the performance of the proposed optimisation method, the quality of the illumination focus was assessed after sequential MMF implant removals and reinsertions. For this purpose, the illumination focus was imaged onto the distal camera without any sample being present. MMF with a 0.22 NA and 50 µm core (Thorlabs, FG050UGA) were used, and calibrations were performed 50 µm

away from the fibre tip. Following the calibration procedure with a MMF implant in the system, the MMF implant was completely removed and subsequently reinserted by attaching the magnets of the MMF implant plate to the magnets that were fixed in the system (Fig. 43B). Illumination foci were recorded just after the calibration (Original), after a number *i* of reinsertions R (R_i) and after applying the sensorless optimisation code ($R_{i,opt}$; Fig. 44A). The intensity and FWHM of the illumination foci were quantified over a total of four reinsertions/optimisations. Intensities between 65% and 95% compared to the original intensity were measured following reinsertions (1 implant; Intensity [%]: R_1: 67 ± 2, R_2: 69 ± 3, R_3: 92.6 ± 1.8, R_4: 80.7 ± 1.7; Fig. 44B). Following sensorless optimisation, intensities above that of the original focus quality were observed (1 implant; Intensity [%]: $R_{1,opt}$: 105.1 ± 1.7, $R_{2,opt}$: 105.6 ± 0.9, $R_{3,opt}$: 111.2 ± 1.3, $R_{4,opt}$: 106.2 ± 0.7; Fig. 44B).

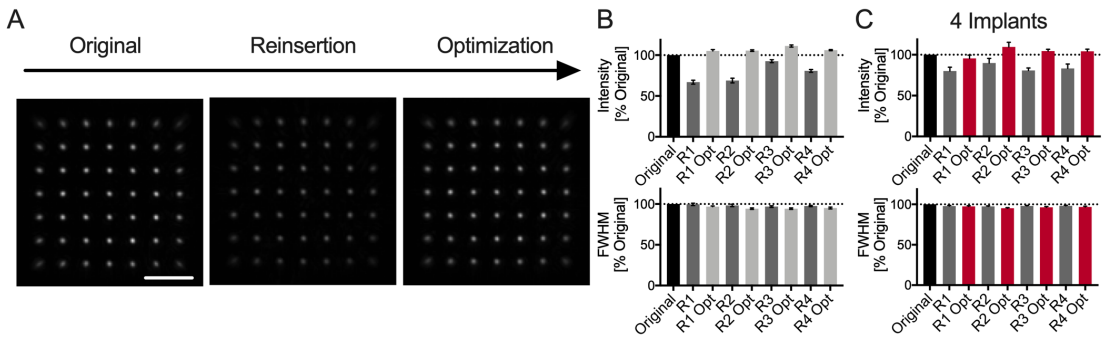

Fig. 44: Focusing light after multiple MMF reinsertions. (A) maximum intensity projection of focus images at different lateral positions (left) immediately after calibration, (middle) after removal/reinsertion, and (right) after sensorless AO optimisation. Scale bar: 20 µm. (B) Peak intensity and lateral width (FWHM) analysis of illumination foci across the FoV for the data shown in (A). (C) Peak intensity and lateral width analysis for 4 distinct implants following sequential removals/reinsertions and sensorless AO optimisation. All data is normalised to the original values.

The FWHM decreased slightly for reinsertions and optimisations but stayed close to 100% compared to the original FWHM of the points (1 implant; FWHM

[%]: R_1: 99.6 ± 1.5, $R_{1,opt}$: 96.8 ± 0.9, R_2: 98.2 ± 1.5, $R_{2,opt}$: 94.3 ± 0.9, R_3: 96.8 ± 1.0, $R_{3,opt}$: 94.3 ± 0.9, R_4: 97.5 ± 0.8, $R_{4,opt}$: 95.1 ± 1.1; Fig. 44B).

The previous measurements were performed with a single implant. To ensure that these results were consistently reproducible, independent of the MMF and headplate, these measurements were repeated with four different implants. Following reinsertions, intensity was on average over 80% for all reinsertions (4 implants; Intensity [%]: R_1: 80 ± 5, R_2: 90 ± 6, R_3: 81 ± 3, R_4: 83 ± 5; Fig. 44C) compared to the original, which could be improved to around 100% using sensorless optimisation (4 implants; Intensity [%]: $R_{1,opt}$: 96 ± 4, $R_{2,opt}$: 110 ± 6, $R_{3,opt}$: 105 ± 2, $R_{4,opt}$: 104 ± 3; Fig. 44C). When assessing the FWHM, focus quality was similar compared to the original across all reinsertions (4 implants; FWHM [%]: R_1: 97.9 ± 0.8, $R_{1,opt}$: 97.5 ± 0.8, R_2: 97.5 ± 0.7, $R_{2,opt}$: 95.3 ± 0.7, R_3: 98.0 ± 0.7, $R_{3,opt}$: 96.4 ± 0.9, R_4: 98.1 ± 0.7, $R_{4,opt}$: 96.8 ± 0.9; Fig. 44C).

Uniform focusing performance across the FoV ensures uniform sampling of objects and is important, as neuronal structures will typically span across the entire FoV (Turcotte et al., 2020b). We assessed the impact of sensorless AO at different locations in the FoV after optimising for a focus near the centre of the FoV. The FWHM and peak intensity of illumination foci were quantified as a function of their distance from the centre of the FoV and constant improvements were measured across the FoV (Fig. 45A). Sensorless optimisation was performed at different radial positions and the changes in focusing characterised across the FoV. No spatial dependence was observed for the improvement in intensity or lateral width, indicating that sensorless AO following fibre reinsertion is not dependent on the position of the optimisation point (Fig. 45B).

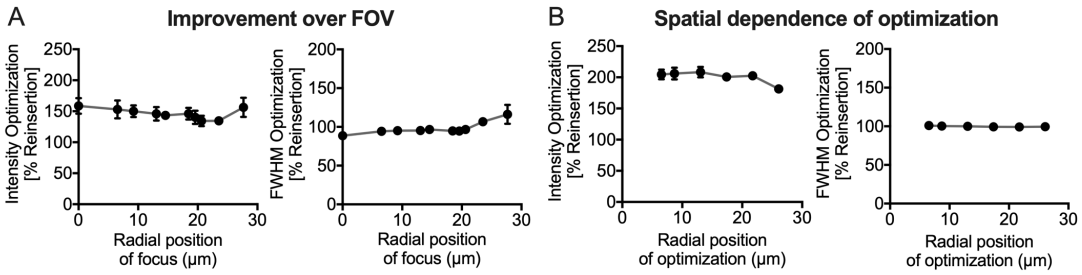

Fig. 45: Spatial dependence of sensorless AO in MMF. (A) Peak intensity and lateral width analysis of illumination foci as a function of their radial position (distance from the core centre) after performing sensorless AO optimisation near the fibre centre. (B) Peak intensity and lateral width analysis of illumination foci across the FoV as a function of the radial position at which after performing sensorless AO was performed. All data is normalised to the pre-AO values.

In summary, the magnetic headplate was sufficient to partially preserve focusing capability across multiple MMF implants following several reinsertions. Combined with sensorless AO, focus characteristics equivalent to pre-removal (Original) were achieved by correcting only for tip, tilt, and defocus.

8.2.3. Repeated fluorescence imaging of beads through a MMF

For chronic *in vivo* imaging, the MMF must be implanted in the brain and the headplate attached to the skull. Hence, the distal camera cannot be used for capturing the illumination as the sensorless optimisation signal. Instead, the optimisation should be based on the signal of interest for imaging, in the case of most neuroscience applications: fluorescence. As such the proximally detected fluorescence was employed for sensorless optimisation. To assess the performance of the proposed repeated imaging methods, 1 µm fluorescent beads were chosen, as they are similar in size to synaptic terminals such as boutons and spines (< 2 µm). Beads were imaged immediately after calibration, after removing and reinserting the implant, and after performing AO (Fig. 46A).

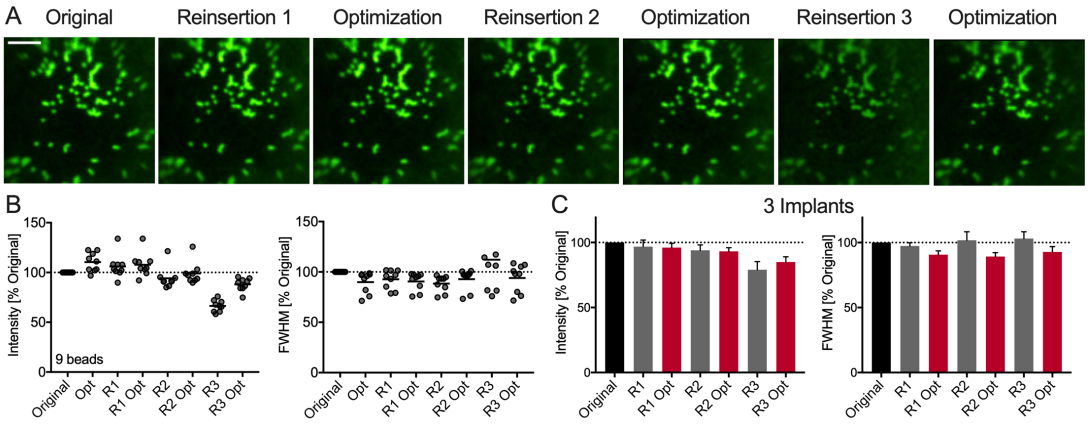

Fig. 46: Repeated imaging of 1 µm fluorescent beads. (A) Images of the same sample acquired from left to right after performing removal/reinsertion and sensorless AO optimisation. Scale bar: 15 µm. (B) Peak intensity and lateral width analysis for the bead imaging data shown in (A). (C) Peak intensity and lateral width analysis for 4 distinct implants following sequential removals/reinsertions and sensorless AO optimisation. All data is normalised to the original values.

Even after three reinsertions, image quality remained high thanks to the custom designed headplate, allowing for precise reinsertion, as illustrated for a single implant in Fig. 46A,B (9 beads; 1 implant; Intensity [%]: Original: 99 ± 4, R_1: 106 ± 4, $R_{1,opt}$: 108 ± 4, R_2: 94.1 ± 0.7, $R_{2,opt}$: 95.3 ± 0.7, R_3: 66 ± 2, $R_{3,opt}$: 88 ± 2; FWHM [%]: Original: 90 ± 4 R_1: 93 ± 3, $R_{1,opt}$: 91 ± 3, R_2: 88 ± 3, $R_{2,opt}$: 93 ± 3, R_3: 112 ± 11, $R_{3,opt}$: 94 ± 5). Importantly, when reinsertions were mechanically less successful, sensorless optimisation provided greater relative improvements and allowed to bring the peak intensity near the original values (as seen from R_3 to $R_{3,opt}$ in Fig. 46A,B). Overall, peak intensity did not drop below 80% following MMF removal and reinsertion compared to the original image and FWHM stayed close to 100% (25 beads; 3 implants; Intensity [%]: R_1: 97 ± 5, R_1,opt: 96 ± 3, R_2: 94 ± 4, $R_{2,opt}$: 93 ± 3, R_3: 79 ± 6, $R_{3,opt}$: 85 ± 4; FWHM [%]: R_1: 97 ± 3, $R_{1,opt}$: 91 ± 3, R_2: 102 ± 7, $R_{2,opt}$: 89 ± 3, R_3: 103 ± 5, $R_{3,opt}$: 93 ± 4; Fig. 46C).

These results demonstrate that repeated high-resolution fluorescence imaging is feasible with the proposed chronic MMF implant combined with AO.

8.2.4. Sensorless adaptive optics improves imaging of live neurones

While fluorescent beads are similar in size compared to synaptic structures, their brightness is much larger than that of living fluorescent brain structures. Moreover, the beads samples were inherently two-dimensional (2D) and had little background, while brain tissue will contain 3D fluorescent structures and have a lower signal-to-background ratio due to out-of-focus signal. Additionally, the insertion of the fibre into tissue may cause bending and translation of the MMF as a result of physical forces exerted by the tissue. To limit the effects of bending, custom-made fibres (doric lenses, MFC-ZF2.5, 60 µm core, NA = 0.37) were coated with a rigid tubing (Turcotte et al., 2020a). Thereby, the MMF was subjected to less deformation when inserted into tissue. However, translation and some degree of fibre bending were inevitable.

To evaluate whether the remaining effects of these static aberrations occurring during insertion can be corrected by sensorless AO, live brain tissue was imaged (Fig. 47). CA3 pyramidal neurones were filled via patch-clamp technique in organotypic hippocampal slices with a fluorescent dye (Alexa 488). Subsequently, slices were transferred to the MMF-based system and imaged immediately after calibration.

Neuronal processes, including dendrites could be identified as bright structures (Fig. 47A,C). The original signal-to-background ratio was calculated to be of 2.7 in the displayed image (Fig. 47A). Following sensorless AO, a greater level of detail could be visualised with small protrusions known as postsynaptic

terminals or spines becoming more visible (Fig. 47C). A substantial relative decrease in background was achieved with the signal-to-background ratio increasing by a factor of 2.3. The improvement provided by correcting for tip, tilt, and defocus is further evidenced by the increased spatial frequency bandwidth as shown by the Fourier transforms of the images (Fig. 47B,D). These results indicate that the sensorless optimisation can indeed be used in living brain tissue to improve image quality.

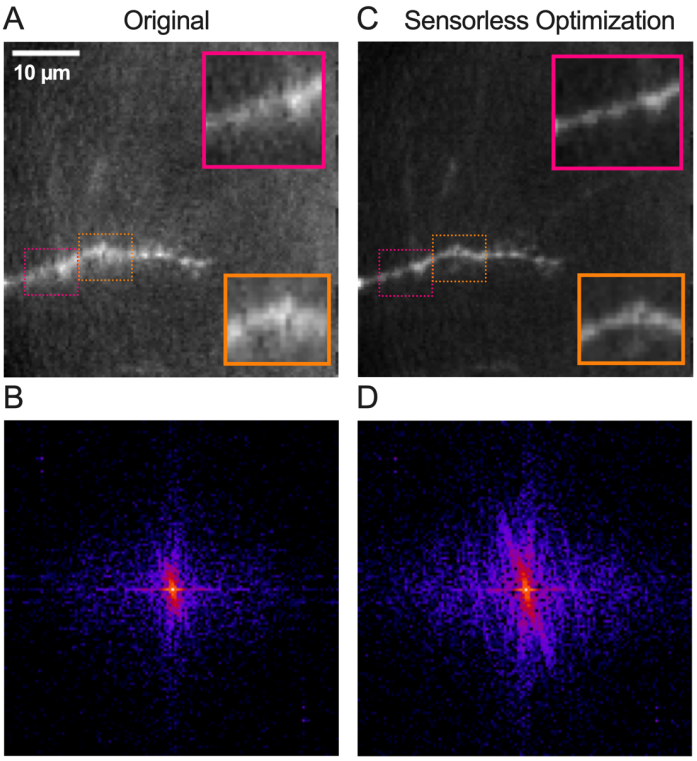

Fig. 47: Imaging of live neurones through an MMF in slices with sensorless AO. (A,C) Images of a dendrite labelled with Alexa Fluor 488, acquired (A) before and (C) after sensorless AO optimisation. Scale bar: 10µm. Inset width: 10µm. Images were normalised to their peak intensity. (B,D) Power frequency spectra of the images shown in (A,C), respectively.

8.2.5. Repeated imaging of 3D fluorescence samples

To perform chronic imaging in living animals, the implant must be attached onto the animal's skull, after the fibre is positioned at the region of interest. In other words, after imaging the desired neuronal structure, the implant must be carefully fixed in place without disrupting the calibration. To test whether this was possible, 3D fluorescent beads were immersed in agar, thus simulating the properties of fluorescently tagged neurones in mouse brains (Fig. 48A). The agar dilution was chosen to roughly match the mechanical properties of brain tissue. Afterwards, a petri dish was attached to cover the bead-agar mixture and provide a solid substrate for attaching the implant. Then, a small hole was drilled into the petri dish, such as for craniotomy, and the MMF was inserted into the agar. Coated fibres (0.37 NA) were used to image beads (1 – 2 µm, green).

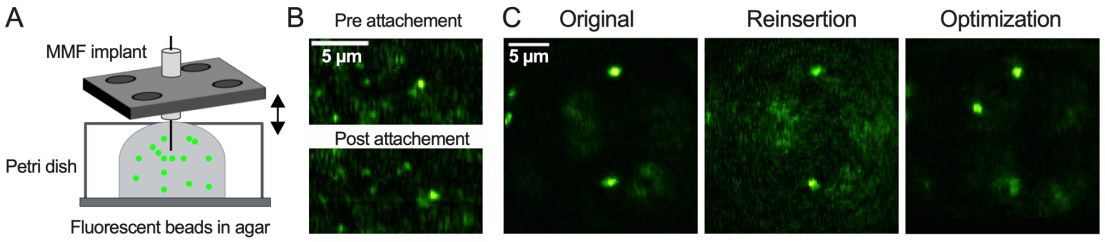

Fig. 48: Repeated imaging in a 3D sample. (A) Schematic representation of the sample consisting of 1-2 µm green fluorescent beads imbedded in agar. (B) Imaging (top) before and (bottom) after affixing the implant onto the petri dish with glue and dental cement. (C) Images of a sample as shown in (A) (left) after attachment of the implant to the sample, (middle) after removal and reinsertion, and (right) after sensorless AO optimisation. Image width: 54 µm.

After having identified a region of interest, with fluorescent beads in focus (Fig. 48B), the implant was attached to the petri dish with superglue and dental cement while carefully avoiding any disruptions of the system. Images were

recorded before and after the implant was attached to the sample, to evaluate potential shifts or disruptions and they show that the implant can be manually attached to the sample without causing any major distortions to the fibre position (Fig. 48B).

In another experiment, the capacity for repeated imaging was evaluated after attachment of the implant to the sample. The sample was first imaged after calibration and implant insertion and attachment (Fig. 48C, left). Next, MMF implant + sample were removed together as a unit, from the optical system and subsequently reinserted. The same beads were visible and in focus after magnet-based reinsertion (Fig. 48C, middle). Sensorless AO optimisation was then performed on the top-most bead and a substantial reduction in the background was observed (Fig. 48C, right). An axial shift was also noticeable and was caused by the top-most bead initially not being in focus. Indeed, defocus can propagate through the fibre (Wen et al., 2020) and our sensorless implementation will thus automatically bring objects of interest into focus. Alternatively, the defocus can be manually adjusted to image the same axial plane. In conclusion, this data proves that the implant including the MMF can be successfully attached to a sample with glue and dental cement while preserving image quality. Furthermore, this configuration is stable and enables repeated imaging with a MMF-based endoscope and sensorless AO.

8.3. Discussion

In this Chapter, I have presented a method for repeated high-resolution imaging with a MMF-based micro-endoscope by precise manual reinsertion of the chronic MMF implant using magnets, followed by further optimisation using

sensorless AO. MMF-based endo-microscopes are particularly well suited for AO as the experimental system already includes a wavefront shaping device, here a LC-SLM. Biological samples often introduce optical aberration due to the heterogeneity in their refractive index distribution or mismatch at interfaces deteriorating image quality (Booth, 2014; Hampson et al., 2021; Ji, 2017). In the foregoing Chapter, I have reported that for MMF endo-microscopy, considering the refractive index of the biological object by performing the calibration in an index-matched solution led to improved focusing ability in brain tissue (Turcotte et al., 2019). While AO can be used to correct for such specimen-induced aberrations (Booth, 2014; Hampson et al., 2021; Ji, 2017), for repeated imaging with a MMF system aberrations are predominant because the system is highly sensitive to any alteration in the relative position between the MMF and the LC-SLM. Hence, we introduced AO to correct for aberrations in the system's illumination path.

In this study, translational changes in the position of the fibre proximal facet were corrected, which translate into tip, tilt, and defocus in the LC-SLM located in a conjugated Fourier plane. Notably, the proximal fibre facet can also be tilted or rotated during repositioning, respectively corresponding to translation and rotation in the LC-SLM plane. Correction for the latter parameters was not necessary, as the custom headplate enabled repositioning of the implant precise enough – with minimal fibre tilt and rotation – to ensure high image quality. Our data support this idea because in all cases imaging performances equivalent or close to the unperturbed system were recovered. Nevertheless, it could be beneficial to introduce further correction modes and even other correction basis for other applications. For instance, sensorless AO could be

combined with other strategies to measure and optimise the altered TM after static deformation (as suggested per Fig. 48; Gordon et al., 2019; Gu et al., 2015; Li et al., 2021).

The results showed that mechanical repositioning of the MMF implant alone was sufficient for repeated imaging of fluorescent beads without loss of spatial resolution with minimal decrease in signal intensity that could be recovered with sensorless optimisation. Importantly, in such 2D bead samples, the absence of out-of-focus objects contributes to the signal-to-background ratio and the image quality remaining high in most cases. However, similar amounts of MMF misalignment after manual repositioning resulted in much larger backgrounds for 3D samples (Fig. 48) due to out-of-focus fluorescence. In such cases, sensorless AO optimisation substantially increased the information content of images. The implementation of AO would also be beneficial for multiphoton fluorescence imaging through MMF, even as limited background would be generated, because the signal depends nonlinearly on the illumination power in the focus (Morales-Delgado et al., 2015b; Turcotte et al., 2020a).

Even though the biggest advantage of MMF-based micro-endoscopes constitutes the possibility to insert them at unlimited depth in a minimally invasive manner, it is important to consider its benefits regarding the surgical preparations necessary for chronic *in vivo* imaging. Chronic imaging of synapse dynamics in cortex is routinely performed using cranial windows (Holtmaat et al., 2009; Yang et al., 2010). Even in deeper brain structures such as the hippocampus, windows are possible following cortical aspiration (Dombeck et al., 2010; Gu et al., 2014). Such windows are typically generated by performing a craniotomy of several millimetres in diameter and subsequently, glass

coverslips are inserted allowing direct imaging with confocal microscopes. However, these windows are often affected by bone regrowth, dura injuries, infections, or simply dirt that accumulates at the cover glass (Holtmaat et al., 2009). Although these factors may be neglectable in acute preparations, for long-term observation of synapses over weeks and months they are doubtlessly impactful. As the surgery procedure for MMF-based micro-endoscopes is much easier and requires only a small craniotomy, MMF-implants are optimal for chronic preparations. In addition, it is not trivial to insert cover glasses above cortical regions of interest that are located on the side of the brain, whereas MMF insertion can be easily performed at any location. Thus, it might be worth to consider using MMF-based micro-endoscopes for synapse imaging even at superficial, cortical regions, given the significantly reduced invasiveness of the surgical procedure. Of course, this will offer reduced FoVs compared to cranial windows and limit the number of synapses that can be monitored simultaneously but might be valuable in some experimental settings.

In conclusion, I have introduced a method for repeated imaging using MMF. Manual repositioning of MMF presents unique obstacles, as a change in relative positioning with respect to the wavefront shaping device invalidates the original calibration, necessary for foci formation and imaging. I tackled this problem using custom 3D printed headplates enabling precise reinsertion of the MMF implant, thus preserving low-quality focusing that can subsequently be transformed into high-quality focusing using sensorless AO. This methodology certainly constitutes an important step towards chronic high-resolution imaging of deep brain structures in living animals using the minimally invasive MMF technology.

9. Conclusions and General Discussion

Since the original characterisations of synaptic plasticity (Bliss and Lømo, 1973; Hebb, 1949; Ramón y Cajal, 1911) a tremendous amount of work has been published within the field of synaptic plasticity. However, our current understanding is still limited especially with regards to the relation between synaptic plasticity and cognitive functions such as learning and memory. Forming these links is challenging, due to a lack of suitable tools to study synapses in relevant brain regions in behaving animals. In this thesis I have proposed and demonstrated substantial advances to a multimode fibre (MMF) based micro-endoscopic system, suitable for minimally invasive deep-brain *in vivo* imaging of synapses. Moreover, fundamental gaps in the field of synaptic plasticity remain: A link between synaptic plasticity and learning and memory is difficult to establish if the impact of endogenous factors such as hormones on synapse dynamics is unclear. Additionally, the field of synaptic plasticity is generally subject to a lack of research focusing on the presynaptic terminal and its signalling mechanisms, which significantly differ from those localised at postsynaptic terminals. Thus, in this thesis I have endeavoured to shed more light on these somewhat underrepresented topics.

Relevance of presynaptic NMDA receptor signalling

One does not have to look far to find that the research on the presynaptic compartment of the synapse is still neglected even nowadays. Over the last couple of years, imaging spine dynamics *in vivo* constitutes an integral part of the synaptic plasticity field (Körber and Stein, 2016; Pfeiffer et al., 2018; Runge et al., 2020; Sadakane et al., 2015; Trachtenberg et al., 2002). However, these

studies mostly focus on spine dynamics (Runge et al., 2020) since they are easier to detect. Some studies exist investigating cortical boutons *in vivo* (De Paola et al., 2006; Grillo et al., 2013; Holtmaat et al., 2008; Sammons et al., 2018) but to my knowledge no such studies exist for the hippocampus (but see Kaifosh et al., 2013). Nevertheless, the importance of presynaptic function has been demonstrated over the years especially in the context of short-term plasticity (Fioravante and Regehr, 2011; Regehr, 2012; Zucker and Regehr, 2002). Importantly, presynaptic regulatory mechanisms endow the synapse with increased computational power, diversifying the output of a neurone (Tong et al., 2020). Here, I contribute a molecular mechanism involving preNMDARs regulating presynaptic Ca^{2+} dynamics and short-term facilitation at hippocampal boutons, that is plastic and adjustable in response to changes in network activity. Considering that short-term plasticity already represents a way to adjust a synapse' responsiveness with regards to previous activity, I have identified another layer of flexibility, comprising different subtypes of presynaptic proteins, in this case, preNMDAR sub-populations.

I show that the downstream effects of preNMDAR sub-populations result from the activation of SK-channels. The interaction between NMDARs and SK-channels is well established at the postsynaptic terminal (Faber, 2010; Griffith et al., 2016; Narasimhan, 2005; Ngo-Anh et al., 2005) and reusing similar signalling motifs pre- and postsynaptically, in other words, making use of one collective protein resource pool seems logical from an evolutionary perspective and is energy efficient for the cell. Here, I have shown the mechanism at Schaffer collateral boutons, however, one might ask the question whether the results presented here could be transferred to synapses in other brain regions.

Indeed, preNMDAR activity has been demonstrated at various cortical and hippocampal synapses (Abrahamsson et al., 2017; Bouvier et al., 2018; Buchanan et al., 2012; Janssen et al., 2005; Lituma et al., 2021; McGuinness et al., 2010; Padamsey et al., 2017b; Rodríguez-Moreno et al., 2013; Sjöström et al., 2003). Nonetheless, on this note, it should be kept in mind that synapses function and are regulated in different ways (Maus et al., 2020), thus, experimental evidence is needed to confirm whether the results presented in this thesis could be translated to other synapses and contribute to their functional outputs. Furthermore, one could speculate about implications for the precise regulation by preNMDAR sub-populations with regards to the individual adjustment of glutamatergic outputs onto different domains of the postsynaptic neurone. Summarized as synapse-type-specific plasticity, it has been proposed that both preNMDAR receptors and K^+ channels can regulate short-term plasticity in a synapse-type-specific manner (summarized in Larsen and Sjöström, 2015). Underlying mechanisms of this regulation have been unidentified so far, thus, I provide a functional framework as to how synapse-type-specificity can be modulated and adjusted. As probable outcome, Ca^{2+} dynamics and AP-waveforms are distinctly regulated at individual synapses, potentially guided by the identity of the postsynaptic neurone. Importantly, it is likely that the postsynaptic neurone to a certain extent directs the balance of preNMDAR sub-populations at specific synapse types through retrograde signals (Larsen and Sjöström, 2015), which could be explored for the preNMDAR/SK-channel regulation in future studies.

Ultimately, the magnitude of importance of NMDARs located at presynaptic terminals is still unknown and might be underestimated. Generally, the inhibition of NMDARs as key players of synaptic plasticity has led to the overall conclusion that their activation is important for learning and memory mechanisms. It has been shown in numerous studies, that inhibition of NMDAR activity, either by inhibitors or genetically, leads to reduced synaptic potentiation and impaired learning and memory (Åhlander et al., 1999; Brigman et al., 2008; Davis et al., 1992; de Lima et al., 2005; Newcomer and Krystal, 2001; Sakimura et al., 1995). Importantly, NMDAR inhibitors used in these studies are never exclusively targeted to post- or presynaptic locations and it is difficult to generate pre- or postsynaptic specific NMDAR knock-out animals. Thus, it is challenging to make concrete statements about the impact of pre- versus postsynaptically located NMDARs on cognitive functions as a discrimination between their functions is only feasible in *in vitro* settings thus far. Even when NMDAR dependent plasticity is demonstrated *in vivo* (Zhang et al., 2015), and its effects are observed postsynaptically, an impact of preNMDARs is likely.

The biggest influence of preNMDARs reflects during short-term plasticity processes. However, it is difficult to determine the behavioural roles of short-term plasticity processes, as it would require targeted and selective elimination of certain short-term plasticity forms. Nevertheless, important roles have been proposed for short-term plasticity in sensory processing (Fortune and Rose, 2002, 2001) and for place fields (Romani and Tsodyks, 2015). In conclusion, understanding preNMDAR signalling in the context of synaptic plasticity will undeniably be important to further our knowledge about the structural representations of learning and memory.

Synaptic plasticity *in vivo*: variability introduced by endogenous factors

Identifying synaptic mechanisms involved in cognitive functions necessitates the performance of *in vivo* experiments, directly monitoring synapse dynamics in anaesthetised or even freely behaving animals. I have provided evidence, that in such studies it is crucial to consider the effects of endogenous factors, such as hormones, since they may directly influence synapse dynamics (Fester and Rune, 2015; Krugers et al., 2010). Thus, careful design of studies is necessary and the original thought to exclude female animals from studies to eliminate the variability introduced by oestrogen is not enough given that oestrogen is locally synthesised in both female and male brains. Accordingly, me and others demonstrated oestrogen-induced effects on spine morphology in neurones from female as well as male animals (Jacome et al., 2016; Lu et al., 2019; Murakami et al., 2006; Sheppard et al., 2019; Tsurugizawa et al., 2005). However, whether brain-derived oestrogen alone causes effects on spines or if cyclic oestrogen secreted by the gonads plays a significant role requires further investigations. Multiple scenarios are possible with brain-derived and cyclic oestrogen interacting, adding their effects or even negatively regulating each other, with differential effects on spine dynamics during the phases of the oestrus cycle. Importantly, not only oestrogen should be considered as an intrinsic variable when studying synaptic plasticity *in vivo*. A large body of literature suggests that other hormones, specifically glucocorticoids affect synapse dynamics (Krugers et al., 2010).

Overall, it is clear that oestrogen affects synaptic plasticity. Furthermore, inhibiting oestrogen signalling or reducing the overall level of oestrogen can

lead to cognitive impairments including worse performance in memory tasks indicated by both rodent and human studies (Daniel, 2006; Dohanich, 2002; Gresack and Frick, 2006; Inagaki et al., 2010; Keenan et al., 2001; Koebele et al., 2021; Krug et al., 2006; Luine et al., 2003; Rapp et al., 2003; Taxier et al., 2020). In future studies, it will be crucial to link these components causally, thus, to identify if the effects of oestrogen on synaptic plasticity are the actual cause of the observed differences in behaviour.

If the latter is true, it is inevitable to consider oestrogen signalling as target for drug development. As pointed out in the introduction, stimulating oestrogen signalling might be beneficial for the treatment of diseases involving anxiety and trauma (Glover et al., 2015, 2012; Lebron-Milad and Milad, 2012). If enhanced oestrogen signalling can improve learning and memory performance by stimulating synaptic plasticity, it could be targeted in neurodegenerative diseases where memory impairment is the major symptom. Some positive effects of oestrogen treatment in such diseases have already been suggested. For example, in the field of verbal learning and memory, enhanced performance in oestrogen-treated women suffering from Alzheimer's disease (AD) was reported (Asthana et al., 2001, 1999). However, other clinical trials could not report any beneficial effects of oestrogen-related treatment of AD, most likely since the underlying pathology of AD is complex (for a full review see Cholerton et al., 2002). Nevertheless, besides its facilitating effects on synaptic plasticity, oestrogen produces a number of other beneficial effects, thus the therapeutical value of oestrogen should be further explored.

Shaping light through an optical fibre: the future of synapse imaging

In order to identify the precise relation between synapse dynamics and cognition, the development of suitable imaging tools is essential (Humeau and Choquet, 2019). The development of two-photon imaging techniques and the use of Thy1 transgenic mice expressing fluorescent proteins has significantly progressed our ability to visualise synapses *in vivo.* Additionally, with the use of micro-endoscopes synapses can be observed *in vivo* in deeper brain regions such as the hippocampus (Attardo et al., 2015; Levene et al., 2004). Generally, micro-endoscopes including fibre optics with GRIN lens-based applications represent the current standard for high-resolution micro-endoscopy. However, using MMFs as central components offers several significant advantages over the use of GRIN lenses. Due to their minimal diameter, MMFs can be inserted without significant tissue damage deep in the brain reducing the device footprint 50 fold compared to when imaging with GRIN lenses (Vasquez-Lopez et al., 2018). Overall, using MMF-based tools can overcome some of the current limitations in synaptic studies in behaving animals including the reduced impact of tissue scattering, since fibres can be implanted at any depth and the size and weight of such imaging devices is minimal which is especially important to encourage natural behaviour in small rodents (Humeau and Choquet, 2019).

Both GRIN lenses and cranial windows have been widely used to image spine dynamics and synaptic plasticity in living animals (Attardo et al., 2015; Holtmaat et al., 2009; Levene et al., 2004; Loewenstein et al., 2011; Moczulska et al., 2013; Resendez et al., 2016; Trachtenberg et al., 2002). However, none of these techniques is actually ideal for this purpose. Without doubt the use of

GRIN lenses and cranial windows is ideal to observe the activity of large volumes of neurones, allowing large field-of-views. However, using these two methods for investigations of spines is less appropriate. Spine dynamics are extremely sensitive to tissue damage (Di Filippo et al., 2013, 2008; Rizzo et al., 2018), and while the use of cranial windows does not require physical interference with brain tissue, it has been shown that the choice of cranial window type can affect dendritic spine turnover rates (Xu et al., 2007). Inconsistencies in spine dynamics are a common phenomenon in today's research. Some report extremely high turnover rates (Attardo et al., 2015; Pfeiffer et al., 2018) while others emphasise the stability of spines over longer periods (Gu et al., 2014). These inconsistencies may derive from different levels of tissue damage, triggering neuroinflammatory processes affecting spine plasticity to different extents. Another explanation would be, that two-photon resolution when imaging spines is not sufficient, thus spine density analysis are challenging owing to illusions such as for example merged spines considered as a single spine. Indeed, Pfeiffer and colleagues show much higher spine density when using superresolution microscopy compared to others (Pfeiffer et al., 2018).

I propose that, as is the general rule for research, the right technique must be chosen dependent on the question asked. Thus, for *in vivo* studies in deep-brain regions focusing on synapse dynamics in relation to behaviour, MMF-based tools are the best choice since they can be inserted at any depth and do not cause any tissue damage that could alter spine dynamics. Moreover, as I show, they can be used for chronic imaging (Schmidt et al., 2022 *accepted at Biomedical Optics Express*) and combined with any technological advances to

improve imaging performance such as multiphoton imaging (Turcotte et al., 2020a) or post-image processing (Turcotte et al., 2020b). Notably, MMF-based imaging bears the potential to be combined with *in vivo* superresolution imaging methods such as STED (Berning et al., 2012), which is important to correctly assess small synaptic structures (Pfeiffer et al., 2018). Finally, while both GRIN lenses and MMFs are flexible and can be used in freely behaving animals, only MMFs can be used for multisite imaging owing to their small size, by inserting multiple MMFs in different brain regions to study interactions of spine dynamics. In conclusion, MMF-based imaging tools are the future of *in vivo* synapse imaging, supporting to tackle the major challenges on our way to understand the structural basis of learning and memory.

10. References

Abbott, L.F., Varela, J.A., Sen, K., Nelson, S.B., 1997. Synaptic depression and cortical gain control. Science 275, 220–224. https://doi.org/10.1126/science.275.5297.221

Abdou, K., Shehata, M., Choko, K., Nishizono, H., Matsuo, M., Muramatsu, S., Inokuchi, K., 2018. Synapse-specific representation of the identity of overlapping memory engrams. Science 360, 1227–1231. https://doi.org/10.1126/science.aat3810

Abraham, W.C., 2008. Metaplasticity: Tuning synapses and networks for plasticity. Nat. Rev. Neurosci. 9, 387–399. https://doi.org/10.1038/nrn2356

Abraham, W.C., 2003. How long will long-term potentiation last? Philos. Trans. R. Soc. B Biol. Sci. 358, 735–744. https://doi.org/10.1098/rstb.2002.1222

Abraham, W.C., Bear, M.F., 1996. Metaplasticity : plasticity of synaptic. Trends Neurosci. 19, 126–130. https://doi.org/10.1016/s0166-2236(96)80018-x

Abraham, W.C., Jones, O.D., Glanzman, D.L., 2019. Is plasticity of synapses the mechanism of long-term memory storage? npj Sci. Learn. 4. https://doi.org/10.1038/s41539-019-0048-y

Abrahamsson, T., You, C., Chou, C., Li, S.Y., Farmer, W.T., Murai, K.K., You, C., Chou, C., Li, S.Y., Mancino, A., Costa, R.P., 2017. Differential Regulation of Evoked and Spontaneous Release by Presynaptic NMDA Receptors. Neuron 96, 839–855. https://doi.org/10.1016/j.neuron.2017.09.030

Adamantidis, A.R., Zhang, F., Aravanis, A.M., Deisseroth, K., De Lecea, L., 2007. Neural substrates of awakening probed with optogenetic control of hypocretin neurons. Nature 450, 420–424. https://doi.org/10.1038/nature06310

Addanki, S., Amiri, I.S., Yupapin, P., 2018. Review of optical fibers-introduction and applications in fiber lasers. Results Phys. 10, 743–750. https://doi.org/10.1016/j.rinp.2018.07.028

Åhlander, M., Misane, I., Schött, P.A., Ögren, S.O., 1999. A behavioral analysis of the spatial learning deficit induced by the NMDA receptor antagonist MK-801 (dizocilpine) in the rat. Neuropsychopharmacology 21, 414–426. https://doi.org/10.1016/S0893-133X(98)00116-X

Akama, K.T., McEwen, B.S., 2003. Estrogen stimulates postsynaptic density-95 rapid protein synthesis via the Akt/protein kinase B pathway. J. Neurosci. 23, 2333–2339. https://doi.org/10.1523/jneurosci.23-06-02333.2003

Al-Juboori, S.I., Dondzillo, A., Stubblefield, E.A., Felsen, G., Lei, T.C., Klug, A., 2013. Light Scattering Properties Vary across Different Regions of the Adult Mouse Brain. PLoS One 8, 1–9. https://doi.org/10.1371/journal.pone.0067626

Al-Mana, D., Ceranic, B., Djahanbakhch, O., Luxon, L.M., 2008. Hormones and the auditory system: A review of physiology and pathophysiology. Neuroscience 153, 881–900. https://doi.org/10.1016/j.neuroscience.2008.02.077

Alexander, B.H., Barnes, H.M., Trimmer, E., Davidson, A.M., Ogola, B.O., Lindsey, S.H., Mostany, R., 2018. Stable density and dynamics of dendritic spines of cortical neurons across the estrous cycle while expressing differential levels of sensory-evoked plasticity. Front. Mol. Neurosci. 11, 1–13. https://doi.org/10.3389/fnmol.2018.00083

Allen, D., Fakler, B., Maylie, J., Adelman, J.P., 2007. Organization and regulation of small conductance Ca2+-activated K+ channel multiprotein complexes. J. Neurosci. 27, 2369–2376. https://doi.org/10.1523/JNEUROSCI.3565-06.2007

Aloisi, A.M., Bonifazi, M., 2006. Sex hormones, central nervous system and pain. Horm. Behav. 50, 1–7. https://doi.org/10.1016/j.yhbeh.2005.12.002

Andreae, L.C., Burrone, J., 2014. The role of neuronal activity and transmitter release on synapse formation. Curr. Opin. Neurobiol. 27, 47–52. https://doi.org/10.1016/j.conb.2014.02.008

Andreska, T., Aufmkolk, S., Sauer, M., Blum, R., 2014. High abundance of BDNF within glutamatergic presynapses of cultured hippocampal neurons. Front. Cell. Neurosci. 8, 1–15. https://doi.org/10.3389/fncel.2014.00107
Aoki, C., Fujisawa, S., Mahadomrongkul, V., Shah, P.J., Nader, K., Erisir, A., 2003. NMDA receptor blockade in intact adult cortex increases trafficking of NR2A subunits into spines, postsynaptic densities, and axon terminals. Brain Res. 963, 139–149. https://doi.org/10.1016/s0006-8993(02)03962-8
Aravanis, A.M., Wang, L.P., Zhang, F., Meltzer, L.A., Mogri, M.Z., Schneider, M.B., Deisseroth, K., 2007. An optical neural interface: in vivo control of rodent motor cortex with integrated fiberoptic and optogenetic technology. J. Neural Eng. 4. https://doi.org/10.1088/1741-2560/4/3/S02
Arnold, A.P., 2009. The organizational-activational hypothesis as the foundation for a unified theory of sexual differentiation of all mammalian tissues. Horm. Behav. 55, 570–578. https://doi.org/10.1016/j.yhbeh.2009.03.011
Ash, R.T., Fahey, P.G., Park, J., Zoghbi, H.Y., Smirnakis, S.M., 2018. Increased axonal bouton stability during learning in the mouse model of MECP2 duplication syndrome. eNeuro 5. https://doi.org/10.1523/ENEURO.0056-17.2018
Asthana, S., Baker, L.D., Craft, S., Stanczyk, F.Z., Veith, R.C., Raskind, M.A., Plymate, S.R., 2001. High-dose estradiol improves cognition for women with ad results of a randomized study. Neurology 57, 605–612. https://doi.org/10.1212/WNL.57.4.605
Asthana, S., Craft, S., Baker, L.D., Raskind, M.A., Birnbaum, R.S., Lofgreen, C.P., Veith, R.C., Plymate, S.R., 1999. Cognitive and neuroendocrine response to transdermal estrogen in postmenopausal women with Alzheimer's disease: Results of a placebo- controlled, double-blind, pilot study. Psychoneuroendocrinology 24, 657–678. https://doi.org/10.1016/S0306-4530(99)00020-7
Attardo, A., Fitzgerald, J.E., Schnitzer, M.J., 2015. Impermanence of dendritic spines in live adult CA1 hippocampus. Nature 523, 592–596. https://doi.org/10.1038/nature14467
Atwood, H.L., Karunanithi, S., 2002. Diversification of synaptic strength: Presynaptic elements. Nat. Rev. Neurosci. 3, 497–516. https://doi.org/10.1038/nrn876
Auberson, Y.P., Allgeier, H., Bischoff, S., Lingenhoehl, K., Moretti, R., Schmutz, M., 2002. 5-Phosphonomethylquinoxalinediones as Competitive NMDA Receptor Antagonists with a Preference for the Human 1A / 2A, Rather than 1A / 2B Receptor Composition. Bioorg. Med. Chem. Lett. 12, 1099–1102.
Azimipour, M., Baumgartner, R., Liu, Y., Jacques, S.L., Eliceiri, K., Pashaie, R., 2014. Extraction of optical properties and prediction of light distribution in rat brain tissue. J. Biomed. Opt. 19, 075001. https://doi.org/10.1117/1.jbo.19.7.075001
Bahr, B.A., 1995. Long-term hippocampal slices: A model system for investigating synaptic mechanisms and pathologic processes. J. Neurosci. Res. 42, 294–305. https://doi.org/10.1002/jnr.490420303
Bailey, C.H., Chen, M., 1988. Long-term memory in Aplysia modulates the total number of varicosities of single identified sensory neurons. Proc. Natl. Acad. Sci. U. S. A. 85, 2373–2377. https://doi.org/10.1073/pnas.85.7.2373
Bailey, C.H., Kandel, E.R., Harris, K.M., 2015. Structural components of synaptic plasticity and memory consolidation. Cold Spring Harb. Perspect. Biol. 7, 1–29. https://doi.org/10.1101/cshperspect.a021758
Balind, S.R., Magó, Á., Ahmadi, M., Kis, N., Varga-Németh, Z., Lőrincz, A., Makara, J.K., 2019. Diverse synaptic and dendritic mechanisms of complex spike burst generation in hippocampal CA3 pyramidal cells. Nat. Commun. 10. https://doi.org/10.1038/s41467-019-09767-w
Balu, M., Baldacchini, T., Carter, J., Krasieva, T.B., Zadoyan, R., Tromberg, B.J., 2009. Effect of excitation wavelength on penetration depth in nonlinear optical microscopy of turbid media. J. Biomed. Opt. 14, 010508. https://doi.org/10.1117/1.3081544

Banerjee, A., Larsen, R.S., Philpot, B.D., Paulsen, O., 2016. Roles of Presynaptic NMDA Receptors in Neurotransmission and Plasticity. Trends Neurosci. 39, 26–39. https://doi.org/10.1016/j.tins.2015.11.001
Bannerman, D.M., Bus, T., Taylor, A., Sanderson, D.J., Schwarz, I., Jensen, V., Hvalby, Ø., Rawlins, J.N.P., Seeburg, P.H., Sprengel, R., 2012. Dissecting spatial knowledge from spatial choice by hippocampal NMDA receptor deletion. Nat. Neurosci. 15, 1153–1159. https://doi.org/10.1038/nn.3166
Bannerman, D.M., Good, M.A., Butcher, S.P., Morris, R.G.M., 1995. Distinct components of spatial learning revealed by prior training and NMDA receptor blockade. Nature 378, 182–186. https://doi.org/10.1038/378182a0
Barha, C.K., Dalton, G.L., Galea, L.A.M., 2010. Low doses of 17α-estradiol and 17β-estradiol facilitate, whereas higher doses of estrone and 17α-and 17β-estradiol impair, contextual fear conditioning in adult female rats. Neuropsychopharmacology 35, 547–559. https://doi.org/10.1038/npp.2009.161
Barnes, S.J., Franzoni, E., Jacobsen, R.I., Erdelyi, F., Szabo, G., Clopath, C., Keller, G.B., Keck, T., 2017. Deprivation-Induced Homeostatic Spine Scaling In Vivo Is Localized to Dendritic Branches that Have Undergone Recent Spine Loss. Neuron 96, 871-882.e5. https://doi.org/10.1016/j.neuron.2017.09.052
Barretto, R.P.J., Ko, T.H., Jung, J.C., Wang, T.J., Capps, G., Waters, A.C., Ziv, Y., Attardo, A., Recht, L., Schnitzer, M.J., 2011. Time-lapse imaging of disease progression in deep brain areas using fluorescence microendoscopy. Nat. Med. 17, 223–229. https://doi.org/10.1038/nm.2292
Barretto, R.P.J., Schnitzer, M.J., 2012a. In vivo microendoscopy of the hippocampus. Cold Spring Harb. Protoc. 7, 1092–1099. https://doi.org/10.1101/pdb.prot071472
Barretto, R.P.J., Schnitzer, M.J., 2012b. In vivo optical microendoscopy for imaging cells lying deep within live tissue. Cold Spring Harb. Protoc. 7, 1029–1034. https://doi.org/10.1101/pdb.top071464
Barria, A., 2007. Subunit-Specific NMDA Receptor Trafficking to Synapses, Protein Trafficking in Neurons, Chapter 10. Academic Press. https://doi.org/10.1016/B978-0-12-369437-9.50015-3
Bartley, A.F., Dobrunz, L.E., 2015. Short-term plasticity regulates the excitation / inhibition ratio and the temporal window for spike integration in CA1 pyramidal cells. Eur. J. Neurosci. 41, 1402–1415. https://doi.org/10.1111/ejn.12898
Bashir, Z.I., Collingridge, G.L., 1994. An investigation of depotentiation of long-term potentiation in the CA1 region of the hippocampus. Exp. Brain Res. 79, 437–443. https://doi.org/10.1007/BF00229183
Bean, B.P., 2007. The action potential in mammalian central neurons. Nat. Rev. Neurosci. 8, 18–20. https://doi.org/10.1038/nrn2148
Bear, M.F., Malenka, R.C., 1994. Synaptic plasticity: LTP and LTD. Curr. Opin. Neurobiol. 4, 389–399. https://doi.org/10.1016/0959-4388(94)90101-5
Becker, J.B., Robinson, T.E., Lorenz, K.A., 1982. Sex difference and estrous cycle variations in amphetamine-elicited rotational behavior. Eur. J. Pharmacol. 80, 65–72. https://doi.org/10.1016/0014-2999(82)90178-9
Becker, J.B., Snyder, P.J., Miller, M.M., Westgate, S.A., Jenuwine, M.J., 1987. The influence of estrous cycle and intrastriatal estradiol on sensorimotor performance in the female rat. Pharmacol. Biochem. Behav. 27, 53–59. https://doi.org/10.1016/0091-3057(87)90476-X
Becker, N., Wierenga, C.J., Fonseca, R., Bonhoeffer, T., Nägerl, U.V., 2008. LTD Induction Causes Morphological Changes of Presynaptic Boutons and Reduces Their Contacts with Spines. Neuron 60, 590–597. https://doi.org/10.1016/j.neuron.2008.09.018
Bednarek, E., Caroni, P., 2011. B-Adducin Is Required for Stable Assembly of New Synapses and Improved Memory Upon Environmental Enrichment. Neuron 69, 1132–1146. https://doi.org/10.1016/j.neuron.2011.02.034
Bellone, C., Nicoll, R.A., 2007. Rapid Bidirectional Switching of Synaptic NMDA

Receptors. Neuron 55, 779–785. https://doi.org/10.1016/j.neuron.2007.07.035
Bender, V.A., Bender, K.J., Brasier, D.J., Feldman, D.E., 2006. Two coincidence detectors for spike timing-dependent plasticity in somatosensory cortex. J. Neurosci. 26, 4166–4177. https://doi.org/10.1523/JNEUROSCI.0176-06.2006
Beral, V., Gaitskell, K., Hermon, C., Moser, K., Reeves, G., Peto, R., 2015. Menopausal hormone use and ovarian cancer risk: Individual participant meta-analysis of 52 epidemiological studies. Lancet 385, 1835–1842. https://doi.org/10.1016/S0140-6736(14)61687-1
Berning, S., Willig, K.I., Steffens, H., Dibaj, P., Hell, S.W., 2012. Nanoscopy in a living mouse brain. Science 335, 551. https://doi.org/10.1126/science.1215369
Berretta, N., Jones, R.S.G., 1996. Tonic facilitation of glutamate release by presynaptic N-methyl-D-aspartate autoreceptors in the entorhinal cortex. Neuroscience 75, 339–344. https://doi.org/10.1016/0306-4522(96)00301-6
Betley, J.N., Xu, S., Cao, Z.F.H., Gong, R., Magnus, C.J., Yu, Y., Sternson, S.M., 2015. Neurons for hunger and thirst transmit a negative-valence teaching signal. Nature 521, 180–185. https://doi.org/10.1038/nature14416
Beuthan, J., Minet, O., Helfmann, J., Herrig, M., Müller, G., 1996. The spatial variation of the refractive index in biological cells. Phys. Med. Biol. 41, 369–382. https://doi.org/10.1088/0031-9155/41/3/002
Bi, G., Poo, M., 2001. Synaptic Modification by Correlated Activity: Hebb's Postulate Revisited. Annu. Rev. Neurosci. 24, 139–166. https://doi.org/10.1146/annurev.neuro.24.1.139
Bianchi, S., Rajamanickam, V.P., Ferrara, L., Di Fabrizio, E., Liberale, C., Di Leonardo, R., 2013. Focusing and imaging with increased numerical apertures through multimode fibers with micro-fabricated optics. Opt. Lett. 38, 4935. https://doi.org/10.1364/ol.38.004935
Bidoret, C., Ayon, A., Barbour, B., Casado, M., 2009. Presynaptic NR2A-containing NMDA receptors implement a high-pass filter synaptic plasticity rule. Proc. Natl. Acad. Sci. U. S. A. 106, 14126–14131. https://doi.org/10.1073/pnas.0904284106
Bildl, W., Strassmaier, T., Thurm, H., Andersen, J., Eble, S., Oliver, D., Knipper, M., Mann, M., Schulte, U., Adelman, J.P., Fakler, B., 2004. Protein kinase CK2 is coassembled with small conductance Ca 2+-activated K+ channels and regulates channel gating. Neuron 43, 847–858. https://doi.org/10.1016/j.neuron.2004.08.033
Binding, J., Ben Arous, J., Léger, J.-F., Gigan, S., Boccara, C., Bourdieu, L., 2011. Brain refractive index measured in vivo with high-NA defocus-corrected full-field OCT and consequences for two-photon microscopy. Opt. Express 19, 4833. https://doi.org/10.1364/oe.19.004833
Bird, C.M., Burgess, N., 2008. The hippocampus and memory: Insights from spatial processing. Nat. Rev. Neurosci. 9, 182–194. https://doi.org/10.1038/nrn2335
Bittner, K.C., Milstein, A.D., Grienberger, C., Romani, S., Magee, J.C., 2017. Behavioral time scale synaptic plasticity underlies CA1 place fields. Science 357, 1033–1036. https://doi.org/10.1126/science.aan3846
Bliss, T.V.P., Collingridge, G.L., 2013. Expression of NMDA receptor-dependent LTP in the hippocampus: bridging the divide. Mol. Brain 6, 1–14. https://doi.org/10.1186/1756-6606-6-5
Bliss, T.V.P., Collingridge, G.L., 1993. A synaptic model of memory: LTP in the hippocampus. Nature 361, 31–39. https://doi.org/10.1038/361031a0
Bliss, T.V.P., Lømo, T., 1973. Long-lasting Potentiation of Synaptic Transmission in the Dentate area of the Anaesthetized Rabbit Following Stimulation of the Perforant Path. J. Physiol. 232, 331–356. https://doi.org/10.1113/jphysiol.1973.sp010273
Bocarsly, M.E., Jiang, W., Wang, C., Dudman, J.T., Ji, N., Aponte, Y., 2015. Minimally invasive microendoscopy system for in vivo functional imaging of deep nuclei in the mouse brain. Biomed. Opt. Express 6, 4546. https://doi.org/10.1364/boe.6.004546
Böhme, M.A., McCarthy, A.W., Grasskamp, A.T., Beuschel, C.B., Goel, P., Jusyte, M.,

Laber, D., Huang, S., Rey, U., Petzoldt, A.G., Lehmann, M., Göttfert, F., Haghighi, P., Hell, S.W., Owald, D., Dickman, D., Sigrist, S.J., Walter, A.M., 2019. Rapid active zone remodeling consolidates presynaptic potentiation. Nat. Commun. 10, 1–16. https://doi.org/10.1038/s41467-019-08977-6
Bollmann, J.H., Sakmann, B., Borst, J.G.G., 2000. Calcium sensitivity of glutamate release in a calyx-type terminal. Science 289, 953–957. https://doi.org/10.1126/science.289.5481.953
Bond, C.T., Maylie, J., Adelman, J.P., 2005. SK channels in excitability, pacemaking and synaptic integration. Curr. Opin. Neurobiol. 15, 305–311. https://doi.org/10.1016/j.conb.2005.05.001
Booth, M.J., 2014. Adaptive optical microscopy: The ongoing quest for a perfect image. Light Sci. Appl. 3, 1–7. https://doi.org/10.1038/lsa.2014.46
Booth, M.J., 2007. Adaptive optics in microscopy. Philos. Trans. R. Soc. A Math. Phys. Eng. Sci. 365, 2829–2843. https://doi.org/10.1098/rsta.2007.0013
Bootman, M.D., Rietdorf, K., Collins, T., Walker, S., Sanderson, M., 2013. Ca2+-sensitive fluorescent dyes and intracellular Ca2+ imaging. Cold Spring Harb. Protoc. 8, 83–99. https://doi.org/10.1101/pdb.top066050
Borovac, J., Bosch, M., Okamoto, K., 2018. Regulation of actin dynamics during structural plasticity of dendritic spines: Signaling messengers and actin-binding proteins. Mol. Cell. Neurosci. 91, 122–130. https://doi.org/10.1016/j.mcn.2018.07.001
Bosch, M., Castro, J., Saneyoshi, T., Matsuno, H., Sur, M., Hayashi, Y., 2014. Structural and molecular remodeling of dendritic spine substructures during long-term potentiation. Neuron 82, 444–459. https://doi.org/10.1016/j.neuron.2014.03.021
Bourne, H.R., Nicoll, R., 1993. Molecular machines integrate coincident synaptic signals. Cell 72, 65–75. https://doi.org/10.1016/s0092-8674(05)80029-7
Bouvier, G., Bidoret, C., Casado, M., Paoletti, P., 2015. Presynaptic NMDA Receptors: Roles and Rules. Neuroscience 311, 322–340. https://doi.org/10.1016/j.neuroscience.2015.10.033
Bouvier, G., Larsen, R.S., Rodríguez-Moreno, A., Paulsen, O., Sjöström, P.J., 2018. Towards resolving the presynaptic NMDA receptor debate. Curr. Opin. Neurobiol. 51, 1–7. https://doi.org/10.1016/j.conb.2017.12.020
Branco, T., Staras, K., Darcy, K.J., Goda, Y., 2008. Local Dendritic Activity Sets Release Probability at Hippocampal Synapses. Neuron 59, 475–485. https://doi.org/10.1016/j.neuron.2008.07.006
Bredt, D.S., Nicoll, R.A., 2003. AMPA receptor trafficking at excitatory synapses. Neuron 40, 361–379. https://doi.org/10.1016/S0896-6273(03)00640-8
Brickley, S.G., Misra, C., Mok, M.H.S., Mishina, M., Cull-Candy, S.G., 2003. NR2B and NR2D subunits coassemble in cerebellar Golgi cells to form a distinct NMDA receptor subtype restricted to extrasynaptic sites. J. Neurosci. 23, 4958–4966. https://doi.org/10.1523/jneurosci.23-12-04958.2003
Brigman, J.L., Feyder, M., Saksida, L.M., Bussey, T.J., Mishina, M., Holmes, A., 2008. Impaired discrimination learning in mice lacking the NMDA receptor NR2A subunit. Learn. Mem. 15, 50–54. https://doi.org/10.1101/lm.777308
Brinton, R.D., 2009. Estrogen-induced plasticity from cells to circuits: predictions for cognitive function. Trends Pharmacol. Sci. 30, 212–222. https://doi.org/10.1016/j.tips.2008.12.006
Brinton, R.D., 2005. Investigative models for determining hormone therapy-induced outcomes in brain: Evidence in support of a healthy cell bias of estrogen action. Ann. N. Y. Acad. Sci. 1052, 57–74. https://doi.org/10.1196/annals.1347.005
Briz, V., Baudry, M., 2014. Estrogen regulates protein synthesis and actin polymerization in hippocampal neurons through different molecular mechanisms. Front. Endocrinol. (Lausanne). 5, 1–14. https://doi.org/10.3389/fendo.2014.00022
Brody, D.L., Yue, D.T., 2000. Relief of G-protein inhibition of calcium channels and

short-term synaptic facilitation in cultured hippocampal neurons. J. Neurosci. 20, 889–898. https://doi.org/10.1523/jneurosci.20-03-00889.2000
Buchanan, K.A., Blackman, A. V., Moreau, A.W., Elgar, D., Costa, R.P., Lalanne, T., Tudor Jones, A.A., Oyrer, J., Sjöström, P.J., 2012. Target-Specific Expression of Presynaptic NMDA Receptors in Neocortical Microcircuits. Neuron 75, 451–466. https://doi.org/10.1016/j.neuron.2012.06.017
Buzsáki, G., da Silva, F.L., 2012. High frequency oscillations in the intact brain. Prog. Neurobiol. 98, 241–249. https://doi.org/10.1016/j.pneurobio.2012.02.004
Caravaca-Aguirre, A.M., Piestun, R., 2017. Single multimode fiber endoscope. Opt. Express 25, 1656. https://doi.org/10.1364/oe.25.001656
Caroni, P., 1997. Overexpression of growth-associated proteins in the neurons of adult transgenic mice. J. Neurosci. Methods 71, 3–9. https://doi.org/10.1016/S0165-0270(96)00121-5
Caroni, P., Donato, F., Muller, D., 2012. Structural plasticity upon learning: Regulation and functions. Nat. Rev. Neurosci. 13, 478–490. https://doi.org/10.1038/nrn3258
Carter, B.C., Jahr, C.E., 2016. Postsynaptic, not presynaptic NMDA receptors are required for spike-timing-dependent LTD induction. Nat. Neurosci. 19, 1218–1224. https://doi.org/10.1038/nn.4343
Cederberg, D., Siesjö, P., 2010. What has inflammation to do with traumatic brain injury? Child's Nerv. Syst. 26, 221–226. https://doi.org/10.1007/s00381-009-1029-x
Cembrowski, M.S., Spruston, N., 2019. Heterogeneity within classical cell types is the rule: lessons from hippocampal pyramidal neurons. Nat. Rev. Neurosci. 20, 193–204. https://doi.org/10.1038/s41583-019-0125-5
Cetin, A., Komai, S., Eliava, M., Seeburg, P.H., Osten, P., 2007. Stereotaxic gene delivery in the rodent brain. Nat. Protoc. 1, 3166–3173. https://doi.org/10.1038/nprot.2006.450
Chabrol, F.P., Arenz, A., Wiechert, M.T., Margrie, T.W., Digregorio, D.A., 2015. Synaptic diversity enables temporal coding of coincident multisensory inputs in single neurons. Nat. Neurosci. 18, 718–727. https://doi.org/10.1038/nn.3974
Chamberlain, S.E.L., Yang, J., Jones, R.S.G., 2008. The role of NMDA receptor subtypes in short-term plasticity in the rat entorhinal cortex. Neural Plast. 2008. https://doi.org/10.1155/2008/872456
Chang, P.K.Y., Boridy, S., McKinney, R.A., Maysinger, D., 2013. Letrozole potentiates mitochondrial and dendritic spine impairments induced by β amyloid. J. Aging Res. 2013. https://doi.org/10.1155/2013/538979
Chang, Y.J., Yang, C.H., Liang, Y.C., Yeh, C.M., Huang, C.C., Hsu, K. Sen, 2009. Estrogen modulates sexually dimorphic contextual fear extinction in rats through estrogen receptor β. Hippocampus 19, 1142–1150. https://doi.org/10.1002/hipo.20581
Chen, J.R., Yan, Y.T., Wang, T.J., Chen, L.J., Wang, Y.J., Tseng, G.F., 2009. Gonadal hormones modulate the dendritic spine densities of primary cortical pyramidal neurons in adult female rat. Cereb. Cortex 19, 2719–2727. https://doi.org/10.1093/cercor/bhp048
Chen, Q., Cichon, J., Wang, W., Qiu, L., Lee, S.J.R., Campbell, N.R., DeStefino, N., Goard, M.J., Fu, Z., Yasuda, R., Looger, L.L., Arenkiel, B.R., Gan, W.B., Feng, G., 2012. Imaging Neural Activity Using Thy1-GCaMP Transgenic Mice. Neuron 76, 297–308. https://doi.org/10.1016/j.neuron.2012.07.011
Chéreau, R., Saraceno, G.E., Angibaud, J., Cattaert, D., Nägerl, U.V., 2017. Superresolution imaging reveals activity-dependent plasticity of axon morphology linked to changes in action potential conduction velocity 114. https://doi.org/10.1073/pnas.1607541114
Chevaleyre, V., Siegelbaum, S.A., 2010. Strong CA2 pyramidal neuron synapses define a powerful disynaptic cortico-hippocampal loop. Neuron 66, 560–572. https://doi.org/10.1016/j.neuron.2010.04.013

Choi, J.H., Sim, S.E., Kim, J. il, Choi, D.I.I., Oh, J., Ye, S., Lee, J., Kim, T.H., Ko, H.G., Lim, C.S., Kaang, B.K., 2018. Interregional synaptic maps among engram cells underlie memory formation. Science 360, 430–435. https://doi.org/10.1126/science.aas9204
Cholerton, B., Gleason, C.E., Baker, L.D., Asthana, S., 2002. Estrogen and Alzheimer's disease: The story so far. Drugs and Aging 19, 405–427. https://doi.org/10.2165/00002512-200219060-00002
Christie, J.M., Jahr, C.E., 2009. Selective expression of ligand-gated ion channels in L5 pyramidal cell axons. J. Neurosci. 29, 11441–11450. https://doi.org/10.1523/JNEUROSCI.2387-09.2009
Christie, J.M., Jahr, C.E., 2008. Dendritic NMDA Receptors Activate Axonal Calcium Channels. Neuron 60, 298–307. https://doi.org/10.1016/j.neuron.2008.08.028
Chudakov, D.M., Lukyanov, S., Lukyanov, K.A., 2005. Fluorescent proteins as a toolkit for in vivo imaging. Trends Biotechnol. 23, 605–613. https://doi.org/10.1016/j.tibtech.2005.10.005
Chung, C., 2013. NMDA receptor as a newly identified member of the metabotropic glutamate receptor family: Clinical implications for neurodegenerative diseases. Mol. Cells 36, 99–104. https://doi.org/10.1007/s10059-013-0113-y
Chung, S., Li, X., Nelson, S.B., 2002. Short-term depression at thalamocortical synapses contributes to rapid adaptation of cortical sensory responses in vivo. Neuron 34, 437–446. https://doi.org/10.1016/S0896-6273(02)00659-1
Citri, A., Malenka, R.C., 2008. Synaptic plasticity: Multiple forms, functions, and mechanisms. Neuropsychopharmacology 33, 18–41. https://doi.org/10.1038/sj.npp.1301559
Čižmár, T., Dholakia, K., 2011. Shaping the light transmission through a multimode optical fibre: complex transformation analysis and applications in biophotonics. Opt. Express 19, 18871. https://doi.org/10.1364/oe.19.018871
Clemens, A.M., Lenschow, C., Beed, P., Li, L., Sammons, R., Naumann, R.K., Wang, H., Schmitz, D., Brecht, M., 2019. Estrus-Cycle Regulation of Cortical Inhibition. Curr. Biol. 29, 605-615.e6. https://doi.org/10.1016/j.cub.2019.01.045
Collin, C., Miyaguchi, K., Segal, M., 1997. Dendritic spine density and LTP induction in cultured hippocampal slices. J. Neurophysiol. 77, 1614–1623. https://doi.org/10.1152/jn.1997.77.3.1614
Collingridge, G.L., Peineau, S., Howland, J.G., Wang, Y.T., 2010. Long-term depression in the CNS. Nat. Rev. Neurosci. 11, 459–473. https://doi.org/10.1038/nrn2867
Conkey, D.B., Caravaca-Aguirre, A.M., Piestun, R., 2012. High-speed scattering medium characterization with application to focusing light through turbid media. Opt. Express 20, 1733. https://doi.org/10.1364/oe.20.001733
Connor, S.A., Wang, Y.T., 2015. A Place at the Table: LTD as a Mediator of Memory Genesis. Neurosci. 22, 359–371. https://doi.org/10.1177/1073858415588498
Córdoba Montoya, D.A., Carrer, H.F., 1997. Estrogen facilitates induction of long term potentiation in the hippocampus of awake rats. Brain Res. 778, 430–438. https://doi.org/10.1016/S0006-8993(97)01206-7
Corlew, R., Brasier, D.J., Feldman, D.E., Philpot, B.D., 2008. Presynaptic NMDA receptors: Newly appreciated roles in cortical synaptic function and plasticity. Neuroscientist 14, 609–625. https://doi.org/10.1177/1073858408322675
Corlew, R., Wang, Y., Ghermazien, H., Erisir, A., Philpot, B.D., 2007. Developmental switch in the contribution of presynaptic and postsynaptic NMDA receptors to long-term depression. J. Neurosci. 27, 9835–9845. https://doi.org/10.1523/JNEUROSCI.5494-06.2007
Cornejo, V.H., Ofer, N., Yuste, R., 2021. Voltage compartmentalization in dendritic spines in vivo. Science eabg0501, 1–10. https://doi.org/10.1126/science.abg0501
Costello, D.A., Watson, M.B., Cowley, T.R., Murphy, N., Royal, C.M., Garlanda, C., Lynch, M.A., 2011. Interleukin-1α and HMGB1 mediate hippocampal dysfunction

in SIGIRR-deficient mice. J. Neurosci. 31, 3871–3879. https://doi.org/10.1523/JNEUROSCI.6676-10.2011
Cowansage, K.K., Shuman, T., Dillingham, B.C., Chang, A., Golshani, P., Mayford, M., 2014. Direct Reactivation of a Coherent Neocortical Memory of Context. Neuron 84, 432–441. https://doi.org/10.1016/j.neuron.2014.09.022
Cui, J., Shen, Y., Li, R., 2012. Estrogen synthesis and signaling pathways during aging: From periphery to brain. Trends Mol. Med. 19, 197–209. https://doi.org/10.1016/j.molmed.2012.12.007
Cull-Candy, S., Brickley, S., Farrant, M., 2001. NMDA receptor subunits : diversity, development and disease. Curr. Opin. Neurobiol. 11, 327–335. https://doi.org/10.1016/s0959-4388(00)00215-4
Cull-Candy, S.G., Leszkiewicz, D.N., 2004. Role of Distinct NMDA Receptor Subtypes at Central Synapses. Sci. STKE 255. https://doi.org/10.1126/stke.2552004re16
Dani, A., Huang, B., Bergan, J., Dulac, C., Zhuang, X., 2010. Superresolution Imaging of Chemical Synapses in the Brain. Neuron 68, 843–856. https://doi.org/10.1016/j.neuron.2010.11.021
Daniel, J.M., 2006. Effects of oestrogen on cognition: What have we learned from basic research? J. Neuroendocrinol. 18, 787–795. https://doi.org/10.1111/j.1365-2826.2006.01471.x
Daniel, J.M., Fader, A.J., Spencer, A.L., Dohanich, G.P., 1997. Estrogen enhances performance of female rats during acquisition of a radial arm maze. Horm. Behav. 32, 217–225. https://doi.org/10.1006/hbeh.1997.1433
Davie, J.T., Kole, M.H.P., Letzkus, J.J., Rancz, E.A., Spruston, N., Stuart, G.J., Häusser, M., 2006. Dendritic patch-clamp recording. Nat. Protoc. 1, 1235–1247. https://doi.org/10.1038/nprot.2006.164
Davis, S., Butcher, S.P., Morris, R.G.M., 1992. The NMDA receptor antagonist D-2-amino-5-phosphonopentanoate (D-AP5) impairs spatial learning and LTP in vivo at intracerebral concentrations comparable to those that block LTP in vitro. J. Neurosci. 12, 21–34. https://doi.org/10.1523/jneurosci.12-01-00021.1992
de Lima, M.N.M., Laranja, D.C., Bromberg, E., Roesler, R., Schröder, N., 2005. Pre- or post-training administration of the NMDA receptor blocker MK-801 impairs object recognition memory in rats. Behav. Brain Res. 156, 139–143. https://doi.org/10.1016/j.bbr.2004.05.016
de Novaes Soares, C., Almeida, O.P., Joffe, H., Cohen, L.S., 2001. Efficacy of estradiol for the treatment of depressive disorders in perimenopausal women: A double-blind, randomized, placebo-controlled trial. Arch. Gen. Psychiatry 58, 529–534. https://doi.org/10.1001/archpsyc.58.6.529
De Paola, V., Holtmaat, A., Knott, G., Song, S., Wilbrecht, L., Caroni, P., Svoboda, K., 2006. Cell type-specific structural plasticity of axonal branches and boutons in the adult neocortex. Neuron 49, 861–875. https://doi.org/10.1016/j.neuron.2006.02.017
De Simoni, A., Griesinger, C.B., Edwards, F.A., 2003. Development of rat CA1 neurones in acute versus organotypic slices : role of experience in synaptic morphology and activity. J. Physiol. 550, 135–147. https://doi.org/10.1113/jphysiol.2003.039099
Debanne, D., Campanac, E., Bialowas, A., Carlier, E., Alcaraz, G., 2011. Axon physiology. Physiol. Rev. 91, 555–602. https://doi.org/10.1152/physrev.00048.2009
Débarre, D., Botcherby, E.J., Watanabe, T., Srinivas, S., Booth, M.J., Wilson, T., 2009. Image-based adaptive optics for two-photon microscopy. Opt. Lett. 34, 2495–2497. https://doi.org/10.1364/ol.34.002495
Deco, G., Rolls, E.T., Romo, R., 2010. Synaptic dynamics and decision making. Proc. Natl. Acad. Sci. U. S. A. 107, 7545–7549. https://doi.org/10.1073/pnas.1002333107
Deisseroth, K., 2011. Optogenetics. Nat. Methods 8, 26–29.

https://doi.org/10.1038/nmeth.f.324
Del Castillo, J., Katz, B., 1954. Quantal components of the end-plate potential. J. Physiol. 124, 560–573. https://doi.org/10.1113/jphysiol.1954.sp005129
Delaney, P.M., Harris, M.R., King, R.G., 1994. Fiber-optic laser scanning confocal microscope suitable for fluorescence imaging. Appl. Opt. 33, 573. https://doi.org/10.1364/ao.33.000573
Deng, P.Y., Klyachko, V.A., 2011. The diverse functions of short-term plasticity components in synaptic computations. Commun. Integr. Biol. 4, 543–548. https://doi.org/10.4161/cib.15870
Denk, W., Strickler, J.H., Webb, W.W., 1990. Two-photon laser scanning fluorescence microscopy. Science 248, 73–76. https://doi.org/10.1126/science.2321027
Denk, W., Svoboda, K., 1997. Photon upmanship: Why multiphoton imaging is more than a gimmick. Neuron 18, 351–357. https://doi.org/10.1016/S0896-6273(00)81237-4
Di Filippo, M., Chiasserini, D., Gardoni, F., Viviani, B., Tozzi, A., Giampà, C., Costa, C., Tantucci, M., Zianni, E., Boraso, M., Siliquini, S., de Iure, A., Ghiglieri, V., Colcelli, E., Baker, D., Sarchielli, P., Fusco, F.R., Di Luca, M., Calabresi, P., 2013. Effects of central and peripheral inflammation on hippocampal synaptic plasticity. Neurobiol. Dis. 52, 229–236. https://doi.org/10.1016/j.nbd.2012.12.009
Di Filippo, M., Sarchielli, P., Picconi, B., Calabresi, P., 2008. Neuroinflammation and synaptic plasticity: theoretical basis for a novel, immune-centred, therapeutic approach to neurological disorders. Trends Pharmacol. Sci. 29, 402–412. https://doi.org/10.1016/j.tips.2008.06.005
Di Leonardo, R., Bianchi, S., 2011. Hologram transmission through multi-mode optical fibers. Opt. Express 19, 247. https://doi.org/10.1364/oe.19.000247
Di Mauro, M., Tozzi, A., Calabresi, P., Pettorossi, V.E., Grassi, S., 2015. Neo-synthesis of estrogenic or androgenic neurosteroids determine whether long-term potentiation or depression is induced in hippocampus of male rat. Front. Cell. Neurosci. 9, 1–13. https://doi.org/10.3389/fncel.2015.00376
Diering, G.H., Huganir, R.L., 2018. The AMPA Receptor Code of Synaptic Plasticity. Neuron 100, 314–329. https://doi.org/10.1016/j.neuron.2018.10.018
Dittman, J.S., Kreitzer, A.C., Regehr, W.G., 2000. Interplay between facilitation, depression, and residual calcium at three presynaptic terminals. J. Neurosci. 20, 1374–1385. https://doi.org/10.1523/jneurosci.20-04-01374.2000
Dobrunz, L.E., Huang, E.P., Stevens, C.F., 1997. Very short-term plasticity in hippocampal synapses. Proc. Natl. Acad. Sci. U. S. A. 94, 14843–14847. https://doi.org/10.1073/pnas.94.26.14843
Dobrunz, L.E., Stevens, C.F., 1997. Heterogeneity of release probability, facilitation, and depletion at central synapses. Neuron 18, 995–1008. https://doi.org/10.1016/S0896-6273(00)80338-4
Docherty, J.R., 2007. Use of knockout technology to resolve pharmacological problems. Br. J. Pharmacol. 150, 1–2. https://doi.org/10.1038/sj.bjp.0706941
Dohanich, G., 2003. Ovarian steroids and Cognitive Function. Curr. Dir. Physchological Sci. 12, 57–61. https://doi.org/10.1111/1467-8721.01226
Dohanich, G., 2002. Gonadal Steroids, Learning, and Memory. Horm. Brain Behav. 2, 265–327. https://doi.org/10.1016/b978-012532104-4/50024-x
Dolphin, A.C., Errington, M.L., Bliss, T.V.P., 1982. Long-term potentiation of the perforant path in vivo is associated with increased glutamate release. Nature 297, 496–497. https://doi.org/10.1038/297496a0
Dombeck, D.A., Harvey, C.D., Tian, L., Looger, L.L., Tank, D.W., 2010. Functional imaging of hippocampal place cells at cellular resolution during virtual navigation. Nat. Neurosci. 13, 1433–1440. https://doi.org/10.1038/nn.2648
Dombret, C., Naulé, L., Trouillet, A.C., Parmentier, C., Hardin-Pouzet, H., Mhaouty-Kodja, S., 2020. Effects of neural estrogen receptor beta deletion on social and mood-related behaviors and underlying mechanisms in male mice. Sci. Rep. 10,

1–14. https://doi.org/10.1038/s41598-020-63427-4
Dong, X.X., Wang, Y., Qin, Z.H., 2009. Molecular mechanisms of excitotoxicity and their relevance to pathogenesis of neurodegenerative diseases. Acta Pharmacol. Sin. 30, 379–387. https://doi.org/10.1038/aps.2009.24
Dore, K., Stein, I.S., Brock, J.A., Castillo, P.E., Zito, K., Sjöström, P.J., 2017. Unconventional NMDA Receptor Signaling. J. Neurosci. 37, 10800–10807. https://doi.org/10.1523/JNEUROSCI.1825-17.2017
Dubois, C.J., Lachamp, P.M., Sun, L., Mishina, M., Liu, S.J., 2016. Presynaptic GluN2D receptors detect glutamate spillover and regulate cerebellar GABA release. J. Neurophysiol. 115, 271–285. https://doi.org/10.1152/jn.00687.2015
Dudel, J., Kuffler, S.W., 1961. Presynaptic inhibition at the crayfish neuromuscular junction. J. Physiol. 155, 543–562. https://doi.org/10.1113/jphysiol.1961.sp006646
Duguid, I.C., Smart, T.G., 2004. Retrograde activation of presynaptic NMDA receptors enhances GABA release at cerebellar interneuron-Purkinje cell synapses. Nat. Neurosci. 7, 525–533. https://doi.org/10.1038/nn1227
Ebihara, T., Kawabata, I., Usui, S., Sobue, K., Okabe, S., 2003. Synchronized formation and remodeling of postsynaptic densities: Long-term visualization of hippocampal neurons expressing postsynaptic density proteins tagged with green fluorescent protein. J. Neurosci. 23, 2170–2181. https://doi.org/10.1523/jneurosci.23-06-02170.2003
Eccles, J.C., Katz, B., Kuffler, S.W., 1941. Nature of the “Endplate Potential” in curarized muscle. J. Neurophysiol. 4, 362–387. https://doi.org/10.1152/jn.1941.4.5.362
Edinger, K.L., Frye, C.A., 2007. Androgens’ performance-enhancing effects in the inhibitory avoidance and water maze tasks may involve actions at intracellular androgen receptors in the dorsal hippocampus. Neurobiol. Learn. Mem. 87, 201–208. https://doi.org/10.1016/j.nlm.2006.08.008
Ehlers, M.D., 2000. Reinsertion or Degradation of AMPA Receptors Determined by Activity-Dependent Endocytic Sorting. Neuron 28, 511–525. https://doi.org/10.1016/s0896-6273(00)00129-x
Eichenbaum, H., Otto, T., Cohen, N.J., 1992. The hippocampus-what does it do? Behav. Neural Biol. 57, 2–36. https://doi.org/10.1016/0163-1047(92)90724-I
Emptage, N., Bliss, T.V.P., Fine, A., 1999. Single synaptic events evoke NMDA receptor-mediated release of calcium from internal stores in hippocampal dendritic spines. Neuron 22, 115–124. https://doi.org/10.1016/S0896-6273(00)80683-2
Emptage, N.J., Reid, C.A., Fine, A., 2001. Calcium stores in hippocampal synaptic boutons mediate short-term plasticity, store-operated Ca2+ entry, and spontaneous transmitter release. Neuron 29, 197–208. https://doi.org/10.1016/S0896-6273(01)00190-8
Emptage, N.J., Reid, C.A., Fine, A., Bliss, T.V.P., 2003. Optical quantal analysis reveals a presynaptic component of LTP at hippocampal Schaffer-associational synapses. Neuron 38, 797–804. https://doi.org/10.1016/S0896-6273(03)00325-8
Engert, F., Bonhoeffer, T., 1999. Dendritic spine changes associated with hippocampal long-term synaptic plasticity. Nature 399, 66–70. https://doi.org/10.1038/19978
Engler-Chiurazzi, E.B., Singh, M., Simpkins, J.W., 2016. From the 90’s to now: A brief historical perspective on more than two decades of estrogen neuroprotection. Brain Res. 1633, 96–100. https://doi.org/10.1016/j.brainres.2015.12.044
Enoki, R., Hu, Y. ling, Hamilton, D., Fine, A., 2009. Expression of Long-Term Plasticity at Individual Synapses in Hippocampus Is Graded, Bidirectional, and Mainly Presynaptic: Optical Quantal Analysis. Neuron 62, 242–253. https://doi.org/10.1016/j.neuron.2009.02.026
Erulkar, S.D., Rahamimoff, R., 1978. The role of calcium ions in tetanic and post-tetanic increase of miniature end-plate potential frequency. J. Physiol. 278, 501–511. https://doi.org/10.1113/jphysiol.1978.sp012320
Euston, D.R., Gruber, A.J., McNaughton, B.L., 2012. The Role of Medial Prefrontal

Cortex in Memory and Decision Making. Neuron 76, 1057–1070. https://doi.org/10.1016/j.neuron.2012.12.002
Faber, E.S.L., 2010. Functional interplay between NMDA receptors , SK channels and voltage-gated Ca2+ channels regulates synaptic excitability in the medial prefrontal cortex. J. Physiol. 588, 1281–1292. https://doi.org/10.1113/jphysiol.2009.185645
Faber, E.S.L., Delaney, A.J., Sah, P., 2005. SK channels regulate excitatory synaptic transmission and plasticity in the lateral amygdala 8, 635–641. https://doi.org/10.1038/nn1450
Faber, E.S.L., Sah, P., 2007. Functions of SK channels in central neurons. Proc. Aust. Physiol. Soc. 38, 25–34. https://doi.org/10.1111/j.1440-1681.2007.04725.x
Faber, E.S.L., Sah, P., 2003. Calcium-Activated Potassium Channels: Multiple Contributions to Neuronal Function. Neurosci. 9, 181–194. https://doi.org/10.1177/1073858403252673
Faber, E.S.L., Sah, P., 2002. Physiological Role of Calcium-Activated Potassium Currents in the Rat Lateral Amygdala. J. Neurosci. 22, 1618–1628. https://doi.org/10.1523/JNEUROSCI.22-05-01618.2002
Fatt, P., Katz, B., 1952. Spontaneous subthreshold activity at motor nerve endings. J. Physiol. 117, 109–128. https://doi.org/10.1113/jphysiol.1952.sp004735
Feldman, D.E., Brecht, M., 2005. Map plasticity in somatosensory cortex. Science 310, 810–815. https://doi.org/10.1126/science.1115807
Feng, B., Tse, H.W., Monaghan, D.T., Skifter, D.A., Morley, R., Jane, D.E., Monaghan, D.T., 2004. Structure – activity analysis of a novel NR2C / NR2D-preferring NMDA receptor antagonist : 1- (phenanthrene-2-carbonyl) piperazine-2 ,3 dicarboxylic acid. Br. J. Pharmacol. 141, 508–516. https://doi.org/10.1038/sj.bjp.0705644
Feng, G., Mellor, R.H., Bernstein, M., Keller-Peck, C., Nguyen, Q.T., Wallace, M., Nerbonne, J.M., Lichtman, J.W., Sanes, J.R., 2000. Imaging Neuronal Subsets in Transgenic Mice Expressing Multiple Spectral Variants of GFP. Neuron 28, 41–51. https://doi.org/10.1016/s0896-6273(00)00084-2
Fenno, L., Yizhar, O., Deisseroth, K., 2011. The development and application of optogenetics. Annu. Rev. Neurosci. 34, 389–412. https://doi.org/10.1146/annurev-neuro-061010-113817
Ferree, N.K., Wheeler, M., Cahill, L., 2012. The influence of emergency contraception on post traumatic stress symptoms following sexual assault Nikole. J. Forensic Nurs. 8, 122–130. https://doi.org/10.1111/j.1939-3938.2012.01134.x
Ferreira, J.S., Papouin, T., Ladépêche, L., Yao, A., Langlais, V.C., Bouchet, D., Dulong, J., Mothet, J.P., Sacchi, S., Pollegioni, L., Paoletti, P., Richard Oliet, S.H., Groc, L., 2017. Co-agonists differentially tune GluN2B-NMDA receptor trafficking at hippocampal synapses. Elife 6, 1–22. https://doi.org/10.7554/eLife.25492
Fester, L., Rune, G.M., 2015. Sexual neurosteroids and synaptic plasticity in the hippocampus. Brain Res. 1621, 162–169. https://doi.org/10.1016/j.brainres.2014.10.033
Fiocchetti, M., Ascenzi, P., Marino, M., 2012. Neuroprotective effects of 17β-estradiol rely on estrogen receptor membrane initiated signals. Front. Physiol. 3 APR, 1–10. https://doi.org/10.3389/fphys.2012.00073
Fioravante, D., Regehr, W.G., 2011. Short-term forms of presynaptic plasticity. Curr. Opin. Neurobiol. 21, 269–274. https://doi.org/10.1016/j.conb.2011.02.003
Fischer, G., Mutel, V., Trube, G., Malherbe, P., Kew, J.N.C., Mohacsi, E., Heitz, M.P., Kemp, J.A., 1997. Ro 25-6981, a highly potent and selective blocker of N-methyl-D- aspartate receptors containing the NR2B subunit. Characterization in vitro. J. Pharmacol. Exp. Ther. 283, 1285–1292.
Fisher, S.A., Fischer, T.M., Carew, T.J., 1997. Multiple overlapping processes underlying short-term synaptic enhancement. Trends Neurosci. 20, 170–177. https://doi.org/10.1016/S0166-2236(96)01001-6
Flusberg, B.A., Cocker, E.D., Piyawattanametha, W., Jung, J.C., Cheung, E.L.M.,

Schnitzer, M.J., 2005. Fiber-optic fluorescence imaging. Nat. Methods 2, 941–950. https://doi.org/10.1038/nmeth820
Flusberg, B.A., Nimmerjahn, A., Cocker, E.D., Mukamel, E.A., Barretto, R.P.J., Ko, T.H., Burns, L.D., Jung, J.C., Schnitzer, M.J., 2008. High-speed, miniaturized fluorescence microscopy in freely moving mice. Nat. Methods 5, 935–938. https://doi.org/10.1038/nmeth.1256
Forsythe, I.D., 1994. Direct patch recording from identified presynaptic terminals mediating glutamatergic EPSCs in the rat CNS, in vitro. J. Physiol. 479, 381–387. https://doi.org/10.1113/jphysiol.1994.sp020303
Forsythe, I.D., Tsujimoto, T., Barnes-Davies, M., Cuttle, M.F., Takahashi, T., 1998. Inactivation of presynaptic calcium current contributes to synaptic depression at a fast central synapse. Neuron 20, 797–807. https://doi.org/10.1016/S0896-6273(00)81017-X
Fortune, E.S., Rose, G.J., 2002. Roles for short-term synaptic plasticity in behavior. J. Physiol. Paris 96, 539–545. https://doi.org/10.1016/S0928-4257(03)00009-3
Fortune, E.S., Rose, G.J., 2001. Short-term synaptic plasticity as a temporal filter. Trends Neurosci. 24, 381–385. https://doi.org/10.1016/S0166-2236(00)01835-X
Fox, C.J., Russell, K.I., Wang, Y.T., Christie, B.R., 2006. Contribution of NR2A and NR2B NMDA Subunits to Bidirectional Synaptic Plasticity in the Hippocampus In Vivo. Hippocampus 16, 907–915. https://doi.org/10.1002/hipo
Foy, M.R., Xu, J., Xie, X., Brinton, R.D., Thompson, R.F., Berger, T.W., 1999. 17β-estradiol enhances NMDA receptor-mediated EPSPs and long-term potentiation. J. Neurophysiol. 81, 925–929. https://doi.org/10.1152/jn.1999.81.2.925
Frank, A.C., Huang, S., Zhou, M., Gdalyahu, A., Kastellakis, G., Silva, T.K., Lu, E., Wen, X., Poirazi, P., Trachtenberg, J.T., Silva, A.J., 2018. Hotspots of dendritic spine turnover facilitate clustered spine addition and learning and memory. Nat. Commun. 9, 1–11. https://doi.org/10.1038/s41467-017-02751-2
Frank, M.G., 2016. Circadian regulation of synaptic plasticity. Biology (Basel). 5. https://doi.org/10.3390/biology5030031
Frey, U., Morris, R.G.M., 1998. Synaptic tagging: Implications for late maintenance of hippocampal long- term potentiation. Trends Neurosci. 21, 181–188. https://doi.org/10.1016/S0166-2236(97)01189-2
Frey, U., Morris, R.G.M., 1997. Synaptic tagging and long-term potentiation. Nature 385, 533–536. https://doi.org/10.1038/385533a0
Frye, C.A., Walf, A.A., 2004. Estrogen and/or Progesterone Administered Systemically or to the Amygdala Can Have Anxiety-, Fear-, and Pain-Reducing Effects in Ovariectomized Rats. Behav. Neurosci. 118, 306–313. https://doi.org/10.1037/0735-7044.118.2.306
Fu, A.K.Y., Hung, K.W., Fu, W.Y., Shen, C., Chen, Y., Xia, J., Lai, K.O., Ip, N.Y., 2011. APCCdh1 mediates EphA4-dependent downregulation of AMPA receptors in homeostatic plasticity. Nat. Neurosci. 14, 181–191. https://doi.org/10.1038/nn.2715
Fu, M., Yu, X., Lu, J., Zuo, Y., 2012. Repetitive motor learning induces coordinated formation of clustered dendritic spines in vivo. Nature 483, 92–96. https://doi.org/10.1038/nature10844
Furlong, S., Coombs, M.R.P., Ghassemi-Rad, J., Hoskin, D.W., 2018. Thy-1 (CD90) Signaling Preferentially Promotes RORγt Expression and a Th17 Response. Front. Cell Dev. Biol. 6, 1–12. https://doi.org/10.3389/fcell.2018.00158
Gabor, C., Lymer, J., Phan, A., Choleris, E., 2015. Rapid effects of the G-protein coupled oestrogen receptor (GPER) on learning and dorsal hippocampus dendritic spines in female mice. Physiol. Behav. 149, 53–60. https://doi.org/10.1016/j.physbeh.2015.05.017
Gähwiler, B.H., 1981. Organotypic monolayer cultures of nervous tissue. J. Neurosci. Methods 4, 329–342. https://doi.org/10.1016/0165-0270(81)90003-0
Gähwiler, B.H., Capogna, M., Debanne, D., McKinney, R.A., Thompson, S.M., 1997.

Organotypic slice cultures: A technique has come of age. Trends Neurosci. 20, 471–477. https://doi.org/10.1016/S0166-2236(97)01122-3
Gallistel, C.R., Matzel, L.D., 2013. The neuroscience of learning: Beyond the hebbian synapse. Annu. Rev. Psychol. 64, 169–200. https://doi.org/10.1146/annurev-psych-113011-143807
Garcia, N.M., Walker, R.S., Zoellner, L.A., 2018. Estrogen, progesterone, and the menstrual cycle: A systematic review of fear learning, intrusive memories, and PTSD. Clin. Psychol. Rev. 66, 80–96. https://doi.org/10.1016/j.cpr.2018.06.005
Giese, K.P., Fedorov, N.B., Filipkowski, R.K., Silva, A.J., 1998. Autophosphorylation at Thr286 of the α calcium-calmodulin kinase II in LTP and learning. Science 279, 870–873. https://doi.org/10.1126/science.279.5352.870
Gill, I., Droubi, S., Giovedi, S., Fedder, K.N., Bury, L.A.D., Bosco, F., Sceniak, M.P., Benfenati, F., Sabo, S.L., 2015. Presynaptic NMDA receptors – dynamics and distribution in developing axons in vitro and in vivo. J. Cell Sci. 128, 768–780. https://doi.org/10.1242/jcs.162362
Girardeau, G., Inema, I., Buzsáki, G., 2017. Reactivations of emotional memory in the hippocampus-amygdala system during sleep. Nat. Neurosci. 20, 1634–1642. https://doi.org/10.1038/nn.4637
Girkin, J.M., Poland, S., Wright, A.J., 2009. Adaptive optics for deeper imaging of biological samples. Curr. Opin. Biotechnol. 20, 106–110. https://doi.org/10.1016/j.copbio.2009.02.009
Glover, E.M., Jovanovic, T., Mercer, K.B., Kerley, K., Bradley, B., Ressler, K.J., Norrholm, S.D., 2012. Estrogen levels are associated with extinction deficits in women with posttraumatic stress disorder. Biol. Psychiatry 72, 19–24. https://doi.org/10.1016/j.biopsych.2012.02.031
Glover, E.M., Jovanovic, T., Norrholm, S.D., 2015. Estrogen and extinction of fear memories: Implications for posttraumatic stress disorder treatment. Biol. Psychiatry 78, 178–185. https://doi.org/10.1016/j.biopsych.2015.02.007
Glover, E.M., Mercer, K.B., Norrholm, S.D., Davis, M., Duncan, E., Bradley, B., Ressler, K.J., Jovanovic, T., 2013. Inhibition of fear is differentially associated with cycling estrogen levels in women. J. Psychiatry Neurosci. 38, 341–348. https://doi.org/10.1503/jpn.120129
Goda, Y., Stevens, C.F., 1996. Synaptic plasticity: The basis of particular types of learning. Curr. Biol. 6, 375–378. https://doi.org/10.1016/S0960-9822(02)00499-2
Gogolla, N., Galimberti, I., DePaola, V., Caroni, P., 2006. Preparation of organotypic hippocampal slice cultures for long-term live imaging. Nat. Protoc. 1, 1165–1171. https://doi.org/10.1038/nprot.2006.168
Goldstein, J.M., Jerram, M., Abbs, B., Whitfield-Gabrieli, S., Makris, N., 2010. Sex differences in stress response circuitry activation dependent on female hormonal cycle. J. Neurosci. 30, 431–438. https://doi.org/10.1523/JNEUROSCI.3021-09.2010
Goldstein, J.M., Seidman, L.J., Horton, N.J., Makris, N., Kennedy, D.N., Caviness, V.S., Faraone, S. V., Tsuang, M.T., 2001. Normal sexual dimorphism of the adult human brain assessed by in vivo magnetic resonance imaging. Cereb. Cortex 11, 490–497. https://doi.org/10.1093/cercor/11.6.490
Gonzalez-Perez, O., Guerrero-Cazares, H., Quiñones-Hinojosa, A., 2010. Targeting of deep brain structures with microinjections for delivery of drugs, viral vectors, or cell transplants. J. Vis. Exp. i, 24–26. https://doi.org/10.3791/2082
Good, M., Day, M., Muir, J.L., 1999. Cyclical changes in endogenous levels of oestrogen modulate the induction of LTD and LTP in the hippocampal CA1 region. Eur. J. Neurosci. 11, 4476–4480. https://doi.org/10.1046/j.1460-9568.1999.00920.x
Göppert-Mayer, M., 2009. Elementary processes with two quantum transitions. Ann. der Phys. 18, 466–479. https://doi.org/10.1002/andp.200910358
Gordon, G.S.D., Gataric, M., Ramos, A.G.C.P., Mouthaan, R., Williams, C., Yoon, J.,

Wilkinson, T.D., Bohndiek, S.E., 2019. Characterizing Optical Fiber Transmission Matrices Using Metasurface Reflector Stacks for Lensless Imaging without Distal Access. Phys. Rev. X 91, 41050. https://doi.org/10.1103/PhysRevX.9.041050
Gould, E., Woolley, C.S., Frankfurt, M., McEwen, B.S., 1990. Gonadal steroids regulate dendritic spine density in hippocampal pyramidal cells in adulthood. J. Neurosci. 10, 1286–1291. https://doi.org/10.1523/JNEUROSCI.10-04-01286.1990
Graham, B.M., Milad, M.R., 2013. Blockade of estrogen by hormonal contraceptives impairs fear extinction in female rats and women. Biol. Psychiatry 73, 371–378. https://doi.org/10.1016/j.biopsych.2012.09.018
Grant, S.G.N., O'Dell, T.J., Karl, K.A., Stein, P.L., Soriano, P., Kandel, E.R., 1992. Impaired long-term potentiation, spatial learning, and hippocampal development in fyn mutant mice. Science 258, 1903–1910. https://doi.org/10.1126/science.1361685
Grasselli, G., Mandolesi, G., Strata, P., Cesare, P., 2011. Impaired sprouting and Axonal Atrophy in cerebellar climbing fibres following in vivo silencing of the growth-associated protein GAP-43. PLoS One 6. https://doi.org/10.1371/journal.pone.0020791
Graves, A.R., Roth, R.H., Tan, H.L., Zhu, Q., Bygrave, A.M., Lopez-Ortega, E., Hong, I., Spiegel, A.C., Johnson, R.C., Vogelstein, J.T., Tward, D.J., Miller, M.I., Huganir, R.L., 2021. Visualizing synaptic plasticity in vivo by large-scale imaging of endogenous AMPA receptors. Elife 10, 1–29. https://doi.org/10.7554/eLife.66809
Greengard, P., Valtorta, F., Czernik, A.J., Benfenati, F., 1993. Synaptic vesicle phosphoproteins and regulation of synaptic function. Science 259, 780–785. https://doi.org/10.1126/science.8430330
Greiser, C.M., Greiser, E.M., Dören, M., 2005. Menopausal hormone therapy and risk of breast cancer: A meta-analysis of epidemiological studies and randomized controlled trials. Hum. Reprod. Update 11, 561–573. https://doi.org/10.1093/humupd/dmi031
Gresack, J.E., Frick, K.M., 2006. Post-training estrogen enhances spatial and object memory consolidation in female mice. Pharmacol. Biochem. Behav. 84, 112–119. https://doi.org/10.1016/j.pbb.2006.04.013
Griffith, T., Tsaneva-Atanasova, K., Mellor, J.R., 2016. Control of Ca 2+ Influx and Calmodulin Activation by SK-Channels in Dendritic Spines. PLoS Comput. Biol. 12, 1–19. https://doi.org/10.1371/journal.pcbi.1004949
Grigoriadis, S., Kennedy, S.H., 2002. Role of estrogen in the treatment of depression. Am. J. Ther. 9, 503–509. https://doi.org/10.1097/00045391-200211000-00008
Grillo, F.W., Song, S., Teles-Grilo Ruivo, L.M., Huang, L., Gao, G., Knott, G.W., MacO, B., Ferretti, V., Thompson, D., Little, G.E., De Paola, V., 2013. Increased axonal bouton dynamics in the aging mouse cortex. Proc. Natl. Acad. Sci. U. S. A. 110. https://doi.org/10.1073/pnas.1218731110
Gross, K.S., Alf, R.L., Polzin, T.R., Frick, K.M., 2021. 17β-estradiol activation of dorsal hippocampal TrkB is independent of increased mature BDNF expression and is required for enhanced memory consolidation in female mice. Psychoneuroendocrinology 125, 105110. https://doi.org/10.1016/j.psyneuen.2020.105110
Grutzendler, J., Kasthuri, N., Gan, W.B., 2002. Long-term dendritic spine stability in the adult cortex. Nature 420, 812–816. https://doi.org/10.1038/nature01276
Grynkiewicz, G., Poenie, M., Tsien, R.Y., 1985. A new generation of Ca2+ indicators with greatly improved fluorescence properties. J. Biol. Chem. 260, 3440–3450. https://doi.org/10.1016/s0021-9258(19)83641-4
Gu, L., Kleiber, S., Schmid, L., Nebeling, F., Chamoun, M., Steffen, J., Wagner, J., Fuhrmann, M., 2014. Long-term in vivo imaging of dendritic spines in the hippocampus reveals structural plasticity. J. Neurosci. 34, 13948–13953. https://doi.org/10.1523/JNEUROSCI.1464-14.2014

Gu, R.Y., Mahalati, R.N., Kahn, J.M., 2015. Design of flexible multi-mode fiber endoscope. Opt. Express 23, 26905. https://doi.org/10.1364/oe.23.026905
Gupta, R.R., Sen, S., Diepenhorst, L.L., Rudick, C.N., Maren, S., 2001. Estrogen modulates sexually dimorphic contextual fear conditioning and hippocampal long-term potentiation (LTP) in rats. Brain Res. 888, 356–365. https://doi.org/10.1016/S0006-8993(00)03116-4
Guskjolen, A., Kenney, J.W., de la Parra, J., Yeung, B. ru A., Josselyn, S.A., Frankland, P.W., 2018. Recovery of "Lost" Infant Memories in Mice. Curr. Biol. 28, 2283-2290.e3. https://doi.org/10.1016/j.cub.2018.05.059
Hablitz, J.J., Johnston, D., 1981. Endogenous nature of spontaneous bursting in hippocampal pyramidal neurons. Cell. Mol. Neurobiol. 1, 325–334. https://doi.org/10.1007/BF00716267
Hadjantonakis, A.K., Nagy, A., 2001. The color of mice: In the light of GFP-variant reporters. Histochem. Cell Biol. 115, 49–58. https://doi.org/10.1007/s004180000233
Haeryfar, S.M.M., Hoskin, D.W., 2004. Thy-1: More than a Mouse Pan-T Cell Marker. J. Immunol. 173, 3581–3588. https://doi.org/10.4049/jimmunol.173.6.3581
Hajszan, T., MacLusky, N.J., Johansen, J.A., Jordan, C.L., Leranth, C., 2007. Effects of androgens and estradiol on spine synapse formation in the prefrontal cortex of normal and testicular feminization mutant male rats. Endocrinology 148, 1963–1967. https://doi.org/10.1210/en.2006-1626
Hampson, K.M., Turcotte, R., Miller, D.T., Kurokawa, K., Males, J.R., Ji, N., Booth, M.J., 2021. Adaptive optics for high-resolution imaging. Nat. Rev. Methods Prim. 1. https://doi.org/10.1038/s43586-021-00066-7
Han, D.H., Park, P., Choi, D. Il, Bliss, T.V.P., Kaang, B.K., 2021. The essence of the engram: Cellular or synaptic? Semin. Cell Dev. Biol. https://doi.org/10.1016/j.semcdb.2021.05.033
Han, J.-H., Kushner, S.A., Yiu, A.P., Hsiang, H.-L., Buch, T., Waisman, A., Bontempi, B., Neve, R.L., Frankland, P.W., Josselyn, 2009. Selective Erasure of a Fear Memory. Science 323, 1492–1496. https://doi.org/10.1126/science.1164139
Hansen, K.B., Yi, F., Perszyk, R., Menniti, F.S., Traynelis, S.F., 2017. NMDA receptors in the central nervous system. Methods Mol. Biol. 1677, 1–80. https://doi.org/10.1007/978-1-4939-7321-7_1
Hao, J., Rapp, P.R., Janssen, W.G.M., Lou, W., Lasley, B.L., Hof, P.R., Morrison, J.H., 2007. Interactive effects of age and estrogen on cognition and pyramidal neurons in monkey prefrontal cortex. Proc. Natl. Acad. Sci. U. S. A. 104, 11465–11470. https://doi.org/10.1073/pnas.0704757104
Happ, D.F., Tasker, R.A., 2016. A method for objectively quantifying propidium iodide exclusion in organotypic hippocampal slice cultures. J. Neurosci. Methods 269, 1–5. https://doi.org/10.1016/j.jneumeth.2016.05.006
Hardingham, G.E., Bading, H., 2010. Synaptic versus extrasynaptic NMDA receptor signalling: Implications for neurodegenerative disorders. Nat. Rev. Neurosci. 11, 682–696. https://doi.org/10.1038/nrn2911
Hardingham, G.E., Fukunaga, Y., Bading, H., 2002. Extrasynaptic NMDARs oppose synaptic NMDARs by triggering CREB shut-off and cell death pathways. Nat. Neurosci. 5, 405–414. https://doi.org/10.1038/nn835
Harris, K.D., Hirase, H., Leinekugel, X., Henze, D.A., Buzsáki, G., 2001. Temporal interaction between single spikes and complex spike bursts in hippocampal pyramidal cells. Neuron 32, 141–149. https://doi.org/10.1016/S0896-6273(01)00447-0
Haruyama, N., Cho, A., B Kulkarni, A., 2009. Overview: Engineering transgenic constructs and mice. Curr. Protoc. Cell Biol. Unit-19.19. https://doi.org/10.1002/0471143030.cb1910s42
Harvey, C.D., Svoboda, K., 2007. Locally dynamic synaptic learning rules in pyramidal neuron dendrites. Nature 450, 1195–1200. https://doi.org/10.1038/nature06416

Harvey, C.D., Yasuda, R., Zhong, H., Svoboda, K., 2008. The Spread of Ras Activity Triggered by Activation of a Single Dendritic Spine. Science 321, 136–140. https://doi.org/10.1126/science.1159675
Harward, S.C., Hedrick, N.G., Hall, C.E., Parra-Bueno, P., Milner, T.A., Pan, E., Laviv, T., Hempstead, B.L., Yasuda, R., McNamara, J.O., 2016. Autocrine BDNF-TrkB signalling within a single dendritic spine. Nature 538, 99–103. https://doi.org/10.1038/nature19766
Hatanaka, Y., Mukai, H., Mitsuhashi, K., Hojo, Y., Murakami, G., Komatsuzaki, Y., Sato, R., Kawato, S., 2009. Androgen rapidly increases dendritic thorns of CA3 neurons in male rat hippocampus. Biochem. Biophys. Res. Commun. 381, 728–732. https://doi.org/10.1016/j.bbrc.2009.02.130
Hausmann, M., 2017. Why sex hormones matter for neuroscience: A very short review on sex, sex hormones, and functional brain asymmetries. J. Neurosci. Res. 95, 40–49. https://doi.org/10.1002/jnr.23857
Hayashi-Takagi, A., Yagishita, S., Nakamura, M., Shirai, F., Wu, Y.I., Loshbaugh, A.L., Kuhlman, B., Hahn, K.M., Kasai, H., 2015. Labelling and optical erasure of synaptic memory traces in the motor cortex. Nature 525, 333–338. https://doi.org/10.1038/nature15257
Hebb, D.O., 1949. The Organization of Behavior. New York, NY Wiley Sons. https://doi.org/10.2307/1418888
Hedrick, N.G., Harward, S.C., Hall, C.E., Murakoshi, H., McNamara, J.O., Yasuda, R., 2016. Rho GTPase complementation underlies BDNF-dependent homo- and heterosynaptic plasticity. Nature 538, 104–108. https://doi.org/10.1038/nature19784
Hedrick, N.G., Yasuda, R., 2017. Regulation of Rho GTPase proteins during spine structural plasticity for the control of local dendritic plasticity. Curr. Opin. Neurobiol. 45, 193–201. https://doi.org/10.1016/j.conb.2017.06.002
Hell, S.W., Bahlmann, K., Schrader, M., Soini, A., Malak, H., Gryczynski, I., Lakowicz, J.R., 1996. Three-photon excitation in fluorescence microscopy. J. Biomed. Opt. 1, 71–74. https://doi.org/10.1117/12.229062
Helmchen, F., Denk, W., 2005. Deep tissue two-photon microscopy. Nat. Methods 2, 932–940. https://doi.org/10.1038/nmeth818
Helmchen, F., Fee, M.S., Tank, D.W., Denk, W., 2001. A miniature head-mounted two-photon microscope: High-resolution brain imaging in freely moving animals. Neuron 31, 903–912. https://doi.org/10.1016/S0896-6273(01)00421-4
Hertz, L., Chen, Y., Simon, S.A., Gutierrez, R., Tandon, S., 2016. Editorial: All 3 types of glial cells are important for memory formation. Front. Integr. Neurosci. 10, 1–4. https://doi.org/10.3389/fnint.2016.00031
Hiroi, R., Neumaier, J.F., 2006. Differential effects of ovarian steroids on anxiety versus fear as measured by open field test and fear-potentiated startle. Behav. Brain Res. 166, 93–100. https://doi.org/10.1016/j.bbr.2005.07.021
Hofer, S.B., Mrsic-Flogel, T.D., Bonhoeffer, T., Hübener, M., 2009. Experience leaves a lasting structural trace in cortical circuits. Nature 457, 313–317. https://doi.org/10.1038/nature07487
Hojo, Y., Hattori, T.A., Enami, T., Furukawa, A., Suzuki, K., Ishii, H.T., Mukai, H., Morrison, J.H., Janssen, W.G.M., Kominami, S., Harada, N., Kimoto, T., Kawato, S., 2004. Adult male rat hippocampus synthesizes estradiol from pregnenolone by cytochromes P45017α and P450 aromatase localized in neurons. Proc. Natl. Acad. Sci. U. S. A. 101, 865–870. https://doi.org/10.1073/pnas.2630225100
Hojo, Y., Murakami, G., Mukai, H., Higo, S., Hatanaka, Y., Ogiue-Ikeda, M., Ishii, H., Kimoto, T., Kawato, S., 2008. Estrogen synthesis in the brain-Role in synaptic plasticity and memory. Mol. Cell. Endocrinol. 290, 31–43. https://doi.org/10.1016/j.mce.2008.04.017
Holahan, M.R., 2017. A shift from a pivotal to supporting role for the growth-associated protein (GAP-43) in the coordination of axonal structural and functional plasticity.

Front. Cell. Neurosci. 11, 1–19. https://doi.org/10.3389/fncel.2017.00266
Holt, C.E., Martin, K.C., Schuman, E.M., 2019. function. Nat. Struct. Mol. Biol. 26, 557–566. https://doi.org/10.1038/s41594-019-0263-5
Holt, C.E., Schuman, E.M., 2013. Perspective The Central Dogma Decentralized : New Perspectives on RNA Function and Local Translation in Neurons. Neuron 80, 648–657. https://doi.org/10.1016/j.neuron.2013.10.036
Holtmaat, A., Bonhoeffer, T., Chow, D.K., Chuckowree, J., De Paola, V., Hofer, S.B., Hübener, M., Keck, T., Knott, G., Lee, W.C.A., Mostany, R., Mrsic-Flogel, T.D., Nedivi, E., Portera-Cailliau, C., Svoboda, K., Trachtenberg, J.T., Wilbrecht, L., 2009. Long-term, high-resolution imaging in the mouse neocortex through a chronic cranial window. Nat. Protoc. 4, 1128–1144. https://doi.org/10.1038/nprot.2009.89
Holtmaat, A., Caroni, P., 2016. Functional and structural underpinnings of neuronal assembly formation in learning. Nat. Neurosci. 19, 1553–1562. https://doi.org/10.1038/nn.4418
Holtmaat, A., De Paola, V., Wilbrecht, L., Knott, G.W., 2008. Imaging of experience-dependent structural plasticity in the mouse neocortex in vivo. Behav. Brain Res. 192, 20–25. https://doi.org/10.1016/j.bbr.2008.04.005
Holtmaat, A., Svoboda, K., 2009. Experience-dependent structural synaptic plasticity in the mammalian brain. Nat. Rev. Neurosci. 10, 647–658. https://doi.org/10.1038/nrn2699
Holtmaat, A.J.G.D., Trachtenberg, J.T., Wilbrecht, L., Shepherd, G.M., Zhang, X., Knott, G.W., Svoboda, K., 2005. Transient and persistent dendritic spines in the neocortex in vivo. Neuron 45, 279–291. https://doi.org/10.1016/j.neuron.2005.01.003
Honjo, H., Iwasa, K., Urabe, M., 1998. Clinical studies of oestrogen therapy for dementia. J. Br. Menopause Soc. 4, 12–17. https://doi.org/10.1177/136218079800400106
Hoppa, M.B., Gouzer, G., Armbruster, M., Ryan, T.A., 2014. Article Control and Plasticity of the Presynaptic Action Potential Waveform at Small CNS Nerve Terminals. Neuron 84, 778–789. https://doi.org/10.1016/j.neuron.2014.09.038
Horton, N.G., Wang, K., Kobat, D., Clark, C.G., Wise, F.W., Schaffer, C.B., Xu, C., 2013. In vivo three-photon microscopy of subcortical structures within an intact mouse brain. Nat. Photonics 7, 205–209. https://doi.org/10.1038/nphoton.2012.336
Hosoi, N., Holt, M., Sakaba, T., 2009. Calcium Dependence of Exo- and Endocytotic Coupling at a Glutamatergic Synapse. Neuron 63, 216–229. https://doi.org/10.1016/j.neuron.2009.06.010
Hruska, M., Henderson, N., Le Marchand, S.J., Jafri, H., Dalva, M.B., 2018. Synaptic nanomodules underlie the organization and plasticity of spine synapses. Nat. Neurosci. 21, 671–682. https://doi.org/10.1038/s41593-018-0138-9
Hsiang, H.L.L., Epp, J.R., van den Oever, M.C., Yan, C., Rashid, A.J., Insel, N., Ye, L., Niibori, Y., Deisseroth, K., Frankland, P.W., Josselyn, S.A., 2014. Manipulating a “cocaine engram” in mice. J. Neurosci. 34, 14115–14127. https://doi.org/10.1523/JNEUROSCI.3327-14.2014
Hua, J.Y., Smear, M.C., Baier, H., Smith, S.J., 2005. Regulation of axon growth in vivo by activity-based competition. Nature 434, 1022–1025. https://doi.org/10.1038/nature03409
Huang, Y.Y., Colino, A., Selig, D.K., Malenka, R.C., 1992. The influence of prior synaptic activity on the induction of long-term potentiation. Science 255, 730–733. https://doi.org/10.1126/science.1346729
Huang, Y.Y., Kandel, E.R., 1995. D1/D5 receptor agonists induce a protein synthesis-dependent late potentiation in the CA1 region of the hippocampus. Proc. Natl. Acad. Sci. U. S. A. 92, 2446–2450. https://doi.org/10.1073/pnas.92.7.2446
Huganir, R.L., Nicoll, R.A., 2013. AMPARs and synaptic plasticity: The last 25 years.

Neuron 80, 704–717. https://doi.org/10.1016/j.neuron.2013.10.025
Humeau, Y., Choquet, D., 2019. The next generation of approaches to investigate the link between synaptic plasticity and learning. Nat. Neurosci. 22, 1536–1543. https://doi.org/10.1038/s41593-019-0480-6
Humpel, C., 2015. Neuroscience forefront review organotypic brain slice cultures: A review. Neuroscience 305, 86–98. https://doi.org/10.1016/j.neuroscience.2015.07.086
Hwang, W.J., Lee, T.Y., Kim, N.S., Kwon, J.S., 2021. The role of estrogen receptors and their signaling across psychiatric disorders. Int. J. Mol. Sci. 22, 1–21. https://doi.org/10.3390/ijms22010373
Ikawa, M., Kominami, K., Yoshimura, Y., Tanaka, K., Nishimune, Y., Okabe, M., 1995. Green fluorescent protein as a marker in transgenic mice. Dev. Growth Differ. 37, 455–459.
Inagaki, T., Gautreaux, C., Luine, V., 2010. Acute Estrogen Treatment Facilitates Recognition Memory Consolidation and Alters Monoamine Levels in Memory-Related Brain Areas. Horm. Behav. 58, 415–126. https://doi.org/10.1016/j.yhbeh.2010.05.013
Inavalli, V.V.G.K., Lenz, M.O., Butler, C., Angibaud, J., Compans, B., Levet, F., Tønnesen, J., Rossier, O., Giannone, G., Thoumine, O., Hosy, E., Choquet, D., Sibarita, J.B., Nägerl, U.V., 2019. A super-resolution platform for correlative live single-molecule imaging and STED microscopy. Nat. Methods 16, 1263–1268. https://doi.org/10.1038/s41592-019-0611-8
Isaac, J.T.R., Nicoll, R.A., Malenka, R.C., 1995. Evidence for silent synapses: Implications for the expression of LTP. Neuron 15, 427–434. https://doi.org/10.1016/0896-6273(95)90046-2
Ishii, H., Tsurugizawa, T., Ogiue-Ikeda, M., Asashima, M., Mukai, H., Murakami, G., Hojo, Y., Kimoto, T., Kawato, S., 2007. Local production of sex hormones and their modulation of hippocampal synaptic plasticity. Neuroscientist 13, 323–334. https://doi.org/10.1177/1073858407013004060l
Ishii, K., Nagaoka, A., Kishida, Y., Okazaki, H., Yagishita, S., Ucar, H., Takahashi, N., Saito, N., Kasai, H., 2018. In Vivo volume dynamics of dendritic spines in the neocortex of wild-type and Fmr1 KO mice. eNeuro 5, 1–13. https://doi.org/10.1523/ENEURO.0282-18.2018
Jääskeläinen, I.P., Ahveninen, J., Andermann, M.L., Belliveau, J.W., Raij, T., Sams, M., 2011. Short-term plasticity as a neural mechanism supporting memory and attentional functions. Brain Res. 1422, 66–81. https://doi.org/10.1016/j.brainres.2011.09.031
Jackman, S.L., Regehr, W.G., 2017. The Mechanisms and Functions of Synaptic Facilitation. Neuron 94, 447–464. https://doi.org/10.1016/j.neuron.2017.02.047
Jacome, L.F., Barateli, K., Buitrago, D., Lema, F., Frankfurt, M., Luine, V.N., 2016. Gonadal hormones rapidly enhance spatial memory and increase hippocampal spine density in male rats. Endocrinology 157, 1357–1362. https://doi.org/10.1210/en.2015-1959
Jacques, S.L., 2013. Optical properties of biological tissues: a review. Phys. Med. Biol. 58, R37-61. https://doi.org/10.1088/0031-9155/58/11/R37
James, G.T., Chang, T.C., Mills, N., Speed, H.E., Dobrunz, L.E., 2006. Responses of Excitatory Hippocampal Synapses to Natural Stimulus Patterns Reveal a Decrease in Short-Term Facilitation and Increase in Short-Term Depression During Postnatal Development. Hippocampus 16, 66–79. https://doi.org/10.1002/hipo.20132
Janssen, W.G.M., Vissavajjhala, P., Andrews, G., Moran, T., Hof, P.R., Morrison, J.H., 2005. Cellular and synaptic distribution of NR2A and NR2B in macaque monkey and rat hippocampus as visualized with subunit-specific monoclonal antibodies. Exp. Neurol. 191, 28–44. https://doi.org/10.1016/j.expneurol.2004.08.020
Jarrard, L.E., 1993. On the role of the hippocampus in learning and memory in the rat.

Behav. Neural Biol. 60, 9–26. https://doi.org/10.1016/0163-1047(93)90664-4
Jasnow, A.M., Schulkin, J., Pfaff, D.W., 2006. Estrogen facilitates fear conditioning and increases corticotropin- releasing hormone mRNA expression in the central amygdala in female mice. Horm. Behav. 49, 197–205. https://doi.org/10.1016/j.yhbeh.2005.06.005
Jennings, J.H., Ung, R.L., Resendez, S.L., Stamatakis, A.M., Taylor, J.G., Huang, J., Veleta, K., Kantak, P.A., Aita, M., Shilling-Scrivo, K., Ramakrishnan, C., Deisseroth, K., Otte, S., Stuber, G.D., 2015. Visualizing hypothalamic network dynamics for appetitive and consummatory behaviors. Cell 160, 516–527. https://doi.org/10.1016/j.cell.2014.12.026
Ji, N., 2017. Adaptive optical fluorescence microscopy. Nat. Methods 14, 374–380. https://doi.org/10.1038/nmeth.4218
Ji, N., Freeman, J., Smith, S.L., 2016. Technologies for imaging neural activity in large volumes. Nat. Neurosci. 19, 1154–1164. https://doi.org/10.1038/nn.4358
Ji, N., Milkie, D.E., Betzig, E., 2010. Adaptive optics via pupil segmentation for high-resolution imaging in biological tissues. Nat. Methods 7, 141–147. https://doi.org/10.1038/nmeth.1411
Ji, N., Sato, T.R., Betzig, E., 2012. Characterization and adaptive optical correction of aberrations during in vivo imaging in the mouse cortex. Proc. Natl. Acad. Sci. U. S. A. 109, 22–27. https://doi.org/10.1073/pnas.1109202108
Jin, Y., Dougherty, S.E., Wood, K., Sun, L., Cudmore, R.H., Abdalla, A., Kannan, G., Pletnikov, M., Hashemi, P., Linden, D.J., 2016. Regrowth of Serotonin Axons in the Adult Mouse Brain Following Injury. Neuron 91, 748–762. https://doi.org/10.1016/j.neuron.2016.07.024
Johansen, J.P., Hamanaka, H., Monfils, M.H., Behnia, R., Deisseroth, K., Blair, H.T., LeDoux, J.E., 2010. Optical activation of lateral amygdala pyramidal cells instructs associative fear learning. Proc. Natl. Acad. Sci. U. S. A. 107, 12692–12697. https://doi.org/10.1073/pnas.1002418107
Johansson, F., Jirenhed, D.A., Rasmussen, A., Zucca, R., Hesslow, G., 2014. Memory trace and timing mechanism localized to cerebellar Purkinje cells. Proc. Natl. Acad. Sci. U. S. A. 111, 14930–14934. https://doi.org/10.1073/pnas.1415371111
Johnson, J.W., Ascher, P., 1987. Glycine potentiates the NMDA response in cultured mouse brain neurons. Nature 325, 529–531. https://doi.org/10.1038/325529a0
Jones, M. V., Westbrook, G.L., 1996. The impact of receptor desensitization on fast synaptic transmission. Trends Neurosci. 19, 96–101. https://doi.org/10.1016/S0166-2236(96)80037-3
Josselyn, S.A., Tonegawa, S., 2020. Memory engrams: Recalling the past and imagining the future. Science 367. https://doi.org/10.1126/science.aaw4325
Jósvay, K., Winter, Z., Katona, R.L., Pecze, L., Marton, A., Buhala, A., Szakonyi, G., Oláh, Z., Vizler, C., 2014. Besides neuro-imaging, the Thy1-YFP mouse could serve for visualizing experimental tumours, inflammation and wound-healing. Sci. Rep. 4, 1–7. https://doi.org/10.1038/srep06776
Ju, W., Morishita, W., Tsui, J., Gaietta, G., Deerinck, T.J., Adams, S.R., Garner, C.C., Tsien, R.Y., Ellisman, M.H., Malenka, R.C., 2004. Activity-dependent regulation of dendritic synthesis and trafficking of AMPA receptors. Nat. Neurosci. 7, 244–253. https://doi.org/10.1038/nn1189
Jung, J.C., Mehta, A.D., Aksay, E., Stepnoski, R., Schnitzer, M.J., 2004. In vivo mammalian brain imaging using one- and two-photon fluorescence microendoscopy. J. Neurophysiol. 92, 3121–3133. https://doi.org/10.1152/jn.00234.2004
Jung, J.C., Schnitzer, M.J., 2003. Multiphoton endoscopy. Opt. Lett. 28, 902. https://doi.org/10.1364/ol.28.000902
Kaifosh, P., Lovett-Barron, M., Turi, G.F., Reardon, T.R., Losonczy, A., 2013. Septo-hippocampal GABAergic signaling across multiple modalities in awake mice. Nat. Neurosci. 16, 1182–1184. https://doi.org/10.1038/nn.3482

Kakkava, E., Romito, M., Conkey, D.B., Loterie, D., Stankovic, K.M., Moser, C., Psaltis, D., 2019. Selective femtosecond laser ablation via two-photon fluorescence imaging through a multimode fiber. Biomed. Opt. Express 10, 423. https://doi.org/10.1364/boe.10.000423
Kandaswamy, U., Deng, P.Y., Stevens, C.F., Klyachko, V.A., 2010. The role of presynaptic dynamics in processing of natural spike trains in hippocampal synapses. J. Neurosci. 30, 15904–15914. https://doi.org/10.1523/JNEUROSCI.4050-10.2010
Kandel, E.R., Dudai, Y., Mayford, M.R., 2014. The molecular and systems biology of memory. Cell 157, 163–186. https://doi.org/10.1016/j.cell.2014.03.001
Kandel, E.R., Spencer, W.A., 1961. Electrophysiology of hippocampal neurons. II. After-potentials and repetitive firing. J. Neurophysiol. 24, 243–259. https://doi.org/10.1152/jn.1961.24.3.243
Karpova, A., Mikhaylova, M., Thomas, U., Knöpfel, T., Behnisch, T., 2006. Involvement of protein synthesis and degradation in long-term potentiation of Schaffer collateral CA1 synapses. J. Neurosci. 26, 4949–4955. https://doi.org/10.1523/JNEUROSCI.4573-05.2006
Kato, A., Hojo, Y., Higo, S., Komatsuzaki, Y., Murakami, G., Yoshino, H., Uebayashi, M., Kawato, S., 2013. Female hippocampal estrogens have a significant correlation with cyclic fluctuation of hippocampal spines. Front. Neural Circuits 7, 1–13. https://doi.org/10.3389/fncir.2013.00149
Katz, B., Miledi, R., 1968. The role of calcium in neuromuscular facilitation. J. Physiol. 195, 481–492. https://doi.org/10.1113/jphysiol.1968.sp008469
Kauer, J.A., Malenka, R.C., Nicoll, R.A., 1988. A persistent postsynaptic modification mediates long-term potentiation in the hippocampus. Neuron 1, 911–917. https://doi.org/10.1016/0896-6273(88)90148-1
Kaufman, A.M., Milnerwood, A.J., Sepers, M.D., Coquinco, A., She, K., Wang, L., Lee, H., Craig, A.M., Cynader, M., Raymond, L.A., 2012. Opposing roles of synaptic and extrasynaptic NMDA receptor signaling in cocultured striatal and cortical neurons. J. Neurosci. 32, 3992–4003. https://doi.org/10.1523/JNEUROSCI.4129-11.2012
Kawata, M., 1995. Roles of steroid hormones and their receptors in structural organization in the nervous system. Neurosci. Res. 24, 1–46. https://doi.org/10.1016/0168-0102(96)81278-8
Kawato, S., Hojo, Y., Kimoto, T., 2002. Histological and metabolism analysis of P450 expression in the brain, Methods in Enzymology. Elsevier Science (USA). https://doi.org/10.1016/S0076-6879(02)57682-5
Keck, T., Keller, G.B., Jacobsen, R.I., Eysel, U.T., Bonhoeffer, T., Hübener, M., 2013. Synaptic scaling and homeostatic plasticity in the mouse visual cortex in vivo. Neuron 80, 327–334. https://doi.org/10.1016/j.neuron.2013.08.018
Keenan, P.A., Ezzat, W.H., Ginsburg, K., Moore, G.J., 2001. Prefrontal cortex as the site of estrogen's effect on cognition. Psychoneuroendocrinology 26, 577–590. https://doi.org/10.1016/S0306-4530(01)00013-0
Kellermayer, B., Ferreira, J.S., Dupuis, J., Levet, F., Grillo-Bosch, D., Bard, L., Linarès-Loyez, J., Bouchet, D., Choquet, D., Rusakov, D.A., Bon, P., Sibarita, J.B., Cognet, L., Sainlos, M., Carvalho, A.L., Groc, L., 2018. Differential Nanoscale Topography and Functional Role of GluN2-NMDA Receptor Subtypes at Glutamatergic Synapses. Neuron 100, 106-119.e7. https://doi.org/10.1016/j.neuron.2018.09.012
Kempadoo, K.A., Mosharov, E. V., Choi, S.J., Sulzer, D., Kandel, E.R., 2016. Dopamine release from the locus coeruleus to the dorsal hippocampus promotes spatial learning and memory. Proc. Natl. Acad. Sci. U. S. A. 113, 14835–14840. https://doi.org/10.1073/pnas.1616515114
Kerchner, G.A., Nicoll, R.A., 2008. Silent synapses and the emergence of a postsynaptic mechanism for LTP. Nat. Rev. Neurosci. 9, 813–825.

https://doi.org/10.1038/nrn2501
Keyser, D.O., Pellmar, T.C., 1994. Synaptic transmission in the hippocampus: Critical role for glial cells. Glia 10, 237–243. https://doi.org/10.1002/glia.440100402
Kim, W. Bin, Cho, J.H., 2017. Synaptic targeting of double-projecting ventral CA1 hippocampal neurons to the medial prefrontal cortex and basal amygdala. J. Neurosci. 37, 4868–4882. https://doi.org/10.1523/JNEUROSCI.3579-16.2017
Kim, J.J., Jung, M.W., 2006. Neural circuits and mechanisms involved in Pavlovian fear conditioning: A critical review. Neurosci. Biobehav. Rev. 30, 188–202. https://doi.org/10.1016/j.neubiorev.2005.06.005
Klausen, M., Dubois, V., Clermont, G., Tonnelé, C., Castet, F., Blanchard-Desce, M., 2019. Dual-wavelength efficient two-photon photorelease of glycine by π-extended dipolar coumarins. Chem. Sci. 10, 4209–4219. https://doi.org/10.1039/c9sc00148d
Klioutchnikov, A., Wallace, D.J., Frosz, M.H., Zeltner, R., Sawinski, J., Pawlak, V., Voit, K.M., Russell, P.S.J., Kerr, J.N.D., 2020. Three-photon head-mounted microscope for imaging deep cortical layers in freely moving rats. Nat. Methods 17, 509–513. https://doi.org/10.1038/s41592-020-0817-9
Klyachko, V.A., Stevens, C.F., 2006. Temperature-dependent shift of balance among the components of short-term plasticity in hippocampal synapses. J. Neurosci. 26, 6945–6957. https://doi.org/10.1523/JNEUROSCI.1382-06.2006
Knierim, J.J., 2015. The hippocampus. Curr. Biol. 25, R1116–R1121. https://doi.org/10.1016/j.cub.2015.10.049
Kobat, D., Durst, M.E., Nishimura, N., Wong, A.W., Schaffer, C.B., Xu, C., 2009. Deep tissue multiphoton microscopy using longer wavelength excitation. Opt. Express 17, 13354. https://doi.org/10.1364/oe.17.013354
Koebele, S. V., Quihuis, A.M., Lavery, C.N., Plumley, Z.M.T., Castaneda, A.J., Bimonte-Nelson, H.A., 2021. Oestrogen treatment modulates the impact of cognitive experience and task complexity on memory in middle-aged surgically menopausal rats. J. Neuroendocrinol. 33, 1–18. https://doi.org/10.1111/jne.13002
Köhler, M., Hirschberg, B., Bond, C.T., Kinzie, J.M., Marrion, N. V., Maylie, J., Adelman, J.P., 1996. Small-conductance, calcium-activated potassium channels from mammalian brain. Science 273, 1709–1714. https://doi.org/10.1126/science.273.5282.1709
Köhr, G., 2006. NMDA receptor function: Subunit composition versus spatial distribution. Cell Tissue Res. 326, 439–446. https://doi.org/10.1007/s00441-006-0273-6
Kokkas, B., 2010. Tissue injury and inflammation. Ann. Gen. Psychiatry 9, 2010. https://doi.org/10.1186/1744-859x-9-s1-s1
Kolb, B., Gibb, R., 2015. Plasticity in the prefrontal cortex of adult rats. Front. Cell. Neurosci. 9, 1–11. https://doi.org/10.3389/fncel.2015.00015
Körber, N., Stein, V., 2016. In vivo imaging demonstrates dendritic spine stabilization by SynCAM 1. Sci. Rep. 6, 1–10. https://doi.org/10.1038/srep24241
Krahe, R., Gabbiani, F., 2004. Burst firing in sensory systems. Nat. Rev. Neurosci. 5, 13–23. https://doi.org/10.1038/nrn1296
Kramár, E.A., Chen, L.Y., Brandon, N.J., Rex, C.S., Liu, F., Gall, C.M., Lynch, G., 2009. Cytoskeletal changes underlie estrogen's acute effects on synaptic transmission and plasticity. J. Neurosci. 29, 12982–12993. https://doi.org/10.1523/JNEUROSCI.3059-09.2009
Krug, R., Born, J., Rasch, B., 2006. A 3-day estrogen treatment improves prefrontal cortex-dependent cognitive function in postmenopausal women. Psychoneuroendocrinology 31, 965–975. https://doi.org/10.1016/j.psyneuen.2006.05.007
Krugers, H.J., Hoogenraad, C.C., Groc, L., 2010. Stress hormones and AMPA receptor trafficking in synaptic plasticity and memory. Nat. Rev. Neurosci. 11, 675–681. https://doi.org/10.1038/nrn2913

Krugers, H.J., Karst, H., Joels, M., 2012. Interactions between noradrenaline and corticosteroids in the brain: From electrical activity to cognitive performance. Front. Cell. Neurosci. 6, 1–10. https://doi.org/10.3389/fncel.2012.00015
Kutsuwada, T., Kashiwabuchi, N., Mori, H., Sakimura, K., Kushiya, E., Araki, K., Meguro, H., Masaki, H., Kumanishi, T., Arakawa, M., Mishina, M., 1992. Molecular diversity of the NMDA receptor channel. Nature 358, 36–41. https://doi.org/10.1038/358036a0
Kwon, H.B., Castillo, P.E., 2008. Role of Glutamate Autoreceptors at Hippocampal Mossy Fiber Synapses. Neuron 60, 1082–1094. https://doi.org/10.1016/j.neuron.2008.10.045
Lacagnina, A.F., Brockway, E.T., Crovetti, C.R., Shue, F., McCarty, M.J., Sattler, K.P., Lim, S.C., Santos, S.L., Denny, C.A., Drew, M.R., 2019. Distinct hippocampal engrams control extinction and relapse of fear memory. Nat. Neurosci. 22, 753–761. https://doi.org/10.1038/s41593-019-0361-z
Lai, C.S.W., Franke, T.F., Gan, W.B., 2012. Opposite effects of fear conditioning and extinction on dendritic spine remodelling. Nature 483, 87–92. https://doi.org/10.1038/nature10792
Lai, K.O., Ip, N.Y., 2013. Structural plasticity of dendritic spines: The underlying mechanisms and its dysregulation in brain disorders. Biochim. Biophys. Acta - Mol. Basis Dis. 1832, 2257–2263. https://doi.org/10.1016/j.bbadis.2013.08.012
Lalo, U., Bogdanov, A., Moss, G.W.J., Frenguelli, B.G., Pankratov, Y., 2018. Role for Astroglia-Derived BDNF and MSK1 in Homeostatic Synaptic Plasticity. Neuroglia 1, 381–394. https://doi.org/10.3390/neuroglia1020026
Lamprecht, R., LeDoux, J., 2004. Structural plasticity and memory. Nat. Rev. Neurosci. 5, 45–54. https://doi.org/10.1038/nrn1301
Lamy, C., Goodchild, S.J., Weatherall, K.L., Jane, D.E., Liégeois, J.F., Seutin, V., Marrion, N. V., 2010. Allosteric block of KCa2 channels by apamin. J. Biol. Chem. 285, 27067–27077. https://doi.org/10.1074/jbc.M110.110072
Lang, C., Barco, A., Zablow, L., Kandel, E.R., Siegelbaum, S.A., Zakharenko, S.S., 2004. Transient expansion of synaptically connected dendritic spines upon induction of hippocampal long-term potentiation. Proc. Natl. Acad. Sci. U. S. A. 101, 16665–16670. https://doi.org/10.1073/pnas.0407581101
Langille, J.J., Gallistel, C.R., 2020. Locating the engram: Should we look for plastic synapses or information-storing molecules? Neurobiol. Learn. Mem. 169, 107164. https://doi.org/10.1016/j.nlm.2020.107164
Larsen, R.S., Corlew, R.J., Henson, M.A., Roberts, A.C., Mishina, M., Watanabe, M., Lipton, S.A., Nakanishi, N., Pérez-Otaño, I., Weinberg, R.J., Philpot, B.D., 2011. NR3A-containing NMDARs promote neurotransmitter release and spike timing-dependent plasticity. Nat. Neurosci. 14, 338–344. https://doi.org/10.1038/nn.2750
Larsen, R.S., Sjöström, P.J., 2015. Synapse-type-specific plasticity in local circuits. Curr. Opin. Neurobiol. 35, 127–135. https://doi.org/10.1016/j.conb.2015.08.001
Lau, C.G., Zukin, R.S., 2007. NMDA receptor trafficking in synaptic plasticity and neuropsychiatric disorders. Nat. Rev. Neurosci. 8, 413–427. https://doi.org/10.1038/nrn2153
Laux, T., Fukami, K., Thelen, M., Golub, T., Frey, D., Caroni, P., 2000. GAP43, MARCKS, and CAP23 modulate PI(4,5)P2 at plasmalemmal rafts, and regulate cell cortex actin dynamics through a common mechanism. J. Cell Biol. 149, 1455–1471. https://doi.org/10.1083/jcb.149.7.1455
Le Duigou, C., Simonnet, J., Teleñczuk, M.T., Fricker, D., Miles, R., 2014. Recurrent synapses and circuits in the CA3 region of the hippocampus: An associative network. Front. Cell. Neurosci. 7, 1–13. https://doi.org/10.3389/fncel.2013.00262
Lebron-Milad, K., Milad, M.R., 2012. Sex differences, gonadal hormones and the fear extinction network: implications for anxiety disorders. Biol. Mood Anxiety Disord. 2, 3. https://doi.org/10.1186/2045-5380-2-3
Lee, S.H., Lutz, D., Drexler, D., Frotscher, M., Shen, J., 2020. Differential modulation of

short-term plasticity at hippocampal mossy fiber and Schaffer collateral synapses by mitochondrial Ca2+. PLoS One 15, 1–16. https://doi.org/10.1371/journal.pone.0240610
Lee, S.J.R., Escobedo-Lozoya, Y., Szatmari, E.M., Yasuda, R., 2009. Activation of CaMKII in single dendritic spines during long-term potentiation. Nature 458, 299–304. https://doi.org/10.1038/nature07842
Lees, R.M., Johnson, J.D., Ashby, M.C., 2020. Presynaptic Boutons That Contain Mitochondria Are More Stable. Front. Synaptic Neurosci. 11, 1–13. https://doi.org/10.3389/fnsyn.2019.00037
Lein, P.J., Barnhart, C.D., Pessah, I.N., 2011. Acute Hippocampal Slice Preparation and Hippocampal Slice Cultures. Methods Mol. Biol. 758, 115–134. https://doi.org/10.1007/978-1-61779-170-3_8
Lephart, E.D., 1996. A review of brain aromatase cytochrome P450. Brain Res. Rev. 22, 1–26. https://doi.org/10.1016/0165-0173(96)00002-1
Leranth, C., Petnehazy, O., MacLusky, N.J., 2003. Gonadal hormones affect spine synaptic density in the CA1 hippocampal subfield of male rats. J. Neurosci. 23, 1588–1592. https://doi.org/10.1523/jneurosci.23-05-01588.2003
Levene, M.J., Dombeck, D.A., Kasischke, K.A., Molloy, R.P., Webb, W.W., 2004. In Vivo Multiphoton Microscopy of Deep Brain Tissue. J. Neurophysiol. 91, 1908–1912. https://doi.org/10.1152/jn.01007.2003
Levene, M.J., Dombeck, D.A., Kasischke, K.A., Molloy, R.P., Williams, R.M., Zipfel, W.R., Webb, W.W., 2003. GRIN lenses for deep in vivo multiphoton imaging. Front. Opt. OSA Tech. Dig. Paper MY3. https://doi.org/10.1364/fio.2003.my3
Li, C., Brake, W.G., Romeo, R.D., Dunlop, J.C., Gordon, M., Buzescu, R., Magarinos, A.M., Allen, P.B., Greengard, P., Luine, V., McEwen, B.S., 2004. Estrogen alters hippocampal dendritic spine shape and enhances synaptic protein immunoreactivity and spatial memory in female mice. Proc. Natl. Acad. Sci. U. S. A. 101, 2185–2190. https://doi.org/10.1073/pnas.0307313101
Li, S., Horsley, S.A.R., Tyc, T., Čižmár, T., Phillips, D.B., 2021. Memory effect assisted imaging through multimode optical fibres. Nat. Commun. 12, 1–13. https://doi.org/10.1038/s41467-021-23729-1
Li, Y.H., Han, T.Z., 2007. Glycine binding sites of presynaptic NMDA receptors may tonically regulate glutamate release in the rat visual cortex. J. Neurophysiol. 97, 817–823. https://doi.org/10.1152/jn.00980.2006
Liao, D., Hessler, N.A., Malinow, R., 1995. Activation of postsynaptically silent synapses during pairing-induced LTP in CA1 region of hippocampal slice. Nature 375, 400–404. https://doi.org/10.1038/375400a0
Lin, M.T., Luja, R., Watanabe, M., Adelman, J.P., Maylie, J., 2008. SK2 channel plasticity contributes to LTP at Schaffer collateral – CA1 synapses. Nat. Neurosci. 11, 170–177. https://doi.org/10.1038/nn2041
Lipták, N., Bosze, Z., Hiripi, L., 2019. GFP transgenic animals in biomedical research: A review of potential disadvantages. Physiol. Res. 68, 525–530. https://doi.org/10.33549/physiolres.934227
Lisman, J.E., 1997. Bursts as a unit of neural information: Making unreliable synapses reliable. Trends Neurosci. 20, 38–43. https://doi.org/10.1016/S0166-2236(96)10070-9
Lisman, J.E., Grace, A.A., 2005. The hippocampal-VTA loop: Controlling the entry of information into long-term memory. Neuron 46, 703–713. https://doi.org/10.1016/j.neuron.2005.05.002
Lituma, P.J., Kwon, H.-B., Alvina, K., Luján, R., Castillo, P.E., 2021. Presynaptic NMDA receptors facilitate short-term plasticity and BDNF release at hippocampal mossy fiber synapses. Elife 10, 1–26. https://doi.org/10.7554/eLife.66612
Liu, D. dan, Yang, Q., Li, S. tian, 2013. Activation of extrasynaptic NMDA receptors induces LTD in rat hippocampal CA1 neurons. Brain Res. Bull. 93, 10–16. https://doi.org/10.1016/j.brainresbull.2012.12.003

Liu, F., Day, M., Muñiz, L.C., Bitran, D., Arias, R., Revilla-Sanchez, R., Grauer, S., Zhang, G., Kelley, C., Pulito, V., Sung, A., Mervis, R.F., Navarra, R., Hirst, W.D., Reinhart, P.H., Marquis, K.L., Moss, S.J., Pangalos, M.N., Brandon, N.J., 2008. Activation of estrogen receptor-β regulates hippocampal synaptic plasticity and improves memory. Nat. Neurosci. 11, 334–343. https://doi.org/10.1038/nn2057

Liu, L., Wong, T.P., Pozza, M.F., Lingenhoehl, K., Wang, Y., Sheng, M., Auberson, Y.P., Wang, Y.T., 2004. Role of NMDA Receptor Subtypes in Governing the Direction of Hippocampal Synaptic Plasticity. Science 304, 1021–1023.

Liu, R., Li, Z., Marvin, J.S., Kleinfeld, D., 2019. Direct wavefront sensing enables functional imaging of infragranular axons and spines. Nat. Methods 16, 615–618. https://doi.org/10.1038/s41592-019-0434-7

Liu, S., Lin, C., Xu, Y., Luo, H., Peng, L., Zeng, X., Zheng, H., Chen, P.R., Zou, P., 2021. A far-red hybrid voltage indicator enabled by bioorthogonal engineering of rhodopsin on live neurons. Nat. Chem. 13, 472–479. https://doi.org/10.1038/s41557-021-00641-1

Liu, X., Ramirez, S., Pang, P.T., Puryear, C.B., Govindarajan, A., Deisseroth, K., Tonegawa, S., 2012. Optogenetic stimulation of a hippocampal engram activates fear memory recall. Nature 484, 381–385. https://doi.org/10.1038/nature11028

Lock, J.T., Parker, I., Smith, I.F., 2015. A comparison of fluorescent Ca2+ indicators for imaging local Ca2+ signals in cultured cells. Cell Calcium 58, 638–648. https://doi.org/10.1016/j.ceca.2015.10.003

Loew, L.M., 2015. Design and Use of Organic Voltage Sensitive Dyes. Adv. Exp. Med. Biol. 859, 27–53. https://doi.org/10.1007/978-3-319-17641-3_2

Loewenstein, Y., Kuras, A., Rumpel, S., 2011. Multiplicative dynamics underlie the emergence of the log- normal distribution of spine sizes in the neocortex in vivo. J. Neurosci. 31, 9481–9488. https://doi.org/10.1523/JNEUROSCI.6130-10.2011

Lømo, T., 2003. The discovery of long-term potentiation. Philos. Trans. R. Soc. B Biol. Sci. 358, 617–620. https://doi.org/10.1098/rstb.2002.1226

Loterie, D., Psaltis, D., Moser, C., 2017. Bend translation in multimode fiber imaging. Opt. Express 25, 6263. https://doi.org/10.1364/oe.25.006263

Lowenstein, D.H., Arsenault, L., 1996. Dentate granule cell layer collagen explant cultures: spontaneous axonal growth and induction by brain-derived neurotrophic factor or basic fibroblast growth factor. Neuroscience 74, 1197–1208. https://doi.org/10.1016/0306-4522(96)00226-6

Lowery, R.L., Majewska, A.K., 2010. Intracranial injection of adeno-associated viral vectors. J. Vis. Exp. 14–16. https://doi.org/10.3791/2140

Lozovaya, N.A., Grebenyuk, S.E., Tsintsadze, T.S., Feng, B., Monaghan, D.T., Krishtal, O.A., 2004. Extrasynaptic NR2B and NR2D subunits of NMDA receptors shape 'superslow' afterburst EPSC in rat hippocampus. J. Physiol. 558, 451–463. https://doi.org/10.1113/jphysiol.2004.063792

Lu, R., Sun, W., Liang, Y., Kerlin, A., Bierfeld, J., Seelig, J.D., Wilson, D.E., Scholl, B., Mohar, B., Tanimoto, M., Koyama, M., Fitzpatrick, D., Orger, M.B., Ji, N., 2017. Video-rate volumetric functional imaging of the brain at synaptic resolution. Nat. Neurosci. 20, 620–628. https://doi.org/10.1038/nn.4516

Lu, Y., Sareddy, G.R., Wang, J., Wang, R., Li, Y., Dong, Y., Zhang, Q., Liu, J., O'Connor, J.C., Xu, J., Vadlamudi, R.K., Brann, D.W., 2019. Neuron-derived estrogen regulates synaptic plasticity and memory. J. Neurosci. 39, 2792–2809. https://doi.org/10.1523/JNEUROSCI.1970-18.2019

Luine, V., Frankfurt, M., 2013. Interactions between estradiol, BDNF and dendritic spines in promoting memory. Neuroscience 239, 34–45. https://doi.org/10.1016/j.neuroscience.2012.10.019

Luine, V.N., Jacome, L.F., Maclusky, N.J., 2003. Rapid enhancement of visual and place memory by estrogens in rats. Endocrinology 144, 2836–2844. https://doi.org/10.1210/en.2003-0004

Luine, V.N., Richards, S.T., Wu, V.Y., Beck, K.D., 1998. Estradiol enhances learning

and memory in a spatial memory task and effects levels of monoaminergic neurotransmitters. Horm. Behav. 34, 149–162. https://doi.org/10.1006/hbeh.1998.1473
Luján, R., Maylie, J., Adelman, J.P., 2009. New sites of action for GIRK and SK channels. Nat. Rev. Neurosci. 10, 475–480. https://doi.org/10.1038/nrn2668
Lüscher, C., Malenka, R.C., 2012. NMDA Receptor-Dependent Long-Term Potentiation and Long-Term Depression (LTP/LTD). Cold Spring Harb. Perspect. Biol. 4. https://doi.org/10.1101/cshperspect.a005710
Lüscher, C., Nicoll, R.A., Malenka, R.C., Muller, D., 2000. Synaptic plasticity and dynamic modulation of the postsynaptic membrane. Nat. Neurosci. 3, 545–550. https://doi.org/10.1038/75714
Lymer, J.M., Sheppard, P.A.S., Kuun, T., Blackman, A., Jani, N., Mahbub, S., Choleris, E., 2018. Estrogens and their receptors in the medial amygdala rapidly facilitate social recognition in female mice. Psychoneuroendocrinology 89, 30–38. https://doi.org/10.1016/j.psyneuen.2017.12.021
MacDermott, A.B., Mayer, M.L., Westbrook, G.L., Smith, S.J., Barker, J.L., 1986. NMDA-receptor activation increases cytoplasmic calcium concentration in cultured spinal cord neurones. Nature 321, 519–522. https://doi.org/10.1038/321519a0
MacDermott, A.B., Role, L.W., Siegelbaum, S.A., 1999. Presynaptic ionotropic receptors and the control of transmitter release. Annu. Rev. Neurosci. 22, 443–485. https://doi.org/10.1146/annurev.neuro.22.1.443
MacGillavry, H.D., Song, Y., Raghavachari, S., Blanpied, T.A., 2013. Nanoscale scaffolding domains within the postsynaptic density concentrate synaptic ampa receptors. Neuron 78, 615–622. https://doi.org/10.1016/j.neuron.2013.03.009
MacLeod, K.M., Horiuchi, T.K., Carr, C.E., 2007. A role for Short-Term Synaptic Facilitation and Depression in the Processing of Intensity Information in the Auditory Brain Stem. J. Neurophysiol. 97, 2863–2874. https://doi.org/10.1152/jn.01030.2006
MacLusky, N.J., Hajszan, T., Leranth, C., 2004. Effects of dehydroepiandrosterone and flutamide on hippocampal CA1 spine synapse density in male and female rats: Implications for the role of androgens in maintenance of hippocampal structure. Endocrinology 145, 4154–4161. https://doi.org/10.1210/en.2004-0477
MacLusky, N.J., Hajszan, T., Prange-Kiel, J., Leranth, C., 2006. Androgen modulation of hippocampal synaptic plasticity. Neuroscience 138, 957–965. https://doi.org/10.1016/j.neuroscience.2005.12.054
MacLusky, N.J., Luine, V.N., Hajszan, T., Leranth, C., 2005. The 17α and 17β isomers of estradiol both induce rapid spine synapse formation in the Ca1 hippocampal subfield of ovariectomized female rats. Endocrinology 146, 287–293. https://doi.org/10.1210/en.2004-0730
Madara, J.C., Levine, E.S., 2008. Presynaptic and postsynaptic NMDA receptors mediate distinct effects of brain-derived neurotrophic factor on synaptic transmission. J. Neurophysiol. 100, 3175–3184. https://doi.org/10.1152/jn.90880.2008
Maddox, S.A., Hartmann, J., Ross, R.A., Ressler, K.J., 2019. Deconstructing the Gestalt: Mechanisms of Fear, Threat, and Trauma Memory Encoding. Neuron 102, 60–74. https://doi.org/10.1016/j.neuron.2019.03.017
Mahalati, R.N., Gu, R.Y., Kahn, J.M., 2013. Resolution limits for imaging through multi-mode fiber. Opt. Express 21, 1656. https://doi.org/10.1364/oe.21.001656
Malenka, R.C., 1995. LTP and LTD: Dynamic and Interactive Processes of Synaptic Plasticity. Neurosci. 1, 35–42. https://doi.org/10.1177/107385849500100106
Malenka, R.C., 1994. Synaptic plasticity in the hippocampus: LTP and LTD. Cell 78, 535–538. https://doi.org/10.1016/0092-8674(94)90517-7
Malenka, R.C., Bear, M.F., 2004. LTP and LTD: An embarrassment of riches. Neuron 44, 5–21. https://doi.org/10.1016/j.neuron.2004.09.012
Malenka, R.C., Nicoll, R.A., 1993. NMDA-receptor-dependent synaptic plasticity:

multiple forms and mechanisms. Trends Neurosci. 16, 15–19. https://doi.org/10.1016/0166-2236(93)90197-t
Malinow, R., Schulman, H., Tsien, R.W., 1989. Inhibition of postsynaptic PKC or CaMKII blocks induction but not expression of LTP. Science 245, 862–866. https://doi.org/10.1126/science.2549638
Maren, S., Fanselow, M.S., 1995. Synaptic plasticity in the basolateral amygdala induced by hippocampal formation stimulation in vivo. J. Neurosci. 15, 7548–7564. https://doi.org/10.1523/jneurosci.15-11-07548.1995
Margrie, T.W., Meyer, A.H., Caputi, A., Monyer, H., Hasan, M.T., Schaefer, A.T., Denk, W., Brecht, M., 2003. Targeted whole-cell recordings in the mammalian brain in vivo. Neuron 39, 911–918. https://doi.org/10.1016/j.neuron.2003.08.012
Markram, H., Gupta, A., Uziel, A., Wang, Y., Tsodyks, M., 1998a. Information processing with frequency-dependent synaptic connections. Neurobiol. Learn. Mem. 70, 101–112. https://doi.org/10.1006/nlme.1998.3841
Markram, H., Pikus, D., Gupta, A., Tsodyks, M., 1998b. Potential for multiple mechanisms, phenomena and algorithms for synaptic plasticity at single synapses. Neuropharmacology 37, 489–500. https://doi.org/10.1016/S0028-3908(98)00049-5
Markram, H., Tsodyks, M., 1997. The information content of action potential trains a synaptic basis. Lect. Notes Comput. Sci. (including Subser. Lect. Notes Artif. Intell. Lect. Notes Bioinformatics) 1327, 13–23. https://doi.org/10.1007/bfb0020126
Markram, H., Tsodyks, M. V., 1996a. Redistribution of synaptic efficacy between neocortical pyramidal neurons 382, 807–810. https://doi.org/10.1038/382807a0
Markram, H., Tsodyks, M. V., 1996b. Redistribution of synaptic efficacy: A mechanism to generate infinite synaptic input diversity from a homogenous population of neurons without changing absolute synaptic efficacies. J. Physiol. Paris 90, 229–232. https://doi.org/10.1016/S0928-4257(97)81429-5
Markus, E.J., Zecevic, M., 1997. Sex differences and estrous cycle changes in hippocampus-dependent fear conditioning. Psychobiology 25, 246–252. https://doi.org/10.3758/BF03331934
Marsh, P., Burns, D., Girkin, J., 2003. Practical implementation of adaptive optics in multiphoton microscopy. Opt. Express 11, 1123. https://doi.org/10.1364/oe.11.001123
Martin, K.C., Kosik, K.S., 2002. Synaptic tagging — who's it? Nat. Rev. Neurosci. 3, 813–820. https://doi.org/10.1038/nrn942
Martin, S.J., Grimwood, P.D., Morris, R.G.M., 2000. Synaptic Plasticity and Memory: An Evaluation of the Hypothesis. Annu. Rev. Neurosci. 23, 649–711. https://doi.org/10.1146/annurev.neuro.23.1.649
Martin, S.J., Morris, R.G.M., 2002. New life in an old idea: The synaptic plasticity and memory hypothesis revisited. Hippocampus 12, 609–636. https://doi.org/10.1002/hipo.10107
Martínez-Cué, C., Rueda, N., 2020. Cellular Senescence in Neurodegenerative Diseases. Front. Cell. Neurosci. 14. https://doi.org/10.3389/fncel.2020.00016
Masland, R.H., 2003. Neuronal cell types. Curr. Biol. 14, R497-500. https://doi.org/10.1016/j.cub.2004.06.035
Massey, P. V, Johnson, B.E., Moult, P.R., Auberson, Y.P., Brown, M.W., Molnar, E., Collingridge, G.L., Bashir, Z.I., 2004. Differential Roles of NR2A and NR2B-Containing NMDA Receptors in Cortical Long-Term Potentiation and Long-Term Depression. J. Neurosci. 24, 7821–7828. https://doi.org/10.1523/JNEUROSCI.1697-04.2004
Mathis, D.M., Furman, J.L., Norris, C.M., 2011. Preparation of acute hippocampal slices from rats and transgenic mice for the study of synaptic alterations during aging and amyloid pathology. J. Vis. Exp. 1–8. https://doi.org/10.3791/2330
Matsuo, N., Reijmers, L.G., Mayford, M.R., 2008. Spine-Type – Specific Recruitment of

Newly Synthesized AMPA Receptors with Learning. Science 319, 1104–1108. https://doi.org/10.1126/science.1149967
Matsuzaki, M., Ellis-Davies, G.C.R., Nemoto, T., Miyashita, Y., Iino, M., Kasai, H., 2001. Dendritic spine geometry is critical for AMPA receptor expression in hippocampal CA1 pyramidal neurons. Nat. Neurosci. 4, 1086–1092. https://doi.org/10.1038/nn736
Matsuzaki, M., Honkura, N., Ellis-Davies, G.C.R., Kasai, H., 2004. Structural basis of long-term potentiation in single dendritic spines. Nature 429, 761–766. https://doi.org/10.1038/nature02617
Maus, L., Lee, C.K., Altas, B., Sertel, S.M., Weyand, K., Rizzoli, S.O., Rhee, J.S., Brose, N., Imig, C., Cooper, B.H., 2020. Ultrastructural Correlates of Presynaptic Functional Heterogeneity in Hippocampal Synapses. Cell Rep. 30, 3632-3643.e8. https://doi.org/10.1016/j.celrep.2020.02.083
Mayer, M.L., Westbrookt, G.L., Guthriet, P.B., 1984. Responses in Spinal Cord Neurones. Nature 309, 261–263.
Mayevsky, A., Chance, B., 1982. Intracellular oxidation-reduction state measured in situ by a multichannel fiber-optic surface fluorometer. Science 217, 537–540. https://doi.org/10.1126/science.7201167
McEwen, B.S., Alves, S.E., 1999. Estrogen actions in the nervous system. Endocr. Rev. 20, 279–307. https://doi.org/10.1210/edrv.20.3.0365
McEwen, B.S., Magarinos, A.M., 2001. Stress and hippocampal plasticity: Implications for the pathophysiology of affective disorders. Hum. Psychopharmacol. 16. https://doi.org/10.1002/hup.266
McEwen, B.S., Milner, T.A., 2017. Understanding the broad influence of sex hormones and sex differences in the brain. J. Neurosci. Res. 95, 24–39. https://doi.org/10.1002/jnr.23809
McGuinness, L., Taylor, C., Taylor, R.D.T., Yau, C., Langenhan, T., Hart, M.L., Christian, H., Tynan, P.W., Donnelly, P., Emptage, N.J., 2010. Presynaptic NMDARs in the Hippocampus Facilitate Transmitter Release at Theta Frequency. Neuron 68, 1109–1127. https://doi.org/10.1016/j.neuron.2010.11.023
Meighan, P.C., Meighan, S.E., Davis, C.J., Wright, J.W., Harding, J.W., 2007. Effects of matrix metalloproteinase inhibition on short- and long-term plasticity of schaffer collateral/CA1 synapses. J. Neurochem. 102, 2085–2096. https://doi.org/10.1111/j.1471-4159.2007.04682.x
Meng, G., Liang, Y., Sarsfield, S., Jiang, W.C., Lu, R., Dudman, J.T., Aponte, Y., Ji, N., 2019. High-throughput synapse-resolving two-photon fluorescence microendoscopy for deep-brain volumetric imaging in vivo. Elife 8, 1–22. https://doi.org/10.7554/eLife.40805
Meyer, D., Bonhoeffer, T., Scheuss, V., 2014. Balance and stability of synaptic structures during synaptic plasticity. Neuron 82, 430–443. https://doi.org/10.1016/j.neuron.2014.02.031
Mhaouty-Kodja, S., 2018. Role of the androgen receptor in the central nervous system. Mol. Cell. Endocrinol. 465, 103–112. https://doi.org/10.1016/j.mce.2017.08.001
Milad, M.R., Igoe, S.A., Lebron-Milad, K., Novales, J.E., 2009. Estrous cycle phase and gonadal hormones influence conditioned fear extinction. Neuroscience 164, 887–895. https://doi.org/10.1016/j.neuroscience.2009.09.011
Miller, E.W., 2016. Small molecule fluorescent voltage indicators for studying membrane potential. Curr. Opin. Chem. Biol. 33, 74–80. https://doi.org/10.1016/j.cbpa.2016.06.003
Min, S.S., Quan, H.Y., Ma, J., Han, J.S., Jeon, B.H., Seol, G.H., 2009. Chronic brain inflammation impairs two forms of long-term potentiation in the rat hippocampal CA1 area. Neurosci. Lett. 456, 20–24. https://doi.org/10.1016/j.neulet.2009.03.079
Mitchell, K.J., Turtaev, S., Padgett, M.J., Čižmár, T., Phillips, D.B., 2016. High-speed spatial control of the intensity, phase and polarisation of vector beams using a digital micro-mirror device. Opt. Express 24. https://doi.org/10.1364/OE.24.029269

Mitsushima, D., Ishihara, K., Sano, A., Kessels, H.W., Takahashi, T., 2011. Contextual learning requires synaptic AMPA receptor delivery in the hippocampus. Proc. Natl. Acad. Sci. U. S. A. 108, 12503–12508. https://doi.org/10.1073/pnas.1104558108
Mizrahi, A., Crowley, J.C., Shtoyerman, E., Katz, L.C., 2004. High-Resolution in Vivo Imaging of Hippocampal Dendrites and Spines. J. Neurosci. 24, 3147–3151. https://doi.org/10.1523/JNEUROSCI.5218-03.2004
Mizuseki, K., Royer, S., Diba, K., Buzsáki, G., 2012. Activity dynamics and behavioral correlates of CA3 and CA1 hippocampal pyramidal neurons. Hippocampus 22, 1659–1680. https://doi.org/10.1002/hipo.22002
Moczulska, K.E., Tinter-Thiede, J., Peter, M., Ushakova, L., Wernle, T., Bathellier, B., Rumpel, S., 2013. Dynamics of dendritic spines in the mouse auditory cortex during memory formation and memory recall. Proc. Natl. Acad. Sci. U. S. A. 110, 18315–18320. https://doi.org/10.1073/pnas.1312508110
Moghadami, S., Jahanshahi, M., Sepehri, H., Amini, H., 2016. Gonadectomy reduces the density of androgen receptor-immunoreactive neurons in male rat's hippocampus: Testosterone replacement compensates it. Behav. Brain Funct. 12, 1–10. https://doi.org/10.1186/s12993-016-0089-9
Mongillo, G., Barak, O., Tsodyks, M., 2008. SynaptiC Theory of Working Memory. Science 319, 1543–1546. https://doi.org/10.1126/science.1150769
Monyer, H., Burnashev, N., Laurie, D.J., Sakmann, B., Seeburg, P.H., 1994. Developmental and regional expression in the rat brain and functional properties of four NMDA receptors. Neuron 12, 529–540. https://doi.org/10.1016/0896-6273(94)90210-0
Monyer, H., Sprengel, R., Schoepfer, R., Herb, A., Higuchi, M., Lomeli, H., Burnashev, N., Sakmann, B., Seeburg, P.H., 1992. Heteromeric NMDA Receptors : Molecular and Functional Distinction of Subtypes. Science 256, 1217–1222. https://doi.org/10.1126/science.256.5060.1217
Morales-Delgado, E.E., Farahi, S., Papadopoulos, I.N., Psaltis, D., Moser, C., 2015a. Delivery of focused short pulses through a multimode fiber. Opt. Express 23, 9109. https://doi.org/10.1364/oe.23.009109
Morales-Delgado, E.E., Psaltis, D., Moser, C., 2015b. Two-photon imaging through a multimode fiber. Opt. Express 23, 32158. https://doi.org/10.1364/oe.23.032158
Morgan, M.A., Pfaff, D.W., 2001. Effects of estrogen on activity and fear-related behaviors in mice. Horm. Behav. 40, 472–482. https://doi.org/10.1006/hbeh.2001.1716
Morris, R.G.M., Anderson, E., Lynch, G.S., Baudry, M., 1986. Selective impairment of learning and blockade of long-term potentiation by an N-methyl-D-aspartate receptor antagonist, AP5. Nature 319, 774–776. https://doi.org/10.1038/319774a0
Moulder, K.L., Jiang, X., Taylor, A.A., Olney, J.W., Mennerick, S., 2006. Physiological activity depresses synaptic function through an effect on vesicle priming. J. Neurosci. 26, 6618–6626. https://doi.org/10.1523/JNEUROSCI.5498-05.2006
Mukai, H., Tsurugizawa, T., Murakami, G., Kominami, S., Ishii, H., Ogiue-Ikeda, M., Takata, N., Tanabe, N., Furukawa, A., Hojo, Y., Ooishi, Y., Morrison, J.H., Janssen, W.G.M., Rose, J.A., Chambon, P., Kato, S., Izumi, S., Yamazaki, T., Kimoto, T., Kawato, S., 2007. Rapid modulation of long-term depression and spinogenesis via synaptic estrogen receptors in hippocampal principal neurons. J. Neurochem. 100, 950–967. https://doi.org/10.1111/j.1471-4159.2006.04264.x
Mulkey, R.M., Herron, C.E., Malenka, R.C., 1993. An essential role for protein phosphatases in hippocampal long-term depression. Science 261, 1051–1055. https://doi.org/10.1126/science.8394601
Murakami, G., Tsurugizawa, T., Hatanaka, Y., Komatsuzaki, Y., Tanabe, N., Mukai, H., Hojo, Y., Kominami, S., Yamazaki, T., Kimoto, T., Kawato, S., 2006. Comparison between basal and apical dendritic spines in estrogen-induced rapid spinogenesis of CA1 principal neurons in the adult hippocampus. Biochem. Biophys. Res. Commun. 351, 553–558. https://doi.org/10.1016/j.bbrc.2006.10.066

Murakoshi, H., Wang, H., Yasuda, R., 2011. Local, persistent activation of Rho GTPases during plasticity of single dendritic spines. Nature 472, 100–106. https://doi.org/10.1038/nature09823
Murchison, C.F., Zhang, X.Y., Zhang, W.P., Ouyang, M., Lee, A., Thomas, S.A., 2004. A distinct role for norepinephrine in memory retrieval. Cell 117, 131–143. https://doi.org/10.1016/S0092-8674(04)00259-4
Murthy, V.N., Schikorski, T., Stevens, C.F., Zhu, Y., 2001. Inactivity produces increases in neurotransmitter release and synapse size. Neuron 32, 673–682. https://doi.org/10.1016/S0896-6273(01)00500-1
Murthy, V.N., Sejnowski, T.J., Stevens, C.F., 1997. Heterogeneous release properties of visualized individual hippocampal synapses. Neuron 18, 599–612. https://doi.org/10.1016/S0896-6273(00)80301-3
Nabavi, S., Kessels, H.W., Alfonso, S., Aow, J., Fox, R., Malinow, R., 2013. Metabotropic NMDA receptor function is required for NMDA receptor-dependent long-term depression. Proc. Natl. Acad. Sci. U. S. A. 110, 4027–4032. https://doi.org/10.1073/pnas.1219454110
Nägerl, U.V., Bonhoeffer, T., 2010. Imaging living synapses at the nanoscale by STED microscopy. J. Neurosci. 30, 9341–9346. https://doi.org/10.1523/JNEUROSCI.0990-10.2010
Nägerl, U.V., Eberhorn, N., Cambridge, S.B., Bonhoeffer, T., 2004. Bidirectional activity-dependent morphological plasticity in hippocampal neurons. Neuron 44, 759–767. https://doi.org/10.1016/j.neuron.2004.11.016
Nägerl, U.V., Willig, K.I., Hein, B., Hell, S.W., Bonhoeffer, T., 2008. Live-cell imaging of dendritic spines by STED microscopy. Proc. Natl. Acad. Sci. U. S. A. 105, 18982–18987. https://doi.org/10.1073/pnas.0810028105
Nair, D., Hosy, E., Petersen, J.D., Constals, A., Giannone, G., Choquet, D., Sibarita, J.B., 2013. Super-resolution imaging reveals that AMPA receptors inside synapses are dynamically organized in nanodomains regulated by PSD95. J. Neurosci. 33, 13204–13224. https://doi.org/10.1523/JNEUROSCI.2381-12.2013
Nakazawa, K., Quirk, M.C., Chitwood, R.A., Watanabe, M., Yeckel, M.F., Sun, L.D., Kato, A., Carr, C.A., Johnston, D., Wilson, M.A., Tonegawa, S., 2002. Requirement for hippocampal CA3 NMDA receptors in associative memory recall. Science 297, 211–218. https://doi.org/10.1126/science.1071795
Nakazawa, K., Sun, L.D., Quirk, M.C., Rondi-Reig, L., Wilson, M.A., Tonegawa, S., 2003. Hippocampal CA3 NMDA receptors are crucial for memory acquisition of one-time experience. Neuron 38, 305–315. https://doi.org/10.1016/S0896-6273(03)00165-X
Nanou, E., Alpert, M.H., Alford, S., Manira, A. El, 2013. Differential regulation of synaptic transmission by pre- and postsynaptic SK channels in the spinal locomotor network. J. Neurophysiol. 109, 3051–3059. https://doi.org/10.1152/jn.00067.2013
Narasimhan, K., 2005. SK channels: a new twist to synaptic plasticity. Nat. Neurosci. 8, 550. https://doi.org/10.1038/nn0505-550
Nebieridze, N., Zhang, X., Chachua, T., Velíšek, L., Stanton, P.K., Velíšková, J., 2012. β-Estradiol unmasks metabotropic receptor-mediated metaplasticity of NMDA receptor transmission in the female rat dentate gyrus. Psychoneuroendocrinology 37, 1845–1854. https://doi.org/10.1016/j.psyneuen.2012.03.023
Neher, E., Sakaba, T., 2008. Multiple Roles of Calcium Ions in the Regulation of Neurotransmitter Release. Neuron 59, 861–872. https://doi.org/10.1016/j.neuron.2008.08.019
Neher, E., Sakmann, B., 1976. Single-channel currents recorded from membrane of denervated frog muscle fibres. Nature 260, 799–802. https://doi.org/10.1038/260799a0
Neubert, F., Beliu, G., Terpitz, U., Werner, C., Geis, C., Sauer, M., Doose, S., 2018. Bioorthogonal Click Chemistry Enables Site-specific Fluorescence Labeling of

Functional NMDA Receptors for Super-Resolution Imaging. Angew. Chemie - Int. Ed. 57, 16364–16369. https://doi.org/10.1002/anie.201808951
Neves, G., Cooke, S.F., Bliss, T.V.P., 2012. Synaptic plasticity, memory and the hippocampus: A neural network approach to causality. Nat. Rev. Neurosci. 9, 65–75. https://doi.org/10.1038/nrn2303
Nevian, T., Sakmann, B., 2006. Spine Ca2+ signaling in spike-timing-dependent plasticity. J. Neurosci. 26, 11001–11013. https://doi.org/10.1523/JNEUROSCI.1749-06.2006
Newcomer, J.W., Farber, N.B., Olney, J.W., 2000. NMDA receptor function, memory, and brain aging. Dialogues Clin. Neurosci. 2, 219–232. https://doi.org/10.31887/dcns.2000.2.3/jnewcomer
Newcomer, J.W., Krystal, J.H., 2001. NMDA Receptor regulation of memory and behavior in humans. Hippocampus 11, 529–542. https://doi.org/10.1002/hipo.1069
Ngo-Anh, T.J., Bloodgood, B.L., Lin, M., Sabatini, B.L., Maylie, J., Adelman, J.P., 2005. SK channels and NMDA receptors form a Ca2+-mediated feedback loop in dendritic spines. Nat. Neurosci. 8, 642–649. https://doi.org/10.1038/nn1449
Niclou, S.P., Danzeisen, C., Eikesdal, H.P., Wiig, H., Brons, N.H.C., Poli, A.M.F., Svendsen, A., Torsvik, A., Enger, P.Ø., Terzis, J.A., Bjerkvig, R., 2008. A novel eGFP-expressing immunodeficient mouse model to study tumor-host interactions. FASEB J. 22, 3120–3128. https://doi.org/10.1096/fj.08-109611
Nicoll, R.A., 2017. A Brief History of Long-Term Potentiation. Neuron 93, 281–290. https://doi.org/10.1016/j.neuron.2016.12.015
Nicoll, R.A., Schmitz, D., 2005. Synaptic plasticity at hippocampal mossy fibre synapses. Nat. Rev. Neurosci. 6, 863–876. https://doi.org/10.1038/nrn1786
Nikonenko, I., Jourdain, P., Muller, D., 2003. Presynaptic remodeling contributes to activity-dependent synaptogenesis. J. Neurosci. 23, 8498–8505. https://doi.org/10.1523/jneurosci.23-24-08498.2003
Noguchi, J., Nagaoka, A., Hayama, T., Ucar, H., Yagishita, S., Takahashi, N., Kasai, H., 2019. Bidirectional in vivo structural dendritic spine plasticity revealed by two-photon glutamate uncaging in the mouse neocortex. Sci. Rep. 9, 1–8. https://doi.org/10.1038/s41598-019-50445-0
Noguchi, J., Nagaoka, A., Watanabe, S., Ellis-Davies, G.C.R., Kitamura, K., Kano, M., Matsuzaki, M., Kasai, H., 2011. In vivo two-photon uncaging of glutamate revealing the structure-function relationships of dendritic spines in the neocortex of adult mice. J. Physiol. 589, 2447–2457. https://doi.org/10.1113/jphysiol.2011.207100
Nosten-Bertrand, M., Errington, M.L., Murphy, K.P.S.J., Tokugawa, Y., Barboni, E., Kozlova, E., Michalovich, D., Morris, R.G.M., Silver, J., Stewart, C.L., Bliss, T.V.P., Morris, R.J., 1996. Normal spatial learning despite regional inhibition of LTP in mice lacking Thy-1. Nature 379, 826–829. https://doi.org/10.1038/379826a0
Nowak, L., Bregestovski, P., Ascher, P., Herbet, A., Prochiantz, A., 1984. Magnesium gates glutamate-activated channels in mouse central neurones. Nature 307, 462–465. https://doi.org/10.1038/307462a0
O'Keefe, J., Dostrovsky, J., 1971. The hippocampus as a spatial map . Preliminary evidence from unit activity in the freely-moving rat. Brain Res. 34, 171–175. https://doi.org/10.1016/0006-8993(71)90358-1
O'Riordan, K.J., Hu, N.W., Rowan, M.J., 2018. Aß Facilitates LTD at Schaffer Collateral Synapses Preferentially in the Left Hippocampus. Cell Rep. 22, 2053–2065. https://doi.org/10.1016/j.celrep.2018.01.085
Ohayon, S., Caravaca-Aguirre, A., Piestun, R., DiCarlo, J.J., 2018. Minimally invasive multimode optical fiber microendoscope for deep brain fluorescence imaging. Biomed. Opt. Express 9, 1492. https://doi.org/10.1364/boe.9.001492
Okabe, M., Ikawa, M., Kominami, K., Nakanishi, T., Nishimune, Y., 1997. "Green mice" as a source of ubiquitous green cells. FEBS Lett. 407, 313–319.

https://doi.org/10.1016/S0014-5793(97)00313-X
Okuyama, T., Kitamura, T., Roy, D.S., Itohara, S., Tonegawa, S., 2016. Ventral CA1 neurons store social memory. Science 353, 1536–1541. https://doi.org/10.1126/science.aaf7003
Orsini, C.A., Kim, J.H., Knapska, E., Maren, S., 2011. Hippocampal and prefrontal projections to the basal amygdala mediate contextual regulation of fear after extinction. J. Neurosci. 31, 17269–17277. https://doi.org/10.1523/JNEUROSCI.4095-11.2011
Österlund, M.K., Gustafsson, J.Å., Keller, E., Hurd, Y.L., 2000. Estrogen receptor β (ERβ) messenger ribonucleic acid (mRNA) expression within the human forebrain: Distinct distribution pattern to ERα mRNA. J. Clin. Endocrinol. Metab. 85, 3840–3846. https://doi.org/10.1210/jcem.85.10.6913
Ouzounov, D.G., Wang, T., Wang, M., Feng, D.D., Horton, N.G., Cruz-Hernández, J.C., Cheng, Y.T., Reimer, J., Tolias, A.S., Nishimura, N., Xu, C., 2017. In vivo three-photon imaging of activity of GcamP6-labeled neurons deep in intact mouse brain. Nat. Methods 14, 388–390. https://doi.org/10.1038/nmeth.4183
Packer, A.M., Peterka, D.S., Hirtz, J.J., Prakash, R., Deisseroth, K., Yuste, R., 2012. Two-photon optogenetics of dendritic spines and neural circuits. Nat. Methods 9, 1202–1205. https://doi.org/10.1038/nmeth.2249
Packer, A.M., Roska, B., Häuser, M., 2013. Targeting neurons and photons for optogenetics. Nat. Neurosci. 16, 805–815. https://doi.org/10.1038/nn.3427
Packer, A.M., Russell, L.E., Dalgleish, H.W.P., Häusser, M., 2015. Simultaneous all-optical manipulation and recording of neural circuit activity with cellular resolution in vivo. Nat. Methods 12, 140–146. https://doi.org/10.1038/nmeth.3217
Padamsey, Z., Emptage, N., 2014. Two sides to long-term potentiation: A view towards reconciliation. Philos. Trans. R. Soc. B Biol. Sci. 369, 18–21. https://doi.org/10.1098/rstb.2013.0154
Padamsey, Z., Emptage, N.J., 2011. Imaging synaptic plasticity. Mol. Brain 4, 1–10. https://doi.org/10.1186/1756-6606-4-36
Padamsey, Z., McGuinness, L., Bardo, S.J., Reinhart, M., Tong, R., Hedegaard, A., Hart, M.L., Emptage, N.J., 2017a. Activity-Dependent Exocytosis of Lysosomes Regulates the Structural Plasticity of Dendritic Spines. Neuron 93, 132–146. https://doi.org/10.1016/j.neuron.2016.11.013
Padamsey, Z., Tong, R., Emptage, N., 2019. Optical Quantal Analysis Using Ca2+ Indicators: A Robust Method for Assessing Transmitter Release Probability at Excitatory Synapses by Imaging Single Glutamate Release Events. Front. Synaptic Neurosci. 11, 1–11. https://doi.org/10.3389/fnsyn.2019.00005
Padamsey, Z., Tong, R., Emptage, N., 2017b. Glutamate is required for depression but not potentiation of long-term presynaptic function. Elife 6, 1–35. https://doi.org/10.7554/eLife.29688
Pala, A., Petersen, C.C.H., 2015. InVivo Measurement of Cell-Type-Specific Synaptic Connectivity and Synaptic Transmission in Layer 2/3 Mouse Barrel Cortex. Neuron 85, 68–75. https://doi.org/10.1016/j.neuron.2014.11.025
Pan, B., Zucker, R.S., 2009. A General Model of Synaptic Transmission and Short-Term Plasticity. Neuron 62, 539–554. https://doi.org/10.1016/j.neuron.2009.03.025
Panja, D., Bramham, C.R., 2014. BDNF mechanisms in late LTP formation: A synthesis and breakdown. Neuropharmacology 76, 664–676. https://doi.org/10.1016/j.neuropharm.2013.06.024
Paoletti, P., 2011. Molecular basis of NMDA receptor functional diversity. Eur. J. Neurosci. 33, 1351–1365. https://doi.org/10.1111/j.1460-9568.2011.07628.x
Paoletti, P., Bellone, C., Zhou, Q., 2013. NMDA receptor subunit diversity: Impact on receptor properties, synaptic plasticity and disease. Nat. Rev. Neurosci. 14, 383–400. https://doi.org/10.1038/nrn3504
Paoletti, P., Neyton, J., 2007. NMDA receptor subunits: function and pharmacology.

Curr. Opin. Pharmacol. 7, 39–47. https://doi.org/10.1016/j.coph.2006.08.011
Papadopoulos, I.N., Farahi, S., Moser, C., Psaltis, D., 2012. Focusing and scanning light through a multimode optical fiber using digital phase conjugation. Opt. Express 20, 10583. https://doi.org/10.1364/oe.20.010583
Papouin, T., Ladépêche, L., Ruel, J., Sacchi, S., Labasque, M., Hanini, M., Groc, L., Pollegioni, L., Mothet, J.P., Oliet, S.H.R., 2012. Synaptic and extrasynaptic NMDA receptors are gated by different endogenous coagonists. Cell 150, 633–646. https://doi.org/10.1016/j.cell.2012.06.029
Park, M., 2018. AMPA receptor trafficking for postsynaptic potentiation. Front. Cell. Neurosci. 12, 1–10. https://doi.org/10.3389/fncel.2018.00361
Patterson, M., Yasuda, R., 2011. Signalling pathways underlying structural plasticity of dendritic spines. Br. J. Pharmacol. 163, 1626–1638. https://doi.org/10.1111/j.1476-5381.2011.01328.x
Paus, T., 2010. Sex differences in the human brain. A developmental perspective. Prog. Brain Res. 186, 13–28. https://doi.org/10.1016/B978-0-444-53630-3.00002-6
Pearson, R., Lewis, M.B., 2005. Fear recognition across the menstrual cycle. Horm. Behav. 47, 267–271. https://doi.org/10.1016/j.yhbeh.2004.11.003
Pelkey, K.A., Chittajallu, R., Craig, M.T., Tricoire, L., Wester, J.C., McBain, C.J., 2017. Hippocampal GABAergic inhibitory interneurons. Physiol. Rev. 97, 1619–1747. https://doi.org/10.1152/physrev.00007.2017
Penn, A.C., Zhang, C.L., Georges, F., Royer, L., Breillat, C., Hosy, E., Petersen, J.D., Humeau, Y., Choquet, D., 2017. Hippocampal LTP and contextual learning require surface diffusion of AMPA receptors. Nature 549, 384–388. https://doi.org/10.1038/nature23658
Peterka, D.S., Takahashi, H., Yuste, R., 2011. Imaging Voltage in Neurons. Neuron 69, 9–21. https://doi.org/10.1016/j.neuron.2010.12.010
Petrini, E.M., Lu, J., Cognet, L., Lounis, B., Ehlers, M.D., Choquet, D., 2009. Endocytic trafficking and recycling maintain a pool of mobile surface AMPA receptors required for synaptic potentiation. Neuron 63, 92–105. https://doi.org/10.1016/j.neuron.2009.05.025
Petrovska, S., Dejanova, B., Jurisic, V., 2012. Estrogens: Mechanisms of neuroprotective effects. J. Physiol. Biochem. 68, 455–460. https://doi.org/10.1007/s13105-012-0159-x
Pfeiffer, T., Poll, S., Bancelin, S., Angibaud, J., Inavalli, V.V.G.K., Keppler, K., Mittag, M., Fuhrmann, M., Nägerl, U.V., 2018. Chronic 2P-STED imaging reveals high turnover of dendritic spines in the hippocampus in vivo. Elife 7, 1–17. https://doi.org/10.7554/eLife.34700
Phan, A., Gabor, C.S., Favaro, K.J., Kaschack, S., Armstrong, J.N., MacLusky, N.J., Choleris, E., 2012. Low doses of 17β-estradiol rapidly improve learning and increase hippocampal dendritic spines. Neuropsychopharmacology 37, 2299–2309. https://doi.org/10.1038/npp.2012.82
Phan, A., Lancaster, K.E., Armstrong, J.N., MacLusky, N.J., Choleris, E., 2011. Rapid effects of estrogen receptor α and β selective agonists on learning and dendritic spines in female mice. Endocrinology 152, 1492–1502. https://doi.org/10.1210/en.2010-1273
Phan, A., Suschkov, S., Molinaro, L., Reynolds, K., Lymer, J.M., Bailey, C.D.C., Kow, L.M., Maclusky, N.J., Pfaff, D.W., Choleris, E., 2015. Rapid increases in immature synapses parallel estrogen-induced hippocampal learning enhancements. Proc. Natl. Acad. Sci. U. S. A. 112, 16018–16023. https://doi.org/10.1073/pnas.1522150112
Picot, M., Billard, J.M., Dombret, C., Albac, C., Karameh, N., Daumas, S., Hardin-Pouzet, H., Mhaouty-Kodja, S., 2016. Neural androgen receptor deletion impairs the temporal processing of objects and hippocampal CA1-dependent mechanisms. PLoS One 11, 1–16. https://doi.org/10.1371/journal.pone.0148328

Pikálek, T.P., Trägårdh, J., Simpson, S., Čižmár, T., 2019. Wavelength dependent characterization of a multimode fibre endoscope. Opt. Express 27, 28239–28253. https://doi.org/10.1364/OE.27.028239
Pinheiro, P.S., Mulle, C., 2008. Presynaptic glutamate receptors: physiological functions and mechanisms of action. Nat. Rev. Neurosci. 9, 423–436. https://doi.org/10.1038/nrn2379
Pittaluga, A., Raiteri, M., 1992. N-methyl-D-aspartic acid (NMDA) and non-NMDA receptors regulating hippocampal norepinephrine release. III. Changes in the NMDA receptor complex induced by their functional cooperation. J. Pharmacol. Exp. Ther. 263, 327–333.
Pittaluga, A., Raiteri, M., 1990. Release-enhancing glycine-dependent presynaptic NMDA receptors exist on noradrenergic terminals of hippocampus. Eur. J. Pharmacol. 191, 231–234. https://doi.org/10.1016/0014-2999(90)94153-o.
Poll, S., Fuhrmann, M., 2018. Long-Term In Vivo Imaging of Structural Plasticity in Rodents. Handb. Behav. Neurosci. 28, 253–262. https://doi.org/10.1016/B978-0-12-812028-6.00014-8
Pont, S., 1987. Thy-1: a lymphoid cell subset marker capable of delivering an activation signal to mouse T lymphocytes. Biochimie 69, 315–320. https://doi.org/10.1016/0300-9084(87)90022-8
Popoff, S.M., Lerosey, G., Carminati, R., Fink, M., Boccara, A.C., Gigan, S., 2010. Measuring the transmission matrix in optics: An approach to the study and control of light propagation in disordered media. Phys. Rev. Lett. 104, 1–4. https://doi.org/10.1103/PhysRevLett.104.100601
Popov, V.I., Davies, H.A., Rogachevsky, V. V., Patrushev, I. V., Errington, M.L., Gabbott, P.L.A., Bliss, T.V.P., Stewart, M.G., 2004. Remodelling of synaptic morphology but unchanged synaptic density during late phase long-term potentiation (LTP): A serial section electron micrograph study in the dentate gyrus in the anaesthetised rat. Neuroscience 128, 251–262. https://doi.org/10.1016/j.neuroscience.2004.06.029
Pozo, K., Goda, Y., 2010. Unraveling mechanisms of homeostatic synaptic plasticity. Neuron 66, 337–351. https://doi.org/10.1016/j.neuron.2010.04.028
Prasher, D.C., 1995. Using GFP to see the light. Trends Genet. 11, 320–323. https://doi.org/10.1016/S0168-9525(00)89090-3
Preston, A.R., Eichenbaum, H., 2013. Interplay of hippocampus and prefrontal cortex in memory. Curr. Biol. 23, R764–R773. https://doi.org/10.1016/j.cub.2013.05.041
Prius-Mengual, J., Pérez-Rodríguez, M., Andrade-Talavera, Y., Rodríguez-Moreno, A., 2019. NMDA Receptors Containing GluN2B/2C/2D Subunits Mediate an Increase in Glutamate Release at Hippocampal CA3–CA1 Synapses. Mol. Neurobiol. 56, 1694–1706. https://doi.org/10.1007/s12035-018-1187-5
Qiao, Q., Ma, L., Li, W., Tsai, J.W., Yang, G., Gan, W.B., 2016. Long-term stability of axonal boutons in the mouse barrel cortex. Dev. Neurobiol. 76, 252–261. https://doi.org/10.1002/dneu.22311
Qin, Z., Chen, C., He, S., Wang, Y., Tam, K.F., Ip, N.Y., Qu, J.Y., 2020. Adaptive optics two-photon endomicroscopy enables deep-brain imaging at synaptic resolution over large volumes. Sci. Adv. 6, 1–12. https://doi.org/10.1126/sciadv.abc6521
Ramón y Cajal, S., 1911. Histologie du système nerveux de l'homme & des vertébrés: Cervelet, cerveau moyen, rétine, couche optique, corps strié, écorce cérébrale générale & régionale, grand sympathique. A. Maloine 2. https://doi.org/10.5962/bhl.title.48637
Rao-Ruiz, P., Visser, E., Mitrić, M., Smit, A.B., van den Oever, M.C., 2021. A Synaptic Framework for the Persistence of Memory Engrams. Front. Synaptic Neurosci. 13, 1–15. https://doi.org/10.3389/fnsyn.2021.661476
Rapp, P.R., Morrison, J.H., Roberts, J.A., 2003. Cyclic estrogen replacement improves cognitive function in aged ovariectomized rhesus monkeys. J. Neurosci. 23, 5708–

5714. https://doi.org/10.1523/jneurosci.23-13-05708.2003
Rasse, T.M., Fouquet, W., Schmid, A., Kittel, R.J., Mertel, S., Sigrist, C.B., Schmidt, M., Guzman, A., Merino, C., Qin, G., Quentin, C., Madeo, F.F., Heckmann, M., Sigrist, S.J., 2005. Glutamate receptor dynamics organizing synapse formation in vivo. Nat. Neurosci. 8, 898–905. https://doi.org/10.1038/nn1484
Rauner, C., Köhr, G., 2011. Triheteromeric NR1/NR2A/NR2B receptors constitute the major N-methyl-D-aspartate receptor population in adult hippocampal synapses. J. Biol. Chem. 286, 7558–7566. https://doi.org/10.1074/jbc.M110.182600
Rebola, N., Srikumar, B.N., Mulle, C., 2010. Activity-dependent synaptic plasticity of NMDA receptors. J. Physiol. 588, 93–99. https://doi.org/10.1113/jphysiol.2009.179382
Redondo, R.L., Kim, J., Arons, A.L., Ramirez, S., Liu, X., Tonegawa, S., 2014. Bidirectional switch of the valence associated with a hippocampal contextual memory engram. Nature 513, 426–430. https://doi.org/10.1038/nature13725
Redondo, R.L., Morris, R.G.M., 2011. Making memories last: The synaptic tagging and capture hypothesis. Nat. Rev. Neurosci. 12, 17–30. https://doi.org/10.1038/nrn2963
Regehr, W.G., 2012. Short-term presynaptic plasticity. Cold Spring Harb. Perspect. Biol. 4, 1–19. https://doi.org/10.1101/cshperspect.a005702
Regehr, W.G., Abbott, L.F., 2004. Synaptic computation. Nature 431, 796–803. https://doi.org/10.1038/nature03010
Reiff, D.F., Thiel, P.R., Schuster, C.M., 2002. Differential regulation of active zone density during long-term strengthening of Drosophila neuromuscular junctions. J. Neurosci. 22, 9399–9409. https://doi.org/10.1523/jneurosci.22-21-09399.2002
Reijmers, L.G., Perkins, B.L., Matsuo, N., Mayford, M., 2007. Localization of a stable neural correlate of associative memory. Science 317, 1230–1233. https://doi.org/10.1126/science.1143839
Rekart, J.L., Holahan, M.R., Routtenberg, A., 2007. Presynaptic Structural Plasticity and Long-Lasting Memory: Focus on Learning-Induced Redistribution of Hippocampal Mossy Fibers, Neural Plasticity and Memory: From Genes to Brain Imaging. Boca Raton (FL): CRC Press/Taylor & Francis. https://doi.org/https://www.ncbi.nlm.nih.gov/books/NBK1848/
Resendez, S.L., Jennings, J.H., Ung, R.L., Namboodiri, V.M.K., Zhou, Z.C., Otis, J.M., Nomura, H., Mchenry, J.A., Kosyk, O., Stuber, G.D., 2016. Visualization of cortical, subcortical and deep brain neural circuit dynamics during naturalistic mammalian behavior with head-mounted microscopes and chronically implanted lenses. Nat. Protoc. 11, 566–597. https://doi.org/10.1038/nprot.2016.021
Richardson, M.P., Strange, B.A., Dolan, R.J., 2004. Encoding of emotional memories depends on amygdala and hippocampus and their interactions. Nat. Neurosci. 7, 278–285. https://doi.org/10.1038/nn1190
Rizzo, F.R., Musella, A., De Vito, F., Fresegna, D., Bullitta, S., Vanni, V., Guadalupi, L., Stampanoni Bassi, M., Buttari, F., Mandolesi, G., Centonze, D., Gentile, A., 2018. Tumor Necrosis Factor and Interleukin-1 β Modulate Synaptic Plasticity during Neuroinflammation. Neural Plast. 2018. https://doi.org/10.1155/2018/8430123
Rizzoli, S.O., Betz, W.J., 2005. Synaptic vesicle pools. Nat. Rev. Neurosci. 6, 57–69. https://doi.org/10.1038/nrn1583
Roberts, T.F., Tschida, K.A., Klein, M.E., Mooney, R., 2010. Rapid spine stabilization and synaptic enhancement at the onset of behavioural learning. Nature 463, 948–952. https://doi.org/10.1038/nature08759
Rodríguez-Moreno, A., Banerjee, A., Paulsen, O., 2010. Presynaptic NMDA receptors and spike timing-dependent depression at cortical synapses. Front. Synaptic Neurosci. 2, 1–6. https://doi.org/10.3389/fnsyn.2010.00018
Rodríguez-Moreno, A., González-Rueda, A., Banerjee, A., Upton, A.L., Craig, M.T., Paulsen, O., 2013. Presynaptic Self-Depression at Developing Neocortical Synapses. Neuron 77, 35–42. https://doi.org/10.1016/j.neuron.2012.10.035

Rodríguez-Moreno, A., Paulsen, O., 2008. Spike timing-dependent long-term depression requires presynaptic NMDA receptors. Nat. Neurosci. 11, 744–745. https://doi.org/10.1038/nn.2125
Rogerson, T., Cai, D.J., Frank, A., Sano, Y., Shobe, J., Lopez-Aranda, M.F., Silva, A.J., 2014. Synaptic tagging during memory allocation. Nat. Rev. Neurosci. 15, 157–169. https://doi.org/10.1038/nrn3667
Romani, S., Tsodyks, M., 2015. Short-term plasticity based network model of place cells dynamics. Hippocampus 25, 94–105. https://doi.org/10.1002/hipo.22355
Rosario, E.R., Chang, L., Head, E.H., Stanczyk, F.Z., Pike, C.J., 2011. Brain levels of sex steroid hormones in men and women during normal aging and in Alzheimer's disease. Neurobiol. Aging 32, 604–613. https://doi.org/10.1016/j.neurobiolaging.2009.04.008
Rossetti, M.F., Cambiasso, M.J., Holschbach, M.A., Cabrera, R., 2016. Oestrogens and Progestagens: Synthesis and Action in the Brain. J. Neuroendocrinol. 28, 1–11. https://doi.org/10.1111/jne.12402
Roth, R.H., Cudmore, R.H., Tan, H.L., Hong, I., Zhang, Y., Huganir, R.L., 2020. Cortical Synaptic AMPA Receptor Plasticity during Motor Learning. Neuron 105, 895-908.e5. https://doi.org/10.1016/j.neuron.2019.12.005
Rotman, Z., Deng, P.Y., Klyachko, V.A., 2011. Short-term plasticity optimizes synaptic information transmission. J. Neurosci. 31, 14800–14809. https://doi.org/10.1523/JNEUROSCI.3231-11.2011
Rowan, M.J.M., DelCanto, G., Yu, J.J., Kamasawa, N., Christie, J.M., 2016. Synapse-level determination of action potential duration by K+ channel clustering in axons Matthew. Neuron 91, 370–383. https://doi.org/10.1016/j.neuron.2016.05.035.Synapse-level
Rowan, M.J.M., Tranquil, E., Christie, J.M., 2014. Distinct Kv channel subtypes contribute to differences in spike signaling properties in the axon initial segment and presynaptic boutons of cerebellar interneurons. J. Neurosci. 34, 6611–6623. https://doi.org/10.1523/JNEUROSCI.4208-13.2014
Roy, D.S., Muralidhar, S., Smith, L.M., Tonegawa, S., 2017. Silent memory engrams as the basis for retrograde amnesia. Proc. Natl. Acad. Sci. U. S. A. 114, E9972–E9979. https://doi.org/10.1073/pnas.1714248114
Rune, G.M., Frotscher, M., 2005. Neurosteroid synthesis in the hippocampus: Role in synaptic plasticity. Neuroscience 136, 833–842. https://doi.org/10.1016/j.neuroscience.2005.03.056
Runge, K., Cardoso, C., de Chevigny, A., 2020. Dendritic Spine Plasticity: Function and Mechanisms. Front. Synaptic Neurosci. 12. https://doi.org/10.3389/fnsyn.2020.00036
Rupprecht, R., Di Michele, F., Hermann, B., Ströhle, A., Lancel, M., Romeo, E., Holsboer, F., 2001. Neuroactive steroids: Molecular mechanisms of action and implications for neuropsychopharmacology. Brain Res. Rev. 37, 59–67. https://doi.org/10.1016/S0165-0173(01)00123-0
Rupprecht, R., Holsboer, F., 1999. Neuroactive steroids: Mechanisms of action and neuropsychopharmacological perspectives. Trends Neurosci. 22, 410–416. https://doi.org/10.1016/S0166-2236(99)01399-5
Ryan, T.J., de San Luis, C.O., Pezzoli, M., Sen, S., 2021. Engram cell connectivity: an evolving substrate for information storage. Curr. Opin. Neurobiol. 67, 215–227. https://doi.org/10.1016/j.conb.2021.01.006
Ryan, T.J., Roy, D.S., Pignatelli, M., Arons, A., Tonegawa, S., 2015. Engram cells retain memory under retrograde amnesia. Science 348, 1007–1013. https://doi.org/10.1126/science.aaa5542
Sadakane, O., Masamizu, Y., Watakabe, A., Terada, S.I., Ohtsuka, M., Takaji, M., Mizukami, H., Ozawa, K., Kawasaki, H., Matsuzaki, M., Yamamori, T., 2015. Long-Term Two-Photon Calcium Imaging of Neuronal Populations with Subcellular Resolution in Adult Non-human Primates. Cell Rep. 13, 1989–1999.

https://doi.org/10.1016/j.celrep.2015.10.050
Sah, P., Faber, E.S.L., 2002. Channels underlying neuronal calcium-activated potassium currents. Prog. Neurobiol. 66, 345–353. https://doi.org/10.1016/s0301-0082(02)00004-7
Sajikumar, S., Frey, J.U., 2004. Late-associativity, synaptic tagging, and the role of dopamine during LTP and LTD. Neurobiol. Learn. Mem. 82, 12–25. https://doi.org/10.1016/j.nlm.2004.03.003
Sakimura, K., Kutsuwada, T., Ito, I., Manabe, T., Takayama, C., Kushiya, E., Yagi, T., Aizawa, S., Inoue, Y., Sugiyama, H., Mishina, M., 1995. Reduced hippocampal LTP and spatial learning in mice lacking cholamines from isolated nerve terminals. Nature 373, 151–155.
Sakmann, B., Neher, E., 1984. Patch clamp techniques for studying ionic channels in excitable membranes. Annu. Rev. Physiol. 46, 455–472. https://doi.org/10.1146/annurev.ph.46.030184.002323
Sammons, R.P., Clopath, C., Barnes, S.J., 2018. Size-Dependent Axonal Bouton Dynamics following Visual Deprivation In Vivo. Cell Rep. 22, 576–584. https://doi.org/10.1016/j.celrep.2017.12.065
Sánchez-Andrade, G., Kendrick, K.M., 2011. Roles of α- and β-estrogen receptors in mouse social recognition memory: Effects of gender and the estrous cycle. Horm. Behav. 59, 114–122. https://doi.org/10.1016/j.yhbeh.2010.10.016
Sandstrom, N.J., Williams, C.L., 2001. Memory retention is modulated by acute estradiol and progesterone replacement. Behav. Neurosci. 115, 384–393. https://doi.org/10.1037//0735-7044.115.2.384
Santos, S.D., Carvalho, A.L., Caldeira, M. V., Duarte, C.B., 2009. Regulation of AMPA receptors and synaptic plasticity. Neuroscience 158, 105–125. https://doi.org/10.1016/j.neuroscience.2008.02.037
Sanz-Clemente, A., Matta, J.A., Isaac, J.T.R., Roche, K.W., 2010. Casein Kinase 2 Regulates the NR2 Subunit Composition of Synaptic NMDA Receptors. Neuron 67, 984–996. https://doi.org/10.1016/j.neuron.2010.08.011
Sanz-Clemente, A., Nicoll, R.A., Roche, K.W., 2013. Diversity in NMDA receptor composition: many regulators, many consequences. Neuroscientist 19, 62–75. https://doi.org/10.1177/1073858411435129
Sarkar, S.N., Smith, L.T., Logan, S.M., Simpkins, J.W., 2010. Estrogen-induced activation of extracellular signal-regulated kinase signaling triggers dendritic resident mRNA translation. Neuroscience 170, 1080–1085. https://doi.org/10.1016/j.neuroscience.2010.07.035
Sattler, R., Tymianski, M., 2001. Molecular mechanisms of glutamate receptor-mediated excitotoxic neuronal cell death. Mol. Neurobiol. 24, 107–129. https://doi.org/10.1385/MN:24:1-3:107
Saucier, D., Cain, D.P., 1995. Spatial learning without NMDA receptor-dependent long-term potentiation. Nature 378, 186–189. https://doi.org/10.1038/378186a0
Scanziani, M., Gähwiler, B.H., Charpak, S., 1998. Target cell-specific modulation of transmitter release at terminals from a single axon 95, 12004–12009. https://doi.org/10.1073/pnas.95.20.12004
Scanziani, M., Häusser, M., 2009. Electrophysiology in the age of light. Nature 461, 930–939. https://doi.org/10.1038/nature08540
Scharfman, H.E., 2016. The enigmatic mossy cell of the dentate gyrus. Nat. Rev. Neurosci. 17, 562–575. https://doi.org/10.1038/nrn.2016.87
Scharfman, H.E., MacLusky, N.J., 2006. Estrogen and brain-derived neurotrophic factor (BDNF) in hippocampus: Complexity of steroid hormone-growth factor interactions in the adult CNS. Front. Neuroendocrinol. 27, 415–435. https://doi.org/10.1016/j.yfrne.2006.09.004
Scharfman, H.E., MacLusky, N.J., 2005. Similarities between actions of estrogen and BDNF in the hippocampus: Coincidence or clue? Trends Neurosci. 28, 79–85. https://doi.org/10.1016/j.tins.2004.12.005

Schinder, A.F., Berninger, B., Poo, M. ming, 2000. Postsynaptic target specificity of neurotrophin-induced presynaptic potentiation. Neuron 25, 151–163. https://doi.org/10.1016/S0896-6273(00)80879-X
Schmidt, P.J., Nieman, L., Danaceau, M.A., Tobin, M.B., Roca, C.A., Murphy, J.H., Rubinow, D.R., 2000. Estrogen replacement in perimenopause-related depression: A preliminary report. Am. J. Obstet. Gynecol. 183, 414–420. https://doi.org/10.1067/mob.2000.106004
Schneggenburger, R., Neher, E., 2000. Intracellular calcium dependence of transmitter release rates at a fast central synapse. Nature 406, 889–893. https://doi.org/10.1038/35022702
Schneggenburger, R., Sakaba, T., Neher, E., 2002. Vesicle pools and short-term synaptic depression: Lessons from a large synapse. Trends Neurosci. 25, 206–212. https://doi.org/10.1016/S0166-2236(02)02139-2
Schneider, H., Pitossi, F., Balschun, D., Wagner, A., Del Rey, A., Besedovsky, H.O., 1998. A neuromodulatory role of interleukin-1β in the hippocampus. Proc. Natl. Acad. Sci. U. S. A. 95, 7778–7783. https://doi.org/10.1073/pnas.95.13.7778
Shah, M.M., Haylett, D.G., 2002. K+ Currents Generated by NMDA Receptor Activation in Rat Hippocampal Pyramidal Neurons. J. Neurophysiol. 87, 2983–2989. https://doi.org/10.1152/jn.00802.2001
Shanmugan, S., Epperson, C.N., 2014. Estrogen and the prefrontal cortex: Towards a new understanding of estrogen's effects on executive functions in the menopause transition. Hum. Brain Mapp. 35, 847–865. https://doi.org/10.1002/hbm.22218
Shansky, R.M., Hamo, C., Hof, P.R., Lou, W., McEwen, B.S., Morrison, J.H., 2010. Estrogen promotes stress sensitivity in a prefrontal cortex-amygdala pathway. Cereb. Cortex 20, 2560–2567. https://doi.org/10.1093/cercor/bhq003
Shen, Y., Specht, S.M., Ioline, D.S.G., Li, R., 1994. The hippocampus: A biological model for studying learning and memory. Prog. Neurobiol. 44, 485–496. https://doi.org/10.1016/0301-0082(94)90008-6
Sheppard, P.A.S., Choleris, E., Galea, L.A.M., 2019. Structural plasticity of the hippocampus in response to estrogens in female rodents. Mol. Brain 12, 28–30. https://doi.org/10.1186/s13041-019-0442-7
Sherwin, B.B., 2007. The clinical relevance of the relationship between estrogen and cognition in women. J. Steroid Biochem. Mol. Biol. 106, 151–156. https://doi.org/10.1016/j.jsbmb.2007.05.016
Shetty, M.S., Sharma, M., Hui, N.S., Dasgupta, A., Gopinadhan, S., Sajikumar, S., 2015. Investigation of synaptic tagging/capture and cross-capture using acute hippocampal slices from rodents. J. Vis. Exp. 2015, 1–9. https://doi.org/10.3791/53008
Shi, S.H., Hayashi, Y., Petralia, R.S., Zaman, S.H., Wenthold, R.J., Svoboda, K., Malinow, R., 1999. Rapid spine delivery and redistribution of AMPA receptors after synaptic NMDA receptor activation. Science 284, 1811–1816. https://doi.org/10.1126/science.284.5421.1811
Shigemoto, R., Kinoshita, A., Wada, E., Nomura, S., Ohishi, H., Takada, M., Flor, P.J., Neki, A., Abe, T., Nakanishi, S., Mizuno, N., 1997. Differential presynaptic localization of metabotropic glutamate receptor subtypes in the rat hippocampus. J. Neurosci. 17, 7503–7522. https://doi.org/10.1523/jneurosci.17-19-07503.1997
Shipton, O., Paulsen, O., 2014. NMDA receptors in hippocampal plasticity. Philos. Trans. R. Soc. 369, 1–17. https://doi.org/10.1098/rstb.2013.0163
Shires, K.L., Da Silva, B.M., Hawthorne, J.P., Morris, R.G.M., Martin, S.J., 2012. Synaptic tagging and capture in the living rat. Nat. Commun. 3, 1–11. https://doi.org/10.1038/ncomms2250
Shors, T.J., Matzel, L.D., 1997. Long-term potentiation: What's learning got to do with it? Behav. Brain Sci. 20, 597–655. https://doi.org/10.1017/s0140525x97001593
Siegel, S.J., Brose, N., Janssen, W.G., Gasic, G.P., Jahn, R., Heinemann, S.F., Morrison, J.H., 1994. Regional, cellular, and ultrastructural distribution of N-

methyl-D- aspartate receptor subunit 1 in monkey hippocampus. Proc. Natl. Acad. Sci. U. S. A. 91, 564–568. https://doi.org/10.1073/pnas.91.2.564
Silva, A.J., Stevens, C.F., Tonegawa, S., Wang, Y., 1992. Deficient hippocampal long-term potentiation in α-calcium-calmodulin kinase II mutant mice. Science 257, 201–206. https://doi.org/10.1126/science.1378648
Sinefeld, D., Paudel, H.P., Ouzounov, D.G., Bifano, T.G., Xu, C., 2015. Adaptive optics in multiphoton microscopy: comparison of two, three and four photon fluorescence. Opt. Express 23, 31472. https://doi.org/10.1364/oe.23.031472
Sivankutty, S., Andresen, E.R., Cossart, R., Bouwmans, G., Monneret, S., Rigneault, H., 2016. Ultra-thin rigid endoscope: two-photon imaging through a graded-index multi-mode fiber. Opt. Express 24, 825. https://doi.org/10.1364/oe.24.000825
Sjöström, P.J., Turrigiano, G.G., Nelson, S.B., 2003. Neocortical LTD via Coincident Activation of Presynaptic NMDA and Cannabinoid Receptors. Neuron 39, 641–654. https://doi.org/10.1016/s0896-6273(03)00476-8
Smith, C.C., McMahon, L.L., 2006. Estradiol-induced increase in the magnitude of long-term potentiation is prevented by blocking NR2B-containing receptors. J. Neurosci. 26, 8517–8522. https://doi.org/10.1523/JNEUROSCI.5279-05.2006
Soares, C., Lee, K.F.H., Nassrallah, W., Béïque, J.C., 2013. Differential subcellular targeting of glutamate receptor subtypes during homeostatic synaptic plasticity. J. Neurosci. 33, 13547–13559. https://doi.org/10.1523/JNEUROSCI.1873-13.2013
Sorrells, S.F., Caso, J.R., Munhoz, C.D., Sapolsky, R.M., 2009. The Stressed CNS: When Glucocorticoids Aggravate Inflammation. Neuron 64, 33–39. https://doi.org/10.1016/j.neuron.2009.09.032.The
Speed, H.E., Dobrunz, L.E., 2009. Developmental changes in short-term facilitation are opposite at temporoammonic synapses compared to schaffer collateral synapses onto CA1 pyramidal cells. Hippocampus 19, 187–204. https://doi.org/10.1002/hipo.20496
Spence, R.D., Voskuhl, R.R., 2012. Neuroprotective effects of estrogens and androgens in CNS inflammation and neurodegeneration. Front. Neuroendocrinol. 33, 105–115. https://doi.org/10.1016/j.yfrne.2011.12.001
Spiteri, T., Ågmo, A., 2009. Ovarian hormones modulate social recognition in female rats. Physiol. Behav. 98, 247–250. https://doi.org/10.1016/j.physbeh.2009.05.001
Srivastava, D.P., Woolfrey, K., Jones, K.A., Shum, C.Y., Lash, L.L., Swanson, G.T., Penzes, P., 2008. Rapid enhancement of two-step wiring plasticity by estrogen and NMDA receptor activity. Proc. Natl. Acad. Sci. U. S. A. 105, 14650–14655. https://doi.org/10.1073/pnas.0810024105
Stefaniuk, M., Gualda, E.J., Pawlowska, M., Legutko, D., Matryba, P., Koza, P., Konopka, W., Owczarek, D., Wawrzyniak, M., Loza-Alvarez, P., Kaczmarek, L., 2016. Light-sheet microscopy imaging of a whole cleared rat brain with Thy1-GFP transgene. Sci. Rep. 6, 1–9. https://doi.org/10.1038/srep28209
Steffens, H., Mott, A.C., Li, S., Wegner, W., Švehla, P., Kan, V.W.Y., Wolf, F., Liebscher, S., Willig, K.I., 2021. Stable but not rigid: Chronic in vivo STED nanoscopy reveals extensive remodeling of spines, indicating multiple drivers of plasticity. Sci. Adv. 7, 1–13. https://doi.org/10.1126/sciadv.abf2806
Stelzer, E.H.K., Hell, S., Lindek, S., Stricker, R., Pick, R., Storz, C., Ritter, G., Salmon, N., 1994. Nonlinear absorption extends confocal fluorescence microscopy into the ultra-violet regime and confines the illumination volume. Opt. Commun. 104, 223–228. https://doi.org/10.1016/0030-4018(94)90546-0
Stevens, C.F., 1998. A million dollar question: Does LTP = Memory? Neuron 20, 1–2. https://doi.org/10.1016/S0896-6273(00)80426-2
Stevens, C.F., Wang, Y., 1995. Facilitation and Depression at Single Central Synapses. Neuron 14, 795–802. https://doi.org/10.1016/0896-6273(95)90223-6
Stewart, M.G., Medvedev, N.I., Popov, V.I., Schoepfer, R., Davies, H.A., Murphy, K., Dallérac, G.M., Kraev, I. V., Rodríguez, J.J., 2005. Chemically induced long-term potentiation increases the number of perforated and complex postsynaptic

densities but does not alter dendritic spine volume in CA1 of adult mouse hippocampal slices. Eur. J. Neurosci. 21, 3368–3378. https://doi.org/10.1111/j.1460-9568.2005.04174.x
Stoppini, L., Buchs, P.A., Muller, D., 1991. A simple method for organotypic cultures of nervous tissue. J. Neurosci. Methods 37, 173–182. https://doi.org/10.1016/0165-0270(91)90128-M
Streich, L., Boffi, J.C., Wang, L., Alhalaseh, K., Barbieri, M., Rehm, R., Deivasigamani, S., Gross, C.T., Agarwal, A., Prevedel, R., 2021. High-resolution structural and functional deep brain imaging using adaptive optics three-photon microscopy. Nat. Methods 18, 1253–1258. https://doi.org/10.1038/s41592-021-01257-6
Stroebel, D., Casado, M., Paoletti, P., 2018. Triheteromeric NMDA receptors: from structure to synaptic physiology. Curr. Opin. Physiol. 2, 1–12. https://doi.org/10.1016/j.cophys.2017.12.004
Südhof, T.C., 2013. Neurotransmitter Release: The Last Millisecond in the Life of a Synaptic Vesicle. Neuron 80. https://doi.org/10.1016/j.neuron.2013.10.022
Sun, H.Y., Dobrunz, L.E., 2006. Presynaptic Kainate Receptor Activation Is a Novel Mechanism for Target Cell-Specific Short-Term Facilitation at Schaffer Collateral Synapses. J. Neurosci. 26, 10796–10807. https://doi.org/10.1523/JNEUROSCI.2746-06.2006
Sun, Y., Smirnov, M., Kamasawa, N., Yasuda, R., 2021. Rapid ultrastructural changes in the PSD and surrounding membrane after induction of structural LTP in single dendritic spines. J. Neurosci. 41, 7003–7014. https://doi.org/10.1523/JNEUROSCI.1964-20.2021
Sutton, M.A., Schuman, E.M., 2006. Dendritic Protein Synthesis, Synaptic Plasticity, and Memory. Cell 127, 49–58. https://doi.org/10.1016/j.cell.2006.09.014
Suzuki, S.S., Smith, G.K., 1985. Burst characteristics of hippocampal complex spike cells in the awake rat. Exp. Neurol. 89, 90–95. https://doi.org/10.1016/0014-4886(85)90267-5
Svoboda, K., Denk, W., Kleinfeld, D., Tank, D.W., 1997. In vivo dendritic calcium dynamics in neocortical pyramidal neurons. Nature 385, 161–165. https://doi.org/10.1038/385161a0
Szabo, V., Ventalon, C., Sars, V. De, Bradley, J., Emiliani, V., 2014. NeuroResource Spatially Selective Holographic Photoactivation and Functional Fluorescence Imaging in Freely Behaving Mice with a Fiberscope. Neuron 84, 1157–1169. https://doi.org/10.1016/j.neuron.2014.11.005
Takeuchi, T., Duszkiewicz, A.J., Morris, R.G.M., 2014. The synaptic plasticity and memory hypothesis: Encoding, storage and persistence. Philos. Trans. R. Soc. B Biol. Sci. 369. https://doi.org/10.1098/rstb.2013.0288
Tanaka, J., Horiike, Y., Matsuzaki, M., Miyazaki, T., Ellis-Davies, G.C.R., Kasai, H., 2008. Protein synthesis and neurotrophin-dependent structural plasticity of single dendritic spines. Science 319, 1683–1688. https://doi.org/10.1126/science.1152864
Tanaka, K.Z., He, H., Tomar, A., Niisato, K., Huang, A.J.Y., McHugh, T.J., 2018. The hippocampal engram maps experience but not place. Science 361, 392–397. https://doi.org/10.1126/science.aat5397
Tang, A.C., Nakazawa, M., Romeo, R.D., Reeb, B.C., Sisti, H., McEwen, B.S., 2005. Effects of long-term estrogen replacement on social investigation and social memory in ovariectomized C57BL/6 mice. Horm. Behav. 47, 350–357. https://doi.org/10.1016/j.yhbeh.2004.10.010
Tang, J., Dani, J.A., 2009. Dopamine Enables In Vivo Synaptic Plasticity Associated with the Addictive Drug Nicotine. Neuron 63, 673–682. https://doi.org/10.1016/j.neuron.2009.07.025
Tang, Y., Janssen, W.G.M., Hao, J., Roberts, J.A., McKay, H., Lasley, B., Allen, P.B., Greengard, P., Rapp, P.R., Kordower, J.H., Hof, P.R., Morrisonn, J.H., 2004. Estrogen Replacement Increases Spinophilin-immunoreactive Spine Number in

the Prefrontal Cortex of Female Rhesus Monkeys. Cereb. Cortex 14, 215–223. https://doi.org/10.1093/cercor/bhg121
Tang, Y.P., Shimizu, E., Dube, G.R., Rampon, C., Kerchner, G.A., Zhuo, M., Liu, G., Tsien, J.Z., 1999. Genetic enhancement of learning and memory in mice. Nature 401, 63–69. https://doi.org/10.1038/43432
Tardin, C., Cognet, L., Bats, C., Lounis, B., Choquet, D., 2003. Direct imaging of lateral movements of AMPA receptors inside synapses. EMBO J. 22, 4656–4665. https://doi.org/10.1093/emboj/cdg463
Taxier, L.R., Gross, K.S., Frick, K.M., 2020. Oestradiol as a neuromodulator of learning and memory. Nat. Rev. Neurosci. 21, 535–550. https://doi.org/10.1038/s41583-020-0362-7
Theer, P., Denk, W., 2006. On the fundamental imaging-depth limit in two-photon microscopy. J. Opt. Soc. Am. A 23, 3139. https://doi.org/10.1364/josaa.23.003139
Thériault, G., Cottet, M., Castonguay, A., McCarthy, N., De Koninck, Y., 2014. Extended two-photon microscopy in live samples with Bessel beams: Steadier focus, faster volume scans, and simpler stereoscopic imaging. Front. Cell. Neurosci. 8, 1–11. https://doi.org/10.3389/fncel.2014.00139
Thierry, A.M., Gioanni, Y., Dégénétais, E., Glowinski, J., 2000. Hippocampo-prefrontal cortex pathway: Anatomical and electrophysiological characteristics. Hippocampus 10, 411–419. https://doi.org/10.1002/1098-1063(2000)10:4<411::AID-HIPO7>3.0.CO;2-A
Thomas, C.G., Miller, A.J., Westbrook, G.L., 2006. Synaptic and extrasynaptic NMDA receptor NR2 subunits in cultured hippocampal neurons. J. Neurophysiol. 95, 1727–1734. https://doi.org/10.1152/jn.00771.2005
Thomson, A.M., 2000. Molecular frequency filters at central synapses. Prog. Neurobiol. 62, 159–196. https://doi.org/10.1016/S0301-0082(00)00008-3
Tonegawa, S., Liu, X., Ramirez, S., Redondo, R., 2015a. Memory Engram Cells Have Come of Age. Neuron 87, 918–931. https://doi.org/10.1016/j.neuron.2015.08.002
Tonegawa, S., Morrissey, M.D., Kitamura, T., 2018. The role of engram cells in the systems consolidation of memory. Nat. Rev. Neurosci. 19, 485–498. https://doi.org/10.1038/s41583-018-0031-2
Tonegawa, S., Pignatelli, M., Roy, D.S., Ryan, T.J., 2015b. Memory engram storage and retrieval. Curr. Opin. Neurobiol. 35, 101–109. https://doi.org/10.1016/j.conb.2015.07.009
Tong, R., Chater, T.E., Emptage, N.J., Goda, Y., 2021. Heterosynaptic cross-talk of pre- and postsynaptic strengths along segments of dendrites. Cell Rep. 34, 108693. https://doi.org/10.1016/j.celrep.2021.108693
Tong, R., Emptage, N.J., Padamsey, Z., 2020. A two-compartment model of synaptic computation and plasticity. Mol. Brain 13, 1–10. https://doi.org/10.1186/s13041-020-00617-1
Tønnesen, J., Katona, G., Rózsa, B., Nägerl, U.V., 2014. Spine neck plasticity regulates compartmentalization of synapses. Nat. Neurosci. 17, 678–685. https://doi.org/10.1038/nn.3682
Tønnesen, J., Nadrigny, F., Willig, K.I., Wedlich-Söldner, R., Nägerl, U.V., 2011. Two-color STED microscopy of living synapses using a single laser-beam pair. Biophys. J. 101, 2545–2552. https://doi.org/10.1016/j.bpj.2011.10.011
Trachtenberg, J.T., Chen, B.E., Knott, G.W., Feng, G., Sanes, J.R., Welker, E., Svoboda, K., 2002. Long-term in vivo imaging of experience-dependent synaptic plasticity in adult cortex. Nature 420, 788–794. https://doi.org/10.1038/nature01273
Travis, Z.D., Sherchan, P., Hayes, W.K., Zhang, J.H., 2019. Surgically-induced brain injury: Where are we now? Chinese Neurosurg. J. 5, 1–11. https://doi.org/10.1186/s41016-019-0181-8
Tropea, D., Majewska, A.K., Garcia, R., Sur, M., 2010. Structural dynamics of synapses in vivo correlate with functional changes during experience-dependent

plasticity in visual cortex. J. Neurosci. 30, 11086–11095. https://doi.org/10.1523/JNEUROSCI.1661-10.2010
Tsien, R.Y., 1989. Fluorescent probes of cell signaling. Annu. Rev. Neurosci. 12, 227–253. https://doi.org/10.1146/annurev.ne.12.030189.001303
Tsodyks, M., Pawelzik, K., Markram, H., 1998. Neural Networks with Dynamic Synapses. Neural Comput. 10, 821–835. https://doi.org/10.1162/089976698300017502
Tsodyks, M. V., Markram, H., 1997. The neural code between neocortical pyramidal neurons depends on neurotransmitter release probability. Proc. Natl. Acad. Sci. U. S. A. 94, 719–723. https://doi.org/10.1073/pnas.94.2.719
Tsurugizawa, T., Mukai, H., Tanabe, N., Murakami, G., Hojo, Y., Kominami, S., Mitsuhashi, K., Komatsuzaki, Y., Morrison, J.H., Janssen, W.G.M., Kimoto, T., Kawato, S., 2005. Estrogen induces rapid decrease in dendritic thorns of CA3 pyramidal neurons in adult male rat hippocampus. Biochem. Biophys. Res. Commun. 337, 1345–1352. https://doi.org/10.1016/j.bbrc.2005.09.188
Tuchin, V. V., 2015. Tissue Optics and Photonics: Light-Tissue Interaction. J. Biomed. Photonics Eng. 1, 3–21. https://doi.org/10.18287/jbpe-2015-1-1-3
Tuchin, V. V., 1997. Light scattering study of tissues. Physics-Uspekhi 40, 495–515. https://doi.org/10.3367/ufnr.0167.199705c.0517
Turcotte, R., Liang, Y., Ji, N., 2017. Adaptive optical versus spherical aberration corrections for in vivo brain imaging. Biomed. Opt. Express 8, 3891. https://doi.org/10.1364/boe.8.003891
Turcotte, R., Schmidt, C.C., Booth, M.J., Emptage, N.J., 2020a. Volumetric Two-photon fluorescence imaging of live neurons using a multimode optical fiber. Opt. Lett. 45, 3–6. https://doi.org/10.1101/2020.04.27.063388
Turcotte, R., Schmidt, C.C., Emptage, N.J., Booth, M.J., 2019. Focusing light in biological tissue through a multimode optical fiber: refractive index matching. Opt. Lett. 44, 2386. https://doi.org/10.1364/ol.44.002386
Turcotte, R., Sutu, E., Schmidt, C.C., Emptage, N.J., Booth, M.J., 2020b. Deconvolution for multimode fiber imaging: modeling of spatially variant PSF. Biomed. Opt. Express 11, 4759. https://doi.org/10.1364/boe.399983
Turrigiano, G., 2012. Homeostatic Synaptic Plasticity : Local and Global Mechanisms for Stabilizing Neuronal Function. Cold Spring Harb. Perspect. Biol. 4, 1–18. https://doi.org/10.1101/cshperspect.a005736
Turrigiano, G.G., 2008. The Self-Tuning Neuron: Synaptic Scaling of Excitatory Synapses. Cell 135, 422–435. https://doi.org/10.1016/j.cell.2008.10.008
Turrigiano, G.G., Leslie, K.R., Desai, N.S., Rutherford, L.C., Nelson, S.B., 1998. Activity-dependent scaling of quantal amplitude in neocortical neurons. Nature 391, 892–896. https://doi.org/10.1038/36103
Turrigiano, G.G., Nelson, S.B., 2004. Homeostatic plasticity in the developing nervous system. Nat. Rev. Neurosci. 5, 97–107. https://doi.org/10.1038/nrn1327
Turtaev, S., Leite, I.T., Altwegg-Boussac, T., Pakan, J.M.P., Rochefort, N.L., Čižmár, T., 2018. High-fidelity multimode fibre-based endoscopy for deep brain in vivo imaging. Light Sci. Appl. 7. https://doi.org/10.1038/s41377-018-0094-x
Turtaev, S., Leite, I.T., Čižmár, T., 2015. Multimode fibres for micro-endoscopy. Optofluidics, Microfluid. Nanofluidics 2, 31–35. https://doi.org/10.1515/optof-2015-0004
Turtaev, S., Leite, I.T., Mitchell, K.J., Padgett, M.J., Phillips, D.B., Čižmár, T., 2017. Comparison of nematic liquid-crystal and DMD based spatial light modulation in complex photonics. Opt. Express 25, 29874. https://doi.org/10.1364/oe.25.029874
Tuscher, J.J., Luine, V., Frankfurt, M., Frick, K.M., 2016. Estradiol-mediated spine changes in the dorsal hippocampus and medial prefrontal cortex of ovariectomized female mice depend on ERK and mTOR activation in the dorsal hippocampus. J. Neurosci. 36, 1483–1489. https://doi.org/10.1523/JNEUROSCI.3135-15.2016

Uddin, M.S., Rahman, M.M., Jakaria, M., Rahman, M.S., Hossain, M.S., Islam, A., Ahmed, M., Mathew, B., Omar, U.M., Barreto, G.E., Ashraf, G.M., 2020. Estrogen Signaling in Alzheimer's Disease: Molecular Insights and Therapeutic Targets for Alzheimer's Dementia. Mol. Neurobiol. 57, 2654–2670. https://doi.org/10.1007/s12035-020-01911-8

Ultanir, S.K., Kim, J.E., Hall, B.J., Deerinck, T., Ellisman, M., Ghosh, A., 2007. Regulation of spine morphology and spine density by NMDA receptor signaling in vivo. Proc. Natl. Acad. Sci. U. S. A. 104, 19553–19558. https://doi.org/10.1073/pnas.0704031104

Van Den Brandt, J., Wang, D., Kwon, S.H., Heinkelein, M., Reichardt, H.M., 2004. Lentivirally generated eGFP-transgenic rats allow efficient cell tracking in vivo. Genesis 39, 94–99. https://doi.org/10.1002/gene.20037

Van Hartesveldt, C., Joyce, J.N., 1986. Effects of estrogen on the basal ganglia. Neurosci. Biobehav. Rev. 10, 1–14. https://doi.org/10.1016/0149-7634(86)90029-1

van Spronsen, M., Hoogenraad, C.C., 2010. Synapse pathology in psychiatric and neurologic disease. Curr. Neurol. Neurosci. Rep. 10, 207–214. https://doi.org/10.1007/s11910-010-0104-8

van Strien, N.M., Cappaert, N.L.M., Witter, M.P., 2009. The anatomy of memory: An interactive overview of the parahippocampal- hippocampal network. Nat. Rev. Neurosci. 10, 272–282. https://doi.org/10.1038/nrn2614

Vandael, D., Okamoto, Y., Borges-Merjane, C., Vargas-Barroso, V., Suter, B.A., Jonas, P., 2021. Subcellular patch-clamp techniques for single-bouton stimulation and simultaneous pre- and postsynaptic recording at cortical synapses. Nat. Protoc. 16, 2947–2967. https://doi.org/10.1038/s41596-021-00526-0

Varela, J.A., Sen, K., Gibson, J., Fost, J., Abbott, L.F., Nelson, S.B., 1997. A quantitative description of short-term plasticity at excitatory synapses in layer 2/3 of rat primary visual cortex. J. Neurosci. 17, 7926–7940. https://doi.org/10.1523/jneurosci.17-20-07926.1997

Vasquez-Lopez, S.A., Turcotte, R., Koren, V., Plöschner, M., Padamsey, Z., Booth, M.J., Čižmár, T., Emptage, N.J., 2018. Subcellular spatial resolution achieved for deep-brain imaging in vivo using a minimally invasive multimode fiber. Light Sci. Appl. 7. https://doi.org/10.1038/s41377-018-0111-0

Vazdarjanova, A., McGaugh, J.L., 1999. Basolateral amygdala is involved in modulating consolidation of memory for classical fear conditioning. J. Neurosci. 19, 6615–6622. https://doi.org/10.1523/jneurosci.19-15-06615.1999

Vetere, G., Tran, L.M., Moberg, S., Steadman, P.E., Restivo, L., Morrison, F.G., Ressler, K.J., Josselyn, S.A., Frankland, P.W., 2019. Memory formation in the absence of experience. Nat. Neurosci. 22, 933–940. https://doi.org/10.1038/s41593-019-0389-0

Vicini, S., Wang, J.F., Li, J.H., Zhu, W.J., Wang, Y.H., Luo, J.H., Wolfe, B.B., Grayson, D.R., 1998. Functional and pharmacological differences between recombinant N-methyl-D-aspartate receptors. J. Neurophysiol. 79, 555–566. https://doi.org/10.1152/jn.1998.79.2.555

Vierk, R., Bayer, J., Freitag, S., Muhia, M., Kutsche, K., Wolbers, T., Kneussel, M., Sommer, T., Rune, G.M., 2015. Structure-function-behavior relationship in estrogen-induced synaptic plasticity. Horm. Behav. 74, 139–148. https://doi.org/10.1016/j.yhbeh.2015.05.008

Vincent, P., Maskos, U., Charvet, I., Bourgeais, L., Stoppini, L., Leresche, N., Changeux, J.P., Lambert, R., Meda, P., Paupardin-Tritsch, D., 2006. Live imaging of neural structure and function by fibred fluorescence microscopy. EMBO Rep. 7, 1154–1161. https://doi.org/10.1038/sj.embor.7400801

Wallace, M., Luine, V., Arellanos, A., Frankfurt, M., 2006. Ovariectomized rats show decreased recognition memory and spine density in the hippocampus and prefrontal cortex. Brain Res. 1126, 176–182.

https://doi.org/10.1016/j.brainres.2006.07.064
Wang, H., Wagner, J.J., 1999. Priming-induced shift in synaptic plasticity in the rat hippocampus. J. Neurophysiol. 82, 2024–2028. https://doi.org/10.1152/jn.1999.82.4.2024
Wang, S., Zhu, J., Xu, T., 2018. 17β-estradiol (E2) promotes growth and stability of new dendritic spines via estrogen receptor β pathway in intact mouse cortex. Brain Res. Bull. 137, 241–248. https://doi.org/10.1016/j.brainresbull.2017.12.011
Wang, T., Xu, C., 2020. Three-photon neuronal imaging in deep mouse brain. Optica 7, 947. https://doi.org/10.1364/optica.395825
Ward, B., McGuinness, L., Akerman, C.J.J., Fine, A., Bliss, T.V.P., Emptage, N.J., 2006. State-Dependent Mechanisms of LTP Expression Revealed by Optical Quantal Analysis. Neuron 52, 649–661. https://doi.org/10.1016/j.neuron.2006.10.007
Warren, S.G., Humphreys, A.G., Juraska, J.M., Greenough, W.T., 1995. LTP varies across the estrous cycle: enhanced synaptic plasticity in proestrus rats. Brain Res. 703, 26–30. https://doi.org/10.1016/0006-8993(95)01059-9
Watkins, J.C., Evans, R.H., 1981. Excitatory amino acid transmitters. Annu. Rev. Pharmacol. Toxicol. 21, 165–204. https://doi.org/10.1146/annurev.pa.21.040181.001121
Watkins, J.C., Jane, D.E., 2006. The glutamate story. Br. J. Pharmacol. 147, 100–108. https://doi.org/10.1038/sj.bjp.0706444
Wegerer, M., Kerschbaum, H., Blechert, J., Wilhelm, F.H., 2014. Low levels of estradiol are associated with elevated conditioned responding during fear extinction and with intrusive memories in daily life. Neurobiol. Learn. Mem. 116, 145–154. https://doi.org/10.1016/j.nlm.2014.10.001
Wegner, W., Mott, A.C., Grant, S.G.N., Steffens, H., Willig, K.I., 2018. In vivo STED microscopy visualizes PSD95 sub-structures and morphological changes over several hours in the mouse visual cortex. Sci. Rep. 8, 1–11. https://doi.org/10.1038/s41598-017-18640-z
Wen, Z., Wang, L., Zhang, X., Ma, Y., Liu, X., Kaminski, C.F., Yang, Q., 2020. Fast volumetric fluorescence imaging with multimode fibers. Opt. Lett. 45, 4931. https://doi.org/10.1364/ol.398177
Wiegert, J.S., Oertner, T.G., 2013. Long-Term depression triggers the selective elimination of weakly integrated synapses. Proc. Natl. Acad. Sci. U. S. A. 110. https://doi.org/10.1073/pnas.1315926110
Williams, R.M., Zipfel, W.R., Webb, W.W., 2001. Multiphoton microscopy in biological research. Curr. Opin. Chem. Biol. 5, 603–608. https://doi.org/10.1016/s1367-5931(00)00241-6
Willig, K.I., Rizzoli, S.O., Westphal, V., Jahn, R., Hell, S.W., 2006. STED microscopy reveals that synaptotagmin remains clustered after synaptic vesicle exocytosis. Nature 440, 935–939. https://doi.org/10.1038/nature04592
Woodhall, G., Evans, D.I., Cunningham, M.O., Jones, R.S.G., 2001. NR2B-containing NMDA autoreceptors at synapses on entorhinal cortical neurons. J. Neurophysiol. 86, 1644–1651. https://doi.org/10.1152/jn.2001.86.4.1644
Woolley, C.S., 2007. Acute effects of estrogen on neuronal physiology. Annu. Rev. Pharmacol. Toxicol. 47, 657–680. https://doi.org/10.1146/annurev.pharmtox.47.120505.105219
Woolley, C.S., 1998. Estrogen-mediated structural and functional synaptic plasticity in the female rat hippocampus. Horm. Behav. 34, 140–148. https://doi.org/10.1006/hbeh.1998.1466
Woolley, C.S., Gould, E., Frankfurt, M., McEwen, B.S., 1990. Naturally occurring fluctuation in dendritic spine density on adult hippocampal pyramidal neurons. J. Neurosci. 10, 4035–4039. https://doi.org/10.1523/jneurosci.10-12-04035.1990
Woolley, C.S., McEwen, B.S., 1993. Roles of estradiol and progesterone in regulation of hippocampal dendritic spine density during the estrous cycle in the rat. J.

Comp. Neurol. 336, 293–306. https://doi.org/10.1002/cne.903360210
Woolley, C.S., McEwen, B.S., 1992. Estradiol mediates fluctuation in hippocampal synapse density during the estrous cycle in the adult rat. J. Neurosci. 12, 2549–2554. https://doi.org/10.1523/jneurosci.12-07-02549.1992
Wu, J.Y., Lam, Y.W., Falk, C.X., Cohen, L.B., Fang, J., Loew, L., Prechtl, J.C., Kleinfeld, D., Tsau, Y., 1998. Voltage-sensitive dyes for monitoring multineuronal activity in the intact central nervous system. Histochem. J. 30, 169–187. https://doi.org/10.1023/A:1003295319615
Wu, L.G., Saggau, P., 1997. Presynaptic inhibition of elicited neurotransmitter release. Trends Neurosci. 20, 204–212. https://doi.org/10.1016/S0166-2236(96)01015-6
Wyllie, D.J.A., Livesey, M.R., Hardingham, G.E., 2013. Influence of GluN2 subunit identity on NMDA receptor function. Neuropharmacology 74, 4–17. https://doi.org/10.1016/j.neuropharm.2013.01.016
Xia, X.M., Fakler, B., Rivard, A., Wayman, G., Johnson-Pais, T., Keen, J.E., Ishii, T., Hirschberg, B., Bond, C.T., Lutsenko, S., Maylie, J., Adelman, J.P., 1998. Mechanism of calcium gating in small-conductance calcium-activated potassium channels. Nature 395, 503–507. https://doi.org/10.1038/26758
Xu, C., Zipfel, W., Shear, J.B., Williams, R.M., Webb, W.W., 1996. Multiphoton fluorescence excitation: New spectral windows for biological nonlinear microscopy. Proc. Natl. Acad. Sci. U. S. A. 93, 10763–10768. https://doi.org/10.1073/pnas.93.20.10763
Xu, H.T., Pan, F., Yang, G., Gan, W.B., 2007. Choice of cranial window type for in vivo imaging affects dendritic spine turnover in the cortex. Nat. Neurosci. 10, 549–551. https://doi.org/10.1038/nn1883
Xu, J., Wu, L.G., 2005. The decrease in the presynaptic calcium current is a major cause of short-term depression at a calyx-type synapse. Neuron 46, 633–645. https://doi.org/10.1016/j.neuron.2005.03.024
Xu, T., Yu, X., Perlik, A.J., Tobin, W.F., Zweig, J.A., Tennant, K., Jones, T., Zuo, Y., 2009. Rapid formation and selective stabilization of synapses for enduring motor memories. Nature 462, 915–919. https://doi.org/10.1038/nature08389
Yamagata, Y., Kobayashi, S., Umeda, T., Inoue, A., Sakagami, H., Fukaya, M., Watanabe, M., Hatanaka, N., Totsuka, M., Yagi, T., Obata, K., Imoto, K., Yanagawa, Y., Manabe, T., Okabe, S., 2009. Kinase-dead knock-in mouse reveals an essential role of kinase activity of Ca2+/calmodulin-dependent protein kinase IIα in dendritic spine enlargement, long-term potentiation, and learning. J. Neurosci. 29, 7607–7618. https://doi.org/10.1523/JNEUROSCI.0707-09.2009
Yang, G., Lai, C.S.W., Cichon, J., Ma, L., Li, W., Gan, W.B., 2014. Sleep promotes branch-specific formation of dendritic spines after learning. Science 344, 1173–1178. https://doi.org/10.1126/science.1249098
Yang, G., Pan, F., Parkhurst, C.N., Grutzendler, J., Gan, W.B., 2010. Thinned-skull cranial window technique for long-term imaging of the cortex in live mice. Nat. Protoc. 5, 213–220. https://doi.org/10.1038/nprot.2009.222
Yang, J., Woodhall, G.L., Jones, R.S.G., 2006. Tonic facilitation of glutamate release by presynaptic NR2B-containing NMDA receptors is increased in the entorhinal cortex of chronically epileptic rats. J. Neurosci. 26, 406–410. https://doi.org/10.1523/JNEUROSCI.4413-05.2006
Yang, Y., Wang, X. Bin, Frerking, M., Zhou, Q., 2008. Spine expansion and stabilization associated with long-term potentiation. J. Neurosci. 28, 5740–5751. https://doi.org/10.1523/JNEUROSCI.3998-07.2008
Yankova, M., Hart, S.A., Woolley, C.S., 2001. Estrogen increases synaptic connectivity between single presynaptic inputs and multiple postsynaptic CA1 pyramidal cells: A serial electron-microscopic study. Proc. Natl. Acad. Sci. U. S. A. 98, 3525–3530. https://doi.org/10.1073/pnas.051624598
Yaroslavsky, A.N., Schulze, P.C., Yaroslavsky, I. V., Schober, R., Ulrich, F., Schwarzmaier, H.J., 2002. Optical properties of selected native and coagulated

human brain tissues in vitro in the visible and near infrared spectral range. Phys. Med. Biol. 47, 2059–2073. https://doi.org/10.1088/0031-9155/47/12/305
Ye, Z., Cudmore, R.H., Linden, D.J., 2019. Estrogen-dependent functional spine dynamics in neocortical pyramidal neurons of the mouse. J. Neurosci. 39, 4874–4888. https://doi.org/10.1523/JNEUROSCI.2772-18.2019
Yong, X.L.H., Zhang, L., Yang, L., Chen, X., Tan, J.Z.A., Yu, X., Chandra, M., Livingstone, E., Widagdo, J., Vieira, M.M., Roche, K.W., Lynch, J.W., Keramidas, A., Collins, B.M., Anggono, V., 2021. Regulation of NMDA receptor trafficking and gating by activity-dependent CaMKIIα phosphorylation of the GluN2A subunit. Cell Rep. 36, 109338. https://doi.org/10.1016/j.celrep.2021.109338
Yuen, G.S., McEwen, B.S., Akama, K.T., 2011. LIM kinase mediates estrogen action on the actin depolymerization factor Cofilin. Brain Res. 1379, 44–52. https://doi.org/10.1016/j.brainres.2010.07.067
Yuste, R., 2005. Fluorescence microscopy today. Nat. Methods 2, 902–904. https://doi.org/10.1038/nmeth1205-902
Zeisel, A., Muñoz-Manchado, A.B., Codeluppi, S., Lönnerberg, P., La Manno, G., Juréus, A., Marques, S., Munguba, H., He, L., Betsholtz, C., Rolny, C., Castelo-Branco, G., Hjerling-Leffler, J., Linnarsson, S., 2015. Cell types in the mouse cortex and hippocampus revealed by single-cell RNA-seq. Science 347, 1138–1141. https://doi.org/10.1126/science.aaa1934
Zhang, F., Gradinaru, V., Adamantidis, A.R., Durand, R., Airan, R.D., De Lecea, L., Deisseroth, K., 2010. Optogenetic interrogation of neural circuits: Technology for probing mammalian brain structures. Nat. Protoc. 5, 439–456. https://doi.org/10.1038/nprot.2009.226
Zhang, X. lei, Sullivan, J.A., Moskal, J.R., Stanton, P.K., 2008. A NMDA receptor glycine site partial agonist, GLYX-13, simultaneously enhances LTP and reduces LTD at Schaffer collateral-CA1 synapses in hippocampus. Neuropharmacology 55, 1238–1250. https://doi.org/10.1016/j.neuropharm.2008.08.018
Zhang, X.M., Luo, J.H., 2013. GluN2A versus GluN2B: Twins, but quite different. Neurosci. Bull. 29, 761–772. https://doi.org/10.1007/s12264-013-1336-9
Zhang, Y., Cudmore, R.H., Lin, D.T., Linden, D.J., Huganir, R.L., 2015. Visualization of NMDA receptor - Dependent AMPA receptor synaptic plasticity in vivo. Nat. Neurosci. 18, 402–409. https://doi.org/10.1038/nn.3936
Zhou, L., Fester, L., Von Blittersdorff, B., Hassu, B., Nogens, H., Prange-Kiel, J., Jarry, H., Wegscheider, K., Rune, G.M., 2010. Aromatase inhibitors induce spine synapse loss in the hippocampus of ovariectomized mice. Endocrinology 151, 1153–1160. https://doi.org/10.1210/en.2009-0254
Zhou, Q., Homma, K.J., Poo, M.M., 2004. Shrinkage of dendritic spines associated with long-term depression of hippocampal synapses. Neuron 44, 749–757. https://doi.org/10.1016/j.neuron.2004.11.011
Zhou, Q., Sheng, M., 2013. NMDA receptors in nervous system diseases. Neuropharmacology 74, 69–75. https://doi.org/10.1016/j.neuropharm.2013.03.030
Zipfel, W.R., Williams, R.M., Webb, W.W., 2003. Nonlinear magic: Multiphoton microscopy in the biosciences. Nat. Biotechnol. 21, 1369–1377. https://doi.org/10.1038/nbt899
Zola-Morgan, S., Squire, L.R., Amaral, D.G., 1986. Human amnesia and the medial temporal region: Enduring memory impairment following a bilateral lesion limited to field CA1 of the hippocampus. J. Neurosci. 6, 2950–2967. https://doi.org/10.1523/jneurosci.06-10-02950.1986
Zong, W., Wu, R., Li, M., Hu, Y., Li, Y., Li, J., Rong, H., Wu, H., Xu, Y., Lu, Y., Jia, H., Fan, M., Zhou, Z., Zhang, Y., Wang, A., Chen, L., Cheng, H., 2017. Fast high-resolution miniature two-photon microscopy for brain imaging in freely behaving mice. Nat. Methods 14, 713–719. https://doi.org/10.1038/nmeth.4305
Zuber, B., Lučić, V., 2019. Molecular architecture of the presynaptic terminal. Curr. Opin. Struct. Biol. 54, 129–138. https://doi.org/10.1016/j.sbi.2019.01.008

Zucker, R.S., Regehr, W.G., 2002. Short-term synaptic plasticity. Annu. Rev. Physiol. 64, 355–405. https://doi.org/10.1146/annurev.physiol.64.092501.114547
Zuo, Y., Lin, A., Chang, P., Gan, W.B., 2005. Development of long-term dendritic spine stability in diverse regions of cerebral cortex. Neuron 46, 181–189. https://doi.org/10.1016/j.neuron.2005.04.001
Zurkovsky, L., Brown, S.L., Boyd, S.E., Fell, J.A., Korol, D.L., 2007. Estrogen modulates learning in female rats by acting directly at distinct memory systems. Neuroscience 144, 26–37. https://doi.org/10.1016/j.neuroscience.2006.09.002

11. Appendix

Supplementary Figures Chapter 4

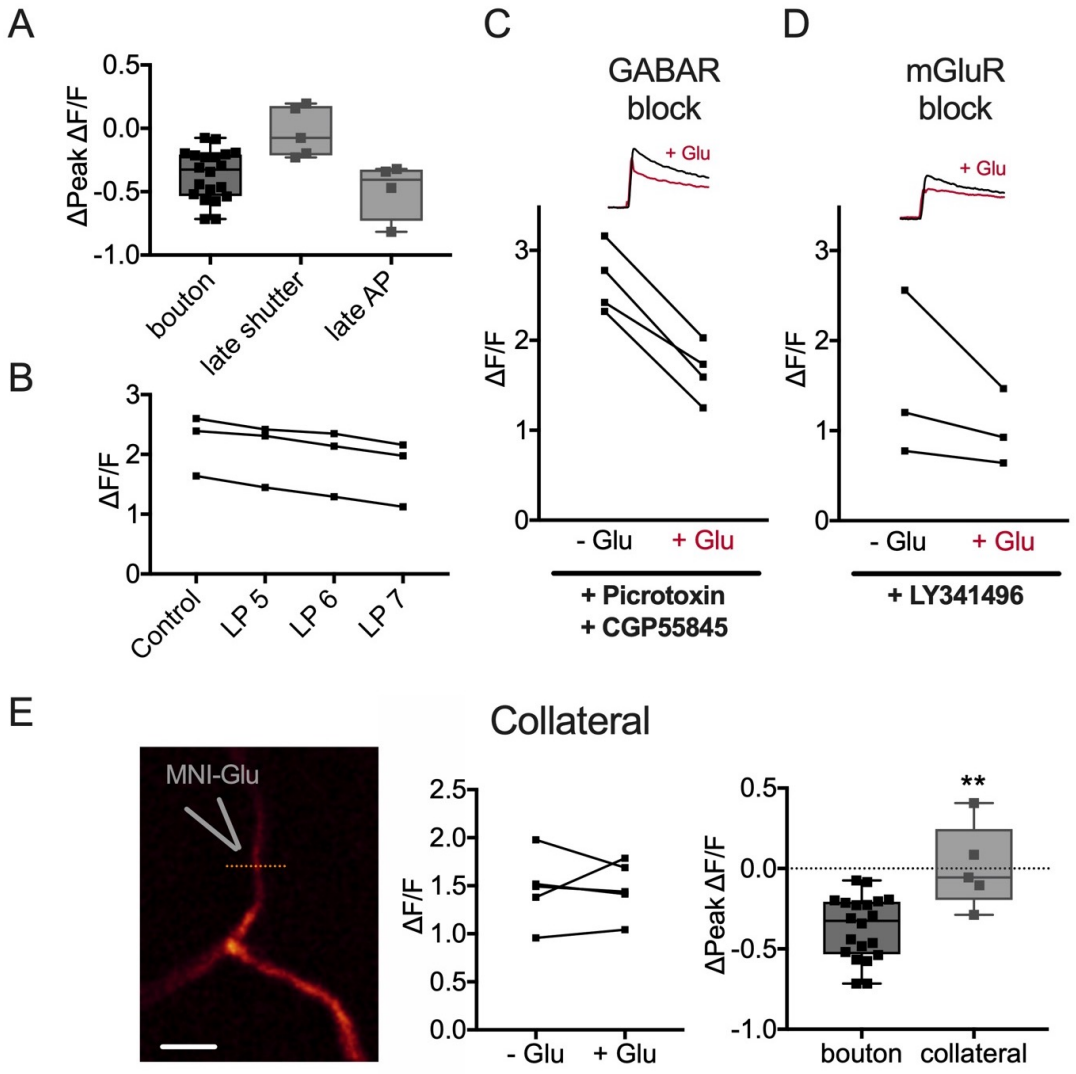

Fig. S4: Modulation of AP-evoked Ca^{2+} influx: Control experiments. (A) Difference in peak APCaTs between trials with and without glutamate photolysis for concurrent experiments (photolysis 0.5 – 5 ms after AP), N = 5, late shutter (20 ms after AP), N = 5, and late AP (20 ms post photolysis), N = 4. The decrease in average peak APCaTs under control conditions is still observable when the AP was delayed but abolished when the shutter opening was delayed. (B) Increasing UV laser intensity linearly decreased APCaTs, likely due to an increase in the concentration of uncaged glutamate. Laser power (LP) 5 – 7 in arbitrary units, N = 3. (C,D) Inhibition of GABA receptors, N = 4 or metabotrobic glutamate receptors (mGluRs), N = 3, with Picrotoxin (30 µM), CGP5845 (5 µM) and LY341495 (100 µM) did not block the decrease in APCaTs. (E) Photolysis experiments were performed at axon collaterals instead of boutons, N = 5. Scale bar = 10 µm. No change in AP-evoked Ca^{2+} transients could be detected following glutamate photolysis at the collateral (Bouton vs. Collateral p = 0.004; Mann Whitney test). Error bars represent SEM.

Supplementary Figures Chapter 5

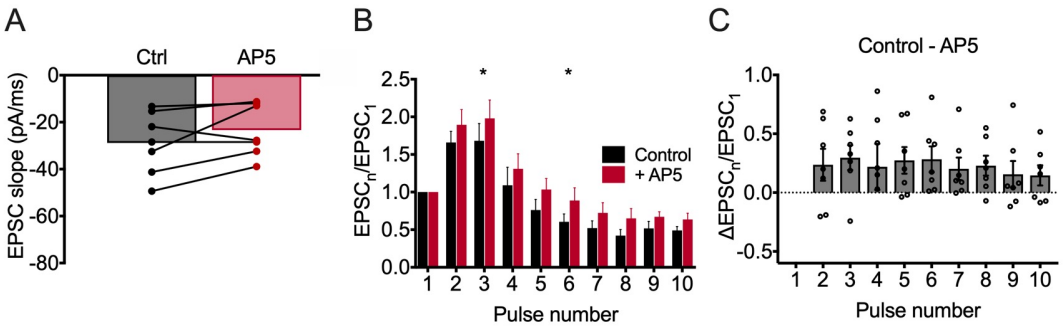

Fig. S5.1: Inhibition of preNMDARs slightly increases short-term facilitation of high-frequency bursts in acute hippocampal slices. (A) The initial EPSC slope does not change during the experiments. **(B)** Average normalised slope during burst stimulation of 10 APs at 200 Hz before (black) and after (red) the addition of 50 µM AP5 in acute hippocampal slices. $GABA_A$- and $GABA_B$-receptors were blocked using Picrotoxin (30 µM) and CGP55845 (5 µM). PreNMDAR blockade significantly increased the magnitude of short-term facilitation in acute slices. (N = 7 cells; $p < 0.05$ for pulses 3 and 6; Wilcoxon signed rank test). (C) **.** Individual data points showing the difference in the normalised EPSC slope of pulse 1-10 before and after the addition of AP5 for experiments shown in (B). Error bars represent SEM. Data was jointly collected with Rudi Tong.

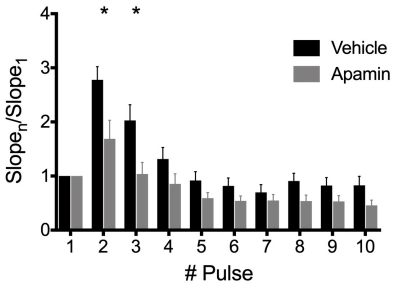

Fig. S5.2: Apamin incubation causes a decrease in the magnitude of facilitation. The average normalised EPSC slope during burst stimulation of 10 APs at 200 Hz in aCSF (black) and apamin (grey) in organotypic slices. Incubation of slices with 1µM apamin caused a decrease in the magnitude of short-term facilitation. (N = 10 cells (control), 9 cells (apamin); $p < 0.05$ for pulses 2 and 3; Mann-Whitney test). Error bars represent SEM.

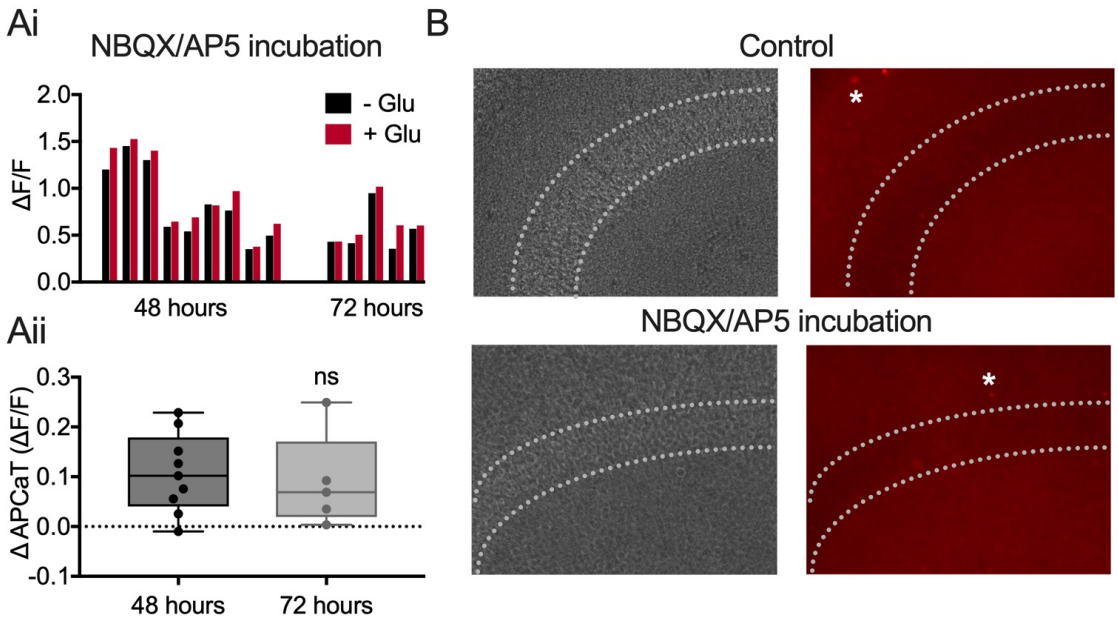

Fig. S5.3: Network activity shifts the balance between GluN2A and GluN2B subpopulations. (Ai) Peak APCaTs for individual experiments following 48 or 72 hours of treatment with NBQX and AP5. (Aii) No difference in effect size could be detected with regards to incubation time. (B) Propidium iodide was used to label dead neurones to assess slice health in control conditions and following NBQX/AP5 incubation. White dotted lines indicate CA3 cell layer, asterisks indicate dead cell bodies outside the cell layer. Drug incubation did not affect slice health.

Supplementary Methods Chapter 5

Propidium iodide cell health essay

Organotypic slices were incubated in 5 g/ml propidium iodide for 30 minutes in the incubator (Happ and Tasker, 2016). Subsequently, images were taken to assess propidium iodide uptake in CA3 neurones. Propidium iodide diffuses into cells with damaged membranes, thus serves as a quantitive marker for cell integrity (see Happ and Tasker, 2016 for details).

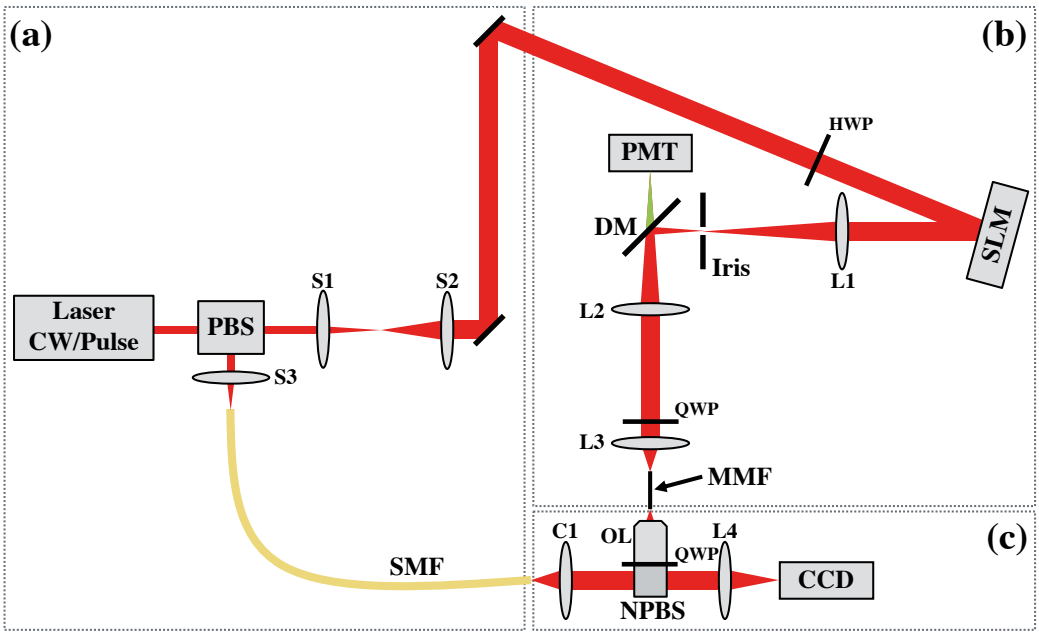

Fig. S7.1: Schematic of the system. (a) The source module contains a laser able to generate CW and pulsed outputs. (b) The imaging module includes an SLM for wavefront control during imaging and calibration, as well as a PMT for detection ofthe fluorescence. (c) The calibration module is used for recording illumination focus data and for evaluating the TM. *Published in Turcotte et al., 2020, Optics Letters, Vol. 45, No. 24.*

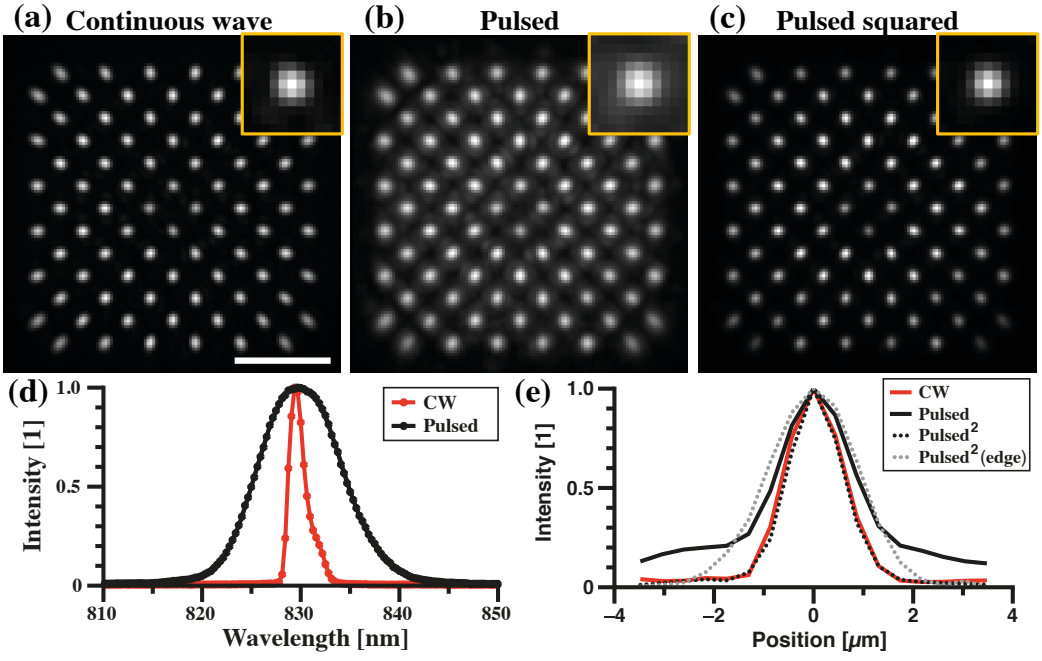

Fig S7.2: Non-linearity of two-photon fluorescence improves focusing quality by suppressing background. (a), (b) Illumination foci achieved with wavefront control

through a MMF and recorded sequentially at different lateral positions (composite maximum intensity projection from images of individual foci) when the laser is operating in (a) CW mode and (b) pulsed mode. (c) Squared of the intensity distribution shown in (b) to illustrate the two-photon illumination. Scale bar: 15 µm; inset width: 4.8 µm. (d) Spectra of the laser source in CW and pulsed mode. (e) Intensity profile for the inset foci shown in (a)–(c) and for a focus at the edge in pulsed mode (squared). *Published in Turcotte et al., 2020, Optics Letters, Vol. 45, No. 24.*

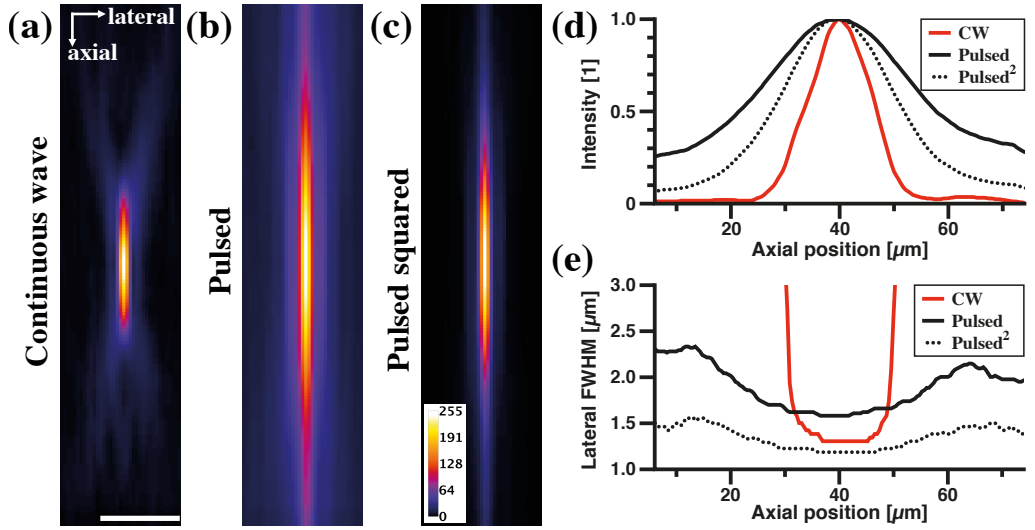

Fig S7.3: Spectral dispersion axially elongates the focus when switching the laser from CW to pulsed mode. (a), (b) Illumination foci achieved with wavefront control through a MMF and recorded sequentially at different axial positions (axial-lateral profile) when the laser is operating in (a) CW mode and (b) pulsed mode. (c) Square of the intensity distribution shown in (b) to illustrate the two-photon excitation. (d) Intensity as a function of the axial position (distance from the distal facet) for the data shown in (a)–(c). (e) Lateral FWHM as a function of the axial position for the data shown in (a)–(c). Scale bar: 10µm. *Published in Turcotte et al., 2020, Optics Letters, Vol. 45, No. 24.*

Supplementary Figures Chapter 8

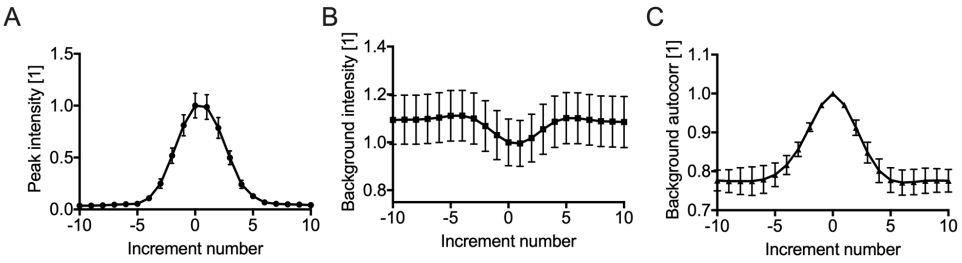

Fig. S8: Metrics for sensorless AO optimisation. (A) peak intensity, (B) background intensity, and (C) background autocorrelation. Each graph is normalised to the value at increment zero. An increment is equal to 0.001π rad for tip and tilt and of $4\times10^{-6}\pi$ rad for defocus around zero bias µm in wavefront correction applied to the LC-SLM.

Details on statement of authorship

The work presented in this thesis is entirely my own work except for the experiments specified below.

In Chapter 4 Figure 10, some data points of the intracellular MK-801 dataset were collected by Dr. Rudi Tong. In the Appendix, Figure S5.1 both Dr. Rudi Tong and I collected and analysed the data. Dr. Rudi Tong kindly provided the photograph in Figure 33B, Chapter 7.

Even though the data was collected by me, the final Figures presented in Chapters 7.2.3. and 7.2.4. as published in the respective papers (Turcotte et al., 2020a, 2019) were generated by Dr. Raphaël Turcotte. Additional experiments in the Appendix, Figure S7.1 - S7.3 were conducted partly or completely by Dr. Raphaël Turcotte. The adaptive optics optimisation code presented in Chapter 8 was designed and implemented by Dr. Raphaël Turcotte, and further experimentally applied and verified by me. Both Dr. Raphaël Turcotte and I collected the data for Figure S8, Appendix (chronic parameters) and Figure 44 (point quality).

All the above and text extracts from publications (referred to in the respective Chapters) have been included in this thesis with permission from all contributing individuals.